



UNIL | Université de Lausanne

Unicentre

CH-1015 Lausanne

<http://serval.unil.ch>

Year : 2014

CIRCADIAN CLOCK ORCHESTRATION OF SIGNALING PATHWAYS INFLUENCES MOUSE METABOLISM

JOUFFE Céline

JOUFFE Céline, 2014, CIRCADIAN CLOCK ORCHESTRATION OF SIGNALING PATHWAYS
INFLUENCES MOUSE METABOLISM

Originally published at : Thesis, University of Lausanne

Posted at the University of Lausanne Open Archive <http://serval.unil.ch>

Document URN : urn:nbn:ch:serval-BIB_3C6DCEACA2365

Droits d'auteur

L'Université de Lausanne attire expressément l'attention des utilisateurs sur le fait que tous les documents publiés dans l'Archive SERVAL sont protégés par le droit d'auteur, conformément à la loi fédérale sur le droit d'auteur et les droits voisins (LDA). A ce titre, il est indispensable d'obtenir le consentement préalable de l'auteur et/ou de l'éditeur avant toute utilisation d'une oeuvre ou d'une partie d'une oeuvre ne relevant pas d'une utilisation à des fins personnelles au sens de la LDA (art. 19, al. 1 lettre a). A défaut, tout contrevenant s'expose aux sanctions prévues par cette loi. Nous déclinons toute responsabilité en la matière.

Copyright

The University of Lausanne expressly draws the attention of users to the fact that all documents published in the SERVAL Archive are protected by copyright in accordance with federal law on copyright and similar rights (LDA). Accordingly it is indispensable to obtain prior consent from the author and/or publisher before any use of a work or part of a work for purposes other than personal use within the meaning of LDA (art. 19, para. 1 letter a). Failure to do so will expose offenders to the sanctions laid down by this law. We accept no liability in this respect.



UNIL | Université de Lausanne

Faculté de biologie
et de médecine

**Département de Pharmacologie et Toxicologie
Nestlé Institute of Health Sciences**

**CIRCADIAN CLOCK ORCHESTRATION OF SIGNALING
PATHWAYS INFLUENCES MOUSE METABOLISM**

Thèse de doctorat ès sciences de la vie (PhD)

présentée à la

Faculté de biologie et de médecine
de l'Université de Lausanne

par

Céline JOUFFE

Master en Sciences Cellulaire et Moléculaire du Vivant de l'Université de Rennes 1 (France)

Jury

Prof. Luc Tappy - Président
Dr. Frédéric Gachon - Directeur de thèse
Prof. Thierry Pedrazzini - Co-directeur
Dr. Dmitri Firsov - Expert
Prof. Urs Albrecht - Expert
Prof. Robbie Loewith - Expert

Lausanne 2014

Imprimatur

Vu le rapport présenté par le jury d'examen, composé de

Président	Monsieur Prof. Luc Tappy
Directeur de thèse	Monsieur Prof. Frédéric Gachon
Co-directeur de thèse	Monsieur Prof. Thierry Pedrazzini
Experts	Monsieur Prof. Dmitri Firsov
	Monsieur Prof. Urs Albrecht
	Monsieur Prof. Roebie Loewith

le Conseil de Faculté autorise l'impression de la thèse de

Madame Céline Jouffe

Master en Sciences de l' Université de Rennes, France

intitulée

**CIRCADIAN CLOCK ORCHESTRATION OF SIGNALING
PATHWAYS INFLUENCES MOUSE METABOLISM**

Lausanne, le 19 décembre 2014

pour La Doyenne
de la Faculté de Biologie et de Médecine



Prof. Luc Tappy

REMERCIEMENTS

Tout d'abord, je tiens à remercier Fred Gachon pour m'avoir donné l'opportunité d'effectuer ces différents travaux au sein de son laboratoire. Je lui suis très reconnaissante pour sa confiance, sa disponibilité, ses conseils et son sens critique qui m'ont beaucoup apportés tout au long de ces cinq années de thèse.

Je tiens à remercier Gaspard Cretenet avec qui j'ai travaillé les deux premières années de ma thèse et qui a été d'une grande aide notamment lors de mon arrivée dans le laboratoire. Un grand merci également à Eva Martin qui a su m'apporter toute l'aide technique dont j'avais besoin pour la réalisation de ces projets.

Je remercie toutes les personnes qui ont participé à l'élaboration de ces différents projets : Laura Symul, Félix Naef, Mojgan Masoodi, Patrick Descombes ainsi que toutes les personnes de la plateforme de génomique du NIHS.

Merci à Dmitri Firsov, Thierry Pedrazzini, Urs Albrecht, Robbie Loewith, et Luc Tappy pour avoir accepté l'invitation à faire partie de mon jury.

Un grand merci à toute l'équipe « Circadian Rhythms », Daniel Mauvoisin, Florian Atger, Eva Martin, Benjamin Weger, Cédric Gobet et Capucine Bolvin pour leur soutien, leurs conseils et la bonne humeur apportés durant ces dernières années.

Je remercie les personnes que j'ai pu rencontrer tout au long de ma thèse au sein du DPT et du NIHS et qui ont joué un rôle essentiel autant sur le plan scientifique que sur le plan moral : Anne, Sabrina, Laurent, Daniel, Gab, Dmitri, Caroline, Chloé, Matthias, Sonia, Aurélie, Laura, Alice, Armand, Julien, Jérôme.

Enfin, je remercie l'ensemble de ma famille qui constitue mon roc sur lequel je peux m'appuyer en permanence et en toute circonstance.

ABSTRACT

Circadian clocks, present in organisms living in a rhythmic environment, constitute the mechanisms allowing anticipation and adaptation of behavior and physiology in response to these environmental variations. As a consequence, most aspects of metabolism and behavior are under the control of this circadian clock. At a molecular level, in all the studied species, the rhythmic expression of the genes involved are generated by interconnected transcriptional and translational feedback loops. In mammals, the heterodimer composed of BMAL1 and its partners CLOCK or NPAS2 constitutes a transcriptional activator regulating transcription of *Per* and *Cry* genes. These genes encode for repressors of the activity of BMAL1:CLOCK or BMAL1: NPAS2 heterodimers, thus closing a negative feedback loop that generates rhythms of approximately 24 hours.

The aim of my doctoral work consisted in the investigation of the role of circadian clock in the regulation of different aspects of mouse metabolism through the rhythmic activation of signaling pathways.

First, we showed that one way how the circadian clock exerts its function as an oscillator is through the regulation of mRNA translation. Indeed, we present evidence showing that circadian clock influences the temporal translation of a subset of mRNAs involved in ribosome biogenesis by controlling the transcription of translation initiation factors as well as the clock-dependent rhythmic activation of signaling pathways involved in their regulation. Moreover, the circadian oscillator regulates the transcription of ribosomal protein mRNAs

and ribosomal RNAs. Thus the circadian clock exerts a major role in coordinating transcription and translation steps underlying ribosome biogenesis.

In the second part, we showed the involvement of the circadian clock in lipid metabolism. Indeed, the three PAR bZip transcription factors DBP, TEF and HLF, are regulated by the molecular clock and play key roles in the control of lipid metabolism. Here we present evidence concerning the circadian expression and activity of PPAR α *via* the circadian transcription of genes involved in the release of fatty acids, natural ligands of PPAR α . It leads to the rhythmic activation of PPAR α itself which could then play its role in the transcription of genes encoding proteins involved in lipid, cholesterol and glucose metabolism. In addition, we considered the possible role of lipid transporters, here SCP2, in the modulation of circadian activation of signaling pathways such as TORC1, PPAR α and SREBP, linked to metabolism, and its feedback on the circadian clock.

In the last part of this work, we studied the effects of these circadian clock-orchestrated pathways in physiology, as clock disruptions have been shown to be linked to metabolic disorders. We performed *in vivo* experiments on genetically and high-fat induced obese mice devoid of functional circadian clock. The results obtained showed that clock disruption leads to impaired triglycerides and glucose homeostasis in addition to insulin secretion and sensitivity.

RESUME

Les rythmes circadiens, présents chez tout organisme vivant dans un environnement rythmique, constituent l'ensemble de mécanismes permettant des réponses comportementales et physiologiques anticipées et adaptées aux variations environnementales. De ce fait, la plupart des aspects liés au métabolisme et au comportement de ces organismes apparaissent être sous le contrôle de l'horloge circadienne contrôlant ces rythmes. Au niveau moléculaire, dans toutes les espèces étudiées, l'expression rythmique de gènes impliqués sont générés par l'interconnexion de boucles de contrôle transcriptionnelles et traductionnelles. Chez les mammifères, l'hétérodimère composé de BMAL1 et de ses partenaires CLOCK ou NPAS2 constitue un activateur transcriptionnel régulant la transcription des gènes *Per* et *Cry*. Ces gènes codent pour des répresseurs de l'activité des hétérodimères BMAL1:CLOCK ou BMAL1:NPAS2. Cela a pour effet de fermer la boucle négative, générant ainsi des rythmes d'environ 24 heures.

Le but de mon travail de thèse a consisté en l'investigation du rôle de l'horloge circadienne dans la régulation de certains aspects du métabolisme chez la souris *via* la régulation de l'activation rythmique des voies de signalisation.

Nous avons tout d'abord montré que l'horloge circadienne exerce sa fonction d'oscillateur notamment au niveau de la régulation de la traduction des ARNm. En effet, nous présentons des preuves montrant que l'horloge circadienne influence la traduction temporelle d'un groupe d'ARNm impliqués dans la biogénèse des ribosomes en contrôlant la transcription de facteurs d'initiation de la traduction ainsi que l'activation rythmique des voies de signalisation qui sont impliquées dans leur régulation. De plus, l'oscillateur circadien régule la

transcription d'ARNm codant pour les protéines ribosomales et d'ARN ribosomaux. De cette façon, l'horloge circadienne exerce un rôle majeur dans la coordination des étapes de transcription et traduction permettant la biogénèse des ribosomes.

Dans la deuxième partie, nous montrons les implications de l'horloge circadienne dans le métabolisme des lipides. En effet, DBP, TEF et HLF, trois facteurs de transcription de la famille des PAR bZip qui sont régulés par l'horloge circadienne, jouent un rôle clé dans le contrôle du métabolisme des lipides par l'horloge circadienne. Nous apportons ici des preuves concernant l'expression et l'activité rythmiques de PPAR α *via* la transcription circadienne de gènes impliqués dans le relargage d'acides gras, ligands naturels de PPAR α , conduisant à l'activation circadienne de PPAR α lui-même, pouvant ainsi jouer son rôle de facteur de transcription de gènes codant pour des protéines impliquées dans le métabolisme des lipides, du cholestérol et du glucose. De plus, nous nous sommes penchés sur le rôle possible de transporteurs de lipides, ici SCP2, dans la modulation de l'activation circadienne de voies de signalisation, telles que TORC1, PPAR α et SREBP, qui sont liées au métabolisme, ainsi que son impact sur l'horloge elle-même.

Dans la dernière partie de ce travail, nous avons étudié les effets de l'activation de ces voies de signalisation régulées par l'horloge circadienne dans le contexte physiologique puisqu'il a été montré que la perturbation de l'horloge pouvait être associée à des désordres métaboliques. Pour ce faire, nous avons fait des expériences *in vivo* sur des souris déficientes pour l'horloge moléculaire pour lesquelles l'obésité est induite génétiquement ou induite par la nourriture riche en lipides. Les résultats que nous obtenons montrent des dérèglements au niveau de l'homéostasie des triglycérides et du glucose ainsi que sur l'expression et la réponse à l'insuline.

RESUME POUR TOUT PUBLIC

Chaque être vivant soumis aux rythmes jour-nuit possède une horloge biologique appelé horloge circadienne. Cette horloge permet aux organismes d'adapter et d'anticiper leur métabolisme aux variations environnementales quotidiennes. Chez les mammifères, cette horloge est présente à la fois dans le cerveau, mais également dans d'autres organes comme le foie, les reins, le pancréas. Au niveau physiologique, en plus de contrôler l'alternance veille-sommeil, cette horloge est impliquée dans la régulation d'autres mécanismes tels que la température corporelle, la pression sanguine, la concentration des certaines hormones dans le sang, ou encore l'activité digestive.

Au niveau moléculaire, des boucles de régulations interconnectées génèrent ces rythmes de 24 heures environ. Ces oscillations permettent ainsi la régulation du métabolisme en agissant sur certaines protéines ou enzymes impliquées dans des voies de signalisations particulières.

Dans le cadre de ce travail, nous nous sommes intéressés aux implications de l'horloge circadienne dans différents aspects du métabolisme. Nous montrons ainsi que l'horloge moléculaire est responsable de l'orchestration de la biogénèse des ribosomes, structure indispensable au mécanisme qui permet la production de protéines. Ce phénomène implique ainsi l'activation coordonnée de plusieurs voies de signalisation au sein de la cellule. D'autre part, nous présentons des résultats montrant le rôle de l'horloge circadienne dans la régulation du métabolisme des lipides et son impact sur les voies de signalisation. Enfin, l'étude de souris obèses nous a permis d'étudier le lien entre l'obésité et l'horloge circadienne.

TABLE OF CONTENT

REMERCIEMENTS	3
ABSTRACT	4
RESUME	6
RESUME POUR TOUT PUBLIC	8
LIST OF ABBREVIATIONS	12
CONTEXT OF DOCTORAL WORK	15
INTRODUCTION	16
I. General introduction	16
II. The circadian clock is hierarchically organized	18
A. The central pacemaker	19
B. Synchronization of peripheral clocks	21
III. The molecular circadian clock	22
A. The principal loop	22
1. The activator complex	22
2. The repressor complex	24
B. The stabilization loop	25
C. Post-transcriptional modifications	26
D. Post-translational modifications	28
1. Phosphorylations and dephosphorylations	28
2. Ubiquitinations	29
3. Sumoylations	29
4. Chromatin remodeling	30
IV. The translational mechanisms in mammals	31
A. Pre-initiation of the translation	32
1. Formation of pre-initiation complex	32
2. Regulation of TORC1 signaling pathway	32
3. Translation initiation regulated by TORC1	33
B. The different steps of translation initiation	35
1. Formation of 43S pre-initiation complex	35
2. Attachment of 43S complex to mRNA	35
3. Ribosome scanning of mRNA 5'UTR	37
4. Initiation of codon recognition	37
5. Commitment of ribosomes to start codon	38
6. Ribosomal subunit joining	38

C.	Translation elongation	39
D.	Termination of translation	39
E.	Ribosome biogenesis	40
1.	40S subunit	41
2.	60S subunit	42
3.	Nuclear export	43
V.	Energy balance	44
A.	SREBP signaling pathway	45
1.	Activation of SREBPs	45
2.	Transcriptional regulation of SREBP1c in liver	46
B.	LXR signaling pathway	48
C.	ChREB signaling pathway	49
1.	Activation of ChREB	50
2.	Alternative transactivation of ChREB in adipose tissue	51
D.	PPAR signaling pathway	53
1.	PPAR α signaling pathway	54
2.	PPAR β/δ signaling pathway	55
3.	PPAR γ signaling pathway	56
E.	Involvement of the circadian clock	57
RESULTS		59
I.	The circadian clock coordinates the ribosome biogenesis	59
II.	Involvements of circadian clock in lipid metabolism	62
A.	Modulation of PPAR α signaling pathway in mouse liver	62
B.	Sterol Carrier Protein 2 dependent diurnal lipid transport modulates rhythmic activation of signaling pathways in mouse liver	63
III.	Metabolic defects in <i>Bmal1</i> knockout mice	66
A.	Metabolic defects in genetically obese <i>Bmal1</i> knockout mice	66
1.	<i>Bmal1</i> KO mice harboring the <i>Ob</i> mutation exhibit premature death	66
2.	ObKO mice exhibit an obese phenotype	68
3.	Glucose homeostasis is impaired in ObKO mice	69
4.	ObKO mice exhibit an impaired glucose clearance but are insulin sensitive	74
5.	ObKO mice exhibit low hepatosteatosis but high circulating triglyceride concentration	76
B.	Metabolic defects in diet-induced obese <i>Bmal1</i> knockout mice	78
1.	<i>Bmal1</i> KO mice fed with high-fat diet become obese prematurely	78
2.	Glucose homeostasis is impaired in diet-induced obese mice	80
3.	<i>Bmal1</i> KO liver exhibit less steatosis	81
4.	Delayed glucose clearance in high-fat diet fed mice	83

DISCUSSION	86
I. Premature death for <i>Bmal1</i> KO mice harboring <i>Ob</i> mutation	86
II. Involvement in bone metabolism	87
III. Food intake consequences	87
IV. Protective effect of <i>Bmal1</i> deletion in obesity	88
V. Involvement of mitochondrial metabolism in insulin sensitivity	89
CONCLUSION	91
EXPERIMENTAL PROCEDURES	94
I. Animal experiments	94
A. Body composition analysis	94
B. Glycemia measurements	95
C. Glucose tolerance test	95
D. Insulin tolerance test	96
II. Serum chemistry analysis	96
III. Glycogen extraction	96
IV. Liver slices	97
REFERENCES	98

LIST OF ABBREVIATIONS

4E-BP1: 4E-binding protein 1	CLOCK: Circadian Locomotor Output Cycles Kaput
5'TOP: 5' Terminal OligoPyrimidine	CREB: Cyclic AMP Response Binding protein
βTrCP: β Transducing repeat-Containing Protein	CRY: CRYptochrome
ABCG5: ATP-Binding Cassette subfamily G member 5	DBP: D-box Binding Protein
ACC: Acetyl-CoA Carboxylase	eEF: eukaryotic Elongation Factor
ACL: ATP-Citrate Lyase	eIF: eukaryotic translation Initiation Factor
ACOT: Acyl CoA Thioesterase	eRF: eukaryotic Releasing Factor
ACS: Acetyl-CoA Synthetase	ERK: Extracellular signal-Regulated protein Kinase
AKT: serine/threonine protein kinase	FAS: Fatty Acid Synthase
AMPK: Adenoside MonoPhosphate-activated protein Kinase	FBXL: F-Box and Leucine-rich repeat protein
BCAA : Branched Chain Amino Acids	FRQ: FReQuency
BMAL1: Brain and Muscle ARNT-Like Protein 1	G6PC: Glucose 6 Phosphatase Catalytic subunit
cAMP: cyclic AMP	GAP: GTPase-Activating Protein
ChREBP: Carbohydrate Response Element Binding Protein	GPAT: Glycerol 3 Phosphate AcylTransferase
ChoRE: Carbohydrate-Response Elements	
CK: Casein Kinase	

GRACE: Glucose Response Activation Conserved Element

GSK (Glycogen Synthetase Kinase)

HAT: Histone AcetylTransferase

HDAC: Histone DeAcetylase

HDL: High Density Lipoproteins

HLF: Hepatic Leukemia Factor

HMGCR: 3-Hydroxy-3-MethylGlutaryl-CoA Reductase

hnRBP: heterogenous nuclear RBP

INSIG: INSulin Induced Gene

IRE1: Inositol Requiring

IRS: Insulin-Receptor Substrates protein

JARID: JumonjiC and ARID domain-containing histone lysine demethylase

L-PK: L-Pyruvate Kinase

LXR: Liver X Receptor

LXRE: Liver X Responsive Element

LID: Low-glucose Inhibitory Domain

MAPK: Mitogen-Activated Protein Kinase

MEF: Mouse Embryonic Fibroblast

miRNA: microRNA

MLX: Max-Like protein X

MNK: MAPK-interacting Kinase

NAD⁺: Nicotinamide Adenine Dinucleotide

NAMPT: NicotinAMide Phosphorybosyl Transferase

NEFA: Non Esterified Fatty Acids

NES: Nuclear Export Sequence

NPAS2 : Neural PAS domain protein 2

NRF2: Nuclear factor erythroid 2-Related Factor 2

p70S6K: p70 ribosomal S6 Kinase

PACAP: Pituary Adenylate Cyclase-Activating Polypeptide

PAR bZip: Proline- and Acidic amino acid-Rich domain basic leucine Zipper

PER1: PERiod

PDK: 3-Phosphoinositide-Dependent protein Kinase

PI3K: PhosphoInositide 3 Kinase

PKA: Protein Kinase A

PP1: Phosphatase Protein 1

PPAR: Peroxisome Proliferator-Activted Receptor

PPRE: Peroxisome Proliferator hormone Responsive Element

RBP: RNA Binding Protein

ROR: Receptor-related Orphan Receptor

ROS: Reactive Oxygen Species

RPS6K: Ribosomal Protein S6 Kinase

rRNA: ribosomal RNA

RXR: Retinoic X Receptor

SCD1: Stearoyl-CoA Desaturase 1

SCP: Sterol Carrier Protein 2

SIRT6: SIRTuins

SREBP: Sterol Regulatory Element
Binding Protein

SCN: SupraChiasmatic Nucleus

T2D: Type 2 Diabetes

TEF: Thyrotroph Embryonic Factor

TORC: Target Of Rapamycin Complex

TSC: Tuberous Sclerosis Complex

UBF: Upstream Binding Factor

UCP2: UnCoupling Protein 2

X5P: Xylulose 5-Phosphate

ZT: Zeitgeber Time

CONTEXT OF THE DOCTORAL WORK

Circadian rhythms, present in organisms exposed to daily light-dark cycles, constitute the mechanisms allowing anticipated and adapted behavior and physiology responses to environmental variations. Indeed, it has been shown that the accumulation of the PAR bZip transcription factors DBP, TEF, and HLF in peripheral organs such as the kidney and liver is circadian clock-dependent. Moreover, these factors control the expression of many enzymes involved in detoxification and drug metabolism³. In a previous study recently realized in our laboratory, it has been shown that reticulum endoplasmic IRE1 α pathway is rhythmically activated with a 12 hour-period. The loss of this rhythmic activation leads to impairment in lipid metabolism resulting in aberrant activation of sterol-regulated SREBP transcription factors⁴. These two studies are good examples of circadian clock-dependent orchestration of metabolism at the transcriptional and post-translational levels. In this doctoral work we investigated the influence of the circadian clock in the activation of signaling pathways regulating metabolism. We also looked at the consequences of the circadian clock-dependent activations in the context of metabolic disorders.

INTRODUCTION

I. General introduction

For centuries, it has been observed that organisms can and must adapt to environmental changes like temperature or light/dark cycles. In the 18th century, Jean-Jacques d'Ortous de Mairan described for the first time in living organisms the existence of an endogenous clock. He observed that mimosa leaves opened during the day and closed during the night. Moreover, the movements of these leaves occurred even without access to the light (figure 1). In 1832, Augustin de Candolle described for the first time evidence of the free running period and the non-requirement for light to synchronize leaves' movements. Indeed, the leaves' movements, which still occur in constant light, exhibit an advanced phase of 2 hours. Similar biological rhythms have been later described in most of the species: in primates and birds⁵, in rodents, in insects, in drosophila⁶ and finally in humans⁷.

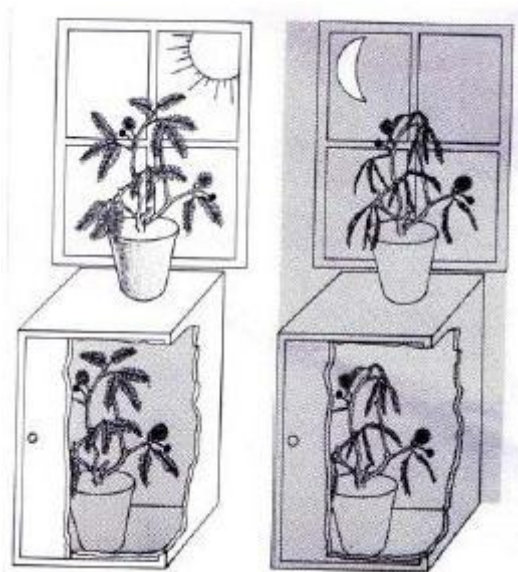


Figure 1: The leaves' movements still occurred even in constant darkness.

Representation of de Mairan's experiment showing that while mimosa was placed in constant darkness, the leaves still opened during the subjective day.

These biological rhythms, qualified as “circadian rhythms” in 1959 by Franz Halberg, coming from the Latin *Circa* and *Diem*, literally meaning “around the day”, were defined by Pittendrigh in 1960⁸ according to their specific characteristics. Circadian rhythms present a period length of about 24 hours, corresponding to one of Earth’s rotations. They are endogenous and self-sustained phenomena. They are almost independent on temperature and light intensity, and can be entrained by environmental cues, such as light, called “*Zeitgeber*”.

Thanks to a 1935 study on beans driven by Bunning, it is known that circadian rhythms are hereditary. Later, some specific mutations in *Drosophila melanogaster* resulted in shortened, lengthened or abolished free period, have been described in 1971⁹. These mutations have been shown to be localized in the *Per (Period)* gene¹⁰. Since the identification of the first clock gene in *Drosophila melanogaster*, decades of studies allowed the identification and characterization of other components of the core clock in most species.

In recent years, the number of studies concerning the regulation and involvement of the circadian rhythms has increased significantly, reflecting how important the circadian rhythms are in different metabolic phenomenon. In fact, disrupted circadian rhythms have been shown to be associated with metabolic disorders such as diabetes, obesity¹¹, vascular diseases¹², and psychiatric disorders¹³.

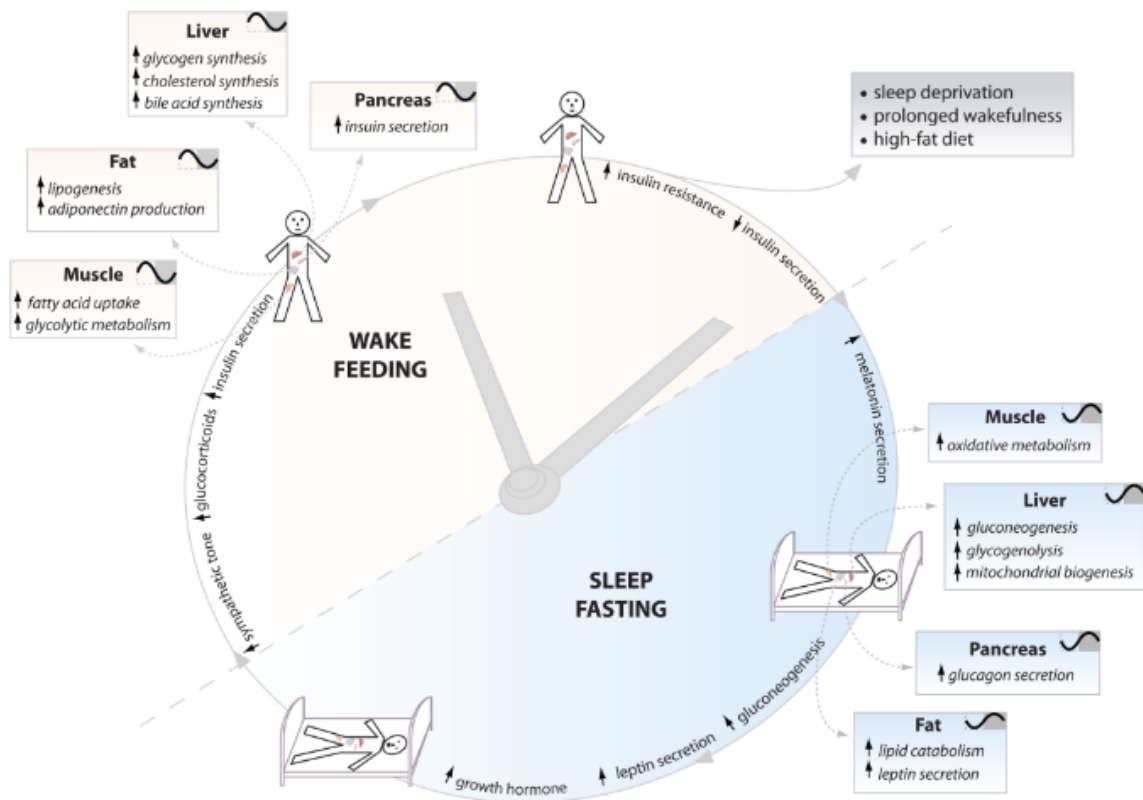


Figure 2: Coordination of behavioral and metabolic processes by the circadian clock according to time of day

Circadian clock coordinates appropriate metabolic response in peripheral tissues at the appropriate time. This coordination, depending on sleep/ wake, fasting/feeding, and dark/light cycles, is essential for maintaining the health of the organism¹⁴.

II. The circadian clock is hierarchically organized

While most tissues, organs¹⁵ and individual cells contain a circadian clock¹⁶, at the level of the whole organism, mammals require a hierarchical organization of the clock with a central pacemaker synchronizing the peripheral clocks (figure 3).

A. The central pacemaker

In mammals, there is a central pacemaker localized in the SCN (SupraChiasmatic Nucleus) (figure 3). In mice, it is composed of two groups of about 10,000 neurons each and is localized in the anterior hypothalamus above the optic chiasm and lateral to the third ventricle¹⁷. The first experiments showing the importance of this structure in circadian rhythms have been realized in rodents. SCN have been ablated, resulting in a loss of the daily rhythms like locomotor activity and drinking behavior¹⁸. When SCN coming from donor with a different period have been transplanted, the circadian rhythms are restored with a period similar to the donor's rhythms¹⁹. The SCN has been shown to be involved in the regulation of many phenomena such as body temperature, locomotor activity, drinking and feeding rhythms, glucose metabolism, neuronal electrical firing, gene expression, and hormone secretion.

As a central pacemaker, this structure also plays a role in the synchronization of the peripheral clocks, such as the one in the liver, when environmental information such as light is detected by photoreceptors located in the eyes *via* the retino-hypothalamus tract into the SCN²⁰. Melanopsin, a photopigment present in specific retinal ganglion cells of the retino-hypothalamus tract²¹, is essential for the synchronization of the circadian rhythms by light²². The transmission of light information is done *via* the activation of melanopsin, followed by a release of glutamate and PACAP (Pituitary Adenylate Cyclase-Activating Polypeptide) leading to molecular mechanisms that use the CREB (Cyclic AMP Response Binding protein) pathway to finally activate the *Per* genes' transcription in the SCN^{23, 24}.

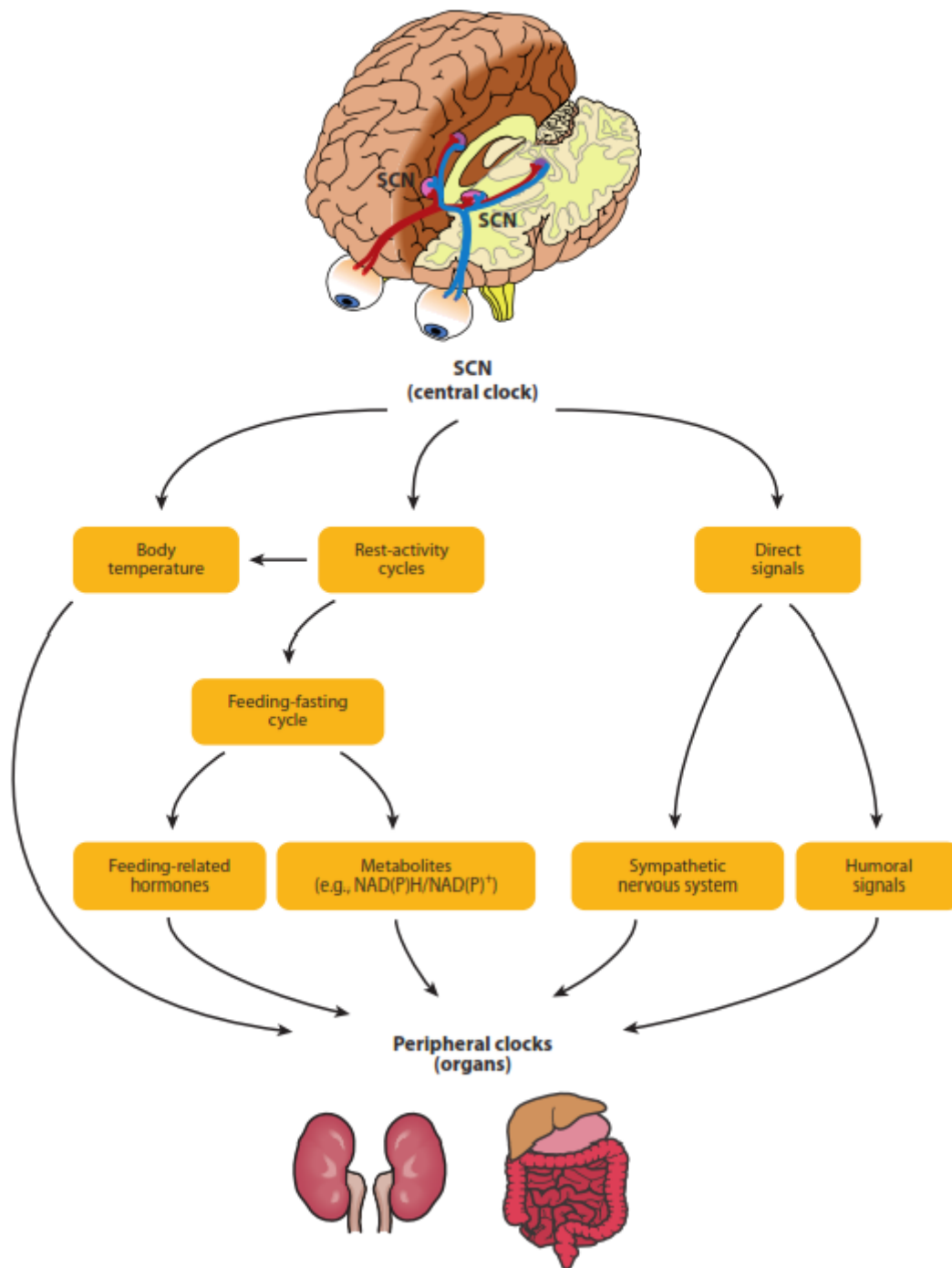


Figure 3: Schematic hierarchical organization of the circadian clock

The SCN synchronized by light signals is able to directly synchronise peripheral clocks through the sympathetic nervous system and humoral signals. In addition, rest-activity cycles driving body temperature variations and feeding-fasting cycles leading to the release of hormones and metabolites constitute indirect SCN-generated information participating in the synchronization of peripheral clocks²⁵.

B. Synchronization of peripheral clocks

Peripheral clocks located in peripheral organs, e.g. the liver or kidneys, have been shown to be rapidly desynchronized²⁶. Indeed experiments on tissue explants showed a persistence of rhythms which became dampened due to progressive cellular desynchrony because of period variation among cells. Peripheral tissues need thus to be synchronized every day to maintain their daily rhythms^{27, 28}. While synchronization of SCN occurred through light as external cue or *Zeitgeber* in peripheral organs it has been suggested that clock synchronization occurred differently with zeitgebers other than light. Indeed, a study showed that circulating metabolites and hormones in the blood could play the role of a zeitgeber for liver and kidney clocks²⁹. Actually, daily fasting-feeding cycles appeared to be important zeitgebers for peripheral clock synchronization, as it has been shown that inverted fasted-feeding cycles lead to the uncoupling of synchronization of peripheral clocks from SCN^{30, 31}. These fasting-feeding cycles lead to rhythmic circulating hormones, metabolites and elevations of temperature, all of which are involved in the synchronization of peripheral clocks²⁵. In addition, the SCN directly synchronizes the peripheral clocks *via* neuronal and humoral outputs. For example, it has been shown that glucocorticoid hormone, which is secreted under the control of SCN *via* the hypothalamic-pituitary-adrenal axis³², exhibits strong oscillations that serve as strong zeitgeber. Moreover, the autonomic nervous system is involved in direct synchronization as shown in surgical liver-denervated animals³³, which exhibit an impaired resetting after light exposure during the night compared to the control animals.

III. The molecular circadian clock

The molecular mechanism that generates a 24-hour oscillation even in absence of external cues^{34, 35} is composed of interconnected transcriptional and translational feedback loops³⁶. The molecular core clock in mammals is schematically described in the figure 4.

A. The principal loop

(1) The activator complex

The first component of the activator complex has been identified in 1994 by Vitaterna and colleagues³⁷. They identified a mutation in a specific gene named *Clock* (*Circadian Locomotor Output Cycles Kaput*) encoding for a transcription factor belonging to the basic helix-loop-helix family³⁸. This mutation, identified in a splicing site, leads *Clock* mRNA to be deleted from the exon 19³⁸, and due to the alterations generated on circadian rhythms, this mutation has been qualified as dominant negative. Indeed, mice harboring the mutation at the heterozygous state exhibited a longer free running period than wild-type mice, and moreover the mutation at the homozygous state confers on *Clock* Δ ¹⁹ mice an arrhythmia after some days in constant darkness³⁷. Later, *Clock* knockout mice were generated and the analysis of their locomotor activity revealed that they still exhibit behavioral rhythmicity in constant darkness but with a shorter free running period compared to heterozygote or wild-type mice³⁹.

The second component of the activator complex was identified by two groups of researchers in 1998 using the two-hybrid technology in yeast^{40, 41}. BMAL1 (Brain and Muscle ARNT-Like Protein 1), whose RNA expression has been described to be similar to *Clock* RNA expression pattern⁴¹, also belongs to the basic helix-loop-helix family of transcription factors

and has been shown to interact directly with CLOCK to form the activator complex. Behavioral rhythmicity studies showed that *Bmal1* knockout mice placed in a constant darkness condition immediately exhibit a completely arrhythmic activity⁴².

The activator complex composed of the heterodimerization of CLOCK and BMAL1 proteins activates the transcription of the repressor complex factors by binding on specific sequences (CACGTG) named E-BOX^{41, 43}.

Later, Garcia *et al.* identified the interaction of BMAL1 and NPAS2 (Neural PAS domain protein 2), another basic helix-loop-helix transcription factor, in the mammalian forebrain⁴⁴. This heterodimer has also been shown to be able to activate the transcription of the components of the repressor complex. However, the rhythmic activity of *Npas2* knockout mice study revealed the same phenotype as that of *Clock* knockout mice, and they still exhibit rhythmic locomotor activity in constant darkness⁴⁵. It thus seems that CLOCK and NPAS2 play a compensatory role for each other in circadian clock mechanisms. This suggestion was later validated by a study of the rhythmicity of *Clock/Npas2* double knockout mice. Indeed, the authors showed that preserving one wild-type allele of *Clock* or *Npas2* while the other gene is completely deleted is sufficient to conserve the rhythmic activity, and complete double knockout mice exhibit the same arrhythmic phenotype in constant darkness found in *Bmal1* knockout mice⁴⁶. BMAL2, identified as a basic helix-loop-helix transcription factor, was cloned in mice in 2001, and while its expression pattern does not exhibit any oscillation⁴⁷, BMAL2 is able to compensate for the absence of BMAL1 in restoring a rhythm in cell culture⁴⁸.

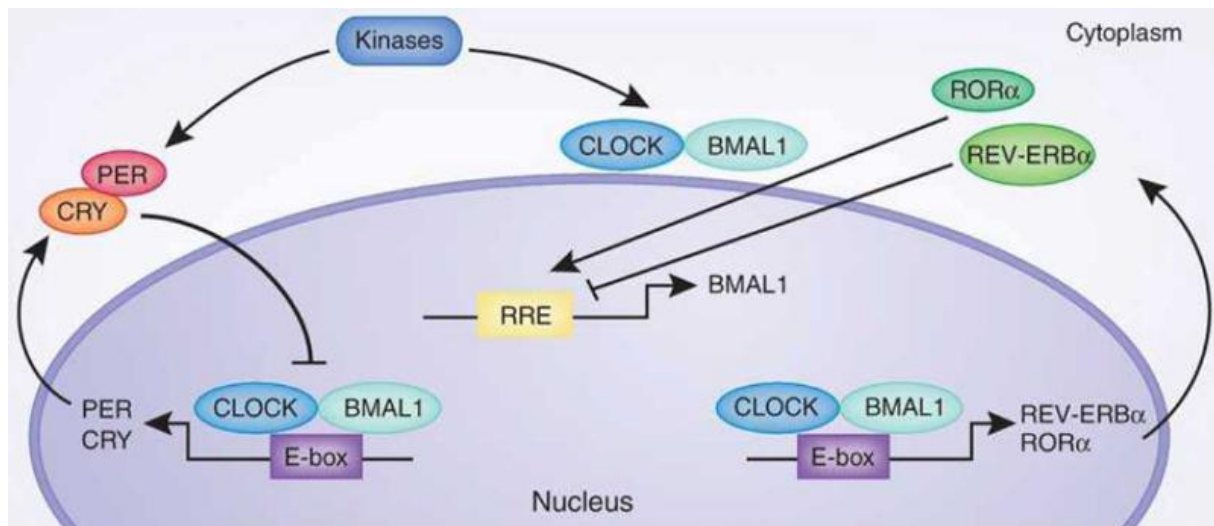


Figure 4: The mammalian molecular clock

BMAL1:CLOCK heterodimers activate clock-controlled gene transcription by direct binding to E-box. PER and CRY protein translation occurs during the night and causes repression of the activator dimer. Degradation of PER and CRY through post-translational modifications provides a new circadian cycle. In addition, REV-ERB and ROR proteins modulate the cycles by their respective inhibition and activation of *Bmal1* transcription through their binding to RRE (ROR Response Element) present in *Bmal1* promoter⁴⁹.

(2) The repressor complex

The repressor complex results in the heterodimerization of PER1 and PER2 (PERiod) proteins⁵⁰ and CRY1 and CRY2 (CRYptochrome) proteins⁵¹. *Per* is the first clock gene identified¹⁰ in *Drosophila melanogaster*. In 1997, the three mammalian *Per* homologs were cloned^{24, 52-56}. Different studies have shown that in the SCN, the three *Per* RNAs are expressed with a rhythmic pattern. In addition, light pulses promote an increase of *Per1* and *Per2* expression during the subjective night^{24, 52, 53, 56}. Mutation in both *Per1* and *Per2* genes leads to complete arrhythmia⁵⁰. The role of the protein CRY1 in the clock core has been demonstrated for the first time in plants⁵⁷. In this study, the authors showed that CRY1 was required to maintain the circadian rhythms in extended darkness. CRY1 and CRY2 proteins were then described in mammals⁵⁸, where they explored the role of CRY2 protein in the

regulation of the circadian rhythms. In their study, van der Horst *et al.* disrupted *Cry1*, *Cry2* or both in mice, and the running wheel activity appeared to be arrhythmic in constant darkness only for mice lacking both *Cry* genes, showing the importance of these genes in the generation of the circadian rhythms⁵¹.

The PER:CRY heterodimers act by negative feedback on their own expression by repressing the transcriptional activity of CLOCK:BMAL1⁵⁹⁻⁶¹. This feedback loop suggests rhythmic *per* and *cry* mRNAs and proteins expression⁶²⁻⁶⁴. Molecular mechanisms involved in repressed CLOCK:BMAL1 activity by PER and CRY requires post-translational modifications. However, recent evidences showed that CRY:PER repression is dependent on their entry into nucleus. It appeared thus that PER facilitates the entry of CRY into nucleus where it acts as repressor of CLOCK:BMAL1 activity⁶⁵.

B. The stabilisation loop

It appears that the core loop is not the only one involved in the generation of circadian rhythms. Indeed, other genes are also involved in the molecular clock oscillation. This is the case of the nuclear receptors REV-ERB α and β belonging to the REV-ERB family. Their expression has been shown to follow a circadian pattern^{16, 66}. In addition, while deletion of *Rev-erba* or *Rev-erb β* causes only subtle defect in circadian behavior, deletion of both genes in mice resulted in complete disruption of locomotor activity⁶⁶. ROR (Receptor-related Orphan Receptor) α , β , and γ belong to the ROR family. Both families of receptors have been shown to be involved in the regulation of transcription *via* their binding on specific sequences in gene promoters: the RRE (ROR Response Element) activate in an opposite way to RORs, and REV-ERBs inhibit the transcription. In context of the regulation of the core oscillator,

RORs and REV-ERBs (expression of REV-ERBs is regulated by the heterodimer CLOCK:BMAL1) activate and inhibit the transcription of *Bmal1*⁶⁷⁻⁷⁰, *Npas2*⁷¹, *Clock*⁷² and *Cry1*⁷³, respectively.

C. Post-transcriptional modifications

Once they are transcribed, mRNA can undergo several regulatory processes to adapt to the needs of protein with respect to time-related functions. It has been suggested in *Drosophila melanogaster* that *Per* mRNA stability could be regulated in a circadian manner as its half-life changes around the clock⁷⁴. Several studies on mice demonstrated that *Per1*, *Per2*, *Per3* and *Cry1* mRNAs are more stable during their rising phase⁷⁴⁻⁷⁶. One aspect of this phenomenon was described in a study where the authors showed the presence of an element involved in the repression of its own expression in the 3'UTR of *Per1*⁷⁷. The interaction of LARK1 (RBM4a), an RBP (RNA Binding Protein) acting as trans-factor and rhythmically expressed in the SCN, together with the 3'UTR of *Per1* has been shown to be involved in the activation of *Per1* mRNA expression⁷⁸. Other RBPs have also been showed to be involved in the regulation of the core oscillator at the post transcriptional level: the hnRBP (heterogenous nuclear RBP) I, D and Q. These particular hnRBP have been shown to interact with some clock gene mRNA to promote instability. For example, hnRBP I promotes the degradation of *Per2* mRNA when it interacts with *Per2* 3'UTR⁷⁵. The same phenomenon occurs with the interaction of hnRBP D and *Cry1* 3'UTR⁷⁶.

The stability of the mRNA can be conferred by the 3' polyA tail stability. It has been shown, first in *Xenopus*⁷⁹ and then in mice⁸⁰, that one deadenylase named 'NOCTURNIN' promotes the destabilization of the mRNA in a rhythmic manner by removing the 3' adenosine residues

from the transcripts⁸¹. Moreover it was recently shown that polyA tail length dynamic present a rhythmic pattern, leading to rhythmic protein expression⁸².

The alternative splicing is an important level of post-transcriptional regulation of gene expression. It has mainly been demonstrated to be involved in the regulation of the core clock in *Drosophila melanogaster*, induced by cold temperature and producing two different isoforms of *Per*⁸³. The same phenomenon has been described in *Neurospora Crassa* for the alternative splicing of *frq*⁸⁴. Recently, evidences demonstrated in mice the circadian control of alternative splicing depending on tissue and that feeding/fasting cycles constitutes an important zeitgeber in the regulation of alternative splicing⁸⁵. In addition, a recent study on mouse brain and liver showed evidence of a light-inducible alternative splicing of *U2AF26* involved in the regulation of *Per1*⁸⁶.

More recently, some evidence has shown that miRNA (microRNA), post-transcriptional regulators, play a role in the regulation of circadian rhythms. For example, the two brain-specific miRNAs miR-219 and miR-132 have been described to be a CLOCK:BMAL heterodimer target and a modulator of clock genes expression in mice SCN⁸⁷, respectively. In mice liver, miR-122⁸⁸ has been shown to be regulated by REV-ERB α , and involved in the regulation of clock gene output. In addition, it has been reported that the free-running period in *Dicer*-deficient MEF (Mouse Embryonic Fibroblasts) was shorter due to lack of three miRNAs (miR-24, miR-29a, miR-30a) involved in PER1 and PER2 translation regulation⁸⁹. Recently, a study on *Dicer* knockout mice showed only a low impact on the liver core clock as the free-running period was delayed by only 40 minutes. But miRNAs have an impact on general rhythmic gene expression⁹⁰.

D. Post-translational modifications

Post-translational modifications on the core clock proteins play a very important role in providing 24 hour-oscillation. These post-translational modifications vary in their nature as the list includes phosphorylations, ubiquitinations, sumoylations, and acetylations.

(1) Phosphorylations and dephosphorylations

CK (Casein Kinase) 1 phosphorylates PER2 on the serine 659 leading to its nuclear retention and stabilization⁹¹, while other phosphorylations on PER proteins have been shown to be involved in their degradation by the proteasome^{92, 93}. CK1 also phosphorylates BMAL1, increasing its transcriptional activity⁹⁴. Another kinase, GSK (Glycogen Synthetase Kinase) 3 β , acts on PERs and CRY2 proteins to favor their nuclear localization^{95, 96}. This kinase is also known to stabilize REV-ERB α . As a consequence, it strengthens *Bmal1* transcriptional repression⁹⁷. AMPK (Adenoside MonoPhosphate-activated protein Kinase) has been shown to phosphorylate CRY1 leading to its instability⁹⁸. In addition, phosphatases are also involved in molecular circadian clock regulation. Indeed, Phosphatase Protein 1 (PP1) acts directly on PER2 leading to the increase of its stability⁹⁹, while PP5 regulates the inhibitory self-phosphorylation of CK1 such that it is indirectly involved in the phosphorylation state of PER2¹⁰⁰.

(2) Ubiquitinations

As mentioned above, some post-translational modifications are linked to degradation by the proteasome. This mechanism requires poly-ubiquitinations on lysine residues of the proteins to be addressed to proteasome¹⁰¹. SFC, a complex composed of several proteins, is involved in the recognition and ubiquitination of phosphorylated proteins to be degraded by the proteasome. PER and CRY proteins undergo degradation to prevent the inhibition of BMAL:CLOCK transcription activity. FBXL (F-Box and Leucine-rich repeat protein) 3, a component of SFC ubiquitin ligase complex, have been shown to be involved in AMPK- and GSK3 β -phosphorylated CRY proteins degradation¹⁰². Two groups of researchers described mutations in *Fbxl3* gene, *Overtime*¹⁰³ and *After-Hours*¹⁰⁴, leading to very long free-running period in constant darkness. In a recent study, FBXL21 has also been shown to be involved in CRY ubiquitination¹⁰⁵. *Fbxl21* knockout mice exhibit a normal running-wheel activity while the free running period of *Fbxl3* knockout mice is extremely long in constant darkness. In addition, mice deleted for both *Fbxl* genes exhibit arrhythmia after few days of constant darkness conditions reflecting their impact on circadian clock. Actually, FBXL21 stabilizes CRYs in the cytoplasm while FBXL3 ubiquitination on CRYs in the nucleus leads to their destabilization. In the same way, CK1-phosphorylated PER proteins undergo degradation *via* polyubiquitination by β TrCP (β Transducing repeat-Containing Protein) 1 and 2^{92, 93}.

(3) Sumoylations

Few examples of sumoylation have been reported, but recent evidence shows that sumoylation is involved in the robustness of circadian rhythms. Indeed, sumoylation in BMAL1 occurs on lysine 259 and is induced by CLOCK¹⁰⁶. This post-translational

modification is required for clock oscillation, as sumoylation of BMAL1 in the nuclear bodies leads to its transactivation and its proteasomal degradation¹⁰⁷.

(4) Chromatin remodeling

Epigenetic factors also influence the circadian clock by modulating gene transcription *via* chromatin remodeling factors. Indeed the regulation of the core clock mechanism in mice liver is accompanied by rhythms in H3 histone acetylation on *Per1*, *Per2* and *Cry1* promoters¹⁰⁸. Moreover, CLOCK proteins have been described as Histone AcetylTransferase (HAT) enzymes¹⁰⁹. This HAT activity is enhanced by the heterodimerisation with BMAL1. More precisely, CLOCK acetylates BMAL1 leading to a facilitated interaction of BMAL1 with CRY proteins. This leads finally to an increase of the negative feedback by CRY proteins¹¹⁰. In addition, some circadian clock repressors are associated with Histone DeAcetylase (HDAC). For example, HDAC can bind *Per1* promoter¹¹¹, and REV-ERB α can associate with HDAC3 on *Bmal1* promoter¹¹².

The methylation state of circadian gene promoters has also been reported to play an important role in their expression regulation. Indeed, rhythmic methylation events of E-boxes present in the circadian genes correlate with the cyclic binding of CLOCK:BMAL1¹¹³. WDR5, a subunit of histone methyl transferase complexes, has been identified as increasing PER-mediated repression¹¹⁴. In addition, it has been shown that JARID (JumonjiC and ARID domain-containing histone lysine demethylase) 1a can associate with CLOCK:BMAL1 and bind *Per2* promoter. It then results in an increased transcription by CLOCK:BMAL1¹¹⁵.

More recently, SIRT (SIRTuins), and more particularly SIRT1^{116, 117} and SIRT6¹¹⁸, have been reported to play a role in the control of circadian clock gene thanks to their function of

histone deacetylase. SIRT6, NAD⁺ (Nicotinamide Adenine Dinucleotide) -dependent enzymes in which deacetylase activity is circadian, bind the BMAL1:CLOCK activator complex and contribute to the regulation of PER2 stability¹¹⁶. SIRT proteins are involved in metabolism, and they thus provide a real link between the circadian clock and the coordination of the metabolism by the circadian rhythms. Indeed, NAMPT (NicotinAMide Phosphorybosyl Transferase), a rate-limiting enzyme involved in NAD⁺ biosynthesis, as consequence of metabolic processes through SIRT1, has been reported to influence *Per2* expression, as its inhibition promotes BMAL1:CLOCK released from suppression by SIRT1. In turn, *Nampt* mRNA expression is upregulated by CLOCK¹¹⁹. More recently, Masri *et al.* reported SIRT6 as being involved in the coordination of SREBP1-dependent circadian transcription¹¹⁸.

IV. The translational mechanisms in mammals

In eukaryote organisms, about 30% of the mass of cellular proteins produced is subject to translational control¹²⁰. Thus, protein synthesis is accurately regulated at the post-transcriptional level. Indeed, mRNAs harbor cis-acting elements involved in the recruitment of trans-acting factors and the subsequent attachment of ribosomes that can scan and translate the mRNA into protein. Essentially, translation is a four step initiation, elongation, termination and recycling of ribosomes for a new translation initiation.

A. Pre-initiation of the translation

(1) Formation of pre-initiation translation complex

Translation initiation constitutes the limiting step of protein synthesis. During this step, the small ribosome subunit is recruited to the 5'-end of mRNA and scans towards the start codon, where the complete ribosome is subsequently assembled, and then the polypeptide can begin¹²¹. The eIF (eukaryotic translation Initiation Factor) 4F complex, composed of eIF4E, eIF4G and eIF4A, is assembled on the 5'-cap structure of mRNA. This leads to the recruitment of the small ribosomal subunit to mRNA. To assemble the eIF4F complex, eIF4E binds to the 5'-cap and recruits eIF4G and eIF4A. 4E-binding protein 1 (4E-BP1; also known as eIF4EBP1) inhibits eIF4G binding to eIF4E. mTORC1-mediated phosphorylation of 4E-BP1 leads to its release from eIF4E, allowing the recruitment of eIF4G and eIF4A¹²².

(2) Regulation of TORC1 signaling pathway

Target Of Rapamycin (TOR) was first identified in 1991¹²³ in yeast. TOR can associate with different partners to compose two different TOR Complexes, TORC1 and TORC2. TORC1, identified as a central sensor in the nutriment detection¹²⁴, is involved in the regulation of cell growth and size by promoting protein synthesis^{125, 126}. TORC1 is regulated by extracellular signals^{124, 126} (figure 5). Indeed, amino-acid, especially Branched Chain Amino Acids (BCAA), availability is an important signal as they positively and directly regulate TORC1 signaling¹²⁷⁻¹²⁹. It has also been shown that hormones or growth factors are involved in TORC1 activation. Indeed, the binding of insulin or insulin-like growth factors to the receptors leads to TORC1 activation *via* the PhosphoInositide 3 Kinase (PI3K) – AKT

pathway. Tuberous Sclerosis Complex (TSC) 1/2, whose activity inhibits TORC1 activity, is inhibited by phosphorylation by AKT¹³⁰. More precisely, TSC1/2 has a GTPase-Activating Protein (GAP) activity with respect to the small GTPases Rheb¹³¹. This activity occurs by stimulating the hydrolysis of GTP-bound Rheb leading to TORC1 inhibition¹³². TORC1 also responds to cellular energy variations. A low cellular energy activates AMPK pathway. In these conditions, AMPK directly phosphorylates TSC2¹³³ and one component of TORC1, Raptor¹³⁴, leading to TORC1 inhibition. Finally, Extracellular signal-Regulated protein Kinase (ERK)¹³⁵ and Mitogen-Activated Protein Kinase (MAPK)-interacting Kinase (MNK) RSK1¹³⁶ pathways are involved in TORC1 regulation as, when activated by stress, they are able to phosphorylate TSC2, leading to TORC1 activation.

(3) Translation initiation regulated by TORC1

mRNAs belonging to the 5' Terminal OligoPyrimidine (5'TOP) mRNA family are characterized by an identifiable pyrimidine-rich motif in the 5' terminal sequence¹³⁷. This motif corresponds to the core of the translational *cis*-regulatory element. Most of the products of these mRNAs are components of the translation machinery, and their expression responds to growth and nutritional stimuli¹³⁷. Indeed, TORC1 regulates the protein synthesis from 5'TOP mRNAs and more particularly the translation initiation complex formation *via* Ribosomal Protein S6 Kinase (RPS6K) and EIF4E-Binding Protein (4E-BP) phosphorylations¹²⁶. In its inactive state, this translation initiation complex is composed of the mRNA cap-binding protein EIF4E bound to the hypophosphorylated form of 4E-BP that acts as a translational repressor. After TORC1 phosphorylation of 4E-BP¹²², it releases EIF4E, which can then interact with the scaffold protein eIF4G and the rest of the EIF4F complex (EIF4A, EIF4B, and EIF4H) to initiate the translation¹³⁸. In parallel, TORC1 phosphorylates

RPS6K, which then phosphorylates other substrates involved in EIF4F complex formation. Indeed, this leads to the phosphorylation of EIF4B, inducing its own recruitment to EIF4A¹³⁹.

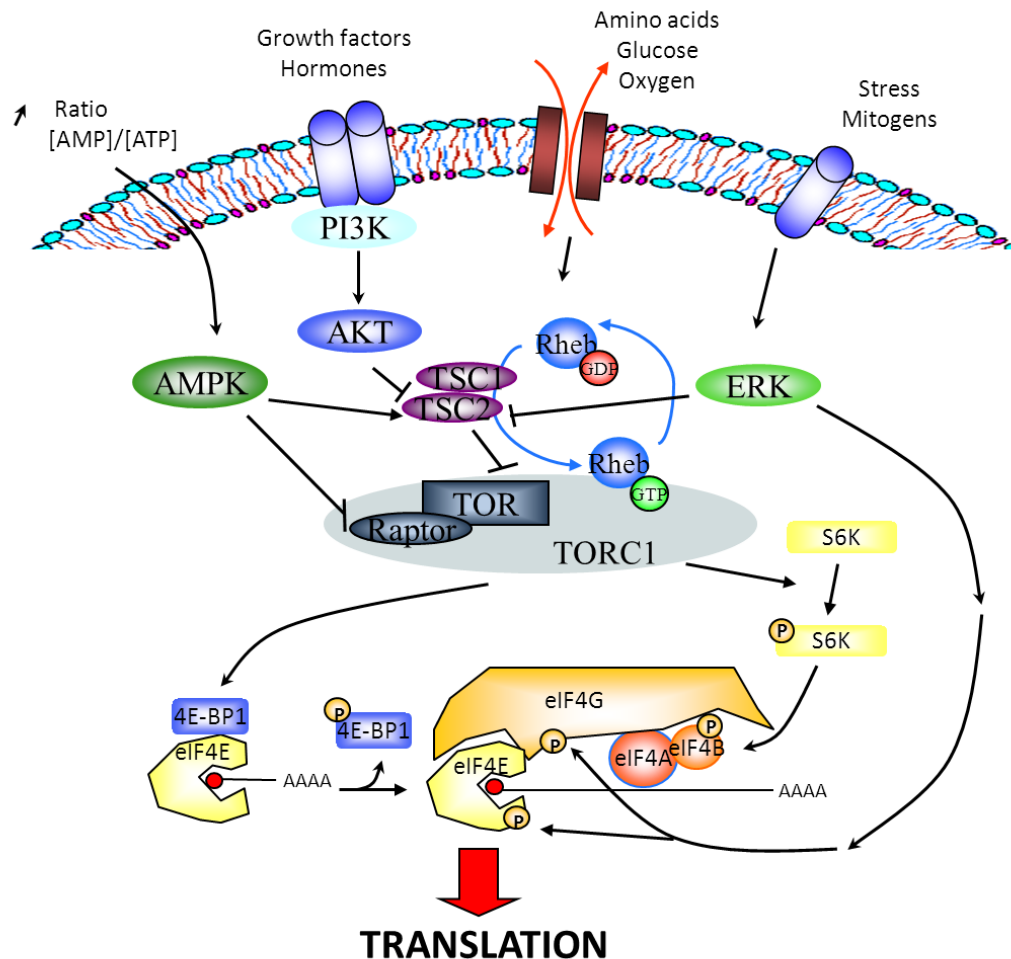


Figure 5: The translation initiation mediated by TORC1 is modulated by metabolism linked signaling pathways.

Activated AKT and REK pathways lead to the activation of mTORC1, which phosphorylates its targets 4E-BP1 and RPS6K, thus allowing the formation of the pre-initiation complex of the translation. In contrast, the activated AMPK signaling pathway represses this formation through its mTORC1 inhibition.

B. The different steps of translation initiation

mRNA scanning and the corresponding polypeptide synthesis is performed by 80S ribosome, which contains a P-site where the initiation codon is base-paired with the anticodon loop of the initiator tRNA (Met- tRNA_i^{Met})¹⁴⁰. Its recruitment requires several steps (figure 6) once activated translation pre-initiation eIF4F complex binds 5' end mRNA.

(1) Formation of 43S pre-initiation complex.

Translation is a cyclical process. Ribosomes undergo recycling at the end of translation process. Indeed, the action of different factors (eIF1, eIF1A and eIF3) leads to the dissociation of the different subunit composing 80S ribosome (60S and 40S subunits) and the release of eRF (eukaryotic Releasing Factor) 1 and 3, mRNA and tRNA. During this recycling step, the 40S subunit is associated to eIF3, eIF1 and eIF1A preventing the 60S subunit from associating again. Thus, eIF3, eIF1 and eIF1A are recruited to 40S subunits during recycling and interact with eIF2-GTP-Met- tRNA_i^{Met} to form 43S complexes. The position of eIF2-GTP-Met- tRNA_i^{Met} on 40S subunits has not been determined. However, in 43S complexes, the Met- tRNA_i^{Met} anticodon loop is probably not inserted as deeply into the P-site as in ribosomal complexes with established codon-anticodon base pairing, and its acceptor end, to which Met is linked, might be rotated towards the E-site¹⁴¹⁻¹⁴³.

(2) Attachment of 43S complex to mRNA.

It has been shown that 43S complexes are intrinsically capable of 5' end-dependent attachment to model mRNAs with completely unstructured 5' UTRs¹⁴⁴.

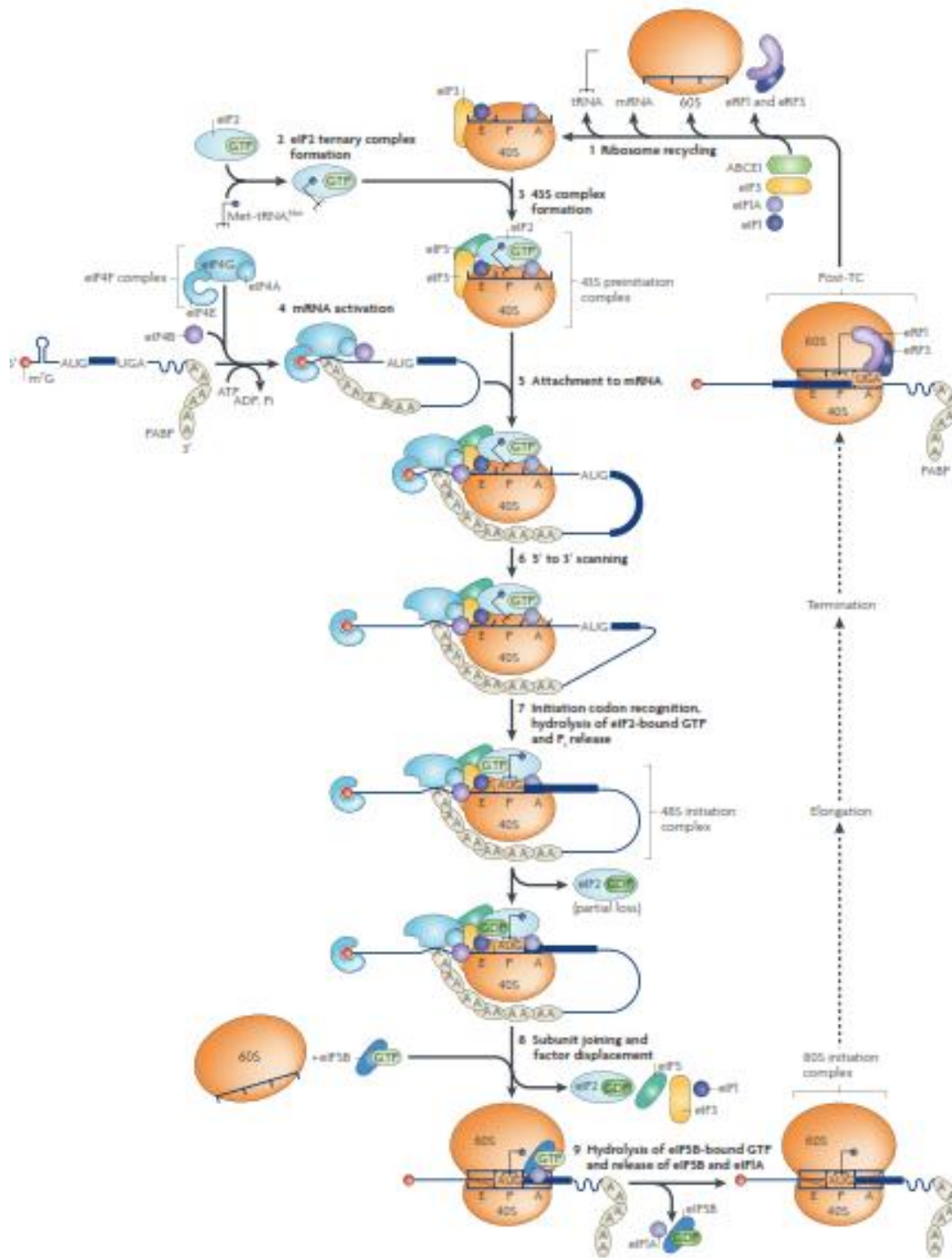


Figure 6: Molecular mechanisms of eukaryotic translation initiation

Translation initiation is constituted of several stages: recycling of ribosomal subunits, formation of 43S pre-initiation complex, attachment of 43S complexes to mRNA, ribosome scanning of mRNA 5' UTRs, initiation of codon recognition, commitment of ribosomes to a start codon, ribosomal subunits joining¹³⁸.

However, natural 5' UTRs possess a sufficiently secondary structure for the loading of 43S complexes onto them to require the cooperative action of eIF4F and eIF4B or eIF4H, which unwind the 5' cap-proximal region of mRNA to prepare it for ribosomal attachment. The recruitment of the 43S complex is achieved by the interaction of cap-eIF4E-eIF4G with eIF3-40S¹⁴⁵.

(3) Ribosome scanning of mRNA 5' UTRs.

After attachment on capped mRNA, the 43S complex scans mRNA downstream of the cap to the initiation codon. Scanning consists of two linked processes: unwinding of secondary structures in the 5' UTR and ribosomal movement along it. 43S complexes can scan unstructured 5' UTRs without factors associated with RNA unwinding and are thus capable of movement along mRNA¹⁴⁴. This movement of 43S complexes requires the scanning-competent conformation induced by eIF1 and eIF1A¹⁴⁶.

Concerning scanning directionality, it has been shown that initiation frequency at the 5' proximal AUG is reduced by the presence of a nearby downstream AUG¹⁴⁷. This suggests that scanning may consist of forward (5' to 3') thrusts alternating with limited relaxation over distances of a few nucleotides in the reverse direction.

(4) Initiation of codon recognition.

To ensure the fidelity of initiation, scanning complexes must have a mechanism that prevents partial base pairing of triplets in the 5' UTR with the Met- tRNA_i^{Met} anticodon and promotes

recognition of the correct initiation codon: usually the first AUG triplet in an optimum 'Kozak' context (GCC(A/G)CCAUGG)^{148, 149}. This role in maintaining the fidelity of initiation is done by eIF1. Indeed, this factor enables 43S complex to discriminate against non-AUG triplets or AUG triplets in non-favorable. In addition, it is involved in cooperation with eIF1A in the dissociation of the ribosomal complexes that aberrantly assemble with such triplets^{144, 149, 150}.

(5) Commitment of ribosomes to a start codon.

Initiation codon recognition is followed by a step during which the arrested ribosome becomes committed to initiation. The commitment step is mediated by eIF5, an eIF2-specific GTPase-activating protein (GAP)¹⁴⁰. The molecular mechanism remains unclear, but two hypothesis have been suggested. The first hypothesis proposes a binding of eIF5 to eIF2's β -subunit but induces the GTPase activity of eIF2's γ -subunit only in eIF2-GTP-Met-tRNA^{Met} complexes that are bound to 40S subunits¹⁵¹. The second hypothesis suggests that eIF5 derepresses eIF2 γ 's GTPase activity¹⁵².

(6) Ribosomal subunit joining.

The joining of 60S subunits and dissociation of eIF1, eIF1A, eIF3 and residual eIF2-GDP are mediated by eIF5B^{153, 154}. Moreover, hydrolysis of eIF5B-bound GTP is required for eIF5B release from assembled 80S ribosomes¹⁴⁰. Interaction of eIF5B with eIF1A^{155, 156} is required for efficient subunit joining and GTP hydrolysis by eIF5B.

Although those eIFs that bind to the interface of the 40S subunit must be released before or at subunit joining, dissociation of eIF3 and eIF4G may be delayed to allow reinitiation following short upstream ORFs¹⁵⁷.

C. Translation elongation

After translation initiation, 80S ribosome is poised on an mRNA with the anticodon of Met-tRNA_i in the P-site base-paired with the start codon. The second codon of the ORF is present in the A-site (Acceptor-site) of the ribosome awaiting binding of the cognate aminoacyl-tRNA. The eEF (eukaryotic Elongation Factor) 1A binds aminoacyl-tRNA in a GTP-dependent manner and then directs the tRNA to the A-site of the ribosome^{158, 159}. Codon recognition by the tRNA triggers GTP hydrolysis by eEF1A, releasing the factor and enabling the aminoacyl-tRNA to be accommodated into the A-site¹⁶⁰. Next, peptide bond formation with the P-site peptidyl-tRNA occurs rapidly with the help of the peptidyl transferase center¹⁶¹. Then the ribosomal subunits triggers movement of the tRNAs with the acceptor ends of the tRNAs in the E- and P-sites and the anticodon loops remaining in the P- and A-sites.

This translocation of the tRNAs to the canonical E- and P-sites requires eEF2¹⁶², whose regulation involves the mTOR pathway through S6K phosphorylation¹⁶³.

D. Termination of the translation

It occurs when the end of the coding sequence is reached by the ribosome and a stop codon (UAA, UGA or UAG) enters the A-site. In eukaryotes, it is catalyzed by two protein factors,

eRF1 and eRF3. eRF1 is responsible for high fidelity stop codon recognition and peptidyl-tRNA hydrolysis, while eRF3 is involved in acceleration of peptide release and termination efficiency at stop codons^{164, 165}. In the post-translocation state of the ribosome, a deacylated tRNA occupies the E-site and the peptidyl-tRNA is in the P-site. The A-site is vacant and available for binding of the next aminoacyl-tRNA in complex with eEF1A¹⁶⁶.

E. Ribosome biogenesis

Deep investigations of ribosome biogenesis have been performed on the yeast *Saccharomyces Cerevisiae*. However, mammalian ribosome biogenesis remains unclear, and the following descriptions refer to described mechanisms in yeast.

In eukaryotes, each ribosome is composed of a small 40S and large 60S subunit. Each subunit itself contains different molecules: ribosomal RNA (rRNA) and ribosomal proteins (40S [18S rRNA, 33 RPs]; 60S [25S, 5.8S, 5S rRNA, 46 RPs]). Ribosome biogenesis requires the activity of all three RNA polymerases (figure 7): RNA polymerase II transcribes the pre-mRNAs of ribosomal proteins and accessory factors involved in ribosome biogenesis¹⁶⁷, RNA polymerase III produces the precursor to 5S rRNA¹⁶⁸, and RNA polymerase I, in part through UBF (Upstream Binding Factor) 1 activation¹⁶⁹, is involved in the transcription of the common precursor to mature 5.8S, 18S and 25S rRNAs¹⁷⁰. Interestingly, mTOR has been shown to regulate all three RNA polymerases².

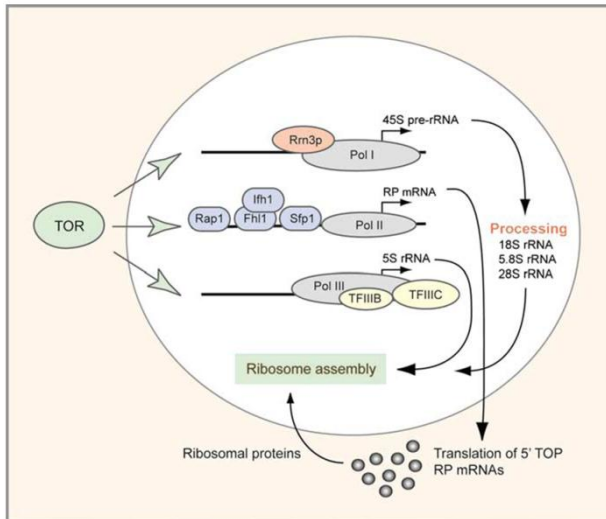


Figure 7: Influence of mTOR in ribosome biogenesis

mTOR regulates the three RNA polymerase I, II and III involved in ribosome component transcription², the pre-rRNA, ribosomal proteins mRNA and 5S rRNA respectively.

In yeast, the biogenesis of both subunits starts with the transcription of the common precursor, the 35S pre-rRNA, by RNA polymerase I (Fig. 8). A large number of non-ribosomal factors and snoRNAs modify nascent rRNA^{171, 172}, leading to pseudouridines formation. Upon cleavage, which can occur co-transcriptionally, the early 40S pre-ribosome (figure 8, left side) is separated from the remaining pre-rRNA, which assembles with large subunit ribosomal proteins and non-ribosomal factors to form the earliest pre-60S ribosomal particles (figure 8, right side)¹⁷².

(1) 40S subunit assembly

The assembly of the first 40S precursor, the 90S particle, occurs co-transcriptionally and starts with the incorporation of UTP-A, UTP-B, and UTP-C¹⁷³. Following cleavage at the U3 snoRNP-dependent sites A0, A1, and A2, which yield the 20S pre-rRNA, the composition of the pre-40S particle changes dramatically. Indeed, most non-ribosomal factors dissociate and a small set of novel biogenesis factors and further Rps proteins are recruited¹⁷⁴. This pre-40S

subunit is rapidly transported out of the nucleolus into the cytoplasm where the cleavage of the 20S pre-rRNA at site D occurs, yielding the mature 18S rRNA ^{175, 176}.

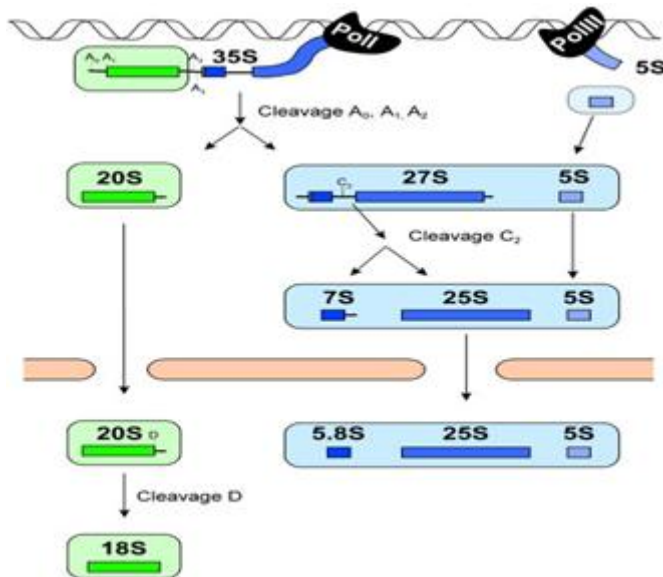


Figure 8: Representation of the major steps in pre-rRNA processing involved in the ribosome subunit formation.

After its transcription, the common pre-rRNA undergo specific sequential cleavages. This maturation leads to the generation of rRNAs constituting the small (green) and the large (blue) subunits of the ribosome ¹.

(2) 60S subunit assembly

Ssf1, the earliest distinct pre-60S particle, contains a mixture of 27SA and 27SB pre-rRNA, ribosomal proteins, and about 30 non-ribosomal proteins, including early diagnostic factors like Noc1 and Rrp5 ^{177, 178}. The next distinct intermediate is defined by the nucleolar Nsa1 particle ¹⁷⁸, since this particle almost exclusively contains the 27SB rRNA part of the 5S subunit. The transition from the nucleolus (Nsa1 particle) to the nucleoplasm (Rix1 particle) is accompanied by major compositional changes of partners ¹⁷⁸. At this step, the 27SB pre-rRNA has been processed almost completely into 25S and 7S/5.8S rRNAs ¹⁷⁹, and its partners prime the pre-60S particle for nuclear export ¹⁸⁰. The final 5.8S processing occurs in the

cytoplasm¹⁸¹, and the release of processing factors allows 60S subunits to be associated with 40S ribosomal subunits¹⁸².

(3) Nuclear export

The nuclear export of both subunits depends on the general export factor Xpo1/Crm1, the regulatory GTPase Ran^{183, 184} and NES (nuclear export sequence) adaptors. Indeed, for the pre-60S subunits, Xpo1 binds to an NES of Nmd3 which interacts with the ribosomal subunits¹⁸⁵. The heterodimer Mex67-Mtr2 also mediates the export of the pre-60S subunits, since it binds 5S rRNA and Mex67, and Mtr2 mutants show impaired pre-60S export¹⁸⁶. Finally, Arx1 also facilitates pre-60 subunit's translocation through its interaction with nucleoporins¹⁸⁷.

The export mechanism of the small subunit is still unclear. Despite the role of Xpo1 in the export of pre-40S ribosomes, no NES-adaptor has been identified to date. However, depletion of a few ribosomal proteins, namely, Rps15, Rps10, Rps26, Rps2, Rps0, and Rps3, were found to cause strong export defects¹⁸⁸, suggesting a direct or indirect involvement in pre-40S export.

V. Energy balance

Organisms must adapt to the fluctuation of nutrient availability. In mammals, surplus of nutrients are mainly stored in adipose tissue as triglyceride. Carbohydrate ingestion stimulates, in the liver, conversion of carbohydrate into triglyceride. Then, triglycerides are mobilized from the liver to adipose tissue for long-term storage. High glucose levels in the circulation after a high-carbohydrate meal leads to the activation of hepatic lipogenesis through various mechanisms. Glucose and lipid metabolisms are thus interconnected, and their fine regulation requires the action of the pancreatic hormones glucagon and insulin. Essentially, glucose activates insulin secretion from pancreatic β -cells leading to the stimulation of glucose uptake and its utilization, and promotion of the synthesis of glycogen and lipogenesis in the liver. In addition, insulin inhibits hepatic glucose production, fat oxidation and ketogenesis, thus shifting the balance to fat storage. Finally, glucose constitutes an important signaling molecule in the regulation of genes encoding for enzymes involved in glycolysis and lipogenesis¹⁸⁹.

Glucose, insulin and glucagon are involved in lipogenesis and glycolysis through the regulation of transcription factors. SREBP (Sterol Regulatory Element Binding Protein) 1c, in the liver, is one important transcriptional regulator of fatty acid and triglyceride synthesis in response to insulin¹⁹⁰⁻¹⁹². Indeed, SREBP1c expression is low in fasted animals, but increases greatly upon feeding, under insulin mediation^{193, 194}. In addition, evidence shows that insulin activates SREBP1c at the post-translational level^{195, 196} leading to the expression of enzymes playing a role in fatty acid and triglyceride synthesis as ATP-citrate lyase (ACL), acetyl-CoA synthetase (ACS), acetyl-CoA carboxylase (ACC), fatty acid synthase (FAS), stearoyl-CoA desaturase-1 (SCD1), and glycerol-3-phosphate acyltransferase (GPAT). In contrast to insulin

stimulation, glucagon inhibits the transcription of SREBP-1c mRNA through the cyclic adenosine 3',5'-monophosphate/protein kinase A signaling pathway^{197, 198}.

A. SREBP signaling pathway

(1) Activation of SREBPs

SREBPs are proteins belonging to the basic helix-loop-helix leucine zipper family of transcription factors. In mammals, three isoforms, SREBP1a, SREBP1c and SREBP2, have been described depending on their tissue localization and their regulatory functions in lipid metabolism. In liver, SREBP1c is especially involved in fatty acids and triglycerides metabolism, whereas SREBP2 plays an important role in the regulation of *de novo* cholesterol biosynthesis as, among other regulating events, it participates in the regulation of the transcription of *Hmgcr* (*3-Hydroxy-3-MethylGlutaryl-CoA Reductase*)¹⁹⁹, which encodes for a rate-limiting enzyme of the cholesterol biosynthesis.

As shown in the figure 9, SREBPs are basically membrane-bound proteins localized in the endoplasmic reticulum. In the presence of sterols or oxysterols, SREBPs remain in the endoplasmic reticulum with the SCAP (SREBP Cleavage-Activating Protein) and INSIG (INSulin Induced Gene) proteins, with this situation corresponding to SREBPs inactive state^{200, 201}. However, in the absence of sterols or oxysterols, SREBPs migrate to the Golgi apparatus to undergo some proteolysis cleavages by Site-1 and Site-2 Proteases (S-1P and S-2P)^{202, 203}, leading to the release of the N-terminal part of SREBPs²⁰⁴, which can play their role of transcription factors in the nucleus on their respective target genes, of which *Fasn* (*Fatty Acid Synthase*) for SREBP1c²⁰⁵ and *Hmgcr* for SREBP2 are two representative examples.

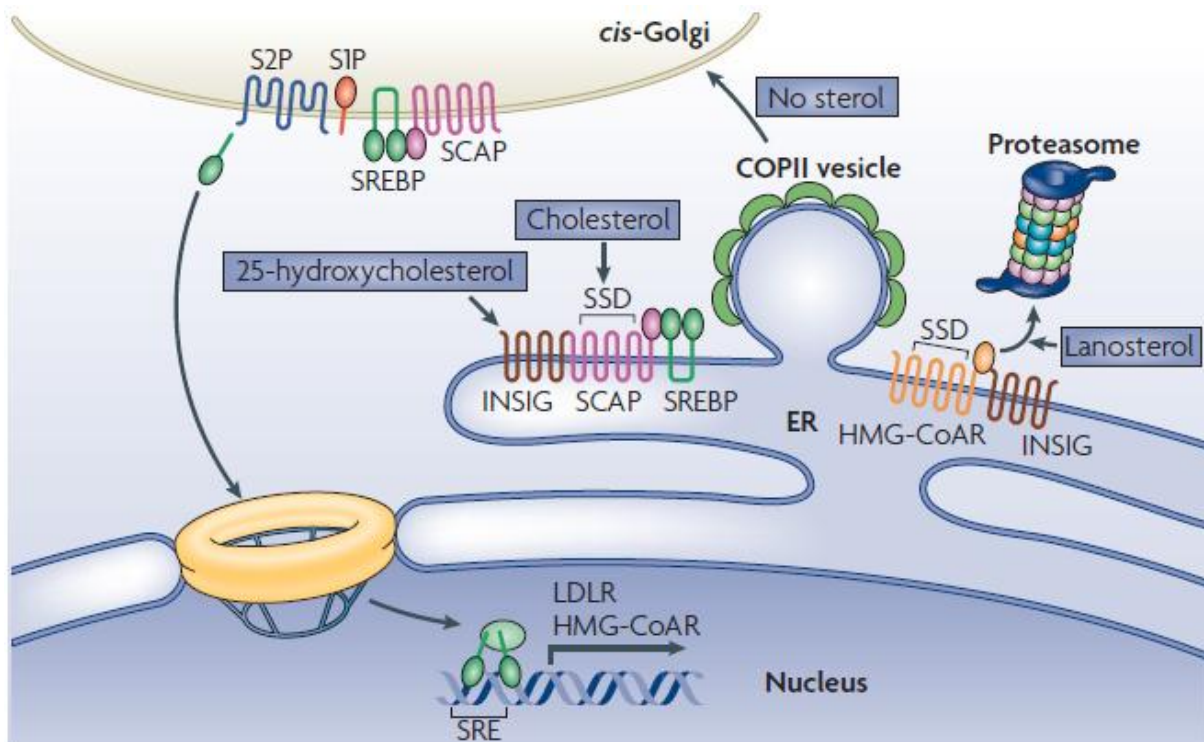


Figure 9: Activation of SREBP as transcription factors

In its inactive state, SREBP remains associated at the membrane of the endoplasmic reticulum. Activation of SREBP, in sterol deprivation conditions, leads to migration to Golgi apparatus where it undergoes several proteolytic processes, thus releasing SREBP transcriptional part²⁰⁶.

(2) Transcriptional regulation of SREBP1c in liver

Insulin interaction with its receptor at the cell surface induces the phosphorylation of IRS (Insulin-Receptor Substrates protein). This initiates a signaling cascade (figure 10) leading to the transcriptional suppression of gluconeogenesis and the activation of lipogenesis^{207, 208}. Tyrosine phosphorylation of IRS by the insulin receptor recruits PI3K, which then phosphorylates phosphatidylinositol (4,5) bisphosphate (PtdIns(4,5)P2) to produce Ptd(3,4,5)P3 (PIP3). PIP3 acts as second messenger and recruits AKT to the plasma

membrane. AKT is then activated by PDK (3-Phosphoinositide-Dependent protein Kinase)1 phosphorylation. As a consequence, AKT activates mTORC1 signaling pathway. Recently, mTORC1 has been reported as an important regulator of SREBP-1c that activates both SREBP-1c transcription²⁰⁹⁻²¹¹ and proteolytic processing in response to insulin stimulation^{210, 212-214}. The inhibition of p70S6K (p70 ribosomal S6 Kinase), one of the major downstream targets of mTORC1, does not present any effect on insulin-induced SREBP1c mRNA expression²¹¹. However, it inhibits SREBP1c proteolytic processes²¹⁰, demonstrating SREBP1c regulation by mTORC1 through distinct mechanisms.

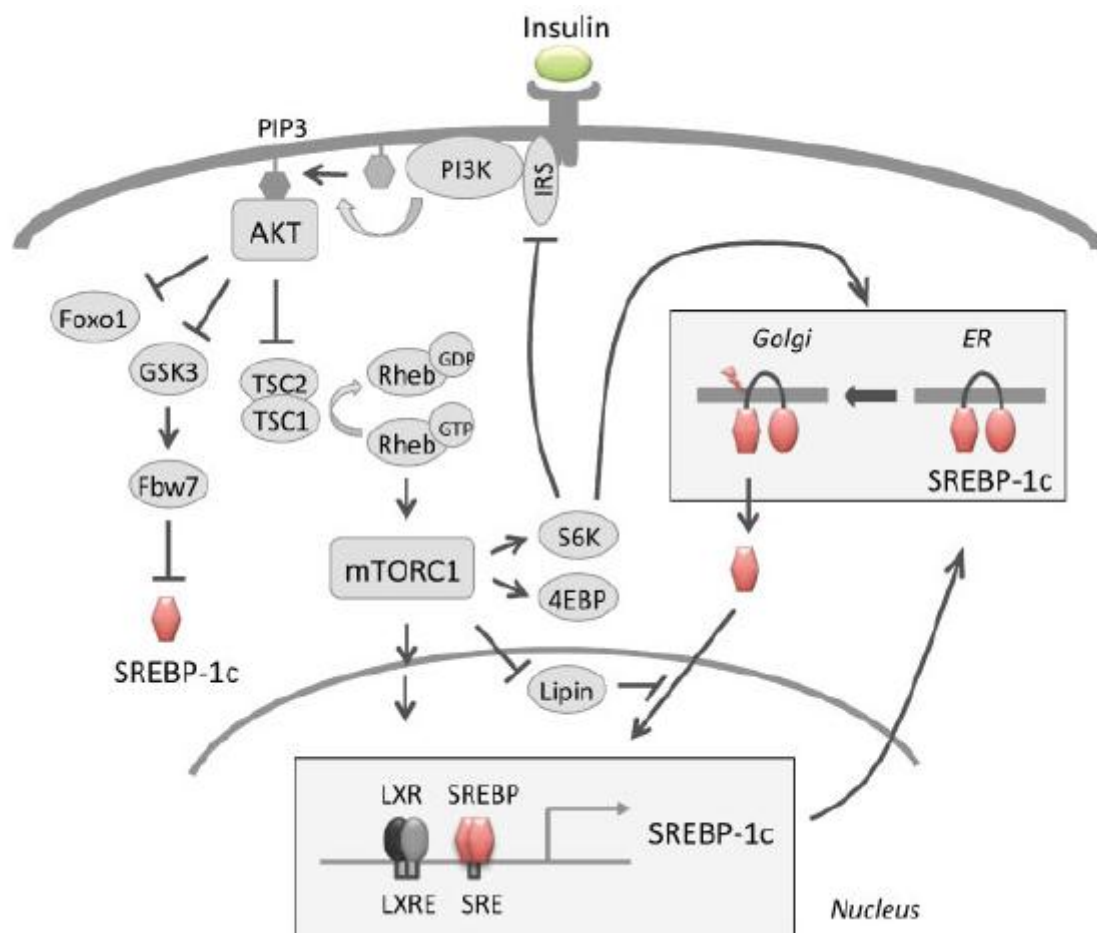


Figure 10: Regulation of SREBP by the insulin signaling pathway.

Insulin activates SREBP-1 through multiple mechanisms. Insulin stimulates SREBP-1c transcription, promotes proteolytic processing, facilitates the nuclear import of the processed protein, and suppresses the proteasomal degradation of SREBP-1²¹⁵.

B. LXR signaling pathway

LXRs belong to a nuclear receptor family of transcription factors. Both LXR isoforms, LXR α mainly expressed in the liver and LXR β , whose expression is ubiquitous^{216, 217}, play the role of transcription factor when activated by the heterodimerization with RXR nuclear receptor²¹⁷ and the binding of specific ligands belonging to the oxysterols family^{216, 217} as shown in figure 11.

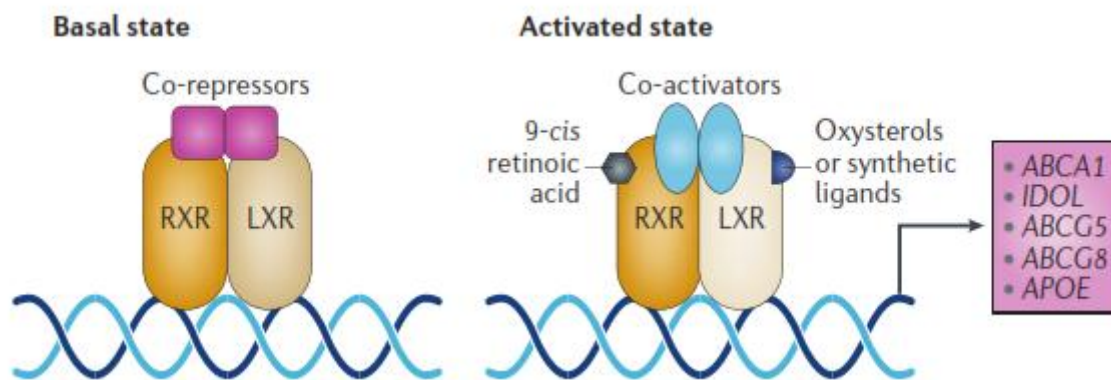


Figure 11: Activation of LXR transcription factor

LXR associated to RXR binds LXRE on target gene promoter. At the basal state, the heterodimer is bound by the repressor, preventing LXR from inducing transcription. In the presence of oxysterols and co-activators, the heterodimer is activated, leading it to play its role of transcription factor²¹⁸.

As transcription factor, the LXR-RXR heterodimers bind to a specific DNA sequence named 'LXRE' (Liver X Responsive Element)²¹⁹ present in the promoter of the LXR target genes as *Abcg5* or *Abcg8* (ATP-binding cassette subfamily g member 5 and 8). LXR target genes encode for proteins, especially transporters, involved in the regulation of a mechanism called reverse cholesterol transport²²⁰. This process allows the excess of cholesterol to return to the liver as HDL (High Density Lipoproteins) to be eliminated in the bile^{219, 221, 222}.

LXR transcription factors also play an important role in fatty acid and triglyceride synthesis. Indeed, LXR α is able to induce SREBP-1c expression *via* LXRE-bound transcription²²³⁻²²⁵. Thus, LXR α lipogenic activity is abrogated in SREBP-1c deficient mice¹⁹⁵, showing the role of LXR in lipogenesis through SREBP-1c. In addition, LXR α deficient mice exhibit reduced expression of SREBP1c in the liver and as a consequence, SREBP1c target genes encoding for lipogenic factors such as SCD1 and FAS also present a decreased expression^{217, 224, 226, 227}. In contrast, SREBP1c expression and lipogenesis increase under high-cholesterol diet^{217, 224, 226, 227}. Importantly, disruption of LXR-binding sites on the SREBP-1c promoter abolished the induction of promoter activity by insulin. This evidence suggests that SREBP-1c induction in response to insulin is dependent on LXR α ²²³. However, no other LXR target genes have been shown to be induced by insulin^{228, 229}. This process appears to be SREBP1c specific, and the mechanism of this LXR α -activated SREBP1c by insulin remains unknown.

C. ChREB signaling pathway

ChREBP (Carbohydrate Response Element Binding Protein) was first identified as a glucose responsive transcription factor involved in the regulation of glycolytic, gluconeogenic, and lipogenic gene expression^{230, 231}. ChREBP activates the transcription of genes encoding for important enzymes belonging to pathways such as L-PK (L-Pyruvate Kinase) for glycolysis, G6PC (Glucose 6 Phosphatase Catalytic subunit) for gluconeogenesis, FAS (Fatty Acid Synthase), ACC (Acetyl CoA Carboxylase) 1, and SCD (Stearyl CoA Desaturase) for lipogenesis²³⁰.

(1) Activation of ChREBP

ChREBP, a transcription factor belonging to the basic helix-loop-helix leucine zipper family²³⁰⁻²³² activated by glucose, is highly expressed in liver, pancreatic β -cells, brown and white adipose tissues, and muscle. ChREBP and MLX (Max-like protein X) form heterodimers^{233, 234} to activate transcription *via* the binding of ChoREs (Carbohydrate-Response Elements). These response elements are composed of two E-box sequences and have been identified in promoters of ChREBP target genes (figure 12).

Two isoforms of ChREBP, ChREBP α and ChREBP β , have recently been identified²³⁵. ChREBP α is mainly located in the cytosol while ChREBP β is located in the nucleus. Under glucose stimulation, ChREBP α isoform is translocated into the nucleus where it binds to ChoRE after its dephosphorylation by protein phosphatase 2A, which is regulated by X5P (Xylulose 5-Phosphate) in the pentose phosphate pathway²³⁶. Under starvation conditions, glucagon increases cAMP levels leading to ChREBP phosphorylation by PKA (cAMP-dependent Protein Kinase) and AMPK. It thus results in ChREBP inactivation²³⁷. In addition, ChREBP activation can be modulated *via* acetylation by HAT (Histone Acetyl-Transferase)²³⁸ and O-GlcNAcylation, which is a nutrition-dependent post-translational modification²³⁹⁻²⁴¹, thus promoting ChREBP transactivation.

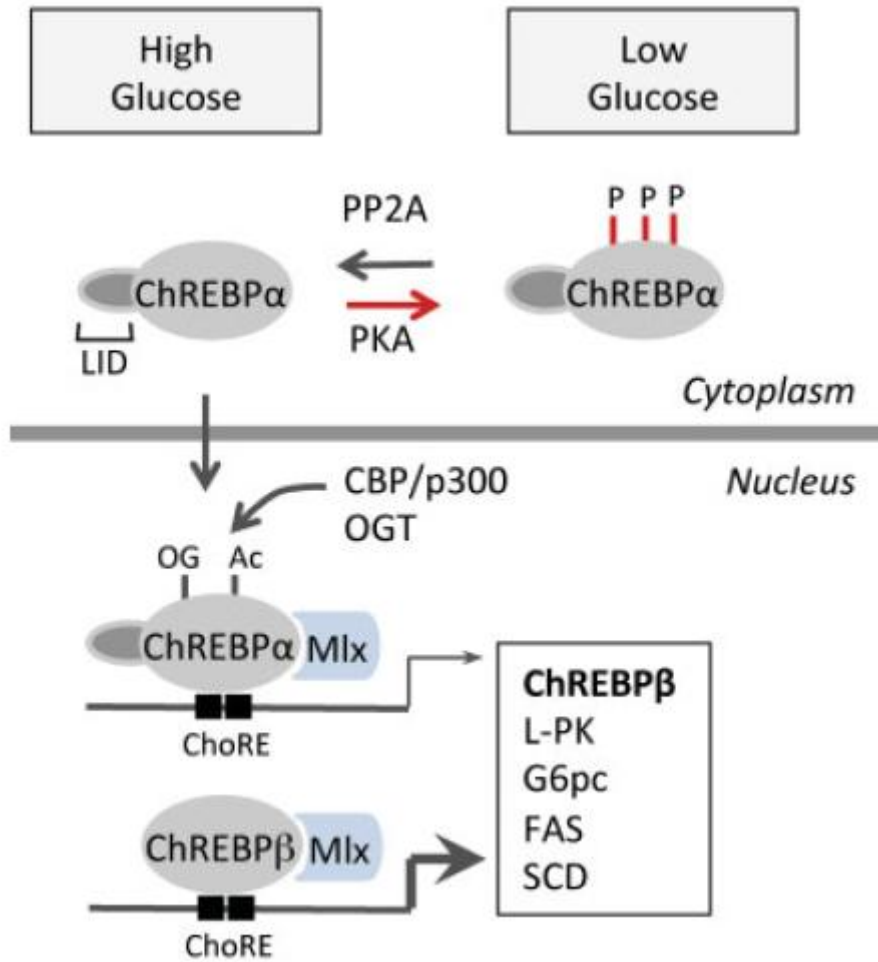


Figure 12: Regulation of ChREBP activity

The phosphorylation/dephosphorylation of ChREBP α by PKA/protein phosphatase 2A (PP2A) is involved in ChREBP α nuclear translocation and activation. Acetylation by coactivator CBP/P300 and O-GlcNAcylation by O-GlcNAc transferase (OGT) also contribute to ChREBP α transcriptional activities. ChREBP α forms a heterodimer with Max-like protein X (MLX) and binds to the carbohydrate-response elements (ChoREs) in the nucleus to induce its target genes involved in glycolytic and lipogenic pathways²¹⁵.

(2) Alternative transactivation of ChREBP in adipose tissue

An alternative transactivation of ChREBP has been proposed (figure 13). ChREBP contains a glucose-sensing module consisting of a low-glucose inhibitory domain (LID) and a glucose response activation conserved element (GRACE). Inhibition of the LID domain on GRACE,

leads ChREBP to remain in an unfavorable conformation for DNA binding and activation. This can be reversed by high glucose²⁴²⁻²⁴⁵. According to this model, deletion of the LID domain produced a constitutively active ChREBP even under low-glucose conditions²⁴⁴. The involvement of the glucose-sensing module and conformational modulation has been implicated in the regulation of ChREBP activity by glucose metabolites, such as glucose 6 phosphate (G6P)^{246, 247}. The mechanism of carbohydrate-mediated ChREBP activation may involve feed-forward regulation, because changes of ChREBP activity can also be reflected on ChREBP mRNA levels^{248, 249}. Recently, ChREBP was shown to be capable of self-regulation in adipose tissue²³⁵. ChREBP β is transcribed from an alternative promoter, differing from ChREBP α . ChREBP β protein, which does not contain LID or nucleus export signals, exhibits constitutively higher transactivation ability than ChREBP α ²⁴⁴. ChREBP β expression increases by cotransfection of ChREBP α and LMX in a glucose dose-dependent manner. The ChoREs are also identified in the promoter region of ChREBP β , and the deletion of these elements completely abolishes the responsiveness of the ChREBP β promoter to ChREBP α /MLX²³⁵. ChREBP α may thus be activated by high-glucose concentrations and induce ChREBP β expression as a feedforward regulation in adipose tissue.

As ChREBP directly regulates genes involved in both glucose and lipid metabolisms some interconnections between ChREBP and PPAR pathways have been established in liver and adipose tissues²⁵⁰.

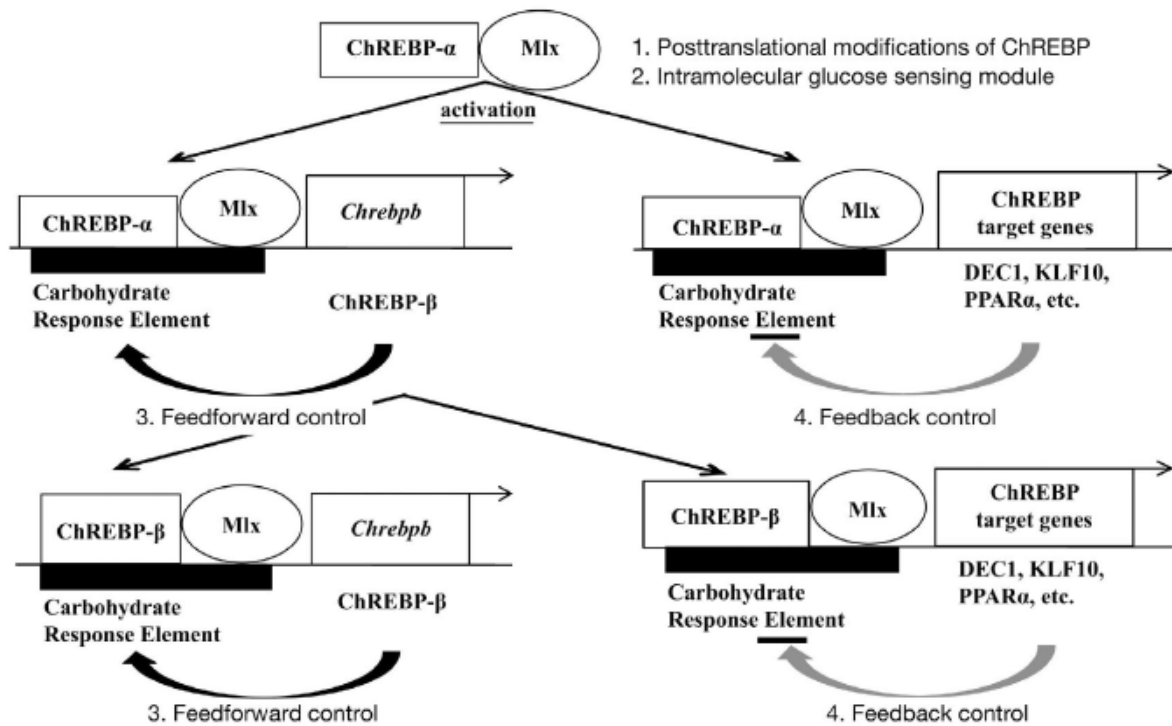


Figure 13: Schematic representation of the mechanisms regulating ChREBP transactivities in adipose tissue

Glucose activates ChREBP- α through (1) posttranslational modification of ChREBP, and (2) an intramolecular glucose sensing module. In turn, ChREBP- α induces ChREBP- β (3. feedforward control). Some ChREBP target genes inhibit both ChREBP- α and β transactivities (4. feedback control)²⁵¹.

D. PPAR signaling pathway

PPAR proteins are nuclear receptors playing the role of transcription factors activated by different ligands, mostly fatty acids. The nature of the ligands depends on the metabolic pathways the PPARs are involved in. Once PPARs interact with the specific ligands, they translocate into the nucleus where they bind to the specific DNA sequence named PPRE (Peroxisome-Proliferator hormone Responsive Element)²⁵² to activate or repress target gene transcription^{253, 254}. In the nucleus, PPAR proteins heterodimerize with RXR (Retinoic X

Receptor), another nuclear receptor. Other proteins, co-activators or co-repressors, interact with this heterodimer, and depending on their nature, the effect of PPARs has been shown to be the activation or the repression of the transcription, respectively.

Three isoforms of PPAR proteins, encoded by three different genes *Nr1c1*, *Nr1c2*, *Nr1c3*²⁵⁵⁻²⁵⁸, have been described: PPAR α , PPAR γ and PPAR β/δ ²⁵⁹. Even though all PPARs are involved in the regulation of lipid metabolism and energy balance, each isoform has its own specificity depending on the tissue where it is expressed and its own function on metabolism regulation events²⁶⁰.

(1) PPAR α signaling pathway

PPAR α (figure 14) is mainly expressed in liver, heart and skeletal muscle, tissues exhibiting a high capacity for fatty acid oxidation. PPAR α is also involved in glucose homeostasis and insulin resistance development²⁶¹. The natural ligands of PPAR α , fatty acids, control the expression of genes involved in lipid metabolism. An increase in fatty acid concentration leads to the activation of PPAR α , which uptakes them under their oxidized form. Liver is the main place where fatty acid oxidation occurs, as this process also has the property of preventing steatosis. During fatty acid influx, transcription of PPAR α target genes is activated leading to the activation of omega- and beta- oxidations in microsomes, mitochondria and peroxisomes^{262, 263}. In liver, an increased PPAR α activity sensing results in increased energy burning and lower fat storage while ineffective PPAR α sensing or fatty acid oxidation leads to low energy burning. This results in a liver steatosis as observed in PPAR α deficient mice²⁶⁴. Thus, PPAR α plays a major role in lipid sensing and energy combustion in the liver where its disruption or impairment can cause fatty liver pathogenesis.

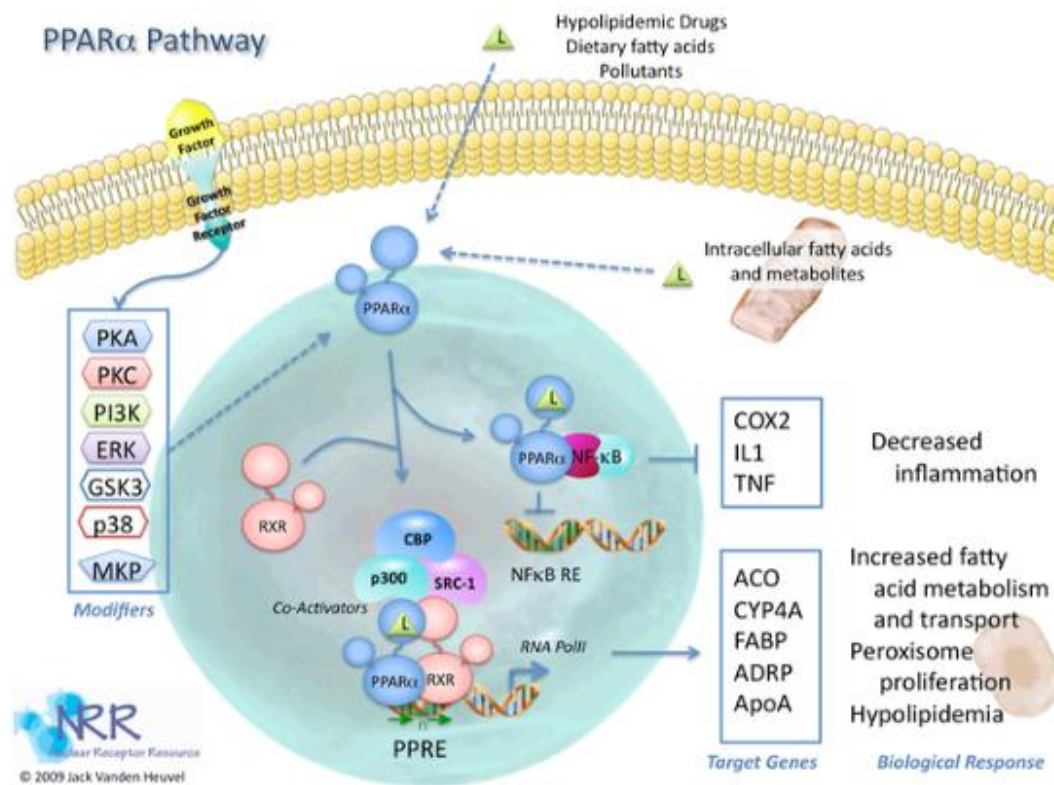


Figure 14: Schematic PPAR α signaling pathway.

Once activated by different signaling pathways including PKA, PI3K, ERK, PPAR α recruits the RXR nuclear receptor and along with some co-activator to activate the transcription of its target genes by binding PPRE.

(2) PPAR β/δ signaling pathway

This isoform of PPAR is ubiquitously expressed in all tissues, but its abundance has been shown to be higher in liver, intestine, adipose tissue, kidney and skeletal muscle. PPAR β/δ is involved in fatty acid oxidation, reducing adiposity, thus preventing obesity development²⁶⁵. PPAR β/δ deficient mice challenged with a high fat regimen exhibit obesity and reduced energy uncoupling²⁶⁵, and in an opposite way, overexpression of this receptor leads to lower lipid accumulation in cardiac cells. These results thus demonstrate the role of PPAR β/δ in fat consumption regulation²⁶⁷.

(3) PPAR γ signaling pathway

PPAR γ has been thoroughly investigated due to its role in macronutrient metabolism. This receptor is abundantly expressed in adipose (white and brown) tissue where it is a central factor in adipogenesis and lipid metabolism regulation. Three PPAR γ isoforms have been identified, and all of them play an important role in adipocyte differentiation and glucose metabolism. However, it has been shown that PPAR γ 2 is regulated in response to nutrient intake and obesity^{268, 269}. Evidence found in *in vivo* experiments demonstrates that PPAR γ 2 deficiency decreases fat accumulation in obese mice. PPAR γ 2 isoform thus prevents lipotoxicity in different mechanisms: promotion of adipose tissue expansion, augmentation of lipid-buffering capacity in peripheral organs (liver, muscle, and pancreatic beta cells), and proliferative response of β -cells to insulin resistance²⁷⁰. Activated PPAR γ in adipocytes guarantees a balanced and adequate secretion of adipocytokines (adiponectin and leptin), mediators of insulin action in peripheral tissues. Insulin sensitivity of the whole body is thus maintained²⁷¹.

PPAR γ also plays an important role in lipid metabolism. Indeed, it is involved in release, transport, and storage of fatty acids as a regulator of genes such as *Lpl* (*Lipoprotein lipase*) or *Cd36*^{268, 270, 272}.

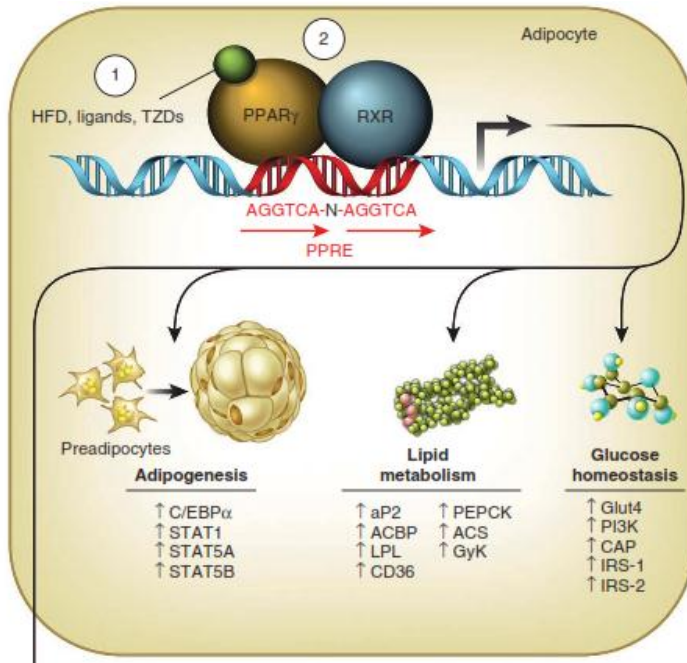


Figure 15: Activated PPAR γ is involved in adipogenesis, lipid metabolism and homeostasis.

Once activated PPAR γ recruits RXR nuclear receptor and some co-activator to activate the transcription of its target genes by binding PPRE²⁷³.

E. Involvement of the circadian clock

It is established that PPARs are connected to the molecular clock by several links. Indeed, PPAR proteins have been shown to be expressed rhythmically in several tissues²⁷⁴⁻²⁷⁶. *Ppara* has been described as a direct target of BMAL1:CLOCK heterodimer *via* the binding of E-box present in its gene promoter²⁷⁷. In a reciprocal way, the deficient PPAR α and deficient PPAR γ mice exhibit alterations in core clock gene expression. Indeed, deficient PPAR α mice showed alterations in rhythmic *Bmal1* and *Per3* expressions in peripheral tissues²⁷⁷ without affecting the rhythms in the SCN²⁷⁸. At the molecular level, PPRE have been found in the promoters of *Bmal1* and *Rev-erba*^{278, 279} and PPAR α has been shown to be involved in the

regulation of *Bmal1* expression by direct interaction with PER2²⁸⁰. In addition, *Rev-erb α* has been described as a target gene of PPAR γ ²⁸¹. PPAR β/δ protein isoform have been less studied in this context. However, *Ppar β/δ* mRNA have been described as a target of miR122 in the liver⁸⁸ expression of which is regulated by REV-ERB α .

Recent evidence demonstrates that circadian rhythms are connected to lipid metabolism. Indeed, REV-ERB α has been shown to be involved in the control of the accumulation of bile acid, suggesting an impact on LXR target genes regulation²⁸². Moreover, *Rev-erba* knockout mice exhibit disrupted circadian accumulation of lipid in both plasma and liver. This observation appears to be due to the impairment of the SREBP pathway and especially of SREBP-1c in the liver²⁸². In the laboratory, it was previously shown that the circadian clock is involved in the maturation of SREBPs, as it is impaired in *Clock*^{A19} dominant negative mutant mice⁴. In addition, SIRT6 was recently shown to be involved in the circadian transcription of SREBP-1c target genes by regulating the chromatin conformation *via* its deacetylase activity, leading to the rhythmic recruitment of SREBP-1c on its target genes promoter.

RESULTS

During this doctoral work, we investigated how the circadian clock influence the different metabolic aspects previously presented in the introduction. We thus present evidence of impacts of the circadian clock on translational events and energy balance.

I. The circadian clock coordinates the ribosome biogenesis

Due to its oscillatory function, the circadian clock has been shown to orchestrate physiology by the rhythmic activation of many key metabolic pathways. In the last decade, many efforts have been made in the characterization of rhythmically expressed genes to determine the role of clock controlled genes on rhythmic physiology^{14, 283}. Indeed, depending on the species and organs, 5 to 10% of the genes have been shown to be rhythmically expressed^{68, 284-286}. However, recent evidences suggest that transcriptional mechanisms are not sufficient to completely explain rhythmic physiology. Indeed, some oscillating proteins have been shown to be encoded by constantly expressed mRNA in mouse liver²⁸⁷⁻²⁸⁹. In addition, among the rhythmically expressed genes, we noticed the presence of several genes encoding proteins involved in mRNA translation, including components of the translation initiation complex^{285, 290}, suggesting a potential role of translation mechanisms in circadian coordination of physiology.

In this study, we investigated the impact of the circadian clock on the translational events in mouse liver. In the liver of wild-type mice, we first described the rhythmic transcription of mRNAs of the components of the translation initiation complex such as *Eif4a*, *Eif4b*, *Eif4g1* and *Eif4bp1*. While no rhythms were observed at the protein level, the phosphorylation of

these components, corresponding to their activation, was observed to be rhythmic throughout the day. We also demonstrated coordinated rhythmic activation of several key pathways, ERK/MAPK, AMPK *via* TSC2 phosphorylation, and PI3K/AKT, involved in regulating the activation of the formation of the translation initiation complex, which occurs during the dark phase. A microarray analysis on polysome-bound mRNAs and total RNAs in mouse liver led us to identify mRNA that are associated with ribosomes in a diurnal manner. These mRNA, targets of TORC1, belong to the 5'-TOP mRNA family and mostly encode for proteins involved in translation such as the ribosomal proteins. This result demonstrates a dynamic translation initiation of 5'-TOP mRNAs starting before the onset of the feeding period, with a maximum in the beginning of the dark period. Western blot performed on cytosolic fractions showed that newly synthesized ribosomal proteins exhibit a rhythmic accumulation during the dark phase. In addition, we showed here that ribosomal proteins mRNA and rRNA exhibit a rhythmic expression before the day-night transition. Moreover, UBF (Upstream Binding Factor) 1, a 45S rRNA transcription regulator, presented rhythmic expression at both mRNA and protein levels.

In *Bmal1* and *Cry1/2* knockout mice, both lacking a functional circadian clock, it appeared that mRNA and protein UBF1 expression is impaired. We also showed that the transcriptional state of the components of the ribosome and of the initiation translation complex is dependent on the molecular clock, because their rhythmic transcription is impaired in deficient circadian clock mice models. Concerning the phosphorylation state of the different factors of initiation translation complex and the signaling pathways involved in their activation, the results obtained revealed disruption in their coordinated activation when the molecular clock is not functional.

Together, these results show the coordination of ribosome biogenesis by the circadian clock via the modulation of rhythmic activation of key pathways regulating translation through the TORC1 pathway, ribosomal proteins translation and finally ribosome biogenesis.

A coordinated rhythmic regulation of transcriptional and translational events for the biogenesis of ribosomes has also been suggested for the filamentous fungus *Neurospora crassa*²⁹¹ and for plants^{292, 293}. Considering the fact that ribosome biogenesis is one of the major energy consuming process in cells²⁹⁴, it must be tightly controlled in order to reduce interferences with other biological processes. It is thus clear that this energy-consuming process must be confined to a time period when energy and nutrients are available in sufficient amounts. In the case of rodents, this is during the night period when the animals are active and consume food. All the elements required for this process must be ready to start ribosome biogenesis during that time. This is achieved by increasing levels of rRNA and ribosomal protein mRNA just before the onset of the night, synchronized with the phosphorylation of EIF4E, which increases 5'-TOP mRNA translation²⁹⁵. Activation of the TORC1 pathway during this period promotes ribosomal protein synthesis, rRNA maturation and ribosome assembly. Accordingly, orchestration of ribosome biogenesis by the circadian clock represents a nice example of anticipation of an obligatory gated process through a complex organization of transcriptional, translational and post-translational events.

The Circadian Clock Coordinates Ribosome Biogenesis

Céline Jouffe^{1#a}, Gaspard Cretenet^{1#b}, Laura Symul², Eva Martin¹, Florian Atger^{1#a}, Felix Naef², Frédéric Gachon^{1#a*}

1 Department of Pharmacology and Toxicology, University of Lausanne, Lausanne, Switzerland, **2** The Institute of Bioengineering, School of Life Sciences, Ecole Polytechnique Fédérale de Lausanne, Lausanne, Switzerland

Abstract

Biological rhythms play a fundamental role in the physiology and behavior of most living organisms. Rhythmic circadian expression of clock-controlled genes is orchestrated by a molecular clock that relies on interconnected negative feedback loops of transcription regulators. Here we show that the circadian clock exerts its function also through the regulation of mRNA translation. Namely, the circadian clock influences the temporal translation of a subset of mRNAs involved in ribosome biogenesis by controlling the transcription of translation initiation factors as well as the clock-dependent rhythmic activation of signaling pathways involved in their regulation. Moreover, the circadian oscillator directly regulates the transcription of ribosomal protein mRNAs and ribosomal RNAs. Thus the circadian clock exerts a major role in coordinating transcription and translation steps underlying ribosome biogenesis.

Citation: Jouffe C, Cretenet G, Symul L, Martin E, Atger F, et al. (2013) The Circadian Clock Coordinates Ribosome Biogenesis. *PLoS Biol* 11(1): e1001455. doi:10.1371/journal.pbio.1001455

Academic Editor: Paul E. Hardin, Texas A&M, United States of America

Received: June 26, 2012; **Accepted:** November 9, 2012; **Published:** January 3, 2013

Copyright: © 2013 Jouffe et al. This is an open-access article distributed under the terms of the Creative Commons Attribution License, which permits unrestricted use, distribution, and reproduction in any medium, provided the original author and source are credited.

Funding: This research was supported by the Swiss National Science Foundation (through individual research grants to F.G. and F.N.), the Canton of Vaud, the European Research Council (through individual Starting Grant to F.G.), the Leenaards Foundation (to F.G. and F.N.) and the Novartis Stiftung für medizinisch-biologische Forschung (to F.G.). The funders had no role in study design, data collection and analysis, decision to publish, or preparation of the manuscript.

Competing Interests: The authors have declared that no competing interests exist.

Abbreviations: AMPK, adenosine monophosphate-activated protein kinase; ERK, extracellular signal-regulated protein kinase; KO, knockout; PI3K, phosphoinositide 3-kinase; RP, ribosomal protein; RPS6, ribosomal protein S6; RT, reverse transcription; SCN, suprachiasmatic nucleus; TOP, terminal oligopyrimidine tract; TORC1, target of rapamycin complex 1; TSC, tuberous sclerosis protein complex; UBF, upstream binding factor; WT, wild type

* E-mail: Frederic.Gachon@rd.nestle.com

^{#a} Current address: Nestlé Institute of Health Sciences, Lausanne, Switzerland

^{#b} Current address: Institut de Génétique Moléculaire de Montpellier, CNRS UMR 5535, Montpellier, France

¶ These authors contributed equally to this work.

Introduction

Circadian rhythms in behavior and physiology reflect the adaptation of organisms exposed to daily light-dark cycles. As a consequence, most aspects of metabolism and behaviour are under the control of these rhythms [1]. At a molecular level, in all the studied species, the rhythmic expression of the genes involved originates in the network of interconnected transcriptional and translational feedback loops [2]. In mammals, the heterodimer composed of BMAL1 and its partners CLOCK or NPAS2 is a transcriptional activator that regulates transcription of the *Period* (*Per*) and *Cryptochrome* (*Cry*) genes that code for repressors of BMAL1 heterodimer activity, thus closing a negative feedback loop that generates rhythms of approximately 24 h [1,2]. Many efforts during the last decade have characterized rhythmically expressed genes and delimit the impact of the circadian clock on physiology. Numerous circadian transcriptome studies in different species and organs show that approximately 10% of the genes are rhythmically expressed. The functions of these genes established the role of the circadian clock in temporally gating rhythmic physiology [1,3]. However, increasing evidence suggests that transcriptional mechanisms are not sufficient to explain numerous observations. For example, it has been shown that many oscillating proteins in mouse liver are encoded by constantly expressed mRNAs [4].

Interestingly, among the rhythmically expressed genes in the liver, we noticed the presence of several genes encoding proteins involved in mRNA translation, including the components of the

translation pre-initiation complex [5,6]. In its inactive state, this complex is composed of the mRNA cap-binding protein eukaryotic translation initiation factor 4E (EIF4E) bound to the hypophosphorylated form of EIF4E-binding protein (4E-BP) that acts as a translational repressor. Upon stimulation, phosphorylation of 4E-BP releases EIF4E, which can then interact with the scaffold protein eIF4G and the rest of the EIF4F complex (EIF4A, EIF4B, and EIF4H) to initiate translation [7]. We therefore investigated whether the circadian clock might coordinate translation in mouse liver. Here we indeed show that the circadian clock controls the transcription of translation initiation factors as well as the rhythmic activation of signaling pathways involved in their regulation. As a consequence, the circadian clock influences the temporal translation of a subset of mRNAs mainly involved in ribosome biogenesis. In addition, the circadian oscillator regulates the transcription of ribosomal protein mRNAs and ribosomal RNAs. These results demonstrate for the first time the major role of the circadian clock in ribosome biogenesis.

Results

Rhythmic Expression and Activation of Components of the Translation Pre-initiation Complex

We investigated whether the circadian clock might coordinate translation in mouse liver. Indeed, quantitative reverse transcrip-

Author Summary

Most living organisms on earth present biological rhythms that play a fundamental role in the coordination of their physiology and behavior. The discovery of the molecular circadian clock gives important insight into the mechanisms involved in the generation of these rhythms. Indeed, this molecular clock orchestrates the rhythmic transcription of clock-controlled genes involved in different aspects of metabolism, for example lipid, carbohydrate, and xenobiotic metabolisms in the liver. However, we show here that the circadian clock could also exert its function through the coordination of mRNA translation. Namely, the circadian clock influences the temporal translation of a subset of mRNAs by controlling the expression and activation of translation initiation factors, as well as the clock-dependent rhythmic activation of signaling pathways involved in their regulation. These rhythmically translated mRNAs are mainly involved in ribosome biogenesis, an energy consuming process, which has to be gated to a period when the cell resources are less limited. Moreover, the role of the circadian oscillator in this process is highlighted by its direct regulation of the transcription of ribosomal protein mRNAs and ribosomal RNAs. Thus our findings suggest that the circadian clock exerts a major role in coordinating transcription and translation steps underlying ribosome biogenesis.

tion (RT)-PCR analyses confirmed that mRNAs of most of the factors involved in translation initiation are rhythmically expressed with a period of 24 h (Figure 1A; statistical analyses are given in Table S1). Interestingly, while we did not observe any significant variations in protein abundance, rhythmic phosphorylations were strongly manifested during two consecutive days, emphasizing the robustness of these rhythms (Figure 1B; quantification and statistical analyses of the data are given on Figure S1 and Table S2). EIF4E is mostly phosphorylated during the day, with a peak at the end of the light period (ZT6-12), whereas EIF4G, EIF4B, 4E-BP1, and ribosomal protein (RP) S6 (RPS6) are mainly phosphorylated during the night, which is, in the case of nocturnal animals like rodents, the period when the animals are active and consume food.

Phosphorylation of these factors is well characterized and involves different signaling pathways [8] whose reported activity perfectly correlates with the observed phosphorylation rhythm. EIF4E is phosphorylated by the extracellular signal-regulated protein kinase (ERK)/mitogen-activated protein kinase (MAPK)-interacting kinase (MNK) pathway [9], which is most active during the day, at the time when EIF4E reaches its maximum phosphorylation (Figure 2A; quantification and statistical analyses of the data are given on Figure S2 and Table S2). On the other hand, EIF4G, EIF4B, 4E-BP1, and RPS6 are mainly phosphorylated by the target of rapamycin (TOR) complex 1 (TORC1) [10], which is activated during the night, at the time when the phosphorylation of these proteins reaches its maximum level. TORC1, in turn, is negatively regulated by the tuberous sclerosis protein complex (TSC), whose activity is under the control of the phosphoinositide 3-kinase (PI3K)/AKT, ERK, and the energy sensing 5' adenosine monophosphate-activated protein kinase (AMPK) pathways [10,11]. As reported [12], AMPK is active during the day and mediates the activation of TSC2, contributing to the repression of TORC1 in the period of energy and nutrient restriction. Conversely, during the night, TORC1 is activated probably through TSC2 inhibition by PI3K via TORC2 [13].

Interestingly, we found that *mTor*, its partner *Raptor*, as well as its regulating kinase *Map3k4*, are also rhythmically expressed, thus potentially further contributing to the rhythmic activation of TORC1 (Figure S3; Table S1). ERK is activated during the day in synchrony with the rhythmic expression of *Mnk2* (Figure S3), contributing to EIF4E phosphorylation during this period. However, its downstream target RPS6 Kinase (RSK) seems to contribute only marginally to the phosphorylation of RPS6 in mouse liver (Figures 1B and 2A). The rhythmic phosphorylation of 4E-BP1 resulted in its release from the mRNA cap-mimicking molecule 7-methyl-GTP from ZT14 to ZT22 (Figure 2B; Table S2), allowing the rhythmic assembly of the EIF4F and potentially mRNA translation.

The rhythmic expression of mRNA encoding translation initiation factors, TORC1 complex component, and a kinase activating these factors is independent of light as it is maintained under constant darkness, even if the phase seems to be advanced (Figure S4A). Interestingly, activation of the TORC1 pathway is also maintained under constant darkness but with an advanced phase (Figure S5A). Since nutrient availability is a potent activator of the TORC1 pathway [13], we asked whether these parameters are also rhythmic under conditions of starvation. We found that expression of mRNA encoding translation initiation factors, TORC1 complex component, and a kinase activating these factors is still rhythmic under starvation (Figure S4B), even when this starvation occurs under constant darkness (Figure S4C). This result unambiguously demonstrates the role of the circadian clock in the expression of these genes. In addition, phosphorylations of RPS6 and 4E-BP1 are still rhythmic under starvation, whether or not the mice are under a light-dark regimen or in constant darkness (Figure S5B and S5C), confirming previously published observations [14]. Interestingly, TORC1 activation is in opposite phase with the clock-dependent rhythmic activation of autophagy in mouse liver [15], a process inhibited by TORC1 but able to generate amino acids that can in turn activate TORC1 [16]. This might suggest that the circadian clock can regulate the two processes in a coordinated fashion. Importantly, rhythmic activation of TORC1 is not restricted to the liver as the same phosphorylation rhythm is found in kidney and heart, albeit with reduced amplitude (Figure S6). Meanwhile, TORC1 activation is constant in brain, lung, and small intestine, suggesting that the rhythmic nutrient availability due to the circadian clock-regulated feeding behavior is not sufficient by itself to explain the rhythmic activation of TORC1.

Characterization of Rhythmically Translated mRNAs

Diurnal binding of 4E-BP to EIF4E suggested that translation might be rhythmic in the liver. To test this hypothesis and to identify potential rhythmically translated genes, we purified polysomal RNAs, a RNA sub-fraction composed mainly of actively translated mRNA, every 2 h during a period of 48 h. We found that relative amount of this polysomal fraction follows a diurnal cycle, showing that a rhythmic translation does occur in mouse liver (Figure S7). This result confirms original observations based on electron microscopy and biochemical studies [17,18]. We therefore decided to characterize these rhythmically translated mRNAs through comparative microarray analysis of polysomal and total RNAs. While the obtained profiles in polysomal and total RNAs fractions are highly similar for most mRNAs (examples of rhythmic mRNAs are given on Figure S8), 249 probes showed a non-uniform ratio in diurnal polysomal over total mRNAs (Figure 3A). This means that approximately 2% of the expressed genes are translated with a rhythm that is not explained by rhythmic mRNA abundance as in most cases, the total mRNA

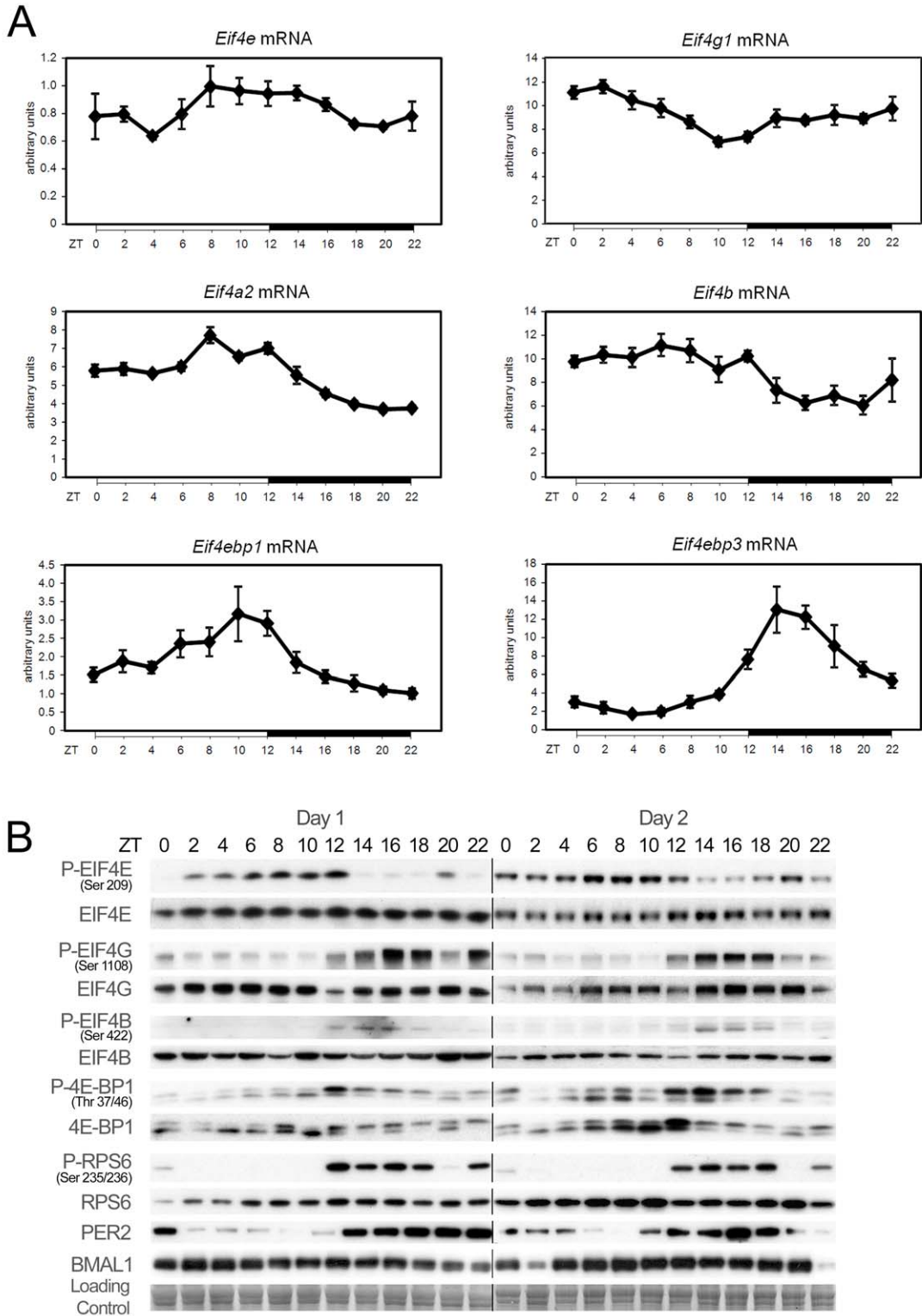


Figure 1. Temporal expression and phosphorylation of translation initiation factors. (A) Temporal mRNA expression profile of translation initiation factors in mouse liver. For each time point, data are mean \pm standard error of the mean (SEM) obtained from four independent animals. (B) Temporal protein expression and phosphorylation of translation initiation factors in mouse liver during two consecutive days. Western blots were realized on total or nuclear (PER2 and BMAL1) liver extracts. PER2 and BMAL1 accumulations are shown as controls for diurnal synchronization of the animals. Naphtol blue black staining of the membranes was used as a loading control. The lines through gels indicate where the images have been cropped. The zeitgeber times (ZT), with ZT0, lights on; ZT12, lights off, at which the animals were sacrificed, are indicated on each panel. doi:10.1371/journal.pbio.1001455.g001

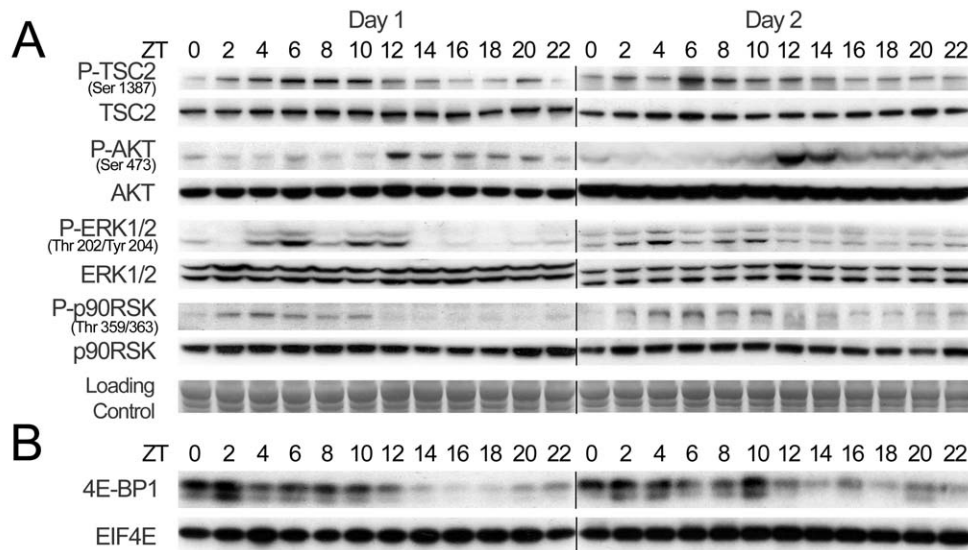


Figure 2. Temporal activation of signaling pathways controlling translation initiation. (A) Temporal expression and phosphorylation of representative proteins of key signaling pathways regulating translation initiation in mouse liver during two consecutive days. Western blots were performed on total liver extracts. Naphtol blue black staining of the membranes was used as a loading control. (B) Temporal binding of EIF4E and 4E-BP1 to 7-methyl-GTP-sepharose during two consecutive days. Total liver extracts were incubated with 7-methyl-GTP beads mimicking the mRNA cap structure. After washing of the beads, bound proteins were analyzed by Western blotting. The zeitgeber times (ZT), with ZT0, lights on; ZT12, lights off, at which the animals were sacrificed, are indicated on each panel. The lines through gels indicate where the images have been cropped. doi:10.1371/journal.pbio.1001455.g002

levels were constant while the polysomes-bound mRNA levels fluctuated during the 24-h cycle (Figures 3B and S9). Among translationally regulated genes, 70% were found in the polysomal fraction during the same time interval, starting at ZT8 before the onset of the feeding period and finishing at the end of the dark period (Tables S3 and S4). Most of these genes belonged to the 5'-terminal oligopyrimidine tract (5'-TOP) family, known to be regulated by TORC1 [19], but also by the level and phosphorylation state of EIF4E [20,21]. 5'-TOP genes are themselves involved in translation via ribosome biogenesis and translation elongation (Table S4).

After confirmations of these results by quantitative RT-PCR (Figure S10), we wished to validate the periodicity in the amount of mRNAs purified in the different fractions obtain during polysomes purification over a 24-h period. Whereas a constitutively translated mRNA such as *Gapdh* is found all the time in the polysomal fraction (with a small decrease in the middle of the light period when overall translation decreases), mRNAs coding for RPs are associated with the polysomal fraction only starting towards the end of the light period (ZT8) and during the dark period (Figure 3C). This result demonstrates a dynamic translation initiation of 5'-TOP mRNA starting before the onset of the feeding period, with a maximum at the beginning of the dark period.

Next, we wanted to confirm that this rhythmic translation had an impact on the protein levels. With respect to RPs, while the half-life of mature ribosomes is approximately 5 d in rodent liver [22], newly synthesized RPs have a half-life of only a few hours, as most of them are rapidly degraded after translation during the ribosome assembly process in the nucleolus [23]. We thus expected a rhythmic expression of this subpopulation of newly synthesized RPs in the soluble cytosolic fraction depleted of ribosomes after sedimentation. Indeed, under these conditions, RPs show a rhythmic abundance with highest expression during the night (Figure 3D; quantification and statistical analyses of the data are

given on Figure S11 and Table S2). In some cases, we noticed a shallow decrease at ZT16-18, potentially reflecting transport of RPs into the nucleolus for ribosome assembly. In addition to translational regulation, we also observed a diurnal expression of RP mRNAs, albeit with a small average peak to trough amplitude of approximately 1.2. Taking into account their relatively long half-life (11 h) [24], we hypothesized that this minor fluctuation might reflect more pronounced rhythmic amplitudes in transcription as amplitude decreases with half-life [25]. In addition, it has recently been shown that the transcription of several RP mRNAs is directly controlled by the molecular oscillator in *Drosophila* head [26]. Indeed, pre-mRNA accumulation of several RP exhibited a rhythmic transcription, with an average amplitude of 3.5-fold with a maximum at ZT8, just before the activation of their translation (Figure 4A; statistical analyses are given in Table S1). In addition, we found that the synthesis of the ribosome constituent precursor 45S rRNA is also rhythmic and synchronized with RP mRNAs transcription, indicating that all elements involved in ribosome biogenesis are transcribed in concert, then translated or matured. In yeast [27] and *Drosophila* [28], transcription of RP mRNAs appears to be coordinated with rRNA transcription, which is a rate limiting step in ribosome biogenesis. On the other hand, in mammals, rRNA transcription is highly regulated by the upstream binding factor (UBF), which establishes and maintains an active chromatin state [29]. Remarkably, we found that UBF1 is rhythmically expressed in mouse liver at both mRNA and protein levels (Figure 4B; quantification and statistical analyses of the data are given in Figure S12A and Tables S1 and S2), in phase with RP mRNAs and rRNAs transcription. In addition, rhythmic transcription of *Ubf1* and *Rpl23* genes is also independent of light and food (Figure S4).

To test whether *Ubf1* transcription is regulated by the circadian clock, we characterized its expression in arrhythmic *Cry1/Cry2* knockout (KO) [30] and *Bmal1* KO [31] mice, which are devoid of a functional circadian clock. Indeed, these mice do exhibit an

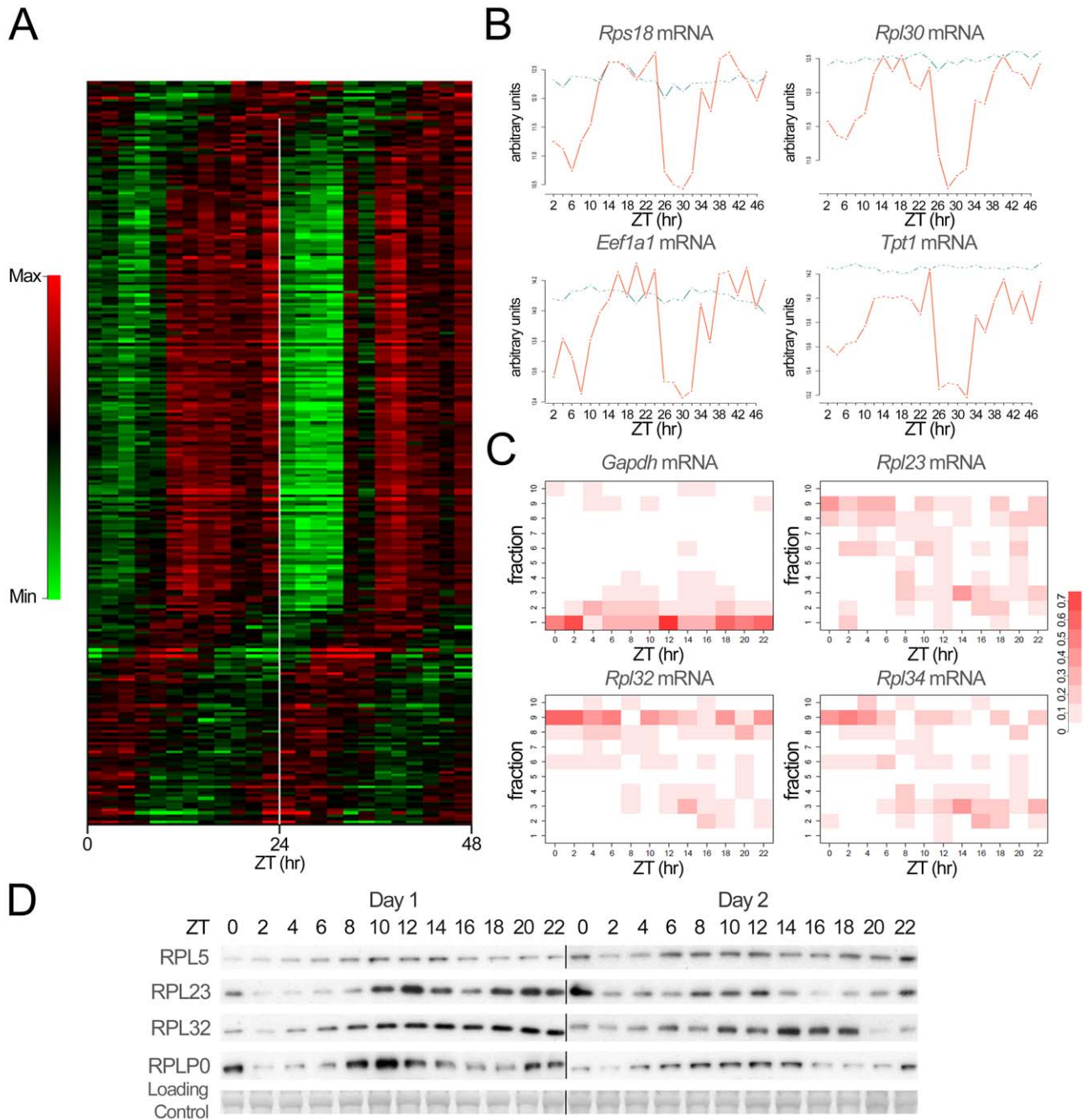


Figure 3. Rhythmic translation of ribosomal proteins in mouse liver. (A) Temporal expression profiles of microarray probes showing a rhythmic ratio of polysomal to total RNAs, ordered by phase. For visualization, data were mean centered and standardized. Log-ratios are color-coded so that red indicates high and green low relative levels of polysomal mRNAs compared to the total fraction. (B) Examples of temporal expression profiles of a subset of rhythmically translated 5'-TOP genes identified in our microarray experiment. Traces represent the levels of mRNA expression measured by microarray in the total RNA (blue line) and polysomal fraction (red line). Data are represented in log scale following standard normalization. (C) Temporal location of *Gapdh* and selected genes showing translational regulation mRNA on the different gradients obtained after polysomes purification. Pools of RNA obtained from four animals were used for each fraction at each time point. The color intensity represents for each time point the relative abundance of the mRNA in each fraction. Fractions 1–2 represent heavy polysomes, 2–3, light polysomes, and 9–10, free mRNAs. Note that even for *Gapdh* mRNA, translation slightly decreases at the end of the light period. (D) Temporal expression of selected rhythmically translated ribosomal proteins in liver cytoplasmic extracts during two consecutive days. Naphtol blue black staining of the membranes was used as a loading control. The lines through gels indicate where the images have been cropped. The zeitgeber times (ZT) at which the animals were sacrificed are indicated on each panel.
doi:10.1371/journal.pbio.1001455.g003

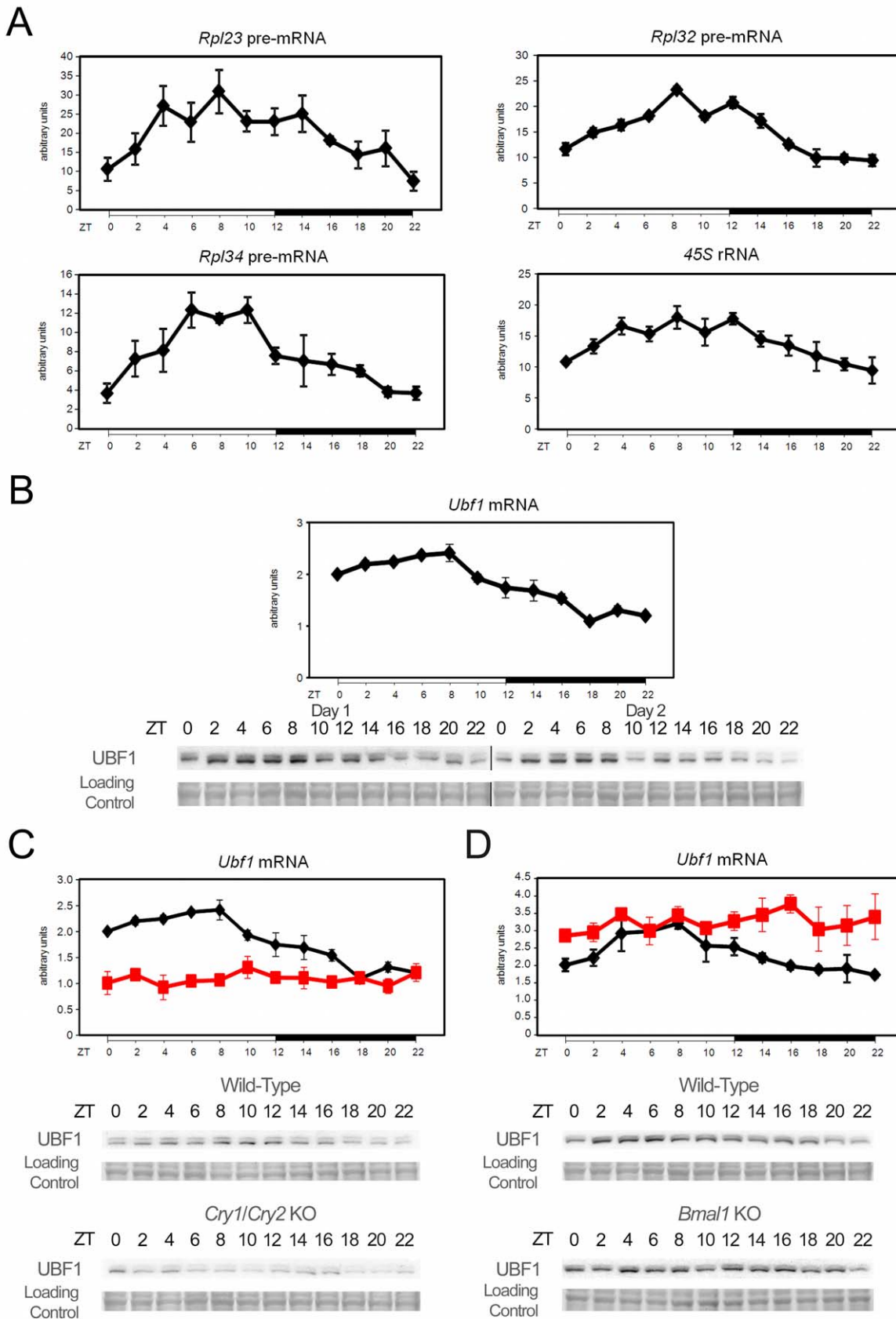


Figure 4. Rhythmic transcription of RP mRNA and rRNA through circadian clock regulated expression of UBF1. (A) Temporal real-time RT-PCR profile of RP pre-mRNA and 45S rRNA precursor expression in mouse liver. For each time point, data are mean \pm standard error of the mean

(SEM) obtained from four independent animals. (B) Temporal *Ubf1* mRNA (upper panel) and protein (lower panel) expression in mouse liver. mRNA were measured by real-time RT-PCR and, for each time point, data are mean \pm SEM obtained from four independent animals. UBF1 protein expression was measured by Western blot on nuclear extracts during two consecutive days. The lines through gels indicate where the images have been cropped. (C–D) Temporal *Ubf1* expression in mice devoid of a functional circadian clock. *Ubf1* expression was measured by real-time RT-PCR with liver RNAs obtained from arrhythmic *Cry1/Cry2* (C) and *Bmal1* (D) KO mice and their control littermates (upper panel). Data are mean \pm SEM obtained from three and two animals, respectively. Black line corresponds to the WT animals and red line to the KO. Protein levels (lower panel) were measured by Western blot on nuclear extracts. The zeitgeber times (ZT) at which the animals were sacrificed are indicated on each panel. Naphtol blue black staining of the membranes was used as a loading control. doi:10.1371/journal.pbio.1001455.g004

arrhythmic pattern of activity under constant darkness, which is in general correlated with an arrhythmic feeding behaviour. As TORC1, as well as other signaling pathways, are in part regulated by feeding through nutrient availability, we expect a temporally discontinuous and erratic activation of these pathways in the KO mice under unrestricted feeding. To verify this hypothesis, we measured activation of the TORC1, AKT, and ERK pathways in *Cry1/Cry2* and *Bmal1* KO kept in constant darkness. As shown in Figure S13A, the rhythmic activation of these signaling pathways is indeed lost under this condition, confirming their arrhythmic activation. To highlight the role of the feeding regimen on this activation, we kept *Cry1/Cry2* KO mice in constant darkness and sacrificed them at CT12. We found a strong inter-individual variability in the activation of the TORC1, AKT, and ERK pathways, reflecting the arrhythmic feeding rhythm of these animals (Figure S13B). To circumvent this caveat and study the rhythmic translation in mice devoid of a functional molecular oscillator, we decided to place *Cry1/Cry2* and *Bmal1* KO under a light-dark regimen to keep a normal diurnal feeding behaviour due to masking. In addition, mice had access to food only during the dark phase to eliminate the effect of a potential disturbed feeding behaviour. Under these conditions, KO mice had a rhythmic feeding behaviour and thus potential differences in protein levels or pathway activity cannot be attributed to the arrhythmic feeding behaviour of these animals. We indeed found that UBF1 rhythmic expression is dependent on a functional circadian clock as it is impaired in both animal models (Figure 4C and 4D; quantification and statistical analyses of the data are given in Figure S12B and Tables S5, S6, S7, S8). However, if UBF1 expression is persistently low in *Cry1/Cry2* KO mice, this expression is constantly high in *Bmal1* KO mice, suggesting the control of *Ubf1* by a circadian clock-regulated transcription repressor. In addition, we observed that these animals lose also the synchrony and coordination of 45S rRNA and RP pre-mRNAs transcription (Figures 5, S14, and S15; statistical analyses of the data are given in Table S5 and S6). Indeed, decreased UBF1 expression in *Cry1/Cry2* KO mice is correlated with lower 45S rRNA transcription, but higher and delayed RP pre-mRNAs transcription. Interestingly, *Bmal1* KO mice present a complete arrhythmic transcription of RP pre-mRNAs, highlighting the crucial role of the circadian clock in the coordination of rRNA and RP mRNAs transcription.

The Circadian Clock Controls Expression and Activation of Components of the Translation Initiation Complex

Rhythmic expression of genes coding for components of the translation initiation complex is strongly dampened or phase-shifted in both KO models, in addition to an altered level of expression (Figures 5, S14, and S15; statistical analyses of the data are given in Tables S5 and S6). However, we did not observe in general any significant variations in protein abundance, excepting a slight increase in EIF4E expression in *Cry1/Cry2* KO mice, reflecting increased mRNA expression (Figure 6A and 6C; quantification and statistical analyses of the data are given in Figures S16, S17; Tables S7 and S8). The variations in EIF4G

levels reflect more the changes in its phosphorylation state, which regulates its stability [32]. While most of the signaling pathways are still rhythmic in *Cry1/Cry2* KO mice, except for the ERK pathway and the downstream phosphorylation of EIF4E, which loses its rhythmic activation, the phase of the activation of the TORC1 and AKT pathways are advanced in comparison to wild-type (WT) mice (Figures 6A and S16; quantification and statistical analyses of the data are given in Table S7). As a consequence, the rhythmic expression of RPs is altered in *Cry1/Cry2* KO mice (Figure 6B; quantification and statistical analyses of the data are given in Table S7), with an increased level of expression, likely because of the increased RP pre-mRNAs and EIF4E levels [20], and a delayed phase of expression. Most of the rhythmic activation of the three pathways is also strongly altered in *Bmal1* KO mice (Figures 6C and S17; quantification and statistical analyses of the data are given in Table S8). As shown in Figure 6D, the phase of RPs rhythmic expression is severely advanced with a maximum of expression in the middle of the day instead of the night (Figure 6D; quantification and statistical analyses of the data are given in Table S8).

Discussion

Regulation of Ribosome Biogenesis by the Circadian Clock

The results presented here show that the molecular circadian clock controls ribosome biogenesis through the coordination of transcriptional, translational, and post-translational regulations. Moreover, the data strongly suggest that a functional molecular oscillator is required for a timely coordinated transcription of translation initiation factors, RP mRNAs, and rRNAs. The clock modulates the rhythmic activation of signaling pathways controlling translation through the TORC1 pathway, translation of RPs, and ribosome biogenesis (Figure 7). Interestingly, it has been reported that the size of the nucleolus, the site of rRNA transcription and ribosome assembly, follows a diurnal pattern with a maximum in the middle of the dark period [33], which thus occurs in synchrony with the observed accumulation of RPs in the liver. The observed rhythmic ribosome biogenesis is substantiated by the previous observation showing that both size and organization of the nucleolus are directly related to ribosome production [34].

Remarkably, a coordinated rhythmic regulation of transcriptional and translational events for the biogenesis of ribosomes has also been suggested for the filamentous fungus *Neurospora crassa* [35] and for plants [36,37]. Since ribosome biogenesis is one of the major energy consuming process in cells [38], its tight control is primordial to reduce interferences with other biological processes. In the case of mouse liver, we estimate that the decrease of translation during the light period is equivalent to 20% of the total translation (Figure S7), in agreement with previously published results [17]. Although moderate, this decrease affects translation of housekeeping genes like *Gapdh* (Figure 3C) and probably the translation of other genes. It means that the increase in ribosome biogenesis

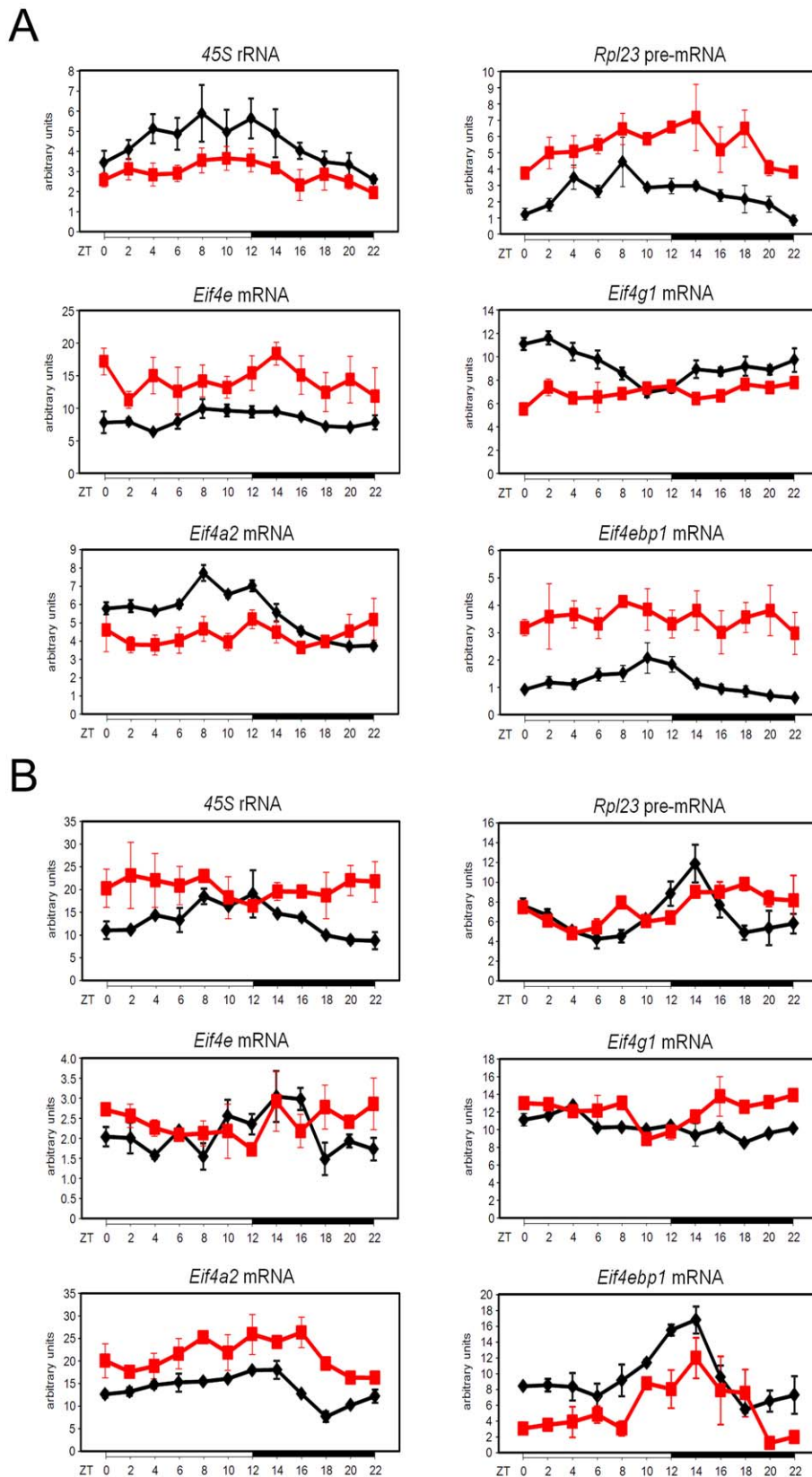


Figure 5. Rhythmic RNA expression of factors involved in ribosomes biogenesis is disrupted in arrhythmic *Cry1/Cry2* and *Bmal1* KO mice. Temporal expression of factors involved in ribosomes biogenesis in *Cry1/Cry2* (A) and *Bmal1* (B) KO mice and their control littermates. Temporal real-time RT-PCR expression profile of 45S rRNA precursor, *Rpl23* pre-mRNA, and translation initiation factors expression in mouse liver. Black line corresponds to the WT animals and red line to the KO. For each time point, data are mean \pm SEM obtained from three (A) and two (B) independent animals. The zeitgeber times (ZT) at which the animals were sacrificed are indicated on each panel.
doi:10.1371/journal.pbio.1001455.g005

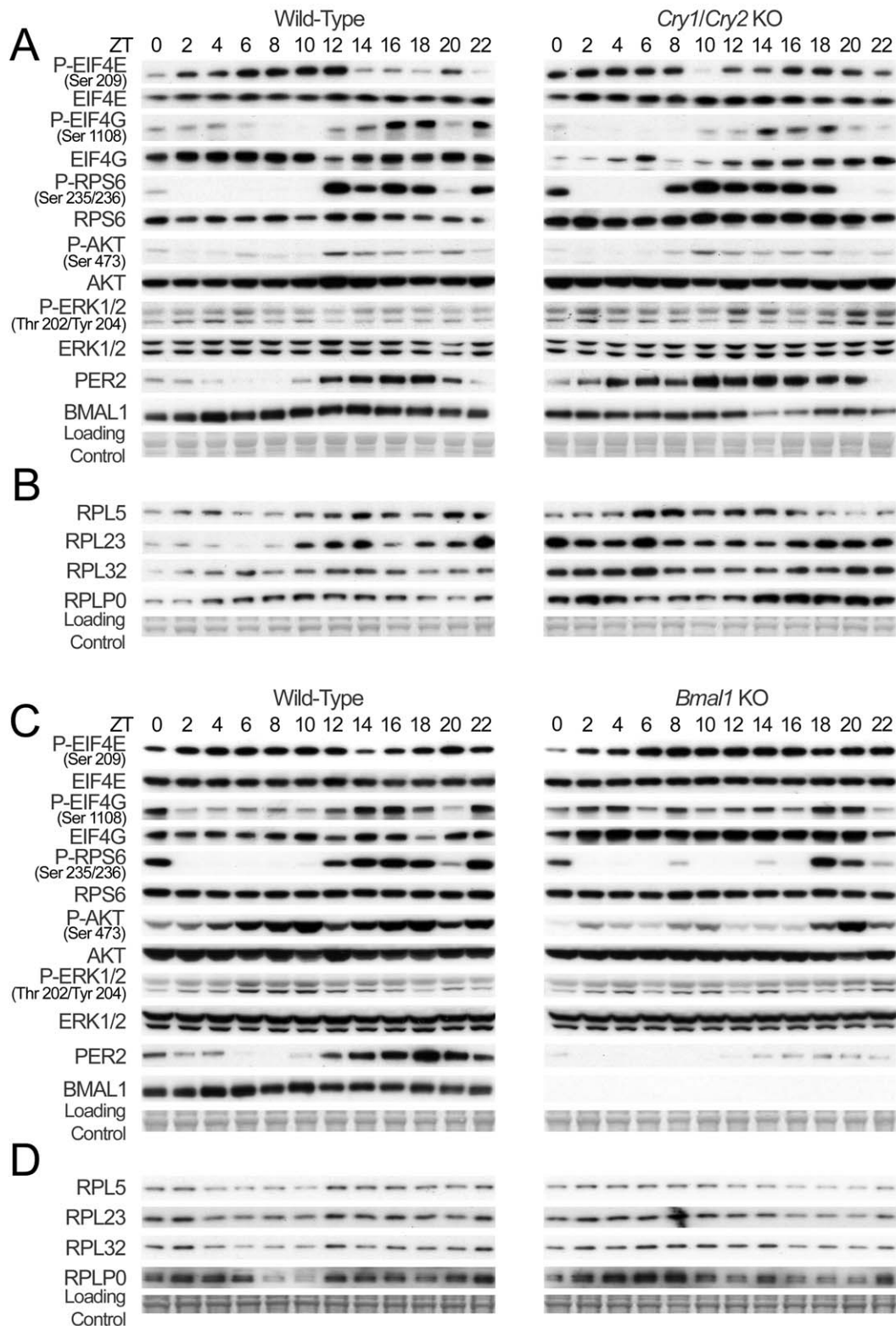


Figure 6. Rhythmic expression and phosphorylation of actors of ribosomes biogenesis is disrupted in arrhythmic *Cry1/Cry2* and *Bmal1* KO mice. (A–C) Temporal expression and phosphorylation of translation initiation factors and representative indicators of signaling pathways controlling their activation in *Cry1/Cry2* (A) and *Bmal1* (C) KO mice and their control littermates. Western blots were realized on total or nuclear (PER2 and BMAL1) liver extracts from WT (left panel) and KO (right panel) animals. (B–D) Temporal expression of selected rhythmically translated ribosomal proteins in liver from *Cry1/Cry2* (B) and *Bmal1* (D) KO mice and their control littermates. Western blots were realized on cytoplasmic extracts from WT (left panel) and KO (right panel) animals. The zeitgeber times (ZT) at which the animals were sacrificed are indicated on each panel. PER2 and BMAL1 accumulations are shown as controls for diurnal synchronization of the animals. Naphtol blue black staining of the membranes was used as a loading control.
doi:10.1371/journal.pbio.1001455.g006

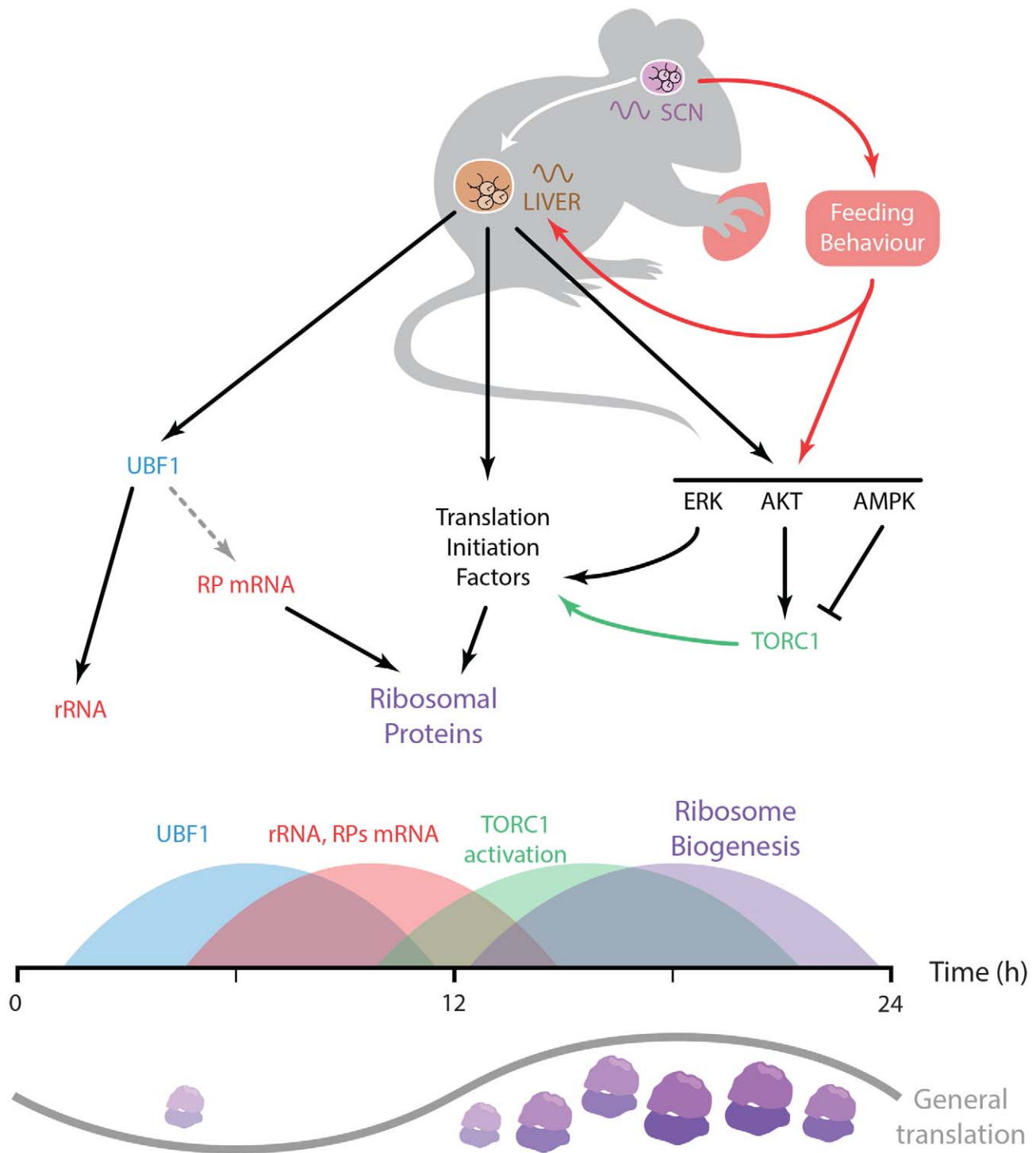


Figure 7. Model describing the coordination of ribosome biogenesis by the circadian clock. The molecular oscillator in the master circadian pacemaker localized in the SCN of the hypothalamus synchronizes peripheral clocks, including liver clock, and, in parallel, regulates feeding behavior, which itself influences peripheral oscillator. The liver circadian clock controls expression of translation initiation factors, and rRNA, and conceivably RP mRNA, through regulation of UBF1. In addition, in association with signals from nutrients, the molecular clock, via the TORC1 pathway, coordinates the rhythmic activation of signaling pathways controlling translation of RP and, in turn, ribosome biogenesis. This succession of events coordinated by the circadian clock finally leads to a subtle rhythmic change of general translation in mouse liver.
doi:10.1371/journal.pbio.1001455.g007

during the night could potentially influence the translation of many other mRNAs, however with a magnitude sufficiently low to not allow its detection by our method.

Nevertheless, it is clear that this energy-consuming process has to be confined to a time when energy and nutrients are available in sufficient amount, which, in the case of rodents, is during the night

period when the animals are active and consume food. Hence, all the elements required for translation have to be ready to start ribosome biogenesis during that time. This is achieved by increasing levels of rRNAs and RP pre-mRNAs just before the onset of the night, synchronized with the phosphorylation of EIF4E that increases 5'-TOP mRNAs translation [21]. Activation of the TORC1 pathway during this period promotes RPs synthesis, rRNAs maturation, and ribosome assembly. In addition activation of the ERK pathway correlates also with ribosome biogenesis [39], strengthening the rhythmic nature of this process. Accordingly, orchestration of ribosome biogenesis by the circadian clock represents a nice example of anticipation of an obligatory gated process through a complex organization of transcriptional, translational, and post-translational events.

Coordination of Rhythmic Activation of Cellular Signaling Pathways by the Circadian Clock

As described in the introduction, the mammalian molecular circadian oscillator consists in interlocked feedback loops of transcription factors that generate a complex network of rhythmically expressed genes [3]. Within the core molecular clock, increasing evidence shows that post-translational modifications play a crucial role in the generation of circadian rhythms [40]. However, the circadian clock is also able to coordinate rhythmic post-translational activation of signaling pathways not directly involved in the molecular oscillator but rather in the sensing of the environment. The first described example consisted in the rhythmic activation of ERK in the suprachiasmatic nucleus (SCN) of the hypothalamus where the master circadian pacemaker is localized: if light stimulates ERK phosphorylation in the SCN in a time-dependent fashion, circadian ERK phosphorylation continues also in constant darkness, suggesting a crucial role of the circadian clock in this process [41]. Interestingly, the same observations have been made for the TORC1 pathway in the SCN [42,43], and for the PI3K/AKT pathway in the retina [44]. Considering the fact that these two pathways have been recently identified as a potent regulators of circadian activity in *Drosophila* [45], we expect that the role of the circadian clock-coordinated signaling pathways on circadian physiology will probably be emphasized in other organisms in the near future.

With respect to rhythmic activation of signaling pathways in the liver, there are only few examples of such regulations. One example is the rhythmic activation of the PI3K/AKT pathway that is associated with food metabolism and rhythmic feeding behavior [46]. Recently, we also described a circadian clock-dependent rhythmic activation of the unfolded protein response regulating liver lipid metabolism [47]. In addition, it has been shown that the circadian clock is also able to regulate autophagy in mouse liver [15]. In this context, our discovery of the rhythmic ribosome biogenesis through coordination of the rhythmic activation of signaling pathways constitutes an important new element in this area of research.

Translation, Circadian Clock, and Longevity

It has long been known that caloric restriction or intermittent fasting increases lifespan in a wide variety of models [48]. Increased lifespan has also been linked to the reduced activation of the TORC1 pathway, which, in turn, provokes a reduced mRNA translation [49,50]. The role of the TORC1 pathway in this translation-dependent extension of lifespan has been genetically confirmed in *Caenorhabditis elegans* [51] and *Drosophila* [52,53]. A similar scenario is also considered in mice since treatment with the TOR inhibitor rapamycin [54] or deletion of the TORC1 downstream protein kinase S6K1 [55] lead to increased lifespan.

In addition, downregulation of various components of the EIF4F complex extends lifespan in *C. elegans* [56–59], whereas inhibition of RPs genes expression extends lifespan in both *Saccharomyces cerevisiae* [60] and *C. elegans* [56]. Hence, keeping ribosome biogenesis, and translation in general, to their minimum levels plays a major role in the regulation of longevity [61]. Interestingly, all the genetically modified animal models presenting a disrupted circadian clock [62–64] or mice subjected to chronic jet lag [65] are subjected to premature aging and reduced lifespan. The deregulation of many other circadian-clock regulated processes can reduce life expectancy, like reduced xenobiotic detoxification [66]. We thus believe that the potential role of disorganized ribosome biogenesis on life expectancy, observed in animals devoid of a circadian clock, will be an exciting subject for further studies.

Material and Methods

Animal Experiments

All animal studies were conducted in accordance with our regional committee for ethics in animal experimentation and the regulations of the veterinary office of the Canton of Vaud. C57Bl/6J mice were purchased from Janvier (Le Genest) or Charles River Laboratory (L'Arbresle). *Bmal1* floxed mice have been previously described [67]. These mice were crossed with mice expressing the CRE recombinase under the control of the CMV promoter [68] to obtain *Bmal1* KO mice. *Cry1/Cry2* double KO mice [30] in the C57Bl/6J genetic background have been previously described [69]. In all experiments, male mice between 10 and 12 wk of age are used. Unless noted otherwise, mice were maintained under standard animal housing conditions, with free access to food and water and in 12-h light/12-h dark cycles. However, for all experiments, animals were fed only at night during 4 d before the experiment to reduce effects of feeding rhythm. For experiments in constant darkness, mice were shifted into complete darkness after the last dark period and then sacrificed every 2 or 4 h during the next 48 h. For starvation experiments, mice were deprived from food during one complete night and then during the following 24 h, mice were sacrificed every 2 or 4 h.

Polysome Purification

Livers were homogenized in lysis buffer containing 20 mM HEPES (pH 7.6), 250 mM NaCl, 10 mM MgCl₂, 10 mM DTT, 20 µg/ml cycloheximid, 10 U/µl RNase inhibitor, and a protease inhibitor cocktail containing 0.5 mM PMSF, 10 µg/ml Aprotinin, 0.7 µg/ml Pepstatin A, and 0.7 µg/ml Leupeptin. The homogenates were centrifuged 10 min at 9,500 g and 1 mg/ml heparin, 0.5% Na deoxycholate, and 0.5% Triton ×100 were added to the supernatant. 50 mg of lysate were deposited on a 36 ml 7% to 47% sucrose gradient in a buffer containing 20 mM HEPES (pH 7.6), 100 mM KCl, 5 mM MgCl₂, and 1 mM DTT. After 4 h 30 min of centrifugation at 130,000 g and 4°C, the gradient was divided in fractions of approximately 1 ml with a peristaltic pump. Optic density of the fractions at 260 nm was measured to establish the polysomal profile in the gradient. Fractions were finally pooled in ten fractions. An example of polysome profile is given on Figure S18. RNAs were then extracted according to the protocol described by Clancy et al. [70] that we slightly modified. Briefly, fractions were precipitated by the addition of three volumes of ethanol and kept overnight at –80°C. After 30 min of centrifugation at 5,200 g, RNAs were extracted from the non-soluble fraction by classical protocol [71].

RNA Extraction and Analysis

Liver RNAs were extracted and analysed by real-time quantitative RT-PCR, mostly as previously described [25]. Briefly, 0.5 µg of liver RNA was reverse transcribed using random hexamers and SuperScript II reverse transcriptase (Life Technologies). The cDNAs equivalent to 20 ng of RNA were PCR amplified in triplicate in an ABI PRISM 7700 Sequence Detection System (Applied Biosystem) using the TaqMan or the SYBR Green technologies. References and sequences of the probes are given in Tables S9 and S10, respectively. *Gapdh* mRNA (total RNA) or 28S rRNA (polysomal RNA) were used as controls.

Microarray Experiments

Liver polysomal and total RNAs were extracted independently from two mice sacrificed every 2 h during 48 h. For polysomal RNAs, we pooled fractions 1 and 2 from the ten fractions obtained during the extraction and containing heavy polysomes. 3 µg of polysomal and total RNAs from each animal from each time point were pooled. These 6 µg of polysomal and total RNAs were used for the synthesis of biotinylated cRNAs according to Affymetrix protocol, and hybridized to mouse Affymetrix Mouse Genome 430 2.0 arrays. The chips were washed and scanned, and the fluorescence signal analysed with Affymetrix software. Data are deposited on the Gene Expression Omnibus database under the reference GSE33726 (<http://www.ncbi.nlm.nih.gov/geo/query/acc.cgi?token=rpwvtogqogkamwrm&acc=GSE33726>).

The raw data of all 48 arrays were normalized together using the robust multiarray average (RMA) method [72]. For the analysis, we filtered out all probesets corresponding to introns using the Ensembl annotation and then only kept genes with a sufficient expression level (we kept genes whose probe signal in the total fraction was above 5 in log₂ scale). For the identification of circadian probesets, the 24-h Fourier component (F24) and the phase were computed using established methods [73]. The associated *p*-value (*p*) was calculated using the Fisher test ($p = (1-s)^{10}$) [73]. For the identification of rhythmically translated genes, the difference between polysomal and total RNAs was subjected to Fourier analysis and we selected probesets giving a *p*-value inferior to 0.001. In addition, we requested that the peak to trough amplitude in the polysomal signal be above 1.2-fold.

Nuclear and Cytoplasmic Protein Extractions and Analysis

Nuclear and cytoplasmic proteins were extracted mostly as described [25]. Briefly, liver were homogenized in sucrose homogenization buffer containing 2.2 M sucrose, 15 mM KCl, 2 mM EDTA, 10 mM HEPES (pH 7.6), 0.15 mM spermin, 0.5 mM spermidin, 1 mM DTT, and the same protease inhibitor cocktail as for polysomes extraction. Lysates were deposited on a sucrose cushion containing 2.05 M sucrose, 10% glycerol, 15 mM KCl, 2 mM EDTA, 10 mM HEPES (pH 7.6), 0.15 mM spermin, 0.5 mM spermidin, 1 mM DTT, and a protease inhibitor cocktail. Tubes were centrifuged during 45 min at 105,000 *g* at 4°C. After ultra-centrifugation, supernatants containing soluble cytoplasmic proteins were harvested, homogenised, and centrifuged for 2 h at 200,000 *g* to remove ribosomes. These supernatants constitute cytoplasmic extracts. The nucleus pellets were suspended in a nucleus lysis buffer composed of 10 mM HEPES (pH 7.6), 100 mM KCl, 0.1 mM EDTA, 10% Glycerol, 0.15 mM spermine, 0.5 mM spermidine, 0.1 mM NaF, 0.1 mM sodium orthovanadate, 0.1 mM ZnSO₄, 1 mM DTT, and the previously described protease inhibitor cocktail. Nuclear extracts were obtained by the addition of an equal volume of NUN buffer composed of 2 M urea, 2% nonidet P-40, 600 mM NaCl, 50 mM HEPES (pH 7.6), 1 mM DTT, and a cocktail of protease

inhibitor, and incubation 20 min on ice. After centrifugation during 10 min at 21,000 *g*, the supernatants were harvested and constitute nuclear extracts.

25 µg of nuclear or 12.5 µg cytoplasmic extracts were used for western blotting. After migration, proteins were transferred to PVDF membranes and Western blotting was realized according to standard procedures. References for the antibodies are given in Table S11.

Total Protein Extraction and Analysis

Organs were homogenized in lysis buffer containing 20 mM HEPES (pH 7.6), 100 mM KCl, 0.1 mM EDTA, 1 mM NaF, 1 mM sodium orthovanadate, 1% Triton X-100, 0.5% Nonidet P-40, 0.15 mM spermin, 0.5 mM spermidin, 1 mM DTT, and a protease inhibitor cocktail. After incubation 30 min on ice, extracts were centrifuged 10 min at 21,000 *g* and the supernatants were harvested to obtain total extracts.

65 µg of extract was used for Western blotting. After migration, proteins were transferred to PVDF membranes and Western blotting was realized according to standard procedures. References for the antibodies are given in Table S11.

7-methyl GTP Sepharose Affinity Protein Purification

7-methyl GTP sepharose 4B beads (GE Healthcare) were washed twice in the previously described liver lysis buffer. 250 µg of liver protein extracts were diluted in 500 µl of lysis buffer containing 1 mM DTT and a cocktail of protease inhibitor and incubated for 2 h on a rotating wheel at 4°C with 20 µl of beads. After incubation, cap-binding-proteins coated beads were washed five times in 500 µl of liver lysis buffer containing 0.5 mM PMSF and 1 mM DTT. 7-methyl GTP bound proteins were eluted by SDS-PAGE loading buffer, separated by SDS-PAGE, transferred to PVDF membranes, and analysed by Western blotting as described.

Statistical Analysis of Genes and Proteins Expression

Mean and standard error of the mean were computed for each time point. The rhythmic characteristics of the expression of each gene or protein were assessed by a Cosinor analysis [74]. This method characterizes a rhythm by the parameters of the fitted cosine function best approximating the data. A period of 24 h was a priori considered. The rhythm characteristics estimated by this linear least squares method include the mesor (rhythm-adjusted mean), the double amplitude (difference between minimum and maximum of fitted cosine function), and the acrophase (time of maximum in fitted cosine function). A rhythm was detected if the null hypothesis was rejected with *p*<0.05. In such a case, the 95% confidence limits of each parameter were computed. The Cosinor 2.3 software used in this study has been elaborated by the Circadian Rhythm Laboratory at University of South Carolina and is freely available at this address: <http://www.circadian.org/software.html>. The statistical significance of differences in the mesor was evaluated by a Student's *t*-test.

Supporting Information

Figure S1 Temporal expression and phosphorylation of translation initiation factors in WT mice. Mean ± standard error of the mean (SEM) (*n* = 3) densitometric values of the Western blot data depicted in Figure 1B were represented according to the zeitgeber time. Statistical analysis of these data is given in Table S2. (TIF)

Figure S2 Temporal expression and phosphorylation of proteins involved in signaling pathways activation and translational initiation in WT mice. (A) Mean \pm standard error of the mean (SEM) ($n=3$) densitometric values of the Western blot data depicted in Figure 2A were represented according to the zeitgeber time. (B) Mean \pm SEM ($n=2$) densitometric values of the Western blot data depicted in Figure 2B were represented according to the zeitgeber time. Statistical analysis of these data is given in Table S2. (TIF)

Figure S3 Temporal expression of TORC1 components and of kinases regulating TORC1 and EIF4E activities in WT mice. (A) Temporal expression of the TORC1 components *mTor* and *Raptor* at the mRNA level (upper panel) and protein level (lower panel) in mouse liver. mRNA expressions were measured by real-time RT-PCR. For each time point, data are mean \pm standard error of the mean (SEM) obtained from four independent animals. Expression of mTOR and RAPTOR and its phosphorylation on Serine 792 were measured by Western blot on total extracts. The phosphorylation of RAPTOR on Serine 792 by AMPK has been shown to reduce TORC1 activity [75] and contributes to the inhibition of TORC1 during the day. Naphtol blue black staining of the membranes was used as a loading control. (B) Temporal expression of *Map4k3* (left panel) and *Mnk2* mRNA (right panel) in mouse liver. mRNA expressions were measured by real-time RT-PCR. For each time point, data are mean \pm SEM obtained from four independent animals. MAP4K3 plays a role in the activation of TORC1 by amino acids [76], whereas MNK2 is involved in the ERK signaling cascade leading to the phosphorylation of EIF4E, which can play a role in 5'-TOP mRNA translation [9]. (TIF)

Figure S4 Rhythmic expression of mRNA encoding translation initiation factors (*Eif4b*, *Eif4ebp3*), the TORC1 complex component *mTor*, the kinase activating these factors *Mnk2*, and proteins involved in rRNA synthesis (*Ubf1*) and ribosome biogenesis (*Rpl23*) is independent of food and light. (A) Temporal expression in constant darkness. (B) Temporal expression during starvation. (C) Temporal expression during starvation in constant darkness. mRNA expressions were measured by real-time RT-PCR. For each time point, data are mean \pm SEM obtained from three independent animals. The circadian (CT) or zeitgeber (ZT) times at which the animals were sacrificed are indicated on the bottom of the figures. (TIF)

Figure S5 Rhythmic activation of TORC1 still occurs in constant conditions. (A) Temporal phosphorylation of TORC1 substrates during 48 h in constant darkness. The lines through gels indicate where the images have been cropped. (B) Temporal phosphorylation of TORC1 substrates during starvation. As reported [14], the period of activation seems to be shorter in these conditions. Interestingly, this activation is antiphasic with the rhythmic activation of autophagy in mouse liver [15], a process inhibited by TORC1 but able to generate amino acids that can in turn activate TORC1 [16]. (C) Temporal phosphorylation of the TORC1 substrate RPS6 during starvation in constant darkness. Temporal expression and phosphorylation of RPS6 and 4E-BP1 were measured by Western blot on total extracts. Naphtol blue black staining of the membranes was used as a loading control. The circadian (CT) or zeitgeber (ZT) times at which the animals were sacrificed are indicated on the top of the figures. (TIF)

Figure S6 Rhythmic activation of TORC1 in different mouse organs. Temporal activation of the TORC1 pathway in mouse organs, revealed by phosphorylation of RPS6. As in the liver, this rhythmic activation is kept in kidney and heart, nevertheless with reduced amplitude (indicated by the blot with a shortest exposure). However, TORC1 activation is constant in brain, lung, and small intestine, suggesting that nutrient availability due to rhythmic feeding is not sufficient to explain this phenomenon. The zeitgeber times (ZT) at which the animals were sacrificed are indicated on each panel. Naphtol blue black staining of the membranes was used as a loading control. (TIF)

Figure S7 The polysomal fraction is rhythmic in mouse liver. Temporal fraction of ribosomes in the polysomal fraction. The percentage is obtained by dividing the optical density obtained for the polysomal fraction by the total of optical density obtained for polysomes and monosomes ($n=5$). The rhythmic nature of this fraction (and thus translation) is confirmed by cosinor analysis ($p \leq 0.005$, $F[2,9] = 11.00$, robustness = 61.3%, Mesor = 76.24, amplitude = 5.50, and phase = 18.09 h). This result confirms past biochemical [17] and morphometric [18] studies describing a rhythmic polysomal fraction in rodent liver with a nadir at ZT6. Interestingly, this time corresponds to the maximum of activity of AMPK [12], which inhibits TORC1 activity through phosphorylation of TSC2 [77] and RAPTOR [75]. The zeitgeber times (ZT) at which the animals were sacrificed are indicated on the bottom of the figure. (TIF)

Figure S8 The temporal profiles of polysomal mRNAs closely follow that of total mRNAs for most circadian genes, as exemplified by the *Period* genes. (A) Temporal profiles ordered by phase in total (left panel) and polysomal RNA (right panel) fractions of microarray probes presenting a rhythmic profile in total mRNA fraction. Data were mean centered and standardized. Log-ratios are color-coded so that red indicates high and green low relative levels of mRNA. For most of the probes, the profiles are strikingly similar in the two fractions, indicating constant translational efficacy along the day. (B) Temporal expression of *Per1* (left panel) and *Per2* (right panel) mRNAs in polysomal (red line) and total (blue line) RNA fractions. Data are represented in log scale without any additional normalization than the one provided by the Affymetrix software. Although a regulation of PER1 expression at the translational level has been proposed [78,79], this hypothesis is not confirmed by our in vivo data as the two profiles are extremely similar. (TIF)

Figure S9 Comparative diurnal expression profile of RNA in total and polysomal fractions. Temporal profiles of total RNA (left panel) and polysomal RNA (right panel) fractions of microarray probes presenting a rhythmic polysomal/total RNA ratio. The profiles are ordered by the phase of the polysomal/total ratio phase. Data were mean centered and standardized. Log-ratios are color-coded so that red indicates high and green low relative levels of mRNA. (TIF)

Figure S10 Diurnal expression of selected 5'-TOP mRNAs in total and polysomal fractions. Temporal real-time RT-PCR profile of selected 5'-TOP mRNA expression in the total RNA (black line) and polysomal RNA (red line) fractions from mouse liver. For each time point, data are mean \pm standard error of the mean (SEM) obtained from four independent animals. In addition to three ribosomal protein mRNA, which are known to

have a 5'-TOP and be regulated by TORC1 [19], we selected also *Receptor of Activated protein Kinase C 1 (Rack1)* or *Guanine Nucleotide Binding protein (G protein)*, *Beta polypeptide 2-Like 1 (Gnb2l1)*, a ribosome constituent [80] known to be regulated by TORC1 [81], which also plays a role in circadian clock regulation [82]. However, a potential role of *Rack1* rhythmic translation on the circadian clock is not documented. The zeitgeber times (ZT) at which the animals were sacrificed are indicated on each panel. (TIF)

Figure S11 Temporal expression of ribosomal proteins in mouse liver. Mean \pm standard error of the mean (SEM) ($n = 3$) densitometric values of the Western blot data depicted in Figure 3D were represented according to the zeitgeber time. Statistical analysis of these data is given in Table S2. (TIF)

Figure S12 Temporal expression of UBF1 in WT, and in *Cry1/Cry2* KO, and *Bmal1* KO mouse liver. (A) Mean \pm standard error of the mean (SEM) ($n = 3$) densitometric values of the Western blot data depicted in Figure 4B were represented according to the zeitgeber time. Statistical analysis of these data is given in Table S2. (B) Mean \pm SEM ($n = 2$) densitometric values of the Western blot data depicted in Figure 4C (*Cry1/Cry2* KO mice) and 4D (*Bmal1* KO mice) were represented according to the zeitgeber time. Statistical analysis of these data is given in Tables S7 and S8, respectively. (TIF)

Figure S13 Activation of the TORC1, PI3K, and ERK pathways in *Cry1/Cry2* and *Bmal1* KO mice kept in constant darkness. (A) Temporal phosphorylation of RPS6, AKT, and ERK in mouse mutant liver. *Cry1/Cry2* and *Bmal1* KO mice were placed in constant darkness for 3 d and then sacrificed every 4 h during a 24-h period. Total liver extracts were used for Western blotting. The circadian (CT) times at which the animals were sacrificed are indicated on the top of the figures. As expected, rhythmic activation of the three pathways is lost under these conditions. (B) Six *Cry1/Cry2* KO mice were kept in constant darkness for one week and then sacrificed at CT12. Phosphorylation of RPS6, AKT and ERK were evaluated by Western blotting on total liver extracts. We observed as expected in these conditions a high degree of variability in the activation of the three pathways, probably due to the arrhythmic food consumption of the animals. However, the ERK pathway seems to be less affected. A quantification of these data is given on the right part of the figure. Naphtol blue black staining of the membranes was used as a loading control. (TIF)

Figure S14 Diurnal expression of genes encoding proteins involved in TORC1 complex, mRNA translation initiation and RPs synthesis in WT and *Cry1/Cry2* KO mice. Temporal real-time RT-PCR expression of genes encoding proteins involved in TORC1 complex (*mTor* and *Raptor*), mRNA translation initiation (*Eif4b* and *Eif4ebp3*), and RP synthesis (*Rpl32* and *Rpl34* pre-mRNA) in total RNA from WT (black line) and *Cry1/Cry2* KO (red line) mouse liver. For each time point, data are mean \pm standard error of the mean (SEM) obtained from four (WT) and three (KO) independent animals. The zeitgeber times (ZT) at which the animals were sacrificed are indicated on each panel. (TIF)

Figure S15 Diurnal expression of genes encoding proteins involved in TORC1 complex, mRNA translation initiation, and RP synthesis in WT and *Bmal1* KO mice.

Temporal real-time RT-PCR expression of genes encoding proteins involved in TORC1 complex (*mTor* and *Raptor*), mRNA translation initiation (*Eif4b* and *Eif4ebp3*), and RP synthesis (*Rpl32* and *Rpl34* pre-mRNA) in total RNA from WT (black line) and *Bmal1* KO (red line) mouse liver. For each time point, data are mean \pm standard error of the mean (SEM) obtained from two independent animals. The zeitgeber times (ZT) at which the animals were sacrificed are indicated on each panel. (TIF)

Figure S16 Temporal expression and phosphorylation of proteins involved in translational initiation, signaling pathways activation, and ribosome biogenesis in *Cry1/Cry2* KO mice. (A) Mean \pm standard error of the mean (SEM) ($n = 2$) densitometric values of the Western blot data depicted in Figure 6A were represented according to the zeitgeber time. (B) Mean \pm SEM ($n = 2$) densitometric values of the Western blot data depicted in Figure 6B were represented according to the zeitgeber time. Statistical analysis of these data is given in Table S7. It is interesting to note that expression of EIF4E is slightly increased in the KO (Student's *t*-test $p \leq 0.05$), in agreement with the increased mRNA expression. It is also the case for RPS6 whose expression increase like most of the other RP proteins (Student's *t*-test $p \leq 3 \times 10^{-6}$). (TIF)

Figure S17 Temporal expression and phosphorylation of proteins involved in translational initiation, signaling pathways activation, and ribosome biogenesis in *Bmal1* KO mice. (A) Mean \pm standard error of the mean (SEM) ($n = 2$) densitometric values of the Western blot data depicted in Figure 6C were represented according to the zeitgeber time. (B) Mean \pm SEM ($n = 2$) densitometric values of the Western blot data depicted in Figure 6D were represented according to the zeitgeber time. Statistical analysis of these data is given in Table S8. (TIF)

Figure S18 Example of polysomes purification profile. Optic density at 260 nm of the 45 sub-fractions obtained after ultracentrifugation of liver extract from mouse sacrificed at ZT8. These fractions are then pooled in ten fractions and the fractions 1 and 2 are pooled to obtain the polysomal fraction used in microarray and RT-PCR experiments. (TIF)

Table S1 Cosinor statistical values related to rhythmic mRNA expression of genes coding for proteins involved in mRNA translation, TORC1 complex, and ribosome biogenesis. A Cosinor statistical analysis was applied to the rhythmic datasets corresponding to the respective expression of the indicated mRNA measured by quantitative PCR in WT mice and shown on Figures 1, 4, and S3. (DOC)

Table S2 Cosinor statistical values related to rhythmic expression and phosphorylations of proteins involved in mRNA translation, TORC1 complex, and ribosome biogenesis. A Cosinor statistical analysis was applied to the rhythmic datasets corresponding to the respective expression of the indicated proteins measured by Western blots quantification in WT mice and shown on Figures S1, S2, S11, and S12. (DOC)

Table S3 Affymetrix microarray probes presenting a rhythmic polysomal/total RNA ratio and in phase with TORC1 activation (complement to Figure 3A). Affymetrix microarray probes presenting a rhythmic polysomal/total RNA

ratio and in phase with TORC1 activation were classified according to the phase of the maximum value (all include between ZT14 and ZT18).
(XLS)

Table S4 Functions of the genes presenting a rhythmic total/polysomal RNA ratio. Most of the genes found regulated at the translational level are known 5'-TOP containing genes. They include almost all the RP coding genes: 28 of the 32 small RP genes and 42 of the 47 large RP genes expressed in mouse [83] are found on the list. The list also includes known 5'-TOP mRNA encoding proteins involved in the regulation of translation: translation initiation factors of the class 2, 3, and 4, first class of translation elongation factors, and poly-A binding proteins [19]. In addition, the list contains genes encoding proteins involved at different steps of translational regulation and ribosome biogenesis: NPM1, a chaperone protein involved in ribosome assembly and rRNA maturation [84]; CCT4, a member of the chaperonin complex that plays a role in ribosome biogenesis [85]; TPT1, a guanine nucleotide exchanger that controls TORC1 activity through regulation of the RHEB GTPase [86]; IGBP1, a regulatory subunit of protein phosphatase 2A that modulates TORC1 activity [87]; PFDN5, a chaperone protein that modulates MYC activity [88]; a transcription factor involved in rRNA and RP mRNA transcription [89]; AHCY, a *S*-adenosyl homocysteine hydrolase that regulates translation also through modulation of MYC activity [90]; GNB2L1 or RACK1, a scaffold protein that interacts with and modulates ribosome activity [80]; UBA52, a protein constitutes by the fusion of a ribosomal protein and ubiquitin [91]; The remaining genes encode proteins with unknown function in translation regulation.
(DOC)

Table S5 Cosinor statistical values related to rhythmic mRNA expression of genes coding for proteins involved in mRNA translation, TORC1 complex, and ribosome biogenesis in WT and *Cry1/Cry2* KO mice. A Cosinor statistical analysis was applied to the rhythmic datasets corresponding to the respective expression of the indicated mRNA measured by quantitative PCR in WT and *Cry1/Cry2* KO mice and shown on Figures 4, 5, and S14.
(DOC)

Table S6 Cosinor statistical values related to rhythmic mRNA expression of genes coding for proteins involved in mRNA translation, TORC1 complex and ribosome biogenesis in WT and *Bmal1* KO mice. A Cosinor statistical analysis was applied to the rhythmic datasets corresponding to the respective expression of the indicated mRNA measured by

quantitative PCR in WT and *Bmal1* KO mice and shown on Figures 4, 5, and S15.
(DOC)

Table S7 Cosinor statistical values related to rhythmic expression and phosphorylation of proteins involved in mRNA translation, TORC1 complex and ribosome biogenesis in WT and *Cry1/Cry2* KO mice. A Cosinor statistical analysis was applied to the rhythmic datasets corresponding to the respective expression of the indicated proteins measured by Western blots quantification in WT and *Cry1/Cry2* KO mice and shown on Figures S12 and S16.
(DOC)

Table S8 Cosinor statistical values related to rhythmic expression and phosphorylation of proteins involved in mRNA translation, TORC1 complex, and ribosome biogenesis in WT and *Bmal1* KO mice. A Cosinor statistical analysis was applied to the rhythmic datasets corresponding to the respective expression of the indicated proteins measured by Western blots quantification in WT and *Bmal1* KO mice and shown on Figures S12 and S17.
(DOC)

Table S9 Taqman probes used for real-time PCR (Applied Biosystems).
(DOC)

Table S10 Sequences of the primers used for SYBR Green real-time PCR.
(DOC)

Table S11 References of the antibodies used for Western blotting [92,93].
(DOC)

Acknowledgments

We thank Mikael Le Clech and Benjamin Bieche for their technical assistance, and David Gatfield and Vjekoslav Dulic for critical reading of the manuscript. Affymetrix microarrays were processed in the Microarray Core Facility of the Institute of Research of Biotherapy, CHRU-INSERM-UMI, Montpellier (France). We also extend our thanks to the Institut de Génétique Humaine, CNRS UPR 1142, Montpellier (France), where a part of this work was conducted, for generous support.

Author Contributions

The author(s) have made the following declarations about their contributions: Conceived and designed the experiments: CJ GC FG. Performed the experiments: CJ GC EM FA FG. Analyzed the data: LS FN FG. Wrote the paper: FG FN.

References

- Bass J, Takahashi JS (2010) Circadian integration of metabolism and energetics. *Science* 330: 1349–1354.
- Zhang EE, Kay SA (2010) Clocks not winding down: unravelling circadian networks. *Nat Rev Mol Cell Biol* 11: 764–776.
- Doherty CJ, Kay SA (2010) Circadian control of global gene expression patterns. *Annu Rev Genet* 44: 419–444.
- Reddy AB, Karp NA, Maywood ES, Sage EA, Deery M, et al. (2006) Circadian orchestration of the hepatic proteome. *Curr Biol* 16: 1107–1115.
- Panda S, Antoch MP, Miller BH, Su AI, Schook AB, et al. (2002) Coordinated transcription of key pathways in the mouse by the circadian clock. *Cell* 109: 307–320.
- Hughes ME, DiTacchio L, Hayes KR, Vollmers C, Pulivarthy S, et al. (2009) Harmonics of circadian gene transcription in mammals. *PLoS Genet* 5: e1000442. doi:10.1371/journal.pgen.1000442
- Jackson RJ, Hellen CUT, Pestova TV (2010) The mechanism of eukaryotic translation initiation and principles of its regulation. *Nat Rev Mol Cell Biol* 11: 113–127.
- Laplanche M, Sabatini DM (2012) mTOR signaling in growth control and disease. *Cell* 149: 274–293.
- Silva RLA, Wendel H-G (2008) MNK, EIF4E and targeting translation for therapy. *Cell Cycle* 7: 553–555.
- Ma XM, Blenis J (2009) Molecular mechanisms of mTOR-mediated translational control. *Nat Rev Mol Cell Biol* 10: 307–318.
- Mendoza MC, Er EE, Blenis J (2011) The Ras-ERK and PI3K-mTOR pathways: cross-talk and compensation. *Trends Biochem Sci* 36: 320–328.
- Lamia KA, Sachdeva UM, DiTacchio L, Williams EC, Alvarez JG, et al. (2009) AMPK regulates the circadian clock by cryptochrome phosphorylation and degradation. *Science* 326: 437–440.
- Zoncu R, Efeyan A, Sabatini DM (2011) mTOR: from growth signal integration to cancer, diabetes and ageing. *Nat Rev Mol Cell Biol* 12: 21–35.
- LeBouton A, Handler S (1971) Persistent circadian rhythmicity of protein synthesis in the liver of starved rats. *Experientia* 27: 1031–1032.
- Ma D, Panda S, Lin JD (2011) Temporal orchestration of circadian autophagy rhythm by C/EBP β . *EMBO J* 30: 4642–4651.
- Neufeld TP (2010) TOR-dependent control of autophagy: biting the hand that feeds. *Curr Opin Cell Biol* 22: 157–168.

17. Fishman B, Wurtman RJ, Munro HN (1969) Daily rhythms in hepatic polysome profiles and tyrosine transaminase activity: role of dietary protein. *Proc Natl Acad Sci U S A* 64: 677–682.
18. Uchiyama Y, Asari A (1984) A morphometric study of the variations in subcellular structures of rat hepatocytes during 24 hours. *Cell Tissue Res* 236: 305–315.
19. Meyuhos O, Drazan A (2009) Ribosomal protein S6 kinase: from TOP mRNAs to cell size. *Prog Mol Biol Transl Sci* 90: 109–153.
20. Mamane Y, Petroulakis E, Martineau Y, Sato T-A, Larsson O, et al. (2007) Epigenetic activation of a subset of mRNAs by eIF4E explains its effects on cell proliferation. *PLoS ONE* 2: e242. doi:10.1371/journal.pone.0000242
21. Bianchini A, Loiarro M, Bielli P, Busà R, Paronetto MP, et al. (2008) Phosphorylation of eIF4E by MNKs supports protein synthesis, cell cycle progression and proliferation in prostate cancer cells. *Carcinogenesis* 29: 2279–2288.
22. Hirsch CA, Hiatt HH (1966) Turnover of liver ribosomes in fed and in fasted rats. *J Biol Chem* 241: 5936–5940.
23. Lam YW, Lamond AI, Mann M, Andersen JS (2007) Analysis of nucleolar protein dynamics reveals the nuclear degradation of ribosomal proteins. *Curr Biol* 17: 749–760.
24. Geyer PK, Meyuhos O, Perry RP, Johnson LF (1982) Regulation of ribosomal protein mRNA content and translation in growth-stimulated mouse fibroblasts. *Mol Cell Biol* 2: 685–693.
25. Gachon F, Fleury Olela F, Schaad O, Descombes P, Schibler U (2006) The circadian PAR-domain basic leucine zipper transcription factors DBP, TEF, and HLF modulate basal and inducible xenobiotic detoxification. *Cell Metab* 4: 25–36.
26. Abruzzi KC, Rodriguez J, Menet JS, Desrochers J, Zadina A, et al. (2011) *Drosophila* CLOCK target gene characterization: implications for circadian tissue-specific gene expression. *Genes Dev* 25: 2374–2386.
27. Laferté A, Favry E, Sentenac A, Riva M, Carles C, et al. (2006) The transcriptional activity of RNA polymerase I is a key determinant for the level of all ribosome components. *Genes Dev* 20: 2030–2040.
28. Grewal SS, Evans JR, Edgar BA (2007) *Drosophila* TIF-IA is required for ribosome synthesis and cell growth and is regulated by the TOR pathway. *J Cell Biol* 179: 1105–1113.
29. Sanij E, Hannan RD (2009) The role of UBF in regulating the structure and dynamics of transcriptionally active rDNA chromatin. *Epigenetics* 4: 374–382.
30. van der Horst GTJ, Muijijens M, Kobayashi K, Takano R, Kanno S-i, et al. (1999) Mammalian Cry1 and Cry2 are essential for maintenance of circadian rhythms. *Nature* 398: 627–630.
31. Bunger MK, Wilsbacher LD, Moran SM, Clendenin C, Radcliffe LA, et al. (2000) Mop3 is an essential component of the master circadian pacemaker in mammals. *Cell* 103: 1009–1017.
32. Berset C, Trachsel H, Altmann M (1998) The TOR (target of rapamycin) signal transduction pathway regulates the stability of translation initiation factor eIF4G in the yeast *Saccharomyces cerevisiae*. *Proc Natl Acad Sci U S A* 95: 4264–4269.
33. Seite R, Pébusque M-J (1985) Chronobiological studies on the nucleolus. *Chronobiol Int* 2: 69–91.
34. Hernandez-Verdun D (2006) The nucleolus: a model for the organization of nuclear functions. *Histochem Cell Biol* 126: 135–148.
35. Dong W, Tang X, Yu Y, Nilsen R, Kim R, et al. (2008) Systems biology of the clock in *Neurospora crassa*. *PLoS ONE* 3: e3105. doi:10.1371/journal.pone.0003105
36. Piques M, Schulze WX, Hohne M, Usadel B, Gibon Y, et al. (2009) Ribosome and transcript copy numbers, polysome occupancy and enzyme dynamics in *Arabidopsis*. *Mol Syst Biol* 5: 314.
37. Xu W, Yang R, Li M, Xing Z, Yang W, et al. (2011) Transcriptome phase distribution analysis reveals diurnal regulated biological processes and key pathways in rice flag leaves and seedling leaves. *PLoS ONE* 6: e17613. doi:10.1371/journal.pone.0017613
38. Warner JR (1999) The economics of ribosome biosynthesis in yeast. *Trends Biochem Sci* 24: 437–440.
39. Asmal M, Colgan J, Naef F, Yu B, Lee Y, et al. (2003) Production of ribosome components in effector CD4⁺ T cells is accelerated by TCR stimulation and coordinated by ERK-MAPK. *Immunity* 19: 535–548.
40. Reischl S, Kramer A (2011) Kinases and phosphatases in the mammalian circadian clock. *FEBS Lett* 585: 1393–1399.
41. Obrietan K, Impey S, Storm DR (1998) Light and circadian rhythmicity regulate MAP kinase activation in the suprachiasmatic nuclei. *Nat Neurosci* 1: 693–700.
42. Cao R, Anderson FE, Jung YJ, Dziema H, Obrietan K (2011) Circadian regulation of mammalian target of rapamycin signaling in the mouse suprachiasmatic nucleus. *Neuroscience* 181: 79–88.
43. Cao R, Lee B, Cho H-y, Saklayen S, Obrietan K (2008) Photic regulation of the mTOR signaling pathway in the suprachiasmatic circadian clock. *Mol Cell Neurosci* 38: 312–324.
44. Ko ML, Jian K, Shi L, Ko GY-P (2009) Phosphatidylinositol 3 kinase–Akt signaling serves as a circadian output in the retina. *J Neurochem* 108: 1607–1620.
45. Zheng X, Sehgal A (2010) AKT and TOR signaling set the pace of the circadian pacemaker. *Curr Biol* 20: 1203–1208.
46. Vollmers C, Gill S, DiTacchio L, Pulivarthy SR, Le HD, et al. (2009) Time of feeding and the intrinsic circadian clock drive rhythms in hepatic gene expression. *Proc Natl Acad Sci U S A* 106: 21453–21458.
47. Cretenet G, Le Clech M, Gachon F (2010) Circadian clock-coordinated 12 hr period rhythmic activation of the IRE1 α pathway controls lipid metabolism in mouse liver. *Cell Metab* 11: 47–57.
48. Bishop NA, Guarente L (2007) Genetic links between diet and lifespan: shared mechanisms from yeast to humans. *Nat Rev Genet* 8: 835–844.
49. Honjoh S, Yamamoto T, Uno M, Nishida E (2009) Signalling through RHEB-1 mediates intermittent fasting-induced longevity in *C. elegans*. *Nature* 457: 726–730.
50. Zid BM, Rogers AN, Katewa SD, Vargas MA, Kolipinski MC, et al. (2009) 4E-BP extends lifespan upon dietary restriction by enhancing mitochondrial activity in *Drosophila*. *Cell* 139: 149–160.
51. Vellai T, Takacs-Vellai K, Zhang Y, Kovacs AL, Orosz L, et al. (2003) Genetics: influence of TOR kinase on lifespan in *C. elegans*. *Nature* 426: 620–620.
52. Kapahi P, Zid BM, Harper T, Koslover D, Sapin V, et al. (2004) regulation of lifespan in *drosophila* by modulation of genes in the TOR signaling pathway. *Curr Biol* 14: 885–890.
53. Luong N, Davies CR, Wessells RJ, Graham SM, King MT, et al. (2006) Activated FOXO-mediated insulin resistance is blocked by reduction of TOR activity. *Cell Metab* 4: 133–142.
54. Harrison DE, Strong R, Sharp ZD, Nelson JF, Astle CM, et al. (2009) Rapamycin fed late in life extends lifespan in genetically heterogeneous mice. *Nature* 460: 392–395.
55. Selman C, Tullet JMA, Wieser D, Irvine E, Lingard SJ, et al. (2009) Ribosomal protein S6 kinase 1 signaling regulates mammalian life span. *Science* 326: 140–144.
56. Hansen M, Taubert S, Crawford D, Libina N, Lee S-J, et al. (2007) Lifespan extension by conditions that inhibit translation in *Caenorhabditis elegans*. *Aging Cell* 6: 95–110.
57. Pan KZ, Palter JE, Rogers AN, Olsen A, Chen D, et al. (2007) Inhibition of mRNA translation extends lifespan in *Caenorhabditis elegans*. *Aging Cell* 6: 111–119.
58. Rogers Aric N, Chen D, McColl G, Czerwiec G, Felkey K, et al. (2011) Life span extension via eIF4G inhibition is mediated by posttranscriptional remodeling of stress response gene expression in *C. elegans*. *Cell Metab* 14: 55–66.
59. Syntichaki P, Troulinaki K, Tavernarakis N (2007) eIF4E function in somatic cells modulates ageing in *Caenorhabditis elegans*. *Nature* 445: 922–926.
60. Steffen KK, MacKay VL, Kerr EO, Tsuchiya M, Hu D, et al. (2008) Yeast life span extension by depletion of 60S ribosomal subunits is mediated by Gcn4. *Cell* 133: 292–302.
61. Kapahi P, Chen D, Rogers AN, Katewa SD, Li PW-L, et al. (2010) With TOR, less is more: a key role for the conserved nutrient-sensing TOR pathway in aging. *Cell Metab* 11: 453–465.
62. Dubrovsky YV, Samsa WE, Kondratov RV (2010) Deficiency of circadian protein CLOCK reduces lifespan and increases age-related cataract development in mice. *Aging (Albany NY)* 2: 936–944.
63. Kondratov RV, Kondratova AA, Gorbacheva VY, Vykhovalnet OV, Antoch MP (2006) Early aging and age-related pathologies in mice deficient in BMAL1, the core component of the circadian clock. *Genes Dev* 20: 1868–1873.
64. Lee S, Donehower LA, Herron AJ, Moore DD, Fu L (2010) Disrupting circadian homeostasis of sympathetic signaling promotes tumor development in mice. *PLoS ONE* 5: e10995. doi:10.1371/journal.pone.0010995
65. Davidson AJ, Sellix MT, Daniel J, Yamazaki S, Menaker M, et al. (2006) Chronic jet-lag increases mortality in aged mice. *Curr Biol* 16: R914–R916.
66. Gachon F, Firsov D (2011) The role of circadian timing system on drug metabolism and detoxification. *Expert Opin Drug Metab Toxicol* 7: 147–158.
67. Storch K-F, Paz C, Signorovitch J, Raviola E, Pawlyk B, et al. (2007) Intrinsic circadian clock of the mammalian retina: importance for retinal processing of visual information. *Cell* 130: 730–741.
68. Schwenk F, Baron U, Rajewsky K (1995) A *cre*-transgenic mouse strain for the ubiquitous deletion of *loxP*-flanked gene segments including deletion in germ cells. *Nucleic Acids Res* 23: 5080–5081.
69. Bur IM, Cohen-Solal AM, Carmignac D, Abecassis P-Y, Chauvet N, et al. (2009) The circadian clock components CRY1 and CRY2 are necessary to sustain sex dimorphism in mouse liver metabolism. *J Biol Chem* 284: 9066–9073.
70. Clancy JL, Nusch M, Humphreys DT, Westman BJ, Beilharz TH, et al. (2007) Methods to analyze microRNA-mediated control of mRNA translation. *Jon L, editor. Methods Enzymol: Academic Press*. pp. 83–111.
71. Chomczynski P, Sacchi N (1987) Single-step method of RNA isolation by acid guanidinium thiocyanate-phenol-chloroform extraction. *Anal Biochem* 162: 156–159.
72. Irizarry RA, Hobbs B, Collin F, Beazer-Barclay YD, Antonellis KJ, et al. (2003) Exploration, normalization, and summaries of high density oligonucleotide array probe level data. *Biostatistics* 4: 249–264.
73. Rey G, Cesbron F, Rougemont J, Reinke H, Brunner M, et al. (2011) Genome-wide and phase-specific DNA-binding rhythms of BMAL1 control circadian output functions in mouse liver. *PLoS Biol* 9: e1000595. doi:10.1371/journal.pbio.1000595
74. Nelson W, Tong YL, Lee JK, Halberg F (1979) Methods for cosinor-rhythmometry. *Chronobiologia* 6: 305–323.

75. Gwinn DM, Shackelford DB, Egan DF, Mihaylova MM, Mery A, et al. (2008) AMPK phosphorylation of raptor mediates a metabolic checkpoint. *Mol Cell* 30: 214–226.
76. Yan L, Mieulet V, Burgess D, Findlay GM, Sully K, et al. (2010) PP2A^{T61c} is an inhibitor of MAP4K3 in nutrient signaling to mTOR. *Mol Cell* 37: 633–642.
77. Inoki K, Zhu T, Guan K-L (2003) TSC2 mediates cellular energy response to control cell growth and survival. *Cell* 115: 577–590.
78. Kojima S, Matsumoto K, Hirose M, Shimada M, Nagano M, et al. (2007) LARK activates posttranscriptional expression of an essential mammalian clock protein, PERIOD1. *Proc Natl Acad Sci U S A* 104: 1859–1864.
79. Lee K-H, Woo K-C, Kim D-Y, Kim T-D, Shin J, et al. (2012) Rhythmic interaction between *Period1* mRNA and hnRNP Q leads to circadian time-dependent translation. *Mol Cell Biol* 32: 717–728.
80. Nilsson J, Sengupta J, Frank J, Nissen P (2004) Regulation of eukaryotic translation by the RACK1 protein: a platform for signalling molecules on the ribosome. *EMBO Rep* 5: 1137–1141.
81. Loreni F, Iadevaia V, Tino E, Caldarola S, Amaldi F (2005) RACK1 mRNA translation is regulated via a rapamycin-sensitive pathway and coordinated with ribosomal protein synthesis. *FEBS Lett* 579: 5517–5520.
82. Robles MS, Boyault C, Knutti D, Padmanabhan K, Weitz CJ (2010) Identification of RACK1 and protein kinase C α as integral components of the mammalian circadian clock. *Science* 327: 463–466.
83. Nakao A, Yoshihama M, Kenmochi N (2004) RPG: the ribosomal protein gene database. *Nucleic Acids Res* 32: D168–D170.
84. Lindström MS (2011) NPM1/B23: a multifunctional chaperone in ribosome biogenesis and chromatin remodeling. *Biochem Res Int* 2011.
85. Kabir MA, Sherman F (2008) Overexpressed ribosomal proteins suppress defective chaperonins in *Saccharomyces cerevisiae*. *FEMS Yeast Res* 8: 1236–1244.
86. Hsu Y-C, Chern JJ, Cai Y, Liu M, Choi K-W (2007) *Drosophila* TC1P is essential for growth and proliferation through regulation of dRheb GTPase. *Nature* 445: 785–788.
87. Grech G, Blázquez-Domingo M, Kolbus A, Bakker WJ, Müllner EW, et al. (2008) Igbp1 is part of a positive feedback loop in stem cell factor-dependent, selective mRNA translation initiation inhibiting erythroid differentiation. *Blood* 112: 2750–2760.
88. Mori K, Maeda Y, Kitaura H, Taira T, Iguchi-Ariga SMM, et al. (1998) MM-1, a novel c-Myc-associating protein that represses transcriptional activity of c-Myc. *J Biol Chem* 273: 29794–29800.
89. van Riggelen J, Yetil A, Felsher DW (2010) MYC as a regulator of ribosome biogenesis and protein synthesis. *Nat Rev Cancer* 10: 301–309.
90. Fernandez-Sanchez ME, Gonatopoulos-Pournatzis T, Preston G, Lawlor MA, Cowling VH (2009) S-Adenosyl homocysteine hydrolase is required for myc-induced mRNA cap methylation, protein synthesis, and cell proliferation. *Mol Cell Biol* 29: 6182–6191.
91. Baker RT, Board PG (1991) The human ubiquitin-52 amino acid fusion protein gene shares several structural features with mammalian ribosomal protein genes. *Nucleic Acids Res* 19: 1035–1040.
92. Brown SA, Ripperger J, Kadener S, Fleury-Olela F, Vilbois F, et al. (2005) PERIOD1-associated proteins modulate the negative limb of the mammalian circadian oscillator. *Science* 308: 693–696.
93. Preitner N, Damiola F, Luis-Lopez-Molina, Zakany J, Duboule D, et al. (2002) The orphan nuclear receptor REV-ERB α controls circadian transcription within the positive limb of the mammalian circadian oscillator. *Cell* 110: 251–260.

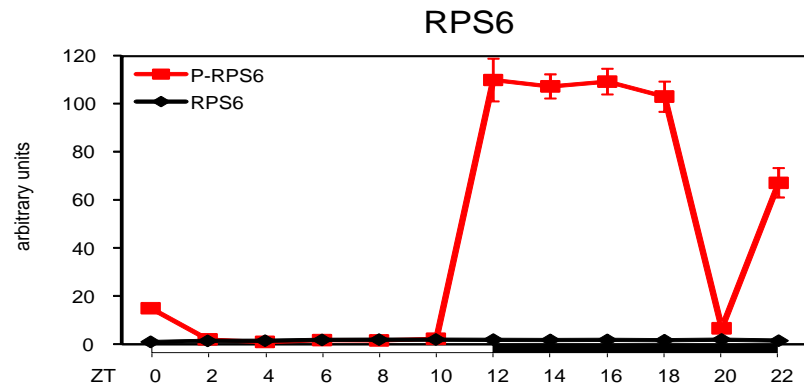
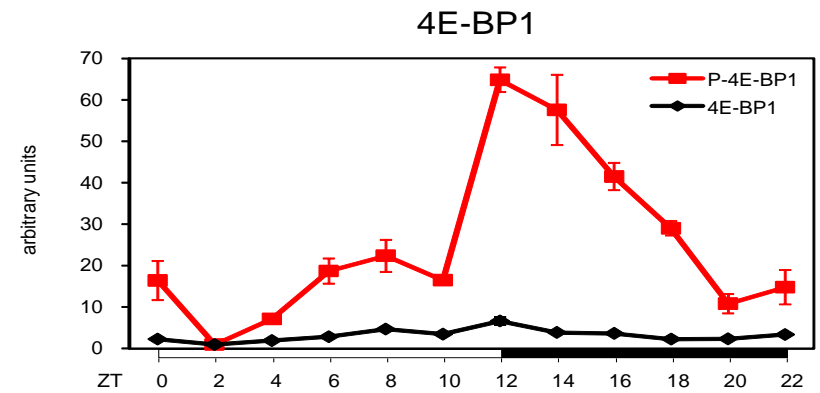
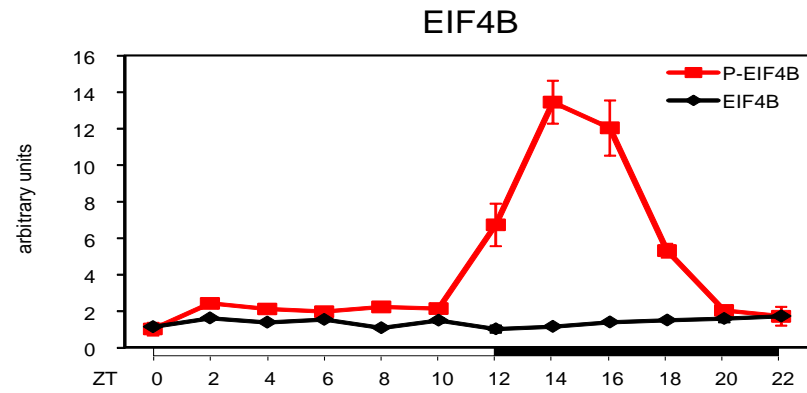
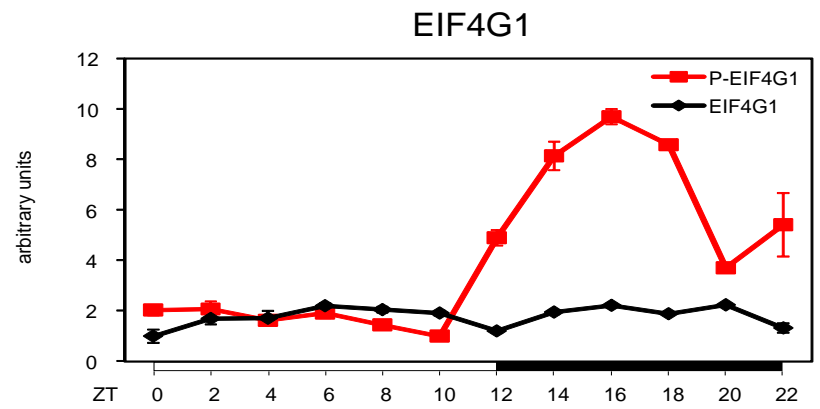
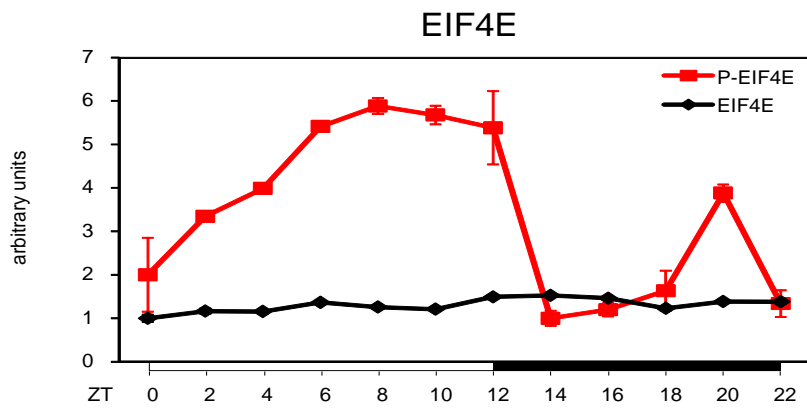
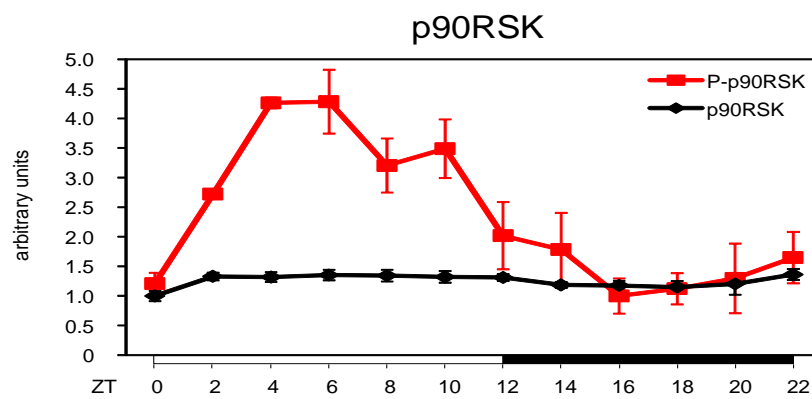
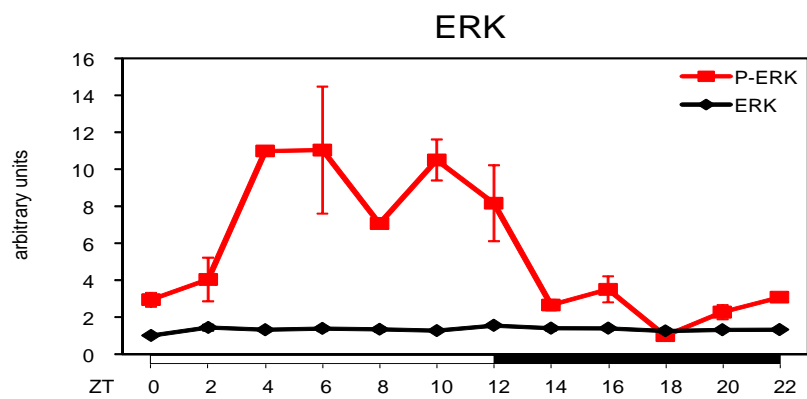
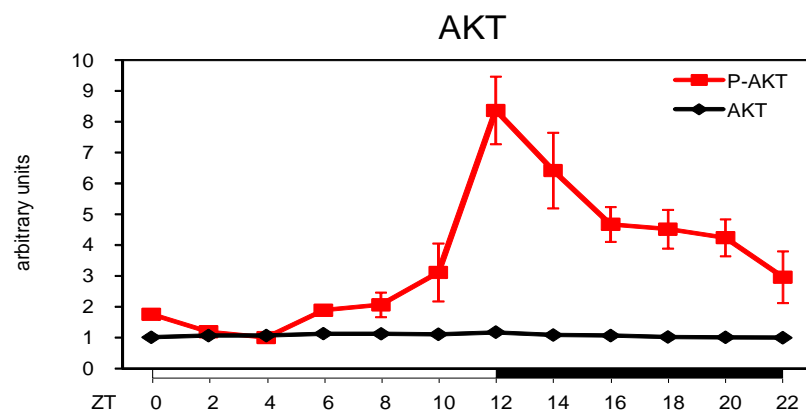
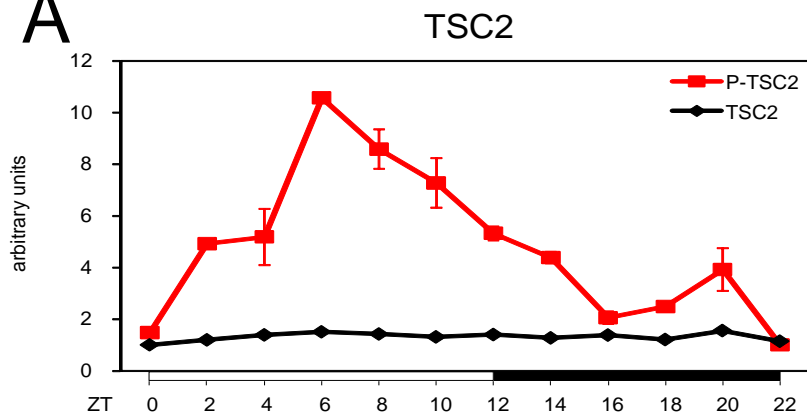
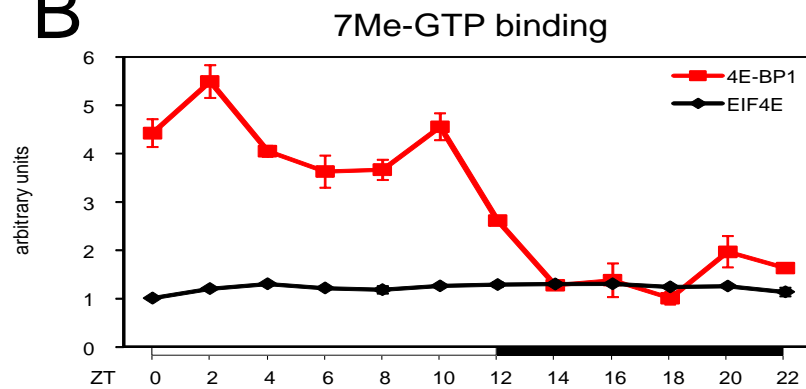
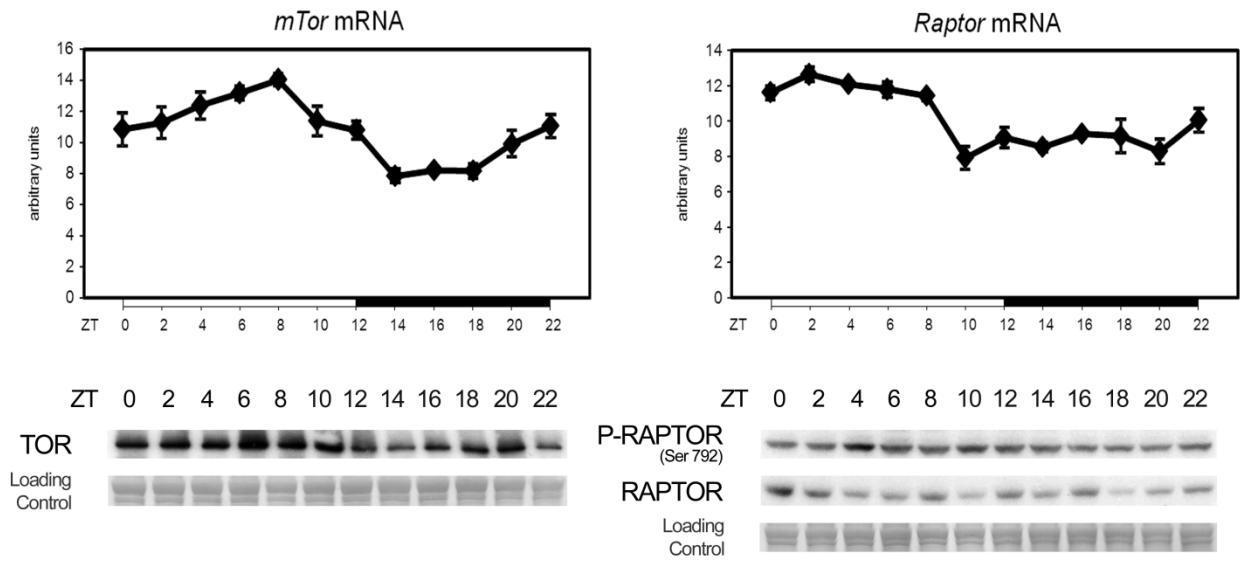
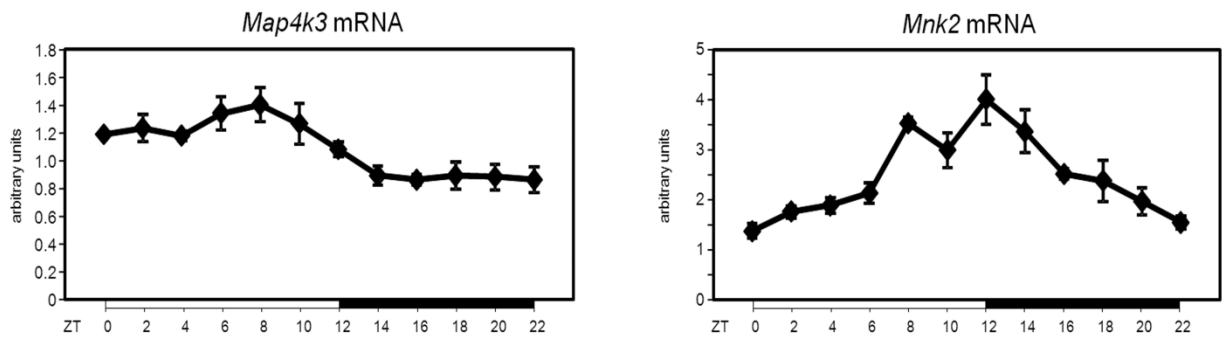


Figure S1

A**B****Figure S2**

A**B****Figure S3**

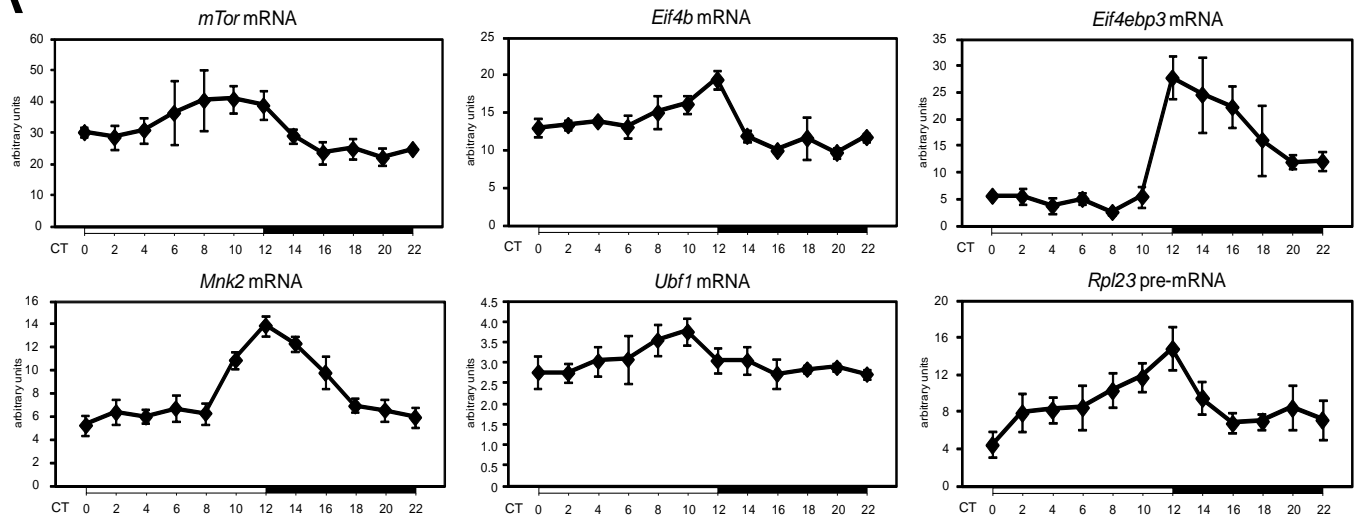
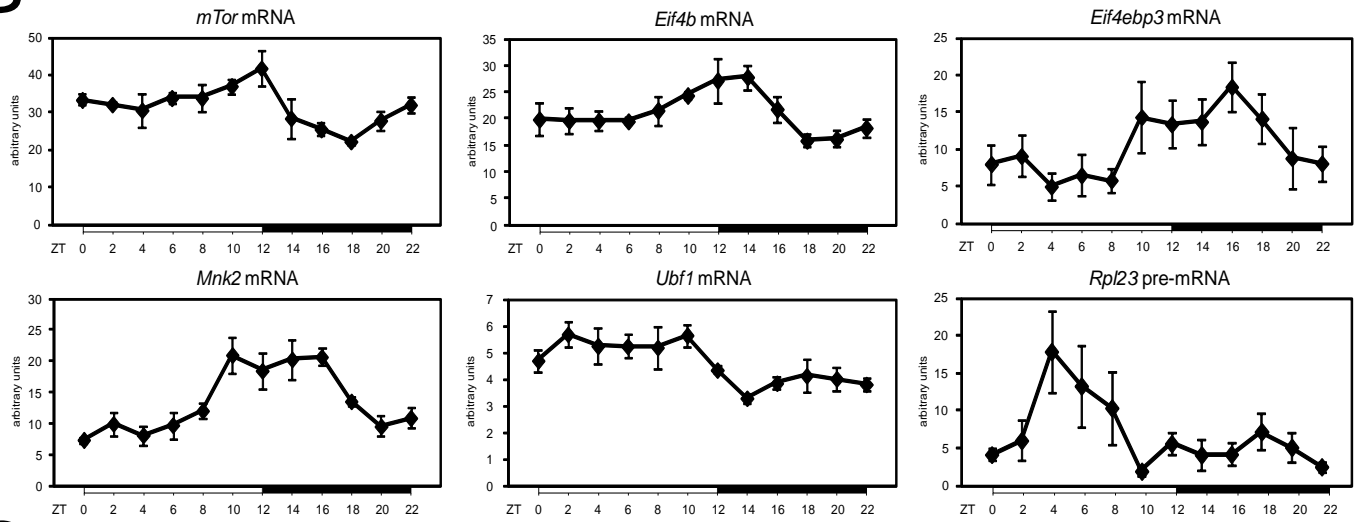
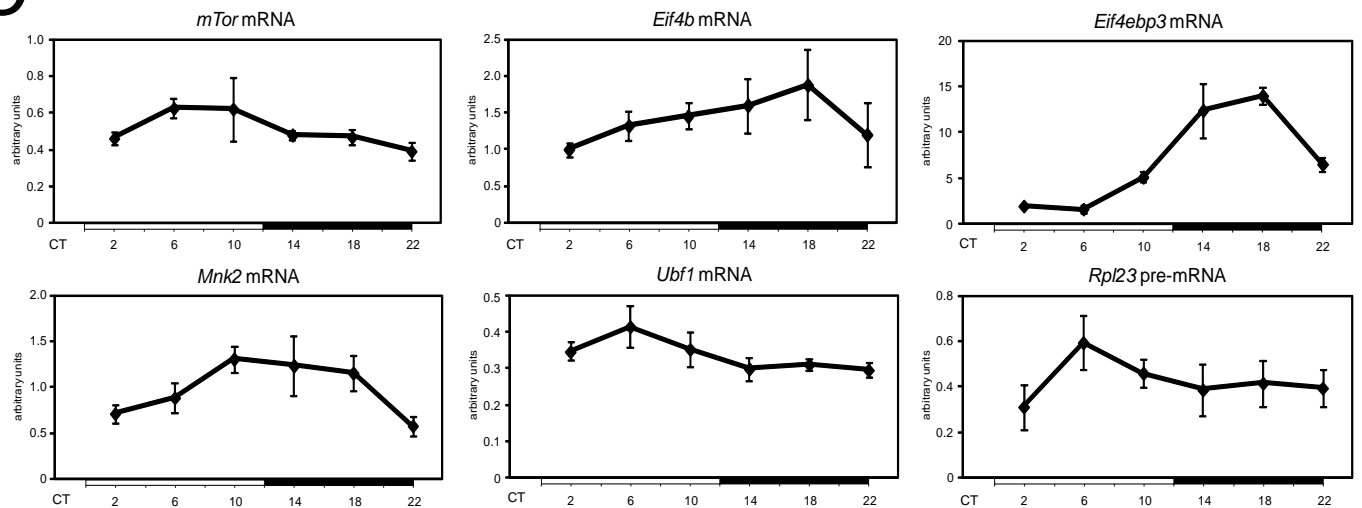
A**B****C**

Figure S4

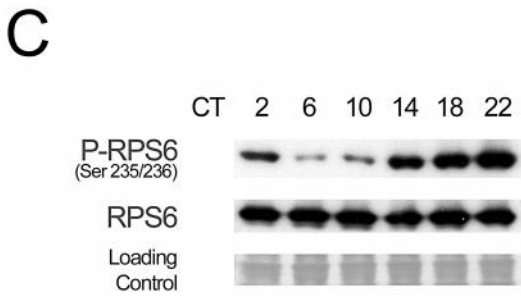
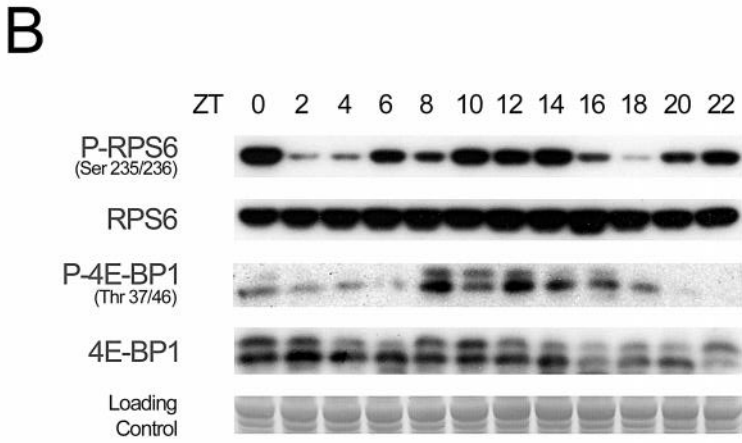
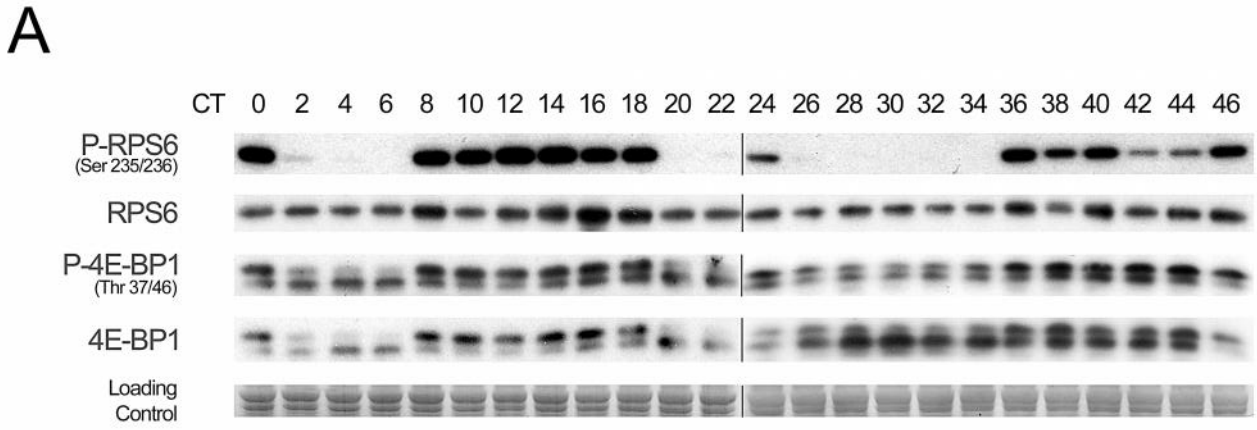


Figure S5

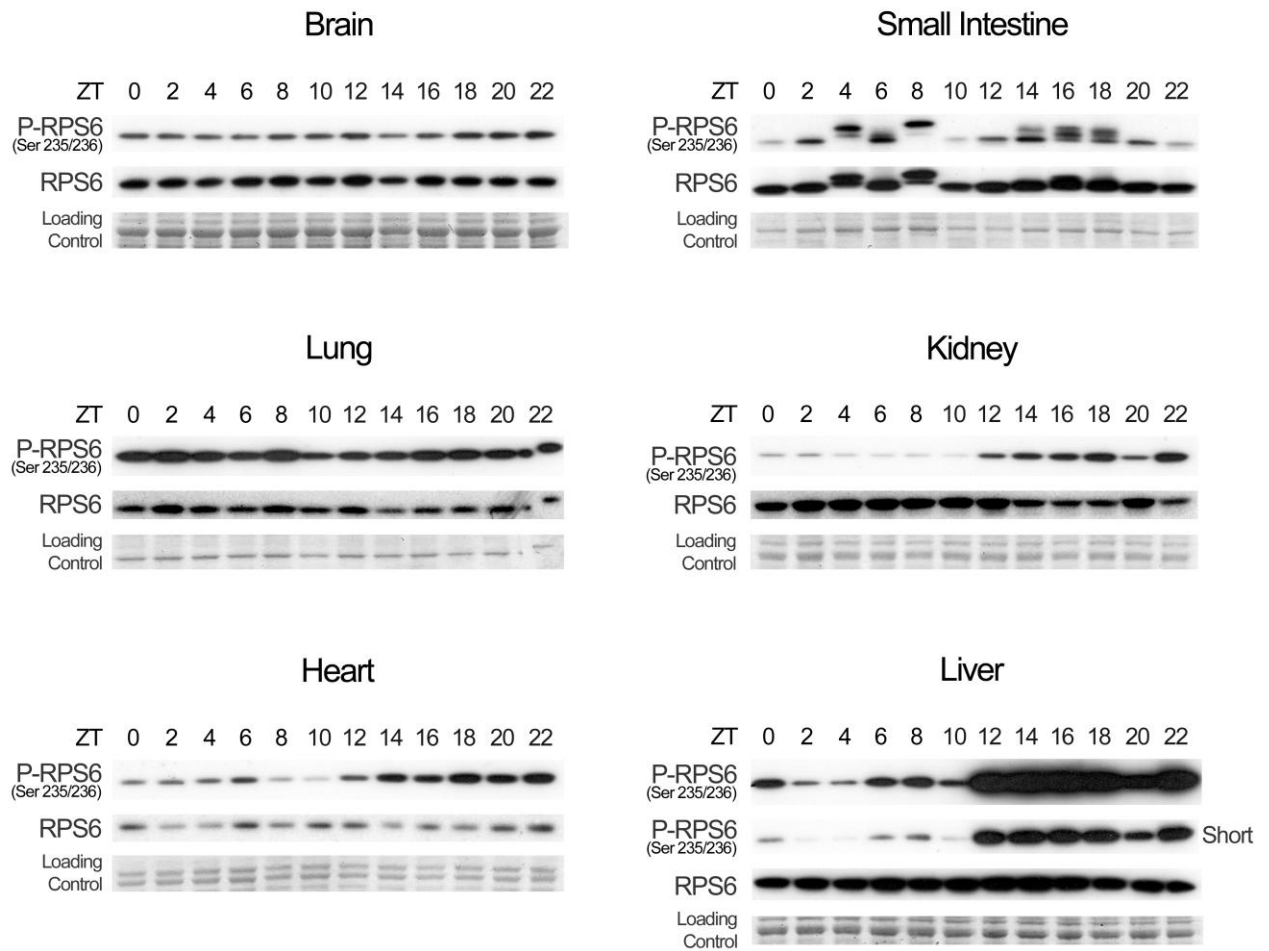


Figure S6

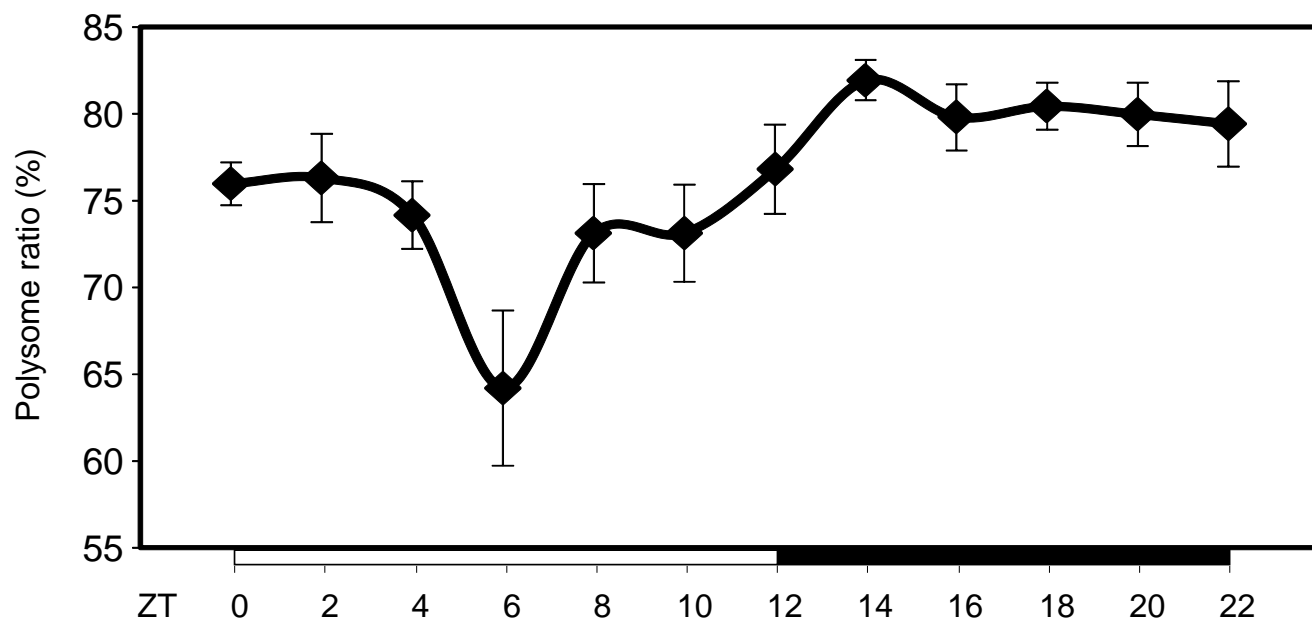


Figure S7

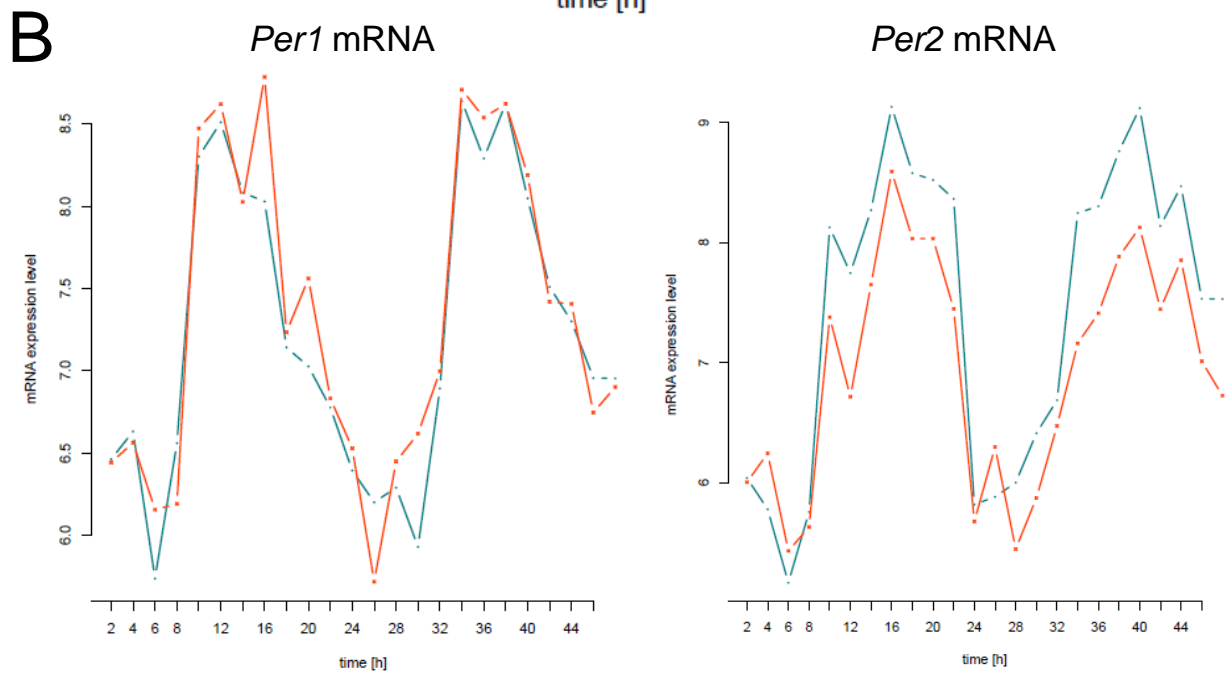
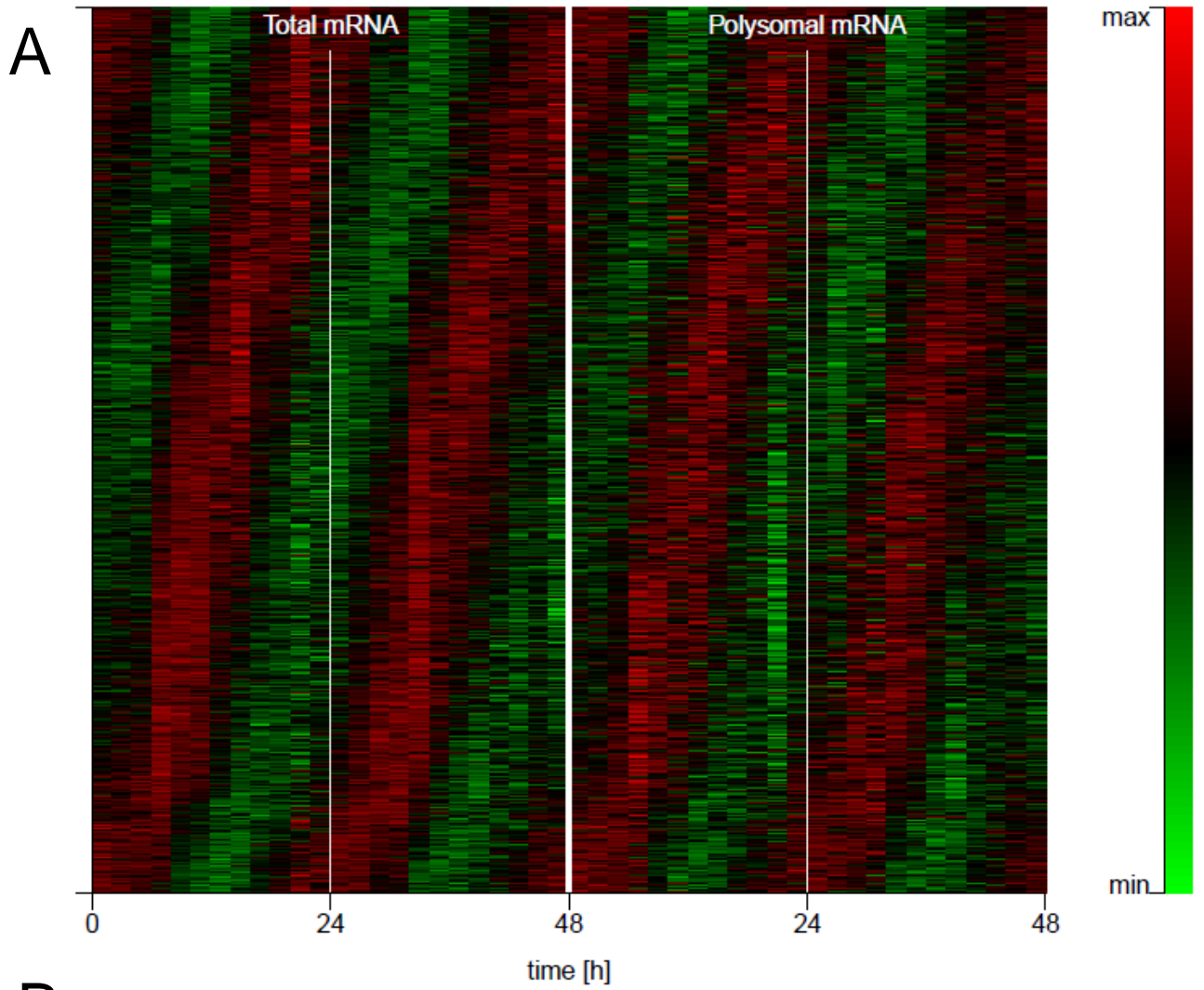


Figure S8

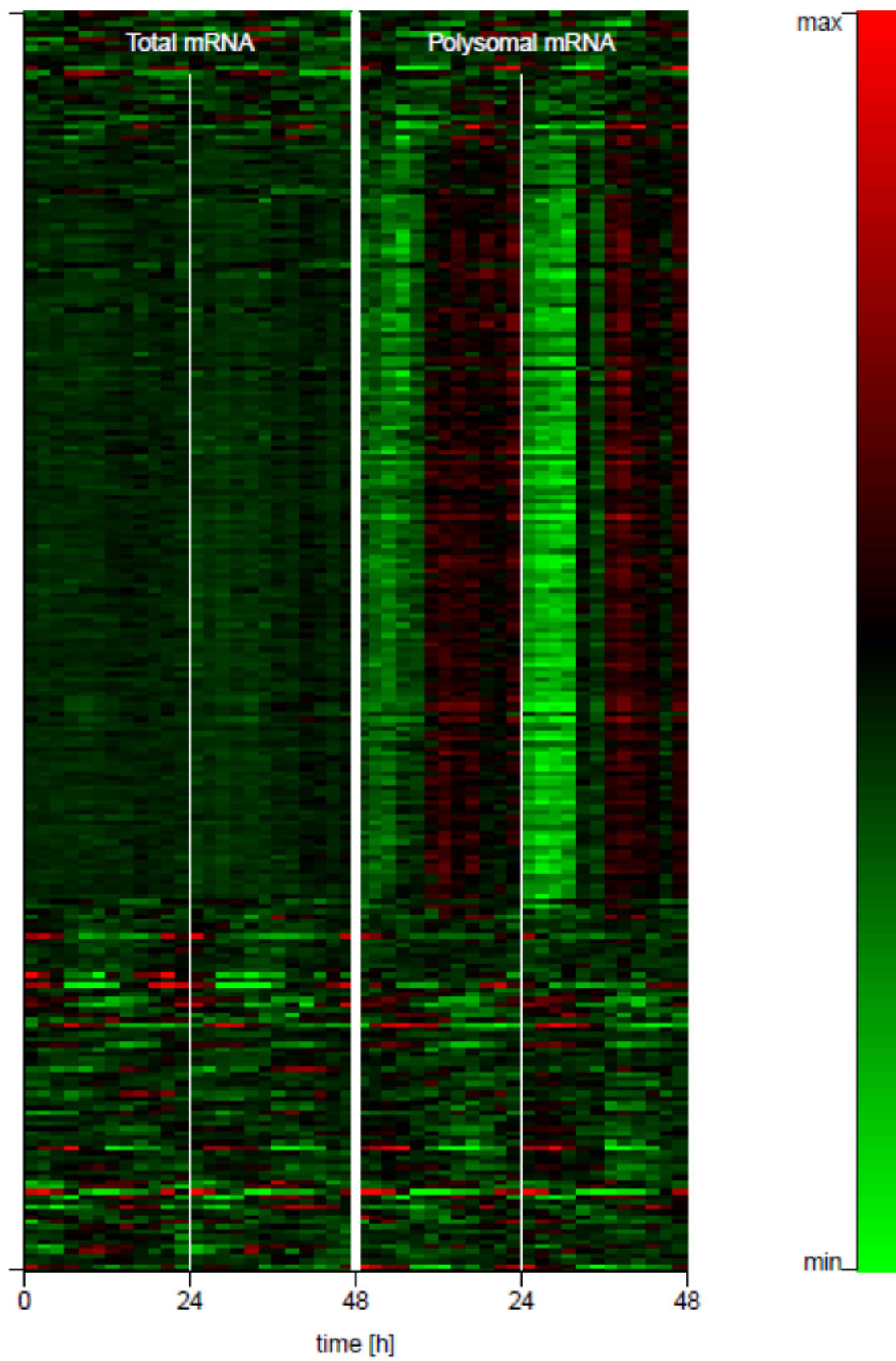
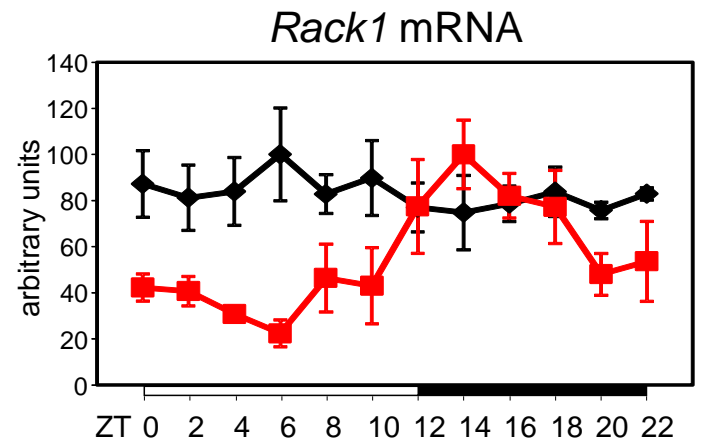
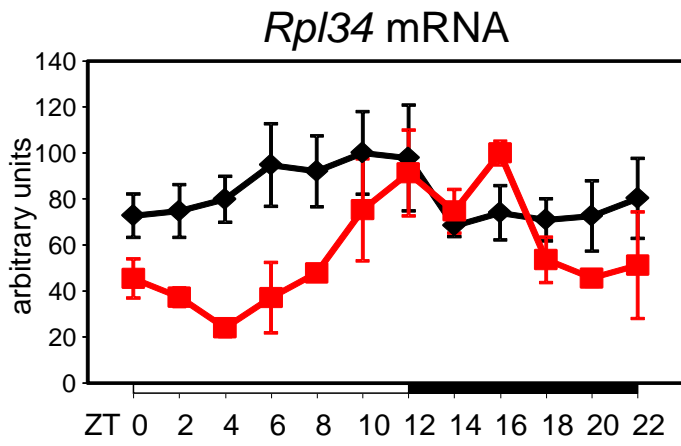
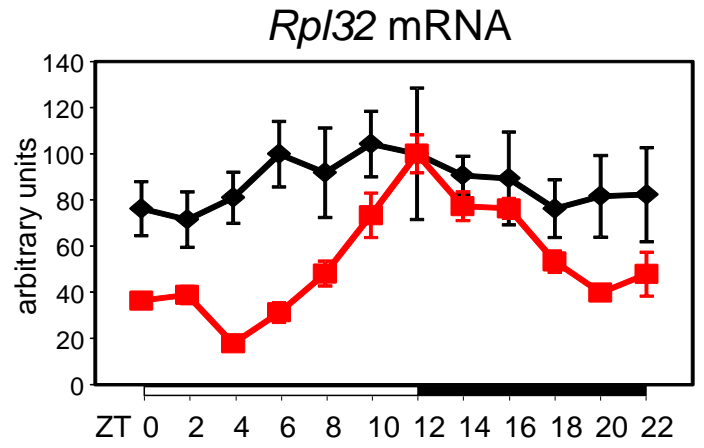
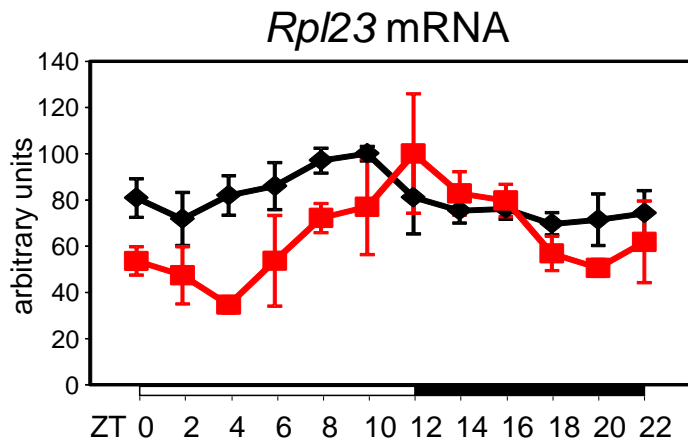


Figure S9



—◆— Total RNA
 —■— Polysomal RNA

Figure S10

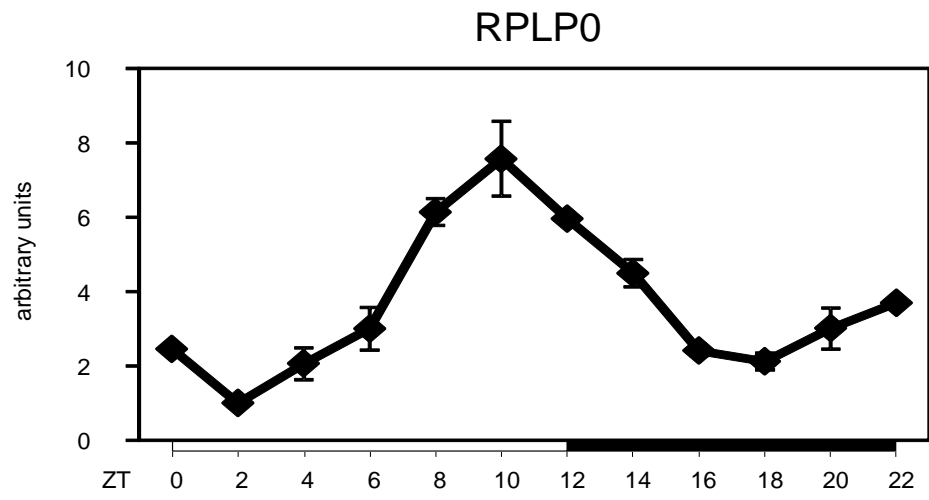
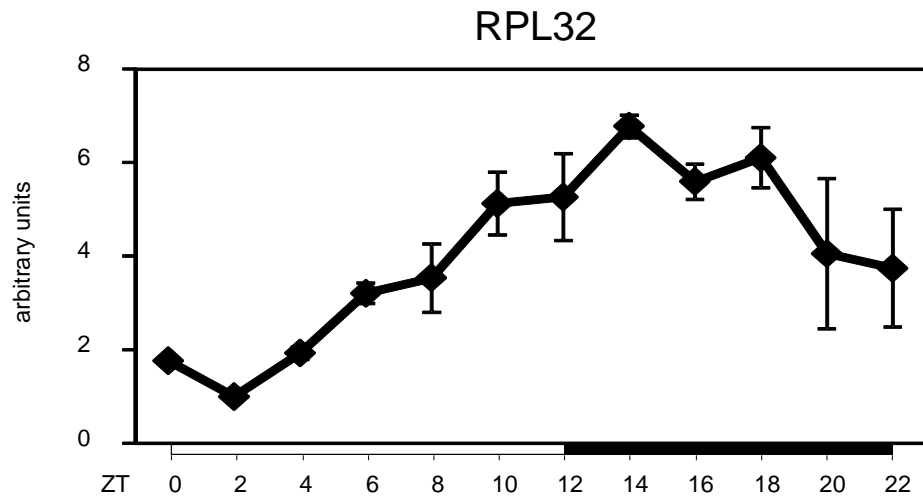
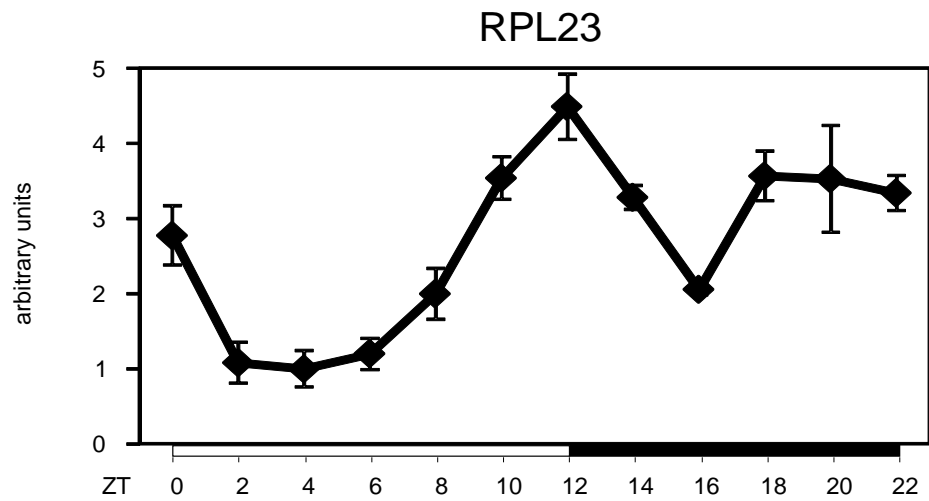
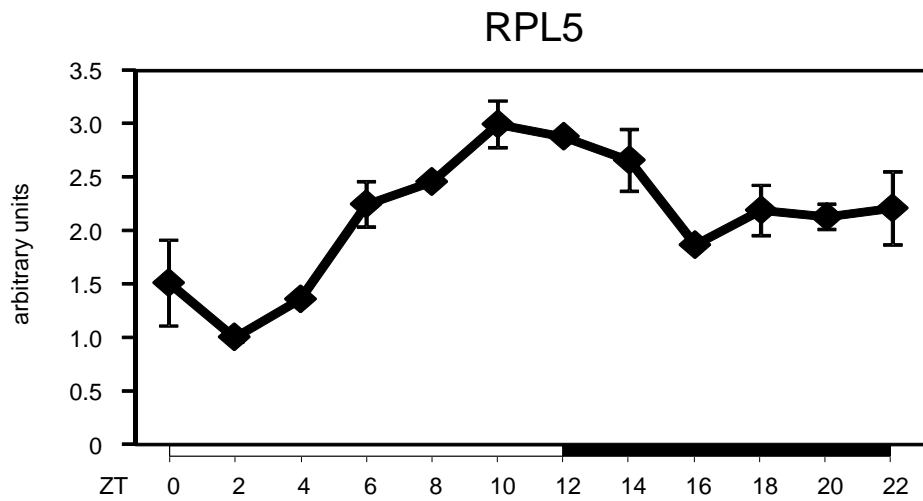
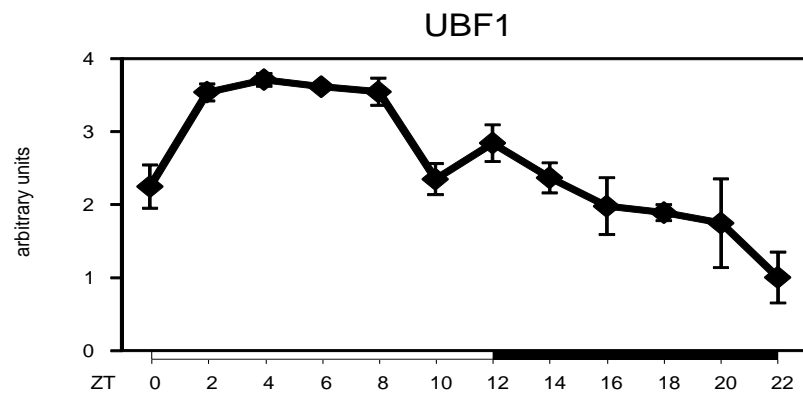
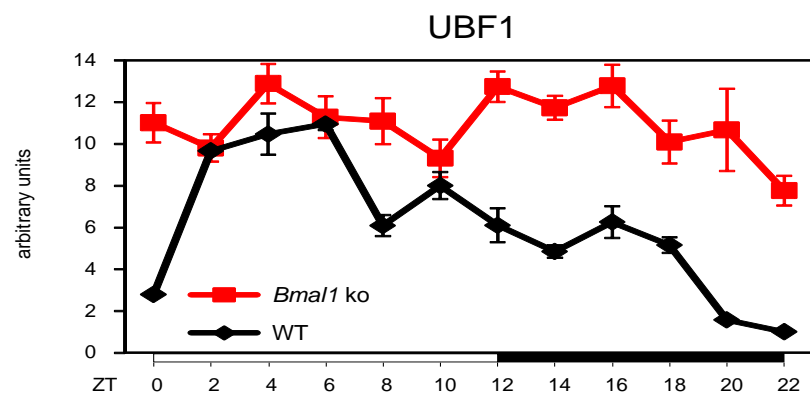
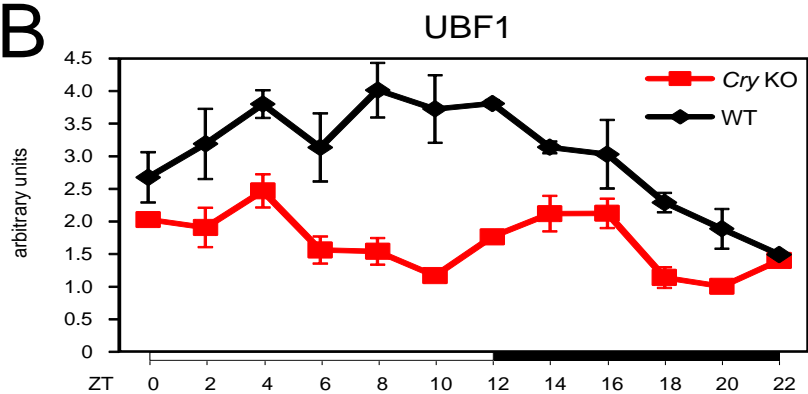
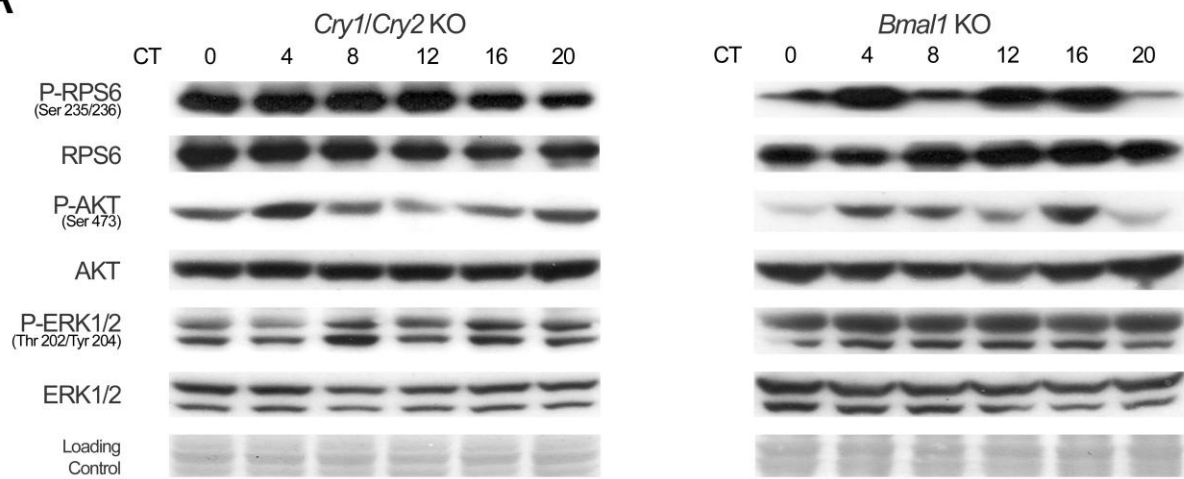
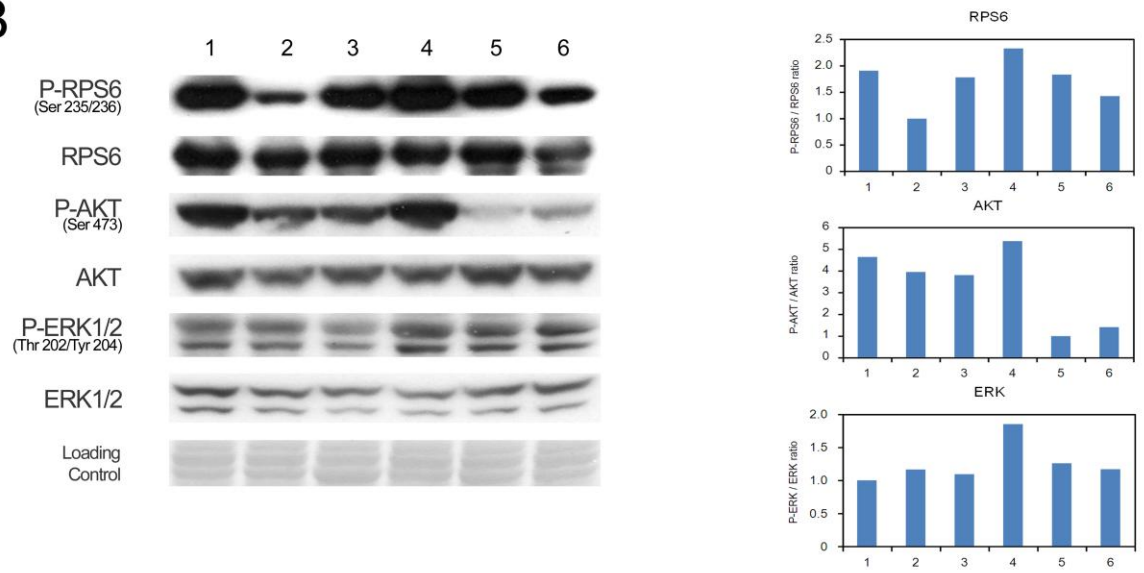
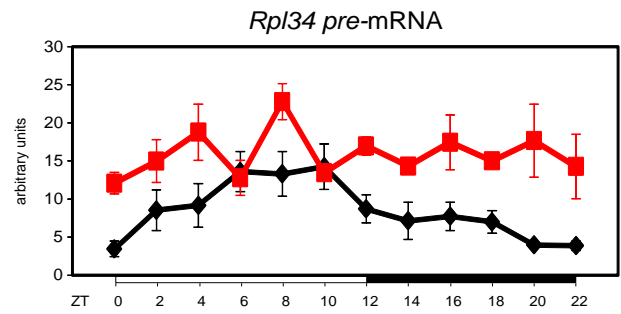
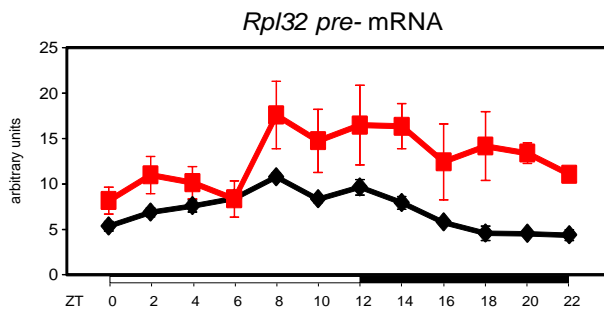
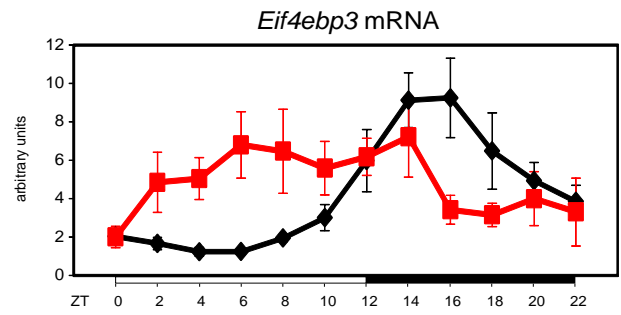
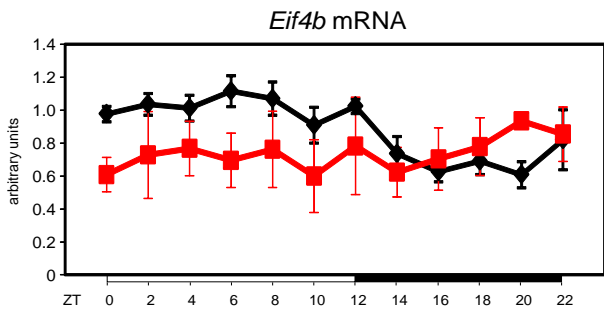
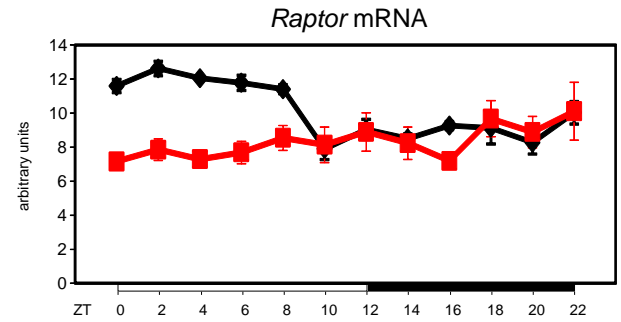
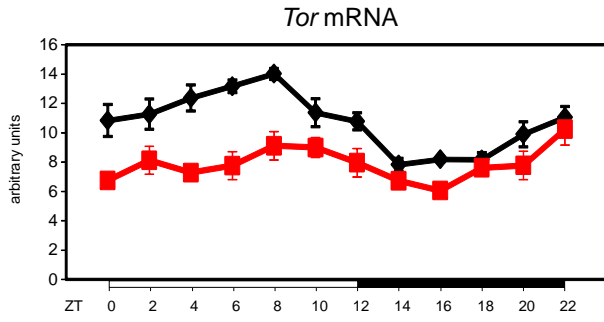


Figure S11

A**B****Figure S12**

A**B****Figure S13**



—◆— WT
 —■— *Cry1/Cry2* KO

Figure S14

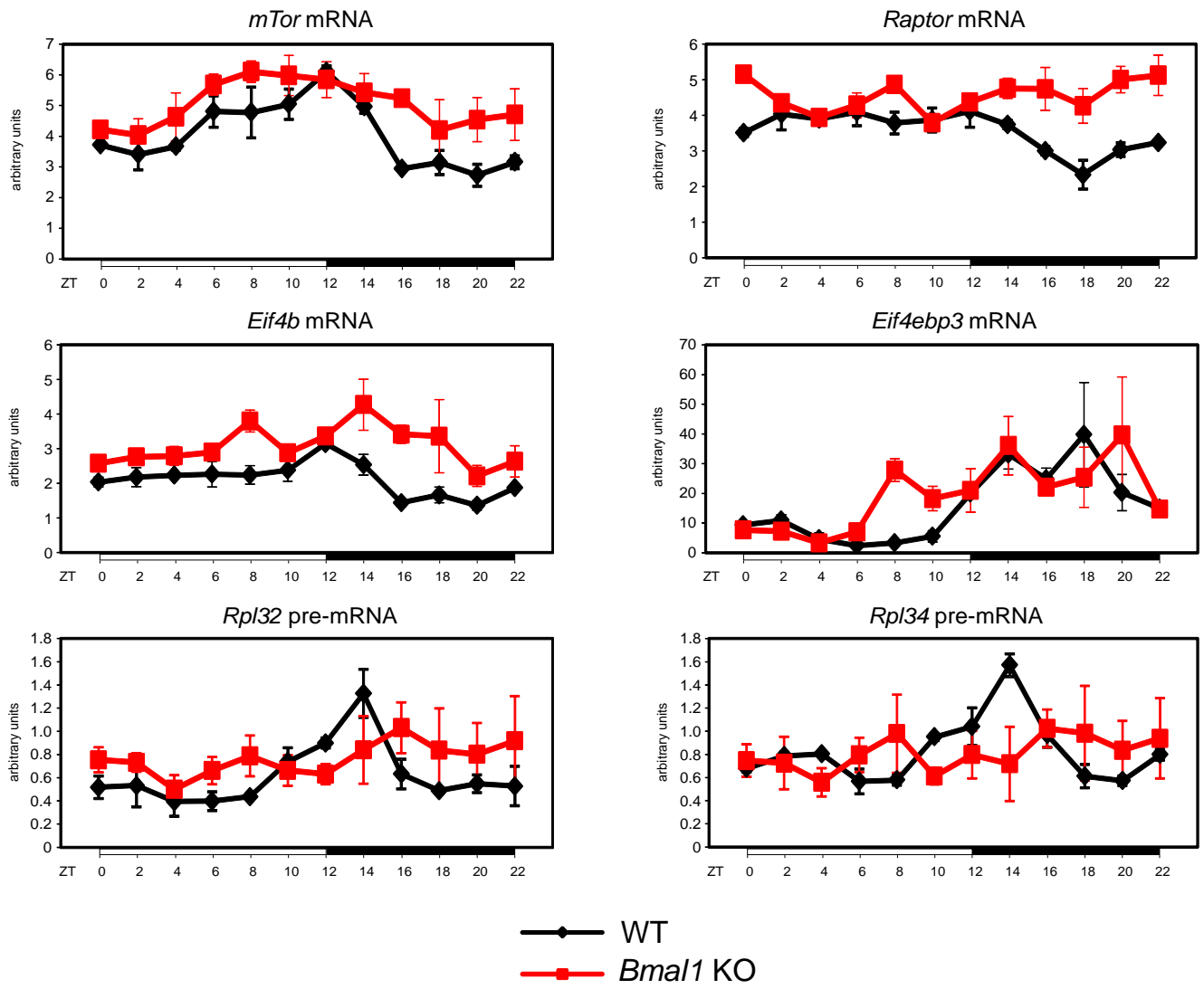
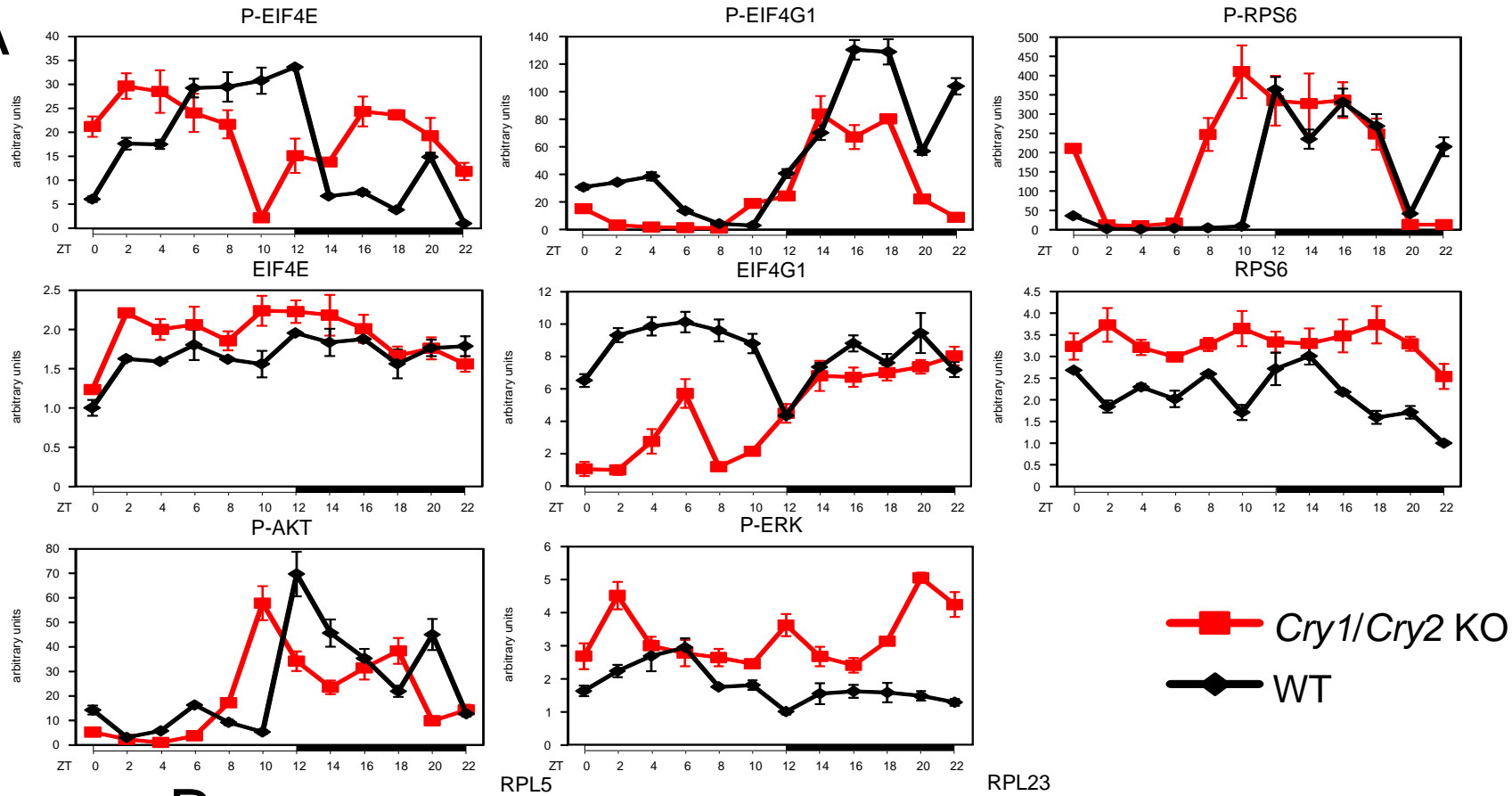
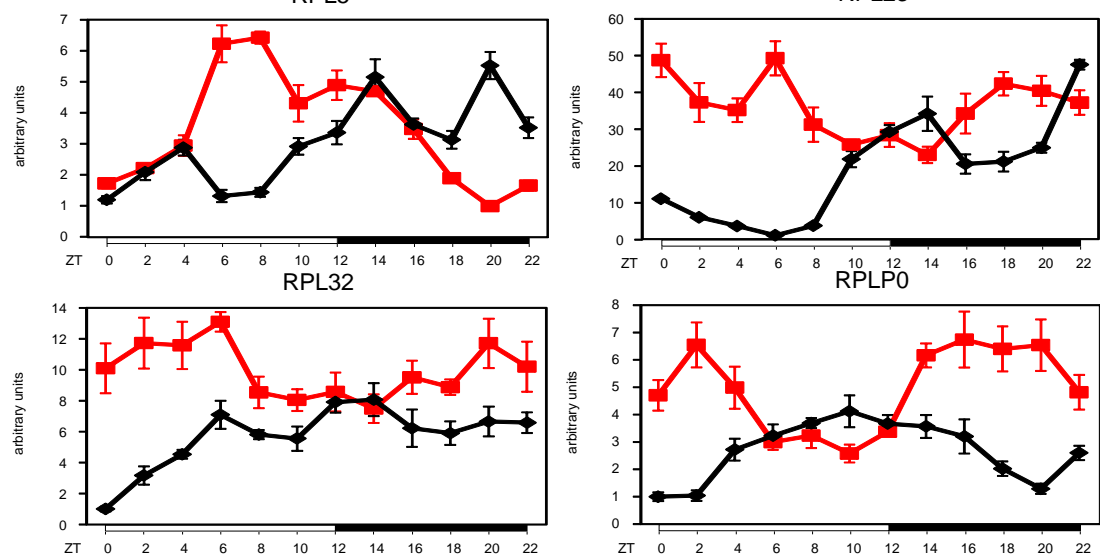
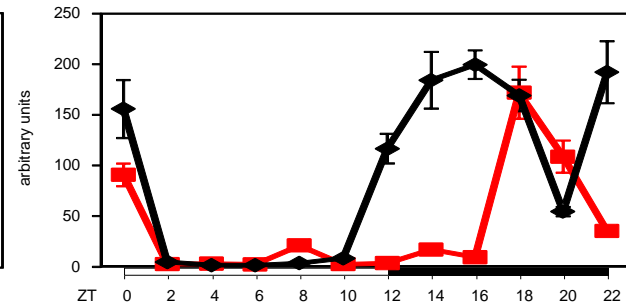
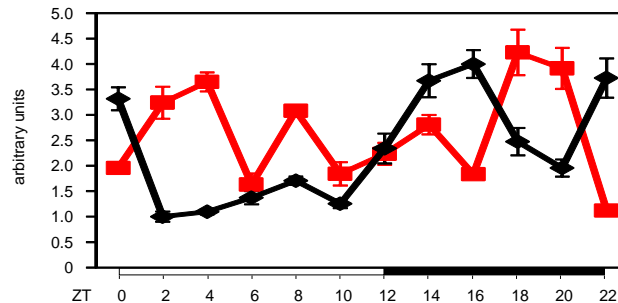
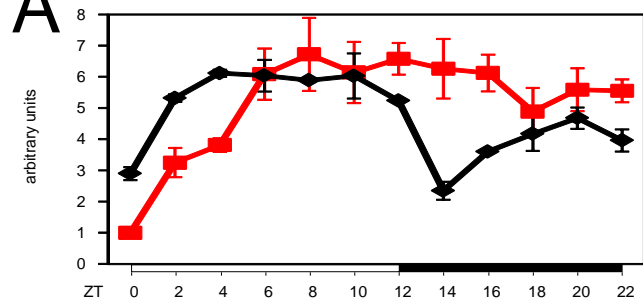
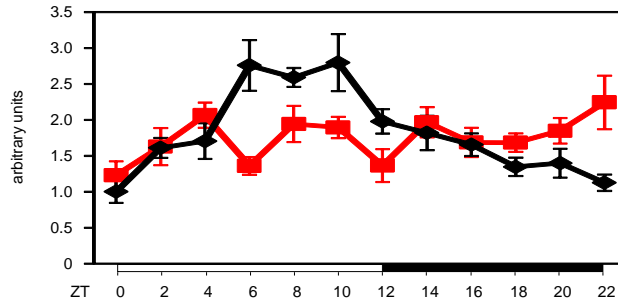
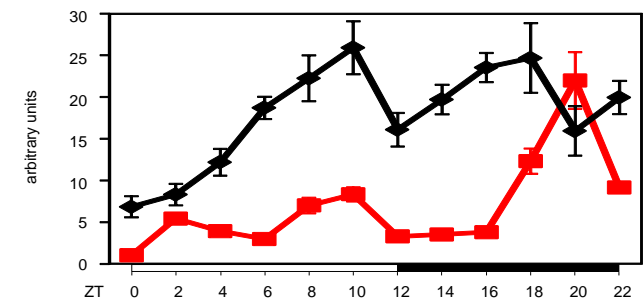
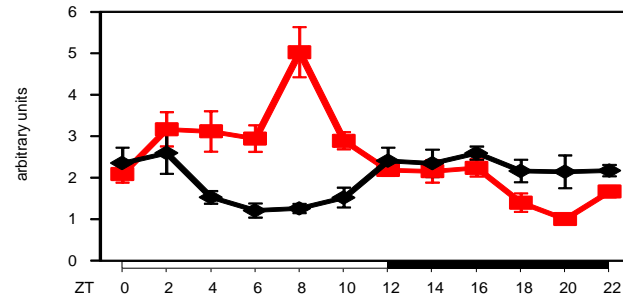
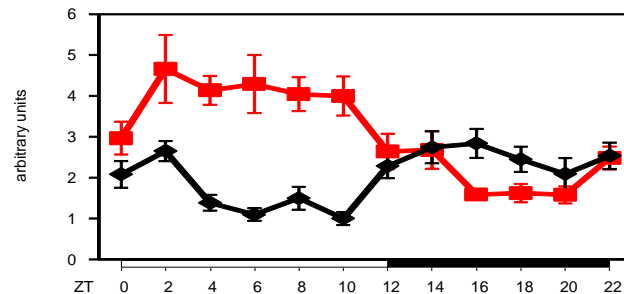
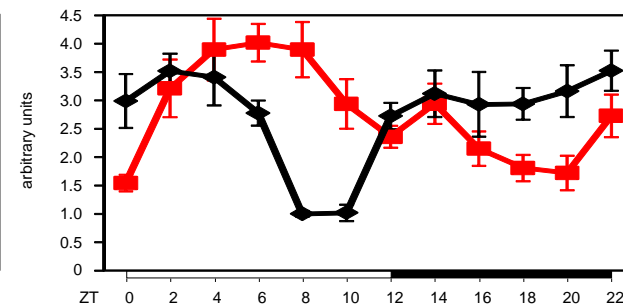
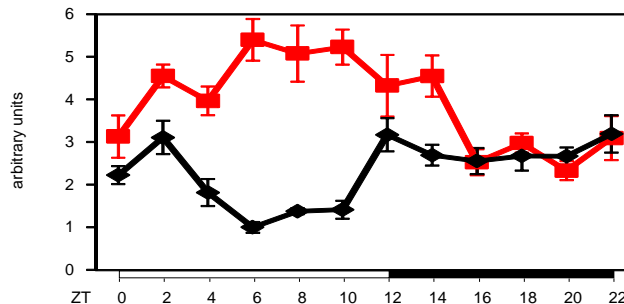


Figure S15

A**B****Figure S16**

A**P-EIF4E****P-EIF4G1****P-RPS6****P-AKT****P-ERK**

—■— *Bmal1* ko
—◆— WT

B**RPL5****RPL23****RPL32****RPLP0****Figure S17**

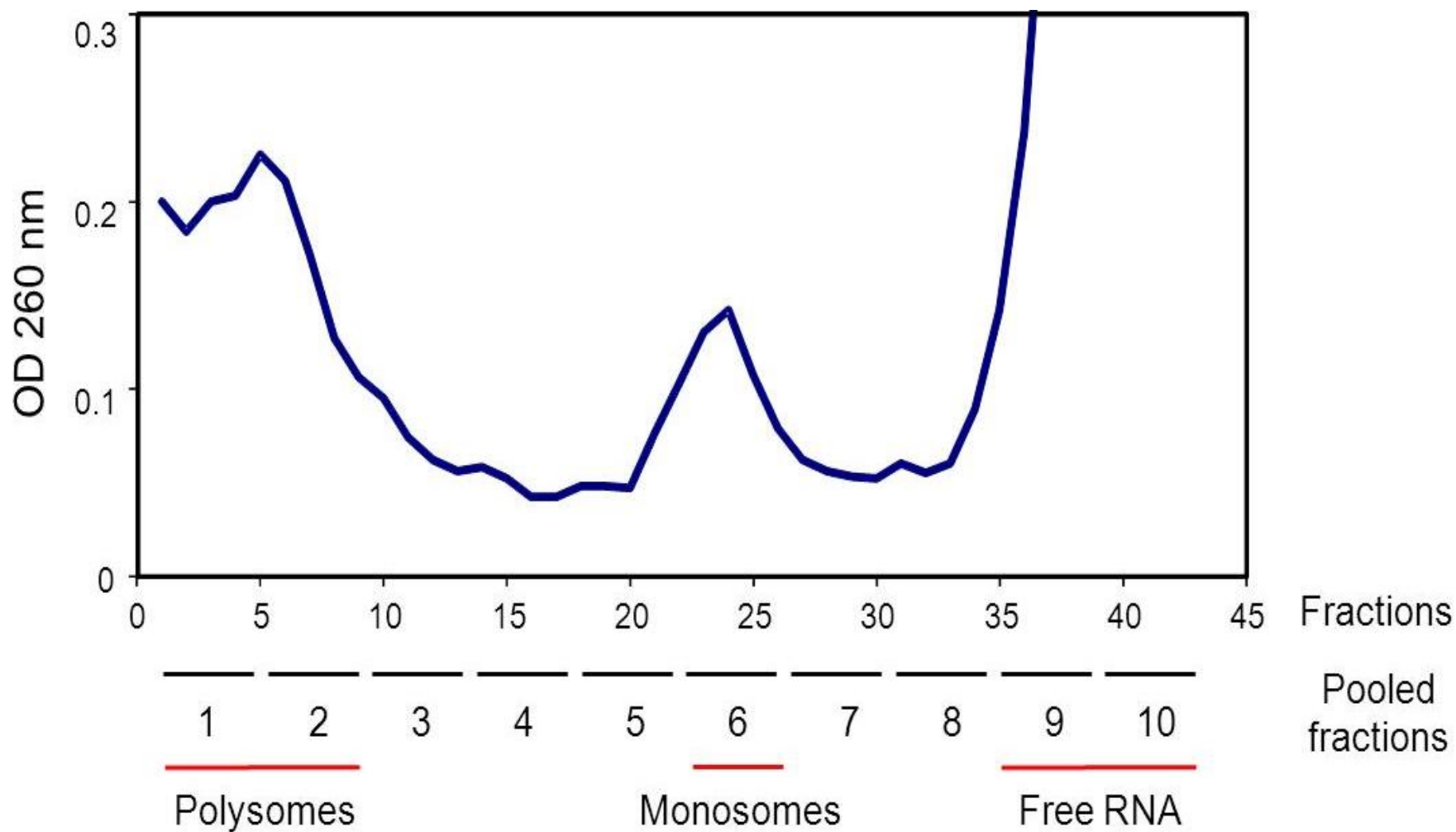


Figure S18

Table S1: Cosinor statistical values related to rhythmic mRNA expression of genes coding for proteins involved in mRNA translation, TORC1 complex and ribosome biogenesis

Gene	p value	F[2,9]	Robustness (%)	Mesor	Amplitude	Acrophase (h)	Fold change
<i>Eif4e</i>	0.01500	6.945	47.6	0.83	0.121	11.3	1.566
<i>Eif4g1</i>	0.00249	13.215	66.1	9.26	1.615	0.7	1.678
<i>Eif4a2</i>	0.00109	17.680	72.9	5.52	1.562	8.1	2.085
<i>Eif4b</i>	0.00043	24.953	79.6	8.85	2.263	5.7	1.835
<i>Eif4ebp1</i>	0.00051	23.339	78.4	1.88	0.860	9.1	3.126
<i>Eif4ebp3</i>	0.00022	32.418	83.7	5.82	4.998	15.8	7.647
<i>mTor</i>	0.00089	19.010	74.5	10.75	2.391	5.3	1.790
<i>Raptor</i>	0.00222	13.753	67.1	10.14	1.954	3.2	1.598
<i>Map4k3</i>	0.00022	32.061	83.6	1.09	0.258	6.1	1.628
<i>Mnk2</i>	0.00026	29.933	82.6	2.45	1.065	11.7	2.929
<i>pre-45S rRNA</i>	0.00025	30.395	82.8	13.90	3.630	9.0	1.913
<i>Pre-Rpl23</i>	0.00222	13.752	67.1	19.53	8.189	9.3	4.141
<i>Pre-Rpl32</i>	0.00011	43.290	87.4	15.17	5.865	8.8	2.480
<i>Pre-Rpl34</i>	0.00044	24.724	79.5	7.51	3.914	8.5	3.348
<i>Ubf1</i>	0.00025	30.734	83.0	1.81	0.577	6.1	2.211

Table S2: Cosinor statistical values related to rhythmic phosphorylation and expression of protein involved in mRNA translation, cell signaling and ribosome biogenesis

Protein	p value	F[2,9]	Robustness (%)	Mesor	Amplitude	Acrophase (h)	Fold change
P-EIF4E	0.01231	7.478	49.9	3.40	2.04	7.51	5.89
P-EIF4G1	0.00185	14.662	68.7	4.21	3.68	16.73	9.69
P-EIF4B	0.01404	7.120	48.4	4.41	4.47	14.64	13.44
P-4E-BP1	0.00488	10.439	59.8	25.06	22.43	13.68	64.81
P-RPS6	0.00604	9.683	57.7	43.96	56.27	15.83	110.02
P-TSC2	0.00212	13.996	67.6	4.76	3.43	7.85	10.57
P-AKT	0.00212	13.993	67.6	3.51	2.63	14.69	8.37
P-ERK	0.00151	15.746	70.4	5.60	4.45	7.33	11.04
P-p90RSK	0.00044	24.711	79.5	2.34	1.51	6.39	4.28
Me-GTP 4E-BP1	0.00299	12.404	64.5	2.97	1.76	4.74	5.49
RPL5	0.01036	7.970	51.9	2.13	0.66	12.52	3.00
RPL23	0.04426	4.471	33.1	2.45	1.02	15.84	4.15
RPL32	0.00007	52.586	89.5	4.01	2.38	14.51	6.78
RPLP0	0.01075	7.864	51.5	3.57	2.20	10.93	7.57
UBF1	0.00328	12.009	63.7	2.57	1.01	6.49	3.71

Affy probes	Genes	Phase	Amplitude	p_value
1434523_x_at	Eif3e	14.18	2.14	3.31E-04
1415716_a_at	Rps27	15.09	3.49	1.08E-04
1450840_a_at	Rpl39	15.18	4.35	3.02E-04
1454778_x_at	Rps28	15.43	2.43	4.61E-04
1423763_x_at	Rps28	15.44	2.47	2.24E-04
1426162_a_at	Rpl7	15.45	2.67	8.68E-04
1415979_x_at	Rpl7	15.56	2.05	3.81E-04
1416603_at	Rpl22	15.60	3.78	1.26E-05
1453118_s_at	Rpl22	15.62	3.54	8.58E-06
1416807_at	Rpl36a	15.64	2.56	4.20E-05
1438655_a_at	Rpl34	15.65	3.66	5.82E-05
1460543_x_at	Rpl37a	15.66	2.87	2.95E-05
1415701_x_at	Rpl23	15.71	2.03	1.67E-05
1435593_x_at	Rps7	15.80	4.04	3.08E-05
1456628_x_at	Rps24	15.82	4.38	3.42E-05
1422475_a_at	Rps3a	15.83	2.93	6.32E-05
1460201_a_at	Rpl24	15.83	1.68	6.74E-05
1433549_x_at	Rps21	15.84	4.76	6.50E-04
1454859_a_at	Rpl23	15.85	2.11	4.33E-05
1437975_a_at	Rpl23a	15.86	2.94	8.83E-06
1451101_a_at	Rps28	15.87	2.10	3.04E-05
1460680_a_at	Rpl23	15.87	2.35	1.86E-04
1428530_x_at	Rps24	15.88	3.94	5.47E-05
1455767_x_at	Rpl21	15.90	2.77	5.11E-04
1455662_x_at	Rps17	15.90	2.64	2.24E-05
1416277_a_at	Rplp1	15.92	2.20	5.58E-04
1434872_x_at	Rpl37	15.93	2.79	1.83E-05
1438986_x_at	Rps17	15.95	2.72	2.61E-05
1429077_x_at	Rpl21	15.95	2.12	1.42E-04
1453362_x_at	Rps24	15.95	3.63	2.39E-05
1419364_a_at	Rps7	15.96	3.26	3.62E-05
1434358_x_at	Rps21	15.98	3.56	1.82E-04
1455364_a_at	Rps7	15.99	4.11	5.77E-05
1416217_a_at	Rpl37a	16.01	2.79	1.20E-05
1423665_a_at	Rpl5	16.04	1.81	5.25E-04
1449255_a_at	Rpl15	16.07	2.17	9.26E-04
1435712_a_at	Rps18	16.11	4.21	9.52E-06
1437510_x_at	Rps17	16.12	2.97	1.38E-05
1425183_a_at	Rpl4	16.12	2.17	6.27E-04
1437976_x_at	Rpl23a	16.12	2.12	2.44E-05
1416026_a_at	Rpl12	16.14	4.10	2.49E-05
1415867_at	Cct4	16.18	1.65	1.03E-04
1416453_x_at	Rps12	16.19	4.44	3.60E-05
1448344_at	Rps12	16.19	4.91	1.67E-05
1435725_x_at	Rpl12	16.19	3.10	2.05E-05
1436064_x_at	Rps24	16.20	2.94	3.77E-06
1428152_a_at	Rpl18a	16.20	2.43	5.25E-06
1436586_x_at	Rps14	16.21	2.53	4.89E-06

1435151_a_at	Rps3	16.21	2.48	1.11E-04
1449196_a_at	Rps27a	16.21	2.63	2.67E-05
1426659_a_at	Rpl23a	16.21	2.76	1.33E-05
1433432_x_at	Rps12	16.22	4.21	1.46E-05
1436995_a_at	Rpl26	16.23	2.97	1.01E-05
1424766_at	Erc6l	16.24	1.91	4.07E-04
1453729_a_at	Rpl37	16.24	2.41	5.41E-06
1459986_a_at	Rps17	16.28	2.63	7.19E-06
1433721_x_at	Rps21	16.30	3.10	1.67E-05
1417317_s_at	Rpl35a	16.30	2.13	1.06E-05
1454856_x_at	Rpl35	16.30	2.88	1.34E-05
1426660_x_at	Rpl23a	16.30	2.40	1.86E-05
1434624_x_at	Rps9	16.31	2.52	8.13E-04
1451068_s_at	Rps25	16.32	2.70	1.68E-05
1416243_a_at	Rpl35	16.33	2.79	2.23E-05
1460175_at	Rps23	16.36	3.02	6.18E-06
1436822_x_at	Rpl17	16.37	3.33	9.70E-05
1417615_a_at	Rpl11	16.38	2.50	5.96E-06
1415736_at	Pfdn5	16.38	2.24	1.00E-05
1420000_s_at	Igfbp1	16.39	2.28	1.51E-04
1418273_a_at	Rpl30	16.39	3.84	6.21E-06
1434231_x_at	Rpl35	16.40	2.91	8.00E-06
1416276_a_at	Rps4x	16.41	2.98	9.17E-06
1433510_x_at	Rpl36	16.41	3.18	5.51E-05
1416088_a_at	Rps15	16.41	2.80	6.80E-04
1456373_x_at	Rps20	16.42	3.44	1.69E-05
1448739_x_at	Rps18	16.42	4.45	8.20E-06
1416099_at	Rpl27	16.43	1.53	8.85E-04
1456436_x_at	Rps20	16.46	3.43	1.22E-05
1454620_x_at	Rps6	16.46	2.03	2.59E-04
1460637_s_at	Pfdn5	16.47	2.55	1.05E-04
1428212_x_at	Rpl31	16.48	2.81	1.14E-05
1453467_s_at	Rps15a	16.50	2.92	1.96E-05
1416519_at	Rpl36	16.50	2.60	3.28E-05
1430288_x_at	Rps21	16.50	3.18	9.15E-06
1416420_a_at	Rpl9	16.53	2.79	9.48E-05
1449243_a_at	Rps19	16.53	5.79	3.12E-06
1455485_x_at	Rpl13a	16.59	2.21	6.35E-06
1448109_a_at	Rpl26	16.59	3.70	9.13E-06
1448157_s_at	Rpl10	16.59	2.05	4.79E-05
1460008_x_at	Rpl31	16.60	2.51	1.85E-05
1416642_a_at	Tpt1	16.60	2.09	8.83E-05
1448245_at	Rpsa	16.61	2.71	2.40E-05
1416054_at	Rps5	16.62	4.26	3.92E-06
1455950_x_at	Rpl35	16.62	2.85	6.60E-06
1416520_x_at	Rpl36	16.62	2.80	1.72E-05
1426661_at	Rpl27a	16.62	2.51	7.04E-06
1435897_at	Rpl32	16.63	5.73	5.97E-06
1434377_x_at	Rps6	16.63	1.75	2.02E-04
1455572_x_at	Rps18	16.63	4.80	2.70E-06

1436840_x_at	Rpl35	16.64	2.79	3.66E-05
1435791_x_at	Rpl17	16.65	3.01	1.58E-04
1423666_s_at	Rpl5	16.67	3.22	8.23E-05
1436924_x_at	Rpl31	16.67	2.71	3.60E-05
1438626_x_at	Rpl14	16.67	3.34	1.11E-04
1436760_a_at	Rps8	16.68	2.52	1.01E-04
1443843_x_at	Rpl9	16.68	2.12	5.70E-05
1427875_a_at	Rpl34	16.69	2.71	4.80E-06
1416089_at	Rps15	16.72	2.81	2.96E-04
1432264_x_at	Cox7a2l	16.74	2.17	8.04E-04
1423855_x_at	Rpl17	16.77	3.44	5.11E-05
1421772_a_at	Cox7a2l	16.78	1.93	9.32E-04
1437196_x_at	Rps16	16.78	2.24	8.63E-06
1455319_x_at	Rps8	16.80	3.16	1.55E-04
1416074_a_at	Rpl28	16.80	3.98	3.12E-04
1415942_at	Rpl10	16.81	2.28	1.94E-04
1450150_a_at	Rpl13	16.81	3.22	4.97E-04
1426793_a_at	Rpl14	16.81	4.69	3.17E-04
1431177_a_at	Rpl10a	16.83	3.27	6.36E-06
1416404_s_at	Rps16	16.84	3.71	9.10E-06
1416141_a_at	Rps6	16.86	1.62	1.58E-04
1435873_a_at	Rpl13a	16.87	2.10	1.29E-05
1417608_a_at	Rpl13a	16.87	2.93	1.75E-05
1416719_a_at	Rps10	16.88	3.17	6.23E-05
1415962_at	Eif3h	16.88	2.47	7.50E-04
1415839_a_at	Npm1	16.89	2.78	6.31E-04
1455693_x_at	Rps6	16.89	1.70	1.18E-04
1434854_a_at	Rps10	16.89	3.32	4.11E-05
1448252_a_at	Eef1b2	16.89	3.59	1.80E-05
1438507_x_at	Rpl14	16.91	3.67	8.91E-05
1436688_x_at	Rpl14	16.91	3.36	4.76E-05
1422859_a_at	Rpl23	16.93	4.08	7.90E-05
1418062_at	Eef1a2	16.98	2.25	3.25E-04
1417762_a_at	Rpl8	17.00	2.32	4.90E-04
1455001_x_at	Rpl13a	17.00	2.62	2.11E-05
1416546_a_at	Rpl6	17.00	2.40	1.95E-05
1422613_a_at	Rpl7a	17.04	2.72	2.83E-04
1456497_x_at	Rps10	17.07	2.94	7.45E-05
1433928_a_at	Rpl13a	17.07	4.12	7.97E-06
1432263_a_at	Cox7a2l	17.10	2.06	6.74E-04
1416142_at	Rps6	17.10	3.62	1.42E-04
1460575_at	Eif2a	17.11	2.41	5.78E-04
1449323_a_at	Rpl3	17.12	3.01	2.47E-06
1438723_a_at	Rps10	17.12	2.73	9.59E-05
1433688_x_at	Rpl14	17.13	3.59	6.32E-05
1452285_a_at	Eif3f	17.16	2.90	3.52E-04
1455168_a_at	Gnb2l1	17.17	2.90	9.28E-05
1419441_at	Rplp0	17.19	3.68	2.36E-04
1433689_s_at	Rps9	17.21	3.65	7.01E-04
1448846_a_at	Rpl29	17.21	2.39	2.18E-04

1415876_a_at	Rps26	17.22	2.26	9.53E-05
1433472_x_at	Rpl38	17.27	2.35	2.70E-04
1455245_x_at	Rpl13	17.27	2.47	7.76E-05
1437610_x_at	Rps8	17.30	2.62	2.71E-04
1455600_at	Rps3	17.35	3.66	1.34E-04
1436046_x_at	Rpl29	17.36	2.44	2.07E-05
1419553_a_at	Rabggtb	17.41	2.73	4.55E-04
1449506_a_at	Eef1d	17.46	2.41	7.50E-04
1451077_at	Rpl5	17.47	3.42	7.82E-04
1460581_a_at	Rpl13	17.50	2.41	2.82E-04
1424635_at	Eef1a1	17.55	1.93	1.63E-06
1455348_x_at	Rpl29	17.56	2.18	1.17E-04
1431766_x_at	Rps2	17.67	2.04	5.50E-04
1451296_x_at	pabpc4	17.70	1.89	6.08E-04
1454627_a_at	Rpl29	17.70	2.29	2.43E-05
1425026_at	Sft2d2	17.72	1.66	4.68E-04
1417125_at	Ahcy	17.74	1.45	1.28E-04
1431765_a_at	Rps2	17.75	2.52	9.82E-04
1426379_at	Eif4b	17.82	2.07	2.16E-04
1450934_at	Eif4a2	17.82	3.62	8.87E-04
1417364_at	Eef1g	17.99	2.79	2.40E-05
1416624_a_at	Uba52	18.39	1.47	9.64E-04

Table S4: Functions of the genes presenting a rhythmic total / polysomal RNA ratio

Ribosomes small subunits	Ribosomes large subunits	Translation initiation factors	Translation elongation factors	Role in ribosome biogenesis	Other functions
Rpsa	Rpl3	Eif2a	Eef1a1	Npm1	Erc61
Rps2	Rpl4	Eif3e	Eef1a2	Cct4	Rabggtb
Rps3	Rpl5	Eif3f	Eef1b2	Tpt1	Sft2d2
Rps3a	Rpl6	Eif3h	Eef1d	Igfbp1	Cox7a2l
Rps4x	Rpl7	Eif4a2	Eef1g	Pfdn5	
Rps5	Rpl7a	Eif4b	pabpc4	Ahcy	
Rps6	Rpl8			Gnb2l1	
Rps7	Rpl9			Uba52	
Rps8	Rpl10				
Rps9	Rpl10a				
Rps10	Rpl11				
Rps12	Rpl12				
Rps14	Rpl13				
Rps15	Rpl13a				
Rps15a	Rpl14				
Rps16	Rpl15				
Rps17	Rpl17				
Rps18	Rpl18a				
Rps19	Rpl21				
Rps20	Rpl22				
Rps21	Rpl23				
Rps23	Rpl23a				
Rps24	Rpl24				
Rps25	Rpl26				
Rps26	Rpl27				
Rps27	Rpl27a				
Rps27a	Rpl28				
Rps28	Rpl29				
	Rpl30				
	Rpl31				
	Rpl32				
	Rpl34				
	Rpl35				
	Rpl35a				
	Rpl36				
	Rpl36a				
	Rpl37				
	Rpl37a				
	Rpl38				
	Rpl39				
	Rplp0				
	Rplp1				

Table S5: Cosinor statistical values related to rhythmic mRNA expression of genes coding for proteins involved in mRNA translation, TORC1 complex and ribosome biogenesis in wild-type and *Cry1/Cry2* KO mice

Gene	Genotype	p value	F[2,9]	Robustness (%)	Mesor	Mesor p value	Amplitude	Acrophase (h)
<i>Eif4e</i>	WT	0.01500	6.945	47.6	8.28	0.00000	1.21	11.26
	KO	n.s.			14.23			
<i>Eif4g1</i>	WT	0.00249	13.215	66.1	9.26	0.00003	1.61	0.70
	KO	n.s.			6.95			
<i>Eif4a2</i>	WT	0.00109	17.680	72.9	5.52	0.00736	1.56	8.06
	KO	n.s.			4.32			
<i>Eif4b</i>	WT	0.00043	24.953	79.6	0.88	0.02120	0.23	5.75
	KO	n.s.			0.74			
<i>Eif4ebp1</i>	WT	0.00062	21.751	77.1	1.20	0.00000	0.55	9.20
	KO	n.s.			3.51			
<i>Eif4ebp3</i>	WT	0.00013	39.929	86.5	4.24	n.s.	3.75	15.82
	KO	0.00583	9.806	58.1	4.84		1.87	9.36
<i>mTor</i>	WT	0.00089	19.010	74.5	10.75	0.00024	2.39	5.25
	KO	n.s.			7.87			
<i>Raptor</i>	WT	0.00222	13.753	67.1	10.14	0.00328	1.95	3.23
	KO	n.s.			8.31			
<i>pre-45S rRNA</i>	WT	0.00019	33.888	84.4	4.36	0.00022	1.29	9.12
	KO	0.00525	10.172	59.1	2.91		0.60	9.42
<i>Pre-Rpl23</i>	WT	0.00571	9.877	58.3	2.46	0.00000	1.11	9.45
	KO	0.00463	10.632	60.3	5.40		1.30	11.55
<i>Pre-Rpl32</i>	WT	0.00011	42.969	87.4	7.01	0.00003	2.72	8.77
	KO	0.01468	7.002	47.8	12.83		3.34	12.97
<i>Pre-Rpl34</i>	WT	0.00068	20.978	76.5	8.41	0.00002	4.61	8.53
	KO	n.s.			15.89			
<i>Ubf1</i>	WT	0.00025	30.734	83.0	1.81	0.00002	0.58	6.14
	KO	n.s.			1.08			

Table S6: Cosinor statistical values related to rhythmic mRNA expression of genes coding for proteins involved in mRNA translation, TORC1 complex and ribosome biogenesis in wild-type and *Bmal1* KO mice

Gene	Genotype	p value	F[2,9]	Robustness (%)	Mesor	Mesor p value	Amplitude	Acrophase (h)
<i>Eif4e</i>	<i>WT</i>	0.01748	6.551	45.7	2.21	n.s.	0.49	12.39
	<i>KO</i>	n.s.			2.40			
<i>Eif4g1</i>	<i>WT</i>	0.02316	5.868	42.1	10.36	0.00225	1.11	3.80
	<i>KO</i>	0.04055	4.647	34.4	12.22		1.46	22.32
<i>Eif4a2</i>	<i>WT</i>	0.01083	7.842	51.4	13.82	0.00002	3.28	9.16
	<i>KO</i>	0.00469	10.585	60.2	21.12		4.13	11.54
<i>Eif4b</i>	<i>WT</i>	0.03973	4.689	34.7	2.11	0.00022	0.48	8.79
	<i>KO</i>	0.03240	5.116	37.6	3.08		0.57	12.29
<i>Eif4ebp1</i>	<i>WT</i>	0.04749	4.333	32.1	9.50	0.00768	3.28	11.84
	<i>KO</i>	0.00734	9.030	55.7	5.47		3.63	12.96
<i>Eif4ebp3</i>	<i>WT</i>	0.00099	18.321	73.7	15.74	n.s.	14.77	16.98
	<i>KO</i>	0.01965	6.260	44.2	19.17		12.18	15.47
<i>mTor</i>	<i>WT</i>	0.00317	12.153	64.0	4.04	0.01286	1.23	9.67
	<i>KO</i>	0.00078	19.924	75.4	5.05		0.92	10.38
<i>Raptor</i>	<i>WT</i>	0.00450	10.745	60.6	3.56	0.00007	0.62	6.86
	<i>KO</i>	n.s.			4.56			
<i>pre-45S rRNA</i>	<i>WT</i>	0.00031	28.143	81.6	13.30	0.00000	4.40	9.84
	<i>KO</i>	0.04012	4.669	34.6	20.43		1.98	1.73
<i>Pre-Rpl23</i>	<i>WT</i>	0.03388	5.020	37.0	6.43	n.s.	2.07	14.17
	<i>KO</i>	0.00338	11.879	63.4	7.38		1.84	17.48
<i>Pre-Rpl32</i>	<i>WT</i>	0.03375	5.029	37.0	0.61	n.s.	0.27	13.85
	<i>KO</i>	0.03433	4.993	36.8	0.76		0.14	17.97
<i>Pre-Rpl34</i>	<i>WT</i>	0.04662	4.369	32.3	0.79	n.s.	0.29	13.23
	<i>KO</i>	n.s.			0.81			
<i>Ubf1</i>	<i>WT</i>	0.00017	35.933	85.2	2.35	0.00002	0.62	7.49
	<i>KO</i>	n.s.			3.23			

Table S7: Cosinor statistical values related to rhythmic phosphorylation and expression of protein involved in mRNA translation, cell signaling and ribosome biogenesis in wild-type and *Cry1/Cry2* KO mice

Gene	Genotype	p value	F[2,9]	Robustness (%)	Mesor	mesor p value	Amplitude	Acrophase (h)
P-EIF4E	<i>WT</i>	0.00325	12.044	63.7	16.52	n.s.	13.57	8.30
	<i>KO</i>	n.s.			19.62			
P-EIF4G1	<i>WT</i>	0.00365	11.559	62.6	54.61	0.09835	51.70	18.33
	<i>KO</i>	0.00274	12.788	65.3	27.29		36.46	15.99
P-RPS6	<i>WT</i>	0.00909	8.360	53.3	125.80	n.s.	157.26	15.88
	<i>KO</i>	0.00603	9.686	57.7	181.56		176.00	12.99
P-AKT	<i>WT</i>	0.04074	4.638	34.3	23.67	n.s.	20.05	15.10
	<i>KO</i>	0.01304	7.320	49.2	19.89		18.77	13.51
P-ERK	<i>WT</i>	0.03083	5.223	38.3	1.79	0.00008	0.56	4.63
	<i>KO</i>	n.s.			3.27			
RPL5	<i>WT</i>	0.03941	5.215	38.2	3.02	n.s.	1.37	16.76
	<i>KO</i>	0.00054	22.830	78.0	3.46		2.28	9.38
RPL23	<i>WT</i>	0.04165	4.593	34.0	18.67	0.00123	13.70	17.15
	<i>KO</i>	0.04366	4.499	33.3	36.04		7.96	0.09
RPL32	<i>WT</i>	0.04843	4.294	31.8	5.71	0.00002	1.90	13.36
	<i>KO</i>	0.02661	5.549	40.3	9.95		1.76	1.60
RPLP0	<i>WT</i>	0.00112	17.533	72.8	2.68	0.00051	1.33	10.85
	<i>KO</i>	0.01775	6.512	45.5	4.92		1.62	19.77
UBF1	<i>WT</i>	0.00099	18.304	73.7	3.01	0.00005	0.97	8.63
	<i>KO</i>	n.s.			1.68			

Table S8: Cosinor statistical values related to rhythmic phosphorylation and expression of protein involved in mRNA translation, cell signaling and ribosome biogenesis in wild-type and *Bmal1* KO mice

Gene	Genotype	p value	F[2,9]	Robustness (%)	Mesor	mesor p value	Amplitude	Acrophase (h)
P-EIF4E	<i>WT</i>	0.03271	5.096	37.5	4.69	n.s.	1.28	6.45
	<i>KO</i>	0.02043	6.166	43.7	5.16		1.74	12.38
P-EIF4G1	<i>WT</i>	0.03883	4.736	35.0	2.33	n.s.	1.07	17.69
	<i>KO</i>	n.s.			2.63			
P-RPS6	<i>WT</i>	0.00813	8.703	54.6	90.65	0.01235	94.45	17.79
	<i>KO</i>	n.s.			38.66			
P-AKT	<i>WT</i>	0.04379	4.493	33.3	17.83	0.00018	5.94	13.44
	<i>KO</i>	n.s.			6.88			
P-ERK	<i>WT</i>	0.00057	22.417	77.7	1.81	n.s.	0.75	8.97
	<i>KO</i>	n.s.			1.74			
RPL5	<i>WT</i>	0.02301	5.883	42.2	2.05	n.s.	0.66	18.59
	<i>KO</i>	0.00010	45.027	87.9	3.06		1.47	5.66
RPL23	<i>WT</i>	0.04263	4.547	33.7	2.02	n.s.	0.49	18.84
	<i>KO</i>	0.00474	10.550	60.1	2.49		1.19	7.00
RPL32	<i>WT</i>	0.04760	4.328	32.0	2.32	0.00036	0.72	19.11
	<i>KO</i>	0.00056	22.488	77.8	3.93		1.34	7.83
RPLP0	<i>WT</i>	0.04692	4.356	32.3	2.76	n.s.	0.82	21.80
	<i>KO</i>	0.00520	10.211	59.2	2.77		0.99	6.63
UBF1	<i>WT</i>	0.02444	5.743	41.4	6.07	0.00013	3.33	7.03
	<i>KO</i>	n.s.			10.92			

Table S9: Taqman probes used for real-time PCR (Applied Biosystems)

Gene	Probe reference
<i>Gapdh</i>	Mm 99999915_g1
<i>28S rRNA</i>	Mm 03682676_s1
<i>Eif4e</i>	Mm 00725633_s1
<i>Eif4g1</i>	Mm 00524099_m1
<i>Eif4a2</i>	Mm 00834357_g1
<i>Eif4b</i>	Mm 00778003_s1
<i>Eif4ebp1</i>	Mm 01620026_g1
<i>Eif4ebp3</i>	Mm 01406408_m1
<i>Rpl23</i>	Mm 00787512_s1
<i>Rpl32</i>	Mm 02528467_g1
<i>Rpl34</i>	Mm 01318199_g1
<i>mTor</i>	Mm 00444968_m1
<i>Raptor</i>	Mm 00712676_m1
<i>Map4k3</i>	Mm 01232993_m1
<i>Mknk2</i>	Mm 00458026_m1
<i>Ubf1</i>	Mm 00456972_m1

Table S10: Sequences of the primers used for SYBR® Green real-time PCR

Gene	Forward primer	Reverse primer
<i>Gapdh</i>	CATGGCCTTCCGTGTTCCCTA	CCTGCTCTTCCGTGTTCCCTA
<i>45S rRNA</i>	GCTGCCTCACCAGTCTTTCT	GCAAGACCCAAACACACACA
<i>Rpl23 intron 3</i>	ATTGATGAACACGGCAAACA	GAGTTCGAGACCGAGACCAG
<i>Rpl32 intron 3</i>	TACAGCAGCAGTCCATGAGG	CACCCCAGGACTCTTTACCA
<i>Rpl34 intron 3</i>	CCTGCCCTGTTTGTGGTAGT	TGGAAATCTTTTCCGTTTGC

Table S11: References of the antibodies used for Western blotting

Protein	Reference	Company
P-EIF4E (Ser 209)	9741	Cell Signaling Technology
EIF4E	2067	Cell Signaling Technology
P-EIF4G (Ser 1108)	2441	Cell Signaling Technology
EIF4G	2469	Cell Signaling Technology
P-EIF4B (Ser 422)	3591	Cell Signaling Technology
EIF4B	3592	Cell Signaling Technology
P-4EBP1 (Thr 37/46)	2855	Cell Signaling Technology
4EBP1	9644	Cell Signaling Technology
P-RPS6 (Ser 235/236)	2211	Cell Signaling Technology
RPS6	2217	Cell Signaling Technology
P-TSC2 (Ser 1387)	5584	Cell Signaling Technology
TSC2	4308	Cell Signaling Technology
P-AKT (Ser 473)	4060	Cell Signaling Technology
AKT	4691	Cell Signaling Technology
P-p44/42 MAPK (ERK1/2) (Thr202 / Tyr 204)	4376	Cell Signaling Technology
P44/42 MAPK (ERK1/2)	9102	Cell Signaling Technology
P-p90RSK (Thr 359/363)	9344	Cell Signaling Technology
p90RSK	9355	Cell Signaling Technology
P-RAPTOR (Ser 792)	2083	Cell Signaling Technology
RAPTOR	2280	Cell Signaling Technology
TOR	2983	Cell Signaling Technology
LP0 Ribosomal Protein	51019-2-AP	ProteinTech Group
L5 Ribosomal Protein	15430-1-AP	ProteinTech Group
L23 Ribosomal Protein	16086-1-AP	ProteinTech Group
L32 Ribosomal Protein	ARP-40219-T100	Aviva Systems Biology
UBF1	sc-9131	Santa Cruz Biotechnology
PER1		Brown et al., 2005
BMAL1		Preitner et al., 2002

II. Involvement of circadian clock in lipid metabolism

A. Modulation of PPAR α signaling pathway in mouse liver

DBP (D-box Binding Protein), TEF (Thyrotroph Embryonic Factor), and HLF (Hepatic Leukemia Factor) are three circadian clock-controlled PAR bZip (Proline- and Acidic amino acid-Rich domain basic leucine Zipper) transcription factors^{113, 296}. These PAR bZip act by binding to D-boxes present on target gene promoters²⁹⁷. Studies in mice deficient for these three transcription factors, PAR bZip KO mice, showed the impact of the circadian clock on several metabolic pathways. Indeed, PAR bZip mice exhibit early aging phenotype, severe epilepsy attacks²⁹⁸, defect in liver xenobiotic detoxification³, cardiac hypertrophy and left ventricular dysfunction associated with a low blood pressure²⁹⁹.

In the present study³⁰⁰, PAR bZip proteins as transcription factors are involved in the rhythmic accumulation and activity of PPAR α . Indeed, in mice depleted of the three PAR bZip (PAR bZip 3KO mice) the expression of PPAR α was damped, as well as *Cyp4a10* and *Cyp4a14* mRNA, two PPAR α target genes. PPAR α activity is stimulated by the binding to fatty acids. Fatty acids availability is driven by LPL (LipoProtein Lipase) and ACOTs (Acyl CoA Thioesterase) enzymes. Here it is proposed that *Acot* gene expressions were under the control of PAR bZip as their diurnal expression was impaired in PAR bZip 3KO mice. However, in mice kept under free-fat diet, PPAR α activity was rescue due to *de novo* fatty acid synthesis as shown by the increased expression of *Fasn* (*Fatty acid synthase*) mRNA.

It appears thus that under normal diet, circadian PAR bZip control free fatty acids release through the control of ACOTs expression. These free fatty acids then play their role of ligands by stimulating PPAR α activation. PPAR α then stimulates transcription of *Acot* and *Lpl*, and in a feed-forward loop reinforces its own expression and activity.

Proline- and acidic amino acid-rich basic leucine zipper proteins modulate peroxisome proliferator-activated receptor α (PPAR α) activity

Frédéric Gachon^{a,b,1}, Nicolas Leuenberger^{c,2}, Thierry Claudel^d, Pascal Gos^a, Céline Jouffe^b, Fabienne Fleury Olela^a, Xavier de Mollerat du Jeu^e, Walter Wahli^c, and Ueli Schibler^{a,1}

^aDepartment of Molecular Biology, National Center of Competence in Research "Frontiers in Genetics," Sciences III, University of Geneva, CH-1211 Geneva 4, Switzerland; ^bDepartment of Pharmacology and Toxicology, University of Lausanne, CH-1005 Lausanne, Switzerland; ^cCenter for Integrative Genomics, National Center of Competence in Research "Frontiers in Genetics," University of Lausanne, CH-1015 Lausanne, Switzerland; ^dLaboratory of Experimental and Molecular Hepatology, Division of Gastroenterology and Hepatology, Department of Medicine, Medical University Graz, A-8036 Graz, Austria; and ^eLife Technologies, Carlsbad, CA 92008

Edited by Steven L. McKnight, University of Texas Southwestern, Dallas, TX, and approved February 4, 2011 (received for review April 7, 2010)

In mammals, many aspects of metabolism are under circadian control. At least in part, this regulation is achieved by core-clock or clock-controlled transcription factors whose abundance and/or activity oscillate during the day. The clock-controlled proline- and acidic amino acid-rich domain basic leucine zipper proteins D-site-binding protein, thyrotroph embryonic factor, and hepatic leukemia factor have previously been shown to participate in the circadian control of xenobiotic detoxification in liver and other peripheral organs. Here we present genetic and biochemical evidence that the three proline- and acidic amino acid-rich basic leucine zipper proteins also play a key role in circadian lipid metabolism by influencing the rhythmic expression and activity of the nuclear receptor peroxisome proliferator-activated receptor α (PPAR α). Our results suggest that, in liver, D-site-binding protein, hepatic leukemia factor, and thyrotroph embryonic factor contribute to the circadian transcription of genes specifying acyl-CoA thioesterases, leading to a cyclic release of fatty acids from thioesters. In turn, the fatty acids act as ligands for PPAR α , and the activated PPAR α receptor then stimulates the transcription of genes encoding proteins involved in the uptake and/or metabolism of lipids, cholesterol, and glucose metabolism.

circadian clock | liver lipid metabolism | nuclear receptors

In mammals, energy homeostasis demands that anabolic and catabolic processes are coordinated with alternating periods of feeding and fasting. There is increasing evidence that inputs from the circadian clock are required in addition to acute regulatory mechanisms to adapt metabolic functions to an animal's daily needs. For example, mice with disrupted hepatocyte clocks display a hypoglycemia during the postabsorptive phase, supposedly because hepatic gluconeogenesis and glucose delivery into the bloodstream are dysregulated in these animals (1).

The regulation of lipid metabolism is also governed by an interaction between acute and circadian regulatory mechanisms, and the three peroxisome proliferator-activated receptors (PPAR α , PPAR β/δ , and PPAR γ) play particularly important roles in these processes (2). Among them, PPAR α acts as a molecular sensor of endogenous fatty acids (FAs) and regulates the transcription of genes involved in lipid uptake and catabolism. Moreover, it accumulates according to a daily rhythm and reaches maximal levels around the beginning of feeding time (3, 4). For liver and many other peripheral tissues, feeding–fasting rhythms are the most dominant zeitgebers (timing cues) (5, 6). This observation underscores the importance of the cross-talk between metabolic and circadian cycles.

Circadian oscillators in peripheral tissues can participate in the control of rhythmic metabolism through circadian transcription factors, which in turn regulate the cyclic transcription of metabolically relevant downstream genes. The three PAR-domain basic

leucine zipper (PAR bZip) proteins, D-site-binding protein (DBP), thyrotroph embryonic factor (TEF), and hepatic leukemia factor (HLF), are examples of such output mediators (for review, see ref. 7). Mice deficient of only one or two members of the PAR bZip gene family display rather mild phenotypes, suggesting that the three members execute partially redundant functions. However, mice deficient of all three PAR bZip genes (henceforth called PAR bZip 3KO mice) have a dramatically reduced life span due to epileptic seizures (8) and impaired xenobiotic detoxification (9).

Genome-wide transcriptome profiling of wild-type and PAR bZip 3KO mice has revealed differentially expressed genes involved in lipid metabolism, many of which are targets of the nuclear receptor PPAR α . Here we present evidence for a pathway in which PAR bZip transcription factors connect the accumulation and activity of PPAR α to circadian oscillators in liver.

Results

***Ppara* Expression in PAR bZip 3KO Mice.** Genome-wide microarray transcriptome profiling studies with liver RNA from wild-type and PAR bZip 3KO mice revealed differentially expressed genes involved in xenobiotic detoxification (9) and lipid metabolism (this paper). The latter included *Ppara*, a gene specifying a nuclear receptor that is well known as a regulator of lipid metabolism, and many PPAR α target genes (10) (Fig. S1A). We validated the reduced accumulation of *Ppara* mRNA and transcripts issued by PPAR α target genes by using quantitative RT-PCR analysis (Fig. 1 A and B and Fig. S1B). The examined PPAR α target genes include *Cyp4a10* and *Cyp4a14*, encoding enzymes involved in FA ω -oxidation (whose expression is strongly reduced in *Ppara* KO mice, see Fig. S2A), and genes specifying enzymes involved in FA β -oxidation (Fig. S1B). PPAR α has also been shown to activate transcription from its own promoter, when activated by PPAR α agonists (11). To evaluate the relevance of this feed-forward loop in circadian *Ppara* transcription, we compared the temporal expression of *Ppara* pre-mRNA in the liver of wild-type mice with that of nonproductive pre-mRNA transcripts issued by the disrupted *Ppara* alleles in *Ppara* KO mice (12). As

Author contributions: F.G., N.L., T.C., X.d.M.d.J., W.W., and U.S. designed research; F.G., N.L., T.C., P.G., C.J., and F.F.O. performed research; X.d.M.d.J. contributed new reagents/analytic tools; F.G., N.L., T.C., W.W., and U.S. analyzed data; and F.G., W.W., and U.S. wrote the paper.

The authors declare no conflict of interest.

This article is a PNAS Direct Submission.

¹To whom correspondence may be addressed. E-mail: frederic.gachon@unil.ch or ueli.schibler@unige.ch.

²Present address: Swiss Laboratory for Doping Analysis, CH-1066 Epalinges, Switzerland.

This article contains supporting information online at www.pnas.org/lookup/suppl/doi:10.1073/pnas.1002862108/-DCSupplemental.

depicted in Fig. 1C, the circadian expression was indeed dampened in these animals, suggesting that PPAR α contributed to the rhythmic transcription of its own gene. Therefore, PAR bZip transcription factors may have activated *Ppara* transcription through an indirect mechanism, for example, by promoting the cyclic generation of PPAR α ligands.

Unexpectedly, hepatic PPAR α protein accumulation was higher in PAR bZip 3KO mice as compared to wild-type mice, in spite of the lower mRNA levels in the former (Fig. 1D). However, nuclear receptors can be destabilized in a ligand-dependent manner (for review, see ref. 13). Hence, the higher protein to mRNA level in hepatocytes of PAR bZip 3KO mice could indicate that in these animals PPAR α was less active and therefore more stable than in the liver of wild-type mice. To examine this conjecture, we measured hepatic PPAR α protein and mRNA accumulation, 4 h after an intraperitoneal injection of the synthetic PPAR α ligand WY14643 into PAR bZip 3KO mice. As shown in Fig. 1E and Fig. S3, the injection of the PPAR α ligand led to a decrease of the protein to mRNA ratio, in keeping with the model of Kamikaze activators postulated by Thomas and Tyers (14). The lower PPAR α protein to mRNA ratio in wild-type as compared to PAR bZip 3KO mice may therefore indicate

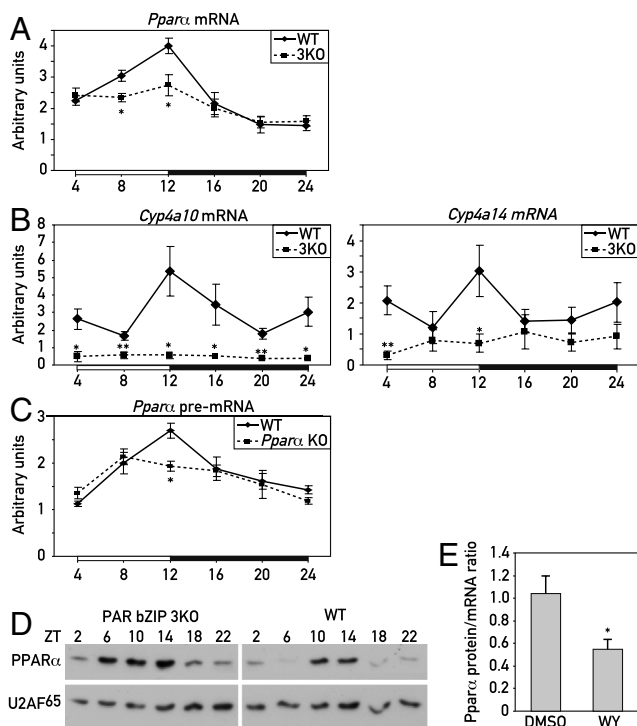


Fig. 1. Expression of PPAR α in PAR bZip 3KO mice. (A) Temporal expression of *Ppara* mRNA in the livers of WT and PAR bZip 3KO mice. RNA levels were estimated by real-time RT-PCR. Mean values \pm SEM obtained from six animals are given. (B) Temporal expression of the PPAR α target genes *Cyp4a10* and *Cyp4a14* in the liver of WT and PAR bZip 3KO mice, as determined by real-time RT-PCR. Mean values \pm SEM obtained from six animals are given. (C) Temporal expression of *Ppara* pre-mRNA transcripts in the livers of WT or *Ppara* KO mice. A PCR amplicon located in the second intron was used in these quantitative RT-PCR experiments. Mean values \pm SEM obtained from four animals are given. (D) Temporal expression of PPAR α protein in liver nuclear extracts from PAR bZip 3KO and WT mice. Signals obtained with U2AF⁶⁵ antibody were used as loading controls (U2AF⁶⁵ is a constitutively expressed splicing factor). (E) Ratio of liver PPAR α protein/*Ppara* mRNA levels after injection of the synthetic PPAR α ligand WY14643 or its solvent (50% DMSO) in PAR bZip 3KO mice at ZT2. Mean values \pm SEM obtained from six animals are given. The raw data used for these computations are presented in Fig. S3. The zeitgeber times (ZT) at which the animals were killed are indicated (* p \leq 0.05, ** p \leq 0.01 KO vs. WT, Student's t test).

that PPAR α had a higher activity in the former animals than in the latter.

PAR bZip Transcription Factors May Stimulate PPAR α Activity Through the Production of PPAR α Ligands. FAs generated by the metabolism of dietary lipids or de novo synthesis are the best known natural ligands for PPAR α (15–17). In liver, FAs can be produced through the hydrolysis of acyl-CoA esters by acyl-CoA thioesterases (ACOTs) (18) and through the hydrolysis of lipids in lipoproteins by lipoprotein lipases (LPLs) (19). Interestingly, members of both of these two enzyme families have been reported to accumulate according to a daily rhythm in the liver (20–22), and our genome-wide transcriptome profiling experiments suggested that the mRNAs for these enzymes were expressed at reduced levels in PAR bZip 3KO mice. As shown in Fig. 2B, the accumulation of transcripts specifying ACOTs displayed temporal expression patterns expected for direct PAR bZip target genes and was indeed blunted in PAR bZip 3KO mice. The *Acot* genes are all located on a 120 kb cluster on mouse chromosome 12, and a perfect PAR bZip DNA binding sequence is located between *Acot1* and *Acot4* (Fig. 2A). At least in vitro, this sequence binds PAR bZip in a diurnal manner (Fig. 2A), which could explain the rhythmic expression of these genes. However, the phase of *Lpl* transcript accumulation was found to be delayed by 12 h when compared to that of *Acot* expression, and we suspected that PAR bZip proteins regulate *Lpl* transcription via an indirect mechanism. Interestingly, *Acot* and *Lpl* reached maximal concentrations at ZT12 and ZT24, respectively, suggesting a bimodal metabolism of FAs in mouse liver: hydrolysis of acyl-CoAs at the day–night transition and hydrolysis of lipids in lipoproteins at the night–day transition.

The transcription of *Acots* and *Lpl* has previously been reported to be regulated by PPAR α (21–23), and the expression of these genes, in addition to that of *Cyp4a10* and *Cyp4a14*, is activated by injection of WY14643 (Fig. S4). We thus decided to examine the role of PPAR α on their diurnal expression by comparing liver RNAs harvested around the clock from *Ppara* KO and wild-type mice. As shown in Fig. S2B, the overall expression levels of *Acots* were only slightly decreased in *Ppara* KO animals for *Acot3* and *Acot4*, not changed for *Acot2*, but 2.5-fold increased for *Acot1*. However, zenith levels were reached about 4–12 h later in *Ppara* KO as compared to wild-type mice. All in all, the changes of *Acot* and *Lpl* expression in PPAR α deficient mice were complex and reflected perhaps a synergistic regulation by PAR bZip transcription factors and PPAR α or other transcription factors.

In the absence of food-derived lipids, PPAR α ligands can also be generated de novo by synthesis of FAs by fatty acid synthase (FASN) (24, 25). Interestingly, *Fasn* expression was enhanced in PAR bZip 3KO animals, supposedly to compensate for the deficient import and/or metabolism of lipids absorbed with the food. Perhaps for the same reasons, the expression of *Fabp1* and *Cd36*, genes encoding proteins involved in FA transport and uptake, was also increased in these mice (Fig. S1B). As described previously (26), *Fasn* expression was decreased in the liver of *Ppara* KO mice, probably reflecting a perturbed activation of the sterol-response element binding protein in these animals (27).

Down-regulation of ACOT expression reduces the activity of PPAR α target genes. Our results insinuated that PAR bZip proteins may stimulate the activity of PPAR α indirectly. According to this scenario, PAR bZip proteins govern the expression of the ACOT isoforms 1 to 4, which in turn liberate FAs from acyl-CoA esters that may serve as PPAR α ligands. In order to examine this possibility, the hepatic expression of ACOT 1 to 4 was down-regulated by the injection of siRNAs into the tail vein (for experimental details, see SI Text, Table S1, and Fig. S5). As shown in Fig. 2C and Fig. S5, a decrease in ACOT2, ACOT3, and

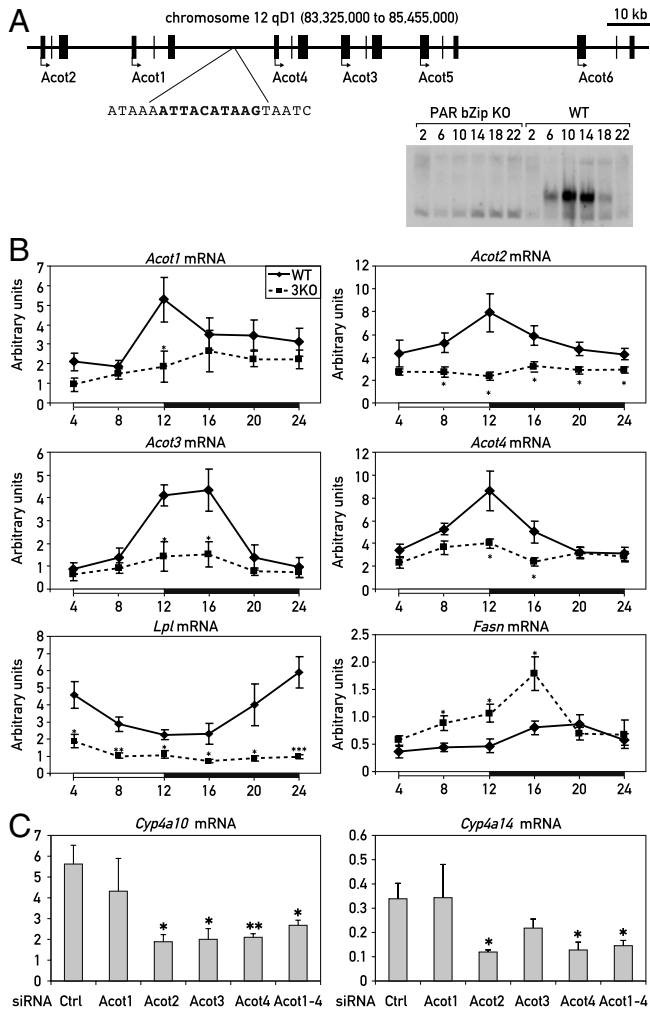


Fig. 2. Regulation of the *Acot* genes cluster and lipid metabolizing enzymes in PAR bZip 3KO. (A) Organization of the mouse *Acot* gene cluster on chromosome 12. A sequence perfectly matching the PAR bZip consensus binding site is located between *Acot1* and *Acot4*. An EMSA experiment with liver nuclear extracts from WT and PAR bZip 3KO mice shows that PAR bZip transcription factors bind this sequence in a diurnal fashion. (B) Temporal expression of acetyl-CoA thioesterase (*Acot*) 1–4, lipoprotein lipase (*Lpl*), and FA synthase (*Fasn*) mRNA in PAR bZip 3KO mice. Real-time RT-PCR experiments were conducted with whole-cell liver RNAs from six animals for each time point. The zeitgeber times (ZT) at which the animals were killed are indicated. Mean values \pm SEM are given. * $p < 0.05$, ** $p < 0.01$, *** $p < 0.001$ KO vs. WT, Student's *t* test. (C) Expression of *Cyp4a10* and *Cyp4a14* mRNA in mouse liver after treatment with siRNAs directed against *Acot* genes. Real-time RT-PCR experiments were conducted with whole-cell liver RNAs from four (control and individual *Acot* siRNA) or six animals (pool of the four precedent *Acot* siRNA). Mean values \pm SEM are given (* $p < 0.05$, ** $p < 0.005$, control siRNA vs. *Acot* siRNA, Student's *t* test).

ACOT4 expression was sufficient to specifically inhibit the expression of the PPAR α target genes *Cyp4a10* and *Cyp4a14*, confirming the role of ACOTs in the activation of PPAR α . Likewise, the intravenous application of an equimolar mixture of ACOT1–4 siRNAs specifically reduced the accumulation of *Cyp4a10* and *Cyp4a14* mRNAs (Fig. 2C and Fig. S5).

Impaired Activity of PPAR α in the Liver of PAR bZip 3KO Mice May Be Due to a Deficiency of FAs. The results presented in the previous section suggested that the down-regulation of ACOTs and LPL in PAR bZip 3KO mice may have caused a decrease in the levels of hepatic FAs that can serve as PPAR α ligands. We thus measured the levels of various FAs in the livers of wild-type and

PAR bZip 3KO mice. In the former, the concentrations of all examined FAs displayed a robust circadian fluctuation with a maximum at ZT12 (Fig. 3A, gray columns). In addition, a second, smaller peak was observed for most of the FAs. This bimodal distribution was consistent with the hypothesis that the temporal expression of ACOTs and LPL (see Fig. 2) were responsible for the hepatic accumulation of FAs. In PAR bZip 3KO mice, the FA levels were low throughout the day (Fig. 3A, white columns). Again, these results were compatible with a down-regulation of ACOTs and LPL in PAR bZip 3KO mice (Fig. 2B). Importantly, several of the examined FAs had previously been identified as PPAR α ligands. For example, C18:1, C18:2, and C18:3 appear to be particularly potent PPAR α ligands (15–17, 28), and the decrease in these FAs probably accounted for the down-regulation of PPAR α target genes in PAR bZip 3KO animals. The blunted activation of the PPAR α pathway in PAR bZip 3KO mice would be expected to manifest itself in a broad dysregulation of hepatic metabolism and associated changes in blood chemistry (26, 29). As depicted in Fig. 3B, PAR bZip 3KO mice showed indeed an increase in the serum concentrations of cholesterol, triglyceride, and glucose, similar to the observations made with *Ppara* KO mice.

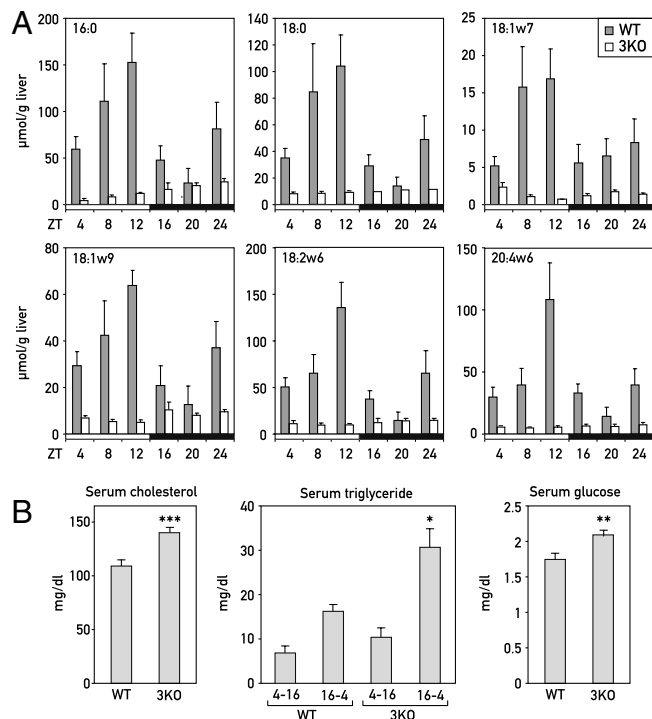


Fig. 3. Lipid metabolism in PAR bZip 3KO mice. (A) Temporal accumulation of FAs (C16:0, C18:0, C18:1w7, C18:1w9, C18:2w6, and C20:4w6) in the livers of WT and PAR bZip 3KO mice. Mean values \pm SEM obtained from four animals are given. The zeitgeber times (ZT) at which the animals were killed are indicated. Note that the profiles of accumulation are daytime dependent for all analyzed FAs in WT animals (ANOVA $F[5,18] = 3.29, 3.72, 9.00, 4.50, 3.86,$ and $4.01,$ and $p < 0.05, 0.025, 0.02, 0.015, 0.025,$ and $0.025,$ respectively), whereas they are low and virtually invariable in KO animals. In all the cases, values were statistically different between WT and KO animals (ANOVA $F[1,46] = 15.85, 13.11, 10.95, 18.00, 13.96,$ and $11.62,$ and $p < 0.0005, 0.001, 0.0025, 0.0001, 0.001,$ and $0.002,$ respectively). (B) Serum concentrations of triglycerides, cholesterol, and glucose in WT and PAR bZip 3KO animals. Mean values \pm SEM obtained from 12 WT and 17 KO animals are given. For triglycerides, values obtained between ZT4 and ZT14 were separated from the values obtained between ZT16 and ZT2, due to their strong circadian variations (* $p < 0.05$, ** $p < 0.01$, *** $p < 0.001$ KO vs. WT, Student's *t* test).

PAR bZip 3KO Mice Have an Impaired Capacity to Adapt to Caloric Restriction. A large number of genes induced by fasting are direct or indirect target genes of PPAR α (30, 31), and *Ppar α* KO mice have indeed difficulties in adapting to caloric restriction (29, 32–36). If the activation of the PPAR α signaling was inhibited in PAR bZip 3KO mice, one would expect that these animals would also have an impaired capacity to adjust their metabolism to reduced food availability. In order to test this hypothesis, we exposed PAR bZip 3KO mice to a feeding regimen in which the quantity of food was reduced to 60% of what these mice absorbed when food was offered ad libitum. As shown in Fig. S6, PAR bZip 3KO mice subjected to this regimen suffered from a rapid and dramatic weight loss, as compared to wild-type mice. However this difference could not be attributed to a difference in energy expenditure, as O₂ consumption and CO₂ production were nearly identical in wild-type and PAR bZip 3KO animals (Fig. S7). We also compared the food anticipatory activity (FAA) of wild-type and PAR bZip 3KO mice (Fig. S8A and B). FAA manifests itself in the onset of enhanced locomotor activity (wheel-running) a few hours before the time when food becomes available. When food availability was limited to a 6-h time span between ZT03 to ZT09, PAR bZip 3KO mice displayed exacerbated FAA and actually shifted a large fraction of their wheel-running activity to this time window during the light phase. As expected, wild-type mice did show FAA but kept running the wheel mainly during the dark phase. These results suggested that the activity associated with food searching equaled or even dominated suprachiasmatic nucleus-driven locomotor activity in PAR bZip 3KO animals when food availability became limiting. Because PPAR α KO mice did not show enhanced FAA (Fig. S8C), the exacerbated FAA cannot have been caused solely by the impaired PPAR α activity in PAR bZip 3KO mice.

PPAR α Ligands Can Be Generated from Food-Derived and de Novo Synthesized Lipids. As discussed above, PPAR α ligands can be generated from diet-derived lipids or de novo synthesis by FASN, and the first pathway appeared to be deficient in PAR bZip 3KO mice. We wished to determine the expression of putative PPAR α target genes and genes with key functions in the production of PPAR α ligands in wild-type and PAR bZip 3KO mice that were fed with a fat-free diet during an extended time span (5 wk). Under these conditions, FAs can be produced exclusively through de novo synthesis. As shown in Fig. 4A, the mRNAs of PPAR α target genes *Cyp4a10* and *Cyp4a14* accumulated to similar levels in wild-type and PAR bZip 3KO mice receiving a fat-free diet, unlike what had been observed in animals fed on normal chow. The similar expression of these PPAR α target genes in mice receiving a fat-free diet suggested that de novo synthesis of FAs serving as PPAR α agonists was not affected by the absence PAR bZip transcription factors, and *Fasn* mRNA was indeed expressed at similar levels in wild-type and PAR bZip 3KO mice receiving fat-free food. Hence, the fat-free diet rescued the deficiency of PPAR α activity in PAR bZip 3KO mice, presumably because de novo synthesis of FAs in liver did not depend upon pathways requiring the circadian PAR bZip proteins. This interpretation was validated by our observation that the hepatic concentrations of various FAs were similar in wild-type and PAR bZip 3KO mice exposed to a fat-free diet (Fig. S9). Interestingly, the expression of *Ppar α* and *Acots* was also rescued by the fat-free diet in PAR bZip 3KO mice and, in keeping with earlier observations (11, 21, 22), both of these genes were indeed activated by PPAR α ligands. *Lpl* expression did not exhibit large differences between mice fed with normal and fat-free chow. Similarly, blood glucose, cholesterol, and triglyceride levels were not significantly different between wild-type and PAR bZip 3KO mice kept on a fat-free diet (Fig. 4B), unlike what we have observed for animals fed with normal chow.

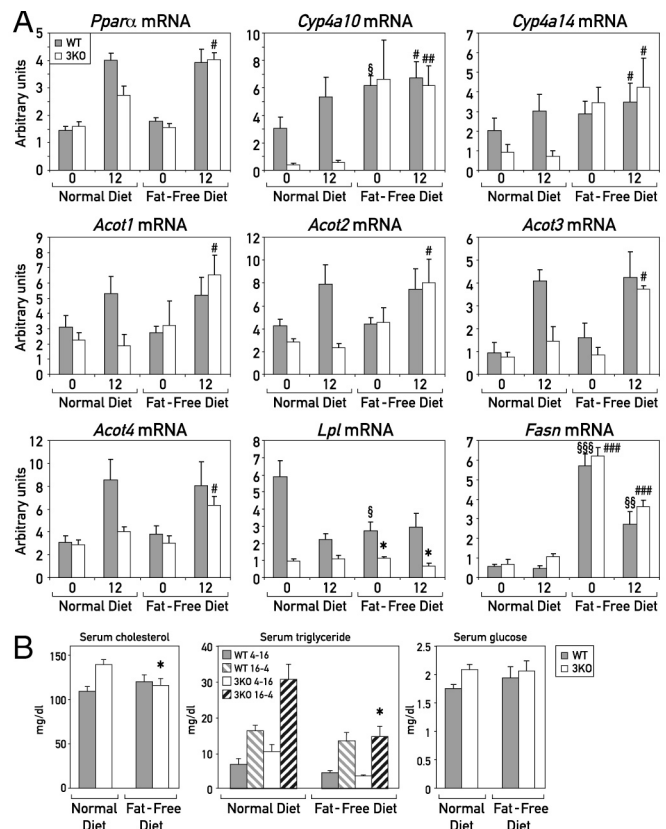


Fig. 4. Effect of fat-free diet on PPAR α target genes expression and serum biochemistry (A) Mice were fed ad libitum during 5 wk with a fat-free diet. For each condition, four mice were killed at ZT0 and ZT12. Total liver RNAs were extracted and analyzed by real-time RT-PCR for the expression of mRNAs specified by PPAR α target genes and *Fasn*, a marker gene of lipogenesis that is induced by the fat-free diet ($\#p \leq 0.05$, $\#\#\#p \leq 0.005$ fat-free vs. normal diet in 3KO; $\$p \leq 0.05$, $\$\$\$p \leq 0.01$, $\$\$\$\$p \leq 0.00005$ fat-free vs. normal diet in WT; $*p \leq 0.05$ KO vs. WT, Student's *t* test). (B) Serum concentrations of triglycerides, cholesterol, and glucose were measured in WT and PAR bZip 3KO animals fed with regular or fat-free chow. Mean values \pm SEM obtained from eight WT and KO animals are given. For FAs, values obtained between ZT4 and ZT14 were separated from the values obtained between ZT16 and ZT2 ($*p \leq 0.05$ fat-free vs. normal diet in 3KO).

Discussion

PAR bZip Transcription Factors DBP, HLF, and TEF Regulate Circadian PPAR α Activity. Here we present evidence for a metabolic clock output pathway operative in hepatocytes, which connects the PAR bZip transcription factors DBP, HLF, and TEF to the circadian activity of PPAR α . This nuclear receptor has long been known to play a key role in the coordination of lipid metabolism and, like several other nuclear receptors, it accumulates in a circadian manner (3, 4). Our studies revealed that *Ppar α* mRNA levels were reduced in PAR bZip 3KO mice. However, PPAR α protein accumulated to higher than wild-type levels in these animals, presumably due to its reduced transactivation potential.

Our gene expression studies, combined with hepatic FAs measurements, offered a plausible biochemical pathway for the PAR bZip-dependent activation of PPAR α , schematized in Fig. 5. PAR bZip proteins drive directly or indirectly the expression of *Acots* and *Lpl*, which in turn release FAs from acyl-CoA esters and lipoproteins, respectively. FAs then serve as ligands of PPAR α and initiate a feed-forward loop, in which PPAR α enhances transcription from its own gene. This scenario is supported by our observation that the siRNA-mediated dampening of ACOT2, ACOT3, and ACOT4 expression led to a down-reg-

ulation of the expression of *Cyp4a10* and *Cyp4a14*, two bona fide target genes of PPAR α .

The accumulation cycles of *Acots* and *Lpl* mRNA had widely different phases, yet both were strongly attenuated in PAR bZip 3KO mice. Whereas the phase of *Acot* expression was compatible with that expected for direct PAR bZip target genes, *Lpl* mRNA reached maximal levels at a time (ZT24) when all three PAR bZip proteins were expressed at nadir values. We thus suspect that *Lpl* transcription was controlled by a complex pathway, in which the precise roles of PPAR α and PAR bZip proteins remain to be clarified. The temporal accumulation of most determined FAs revealed a major peak at ZT12, when *Acots* were maximally expressed, and a minor peak at ZT24, when *Lpl* was maximally expressed. The control of FAs catabolism through oxidation and lipid uptake are major functions of PPAR α . On first sight, the low hepatic FAs levels in PAR bZip 3KO mice, in which PPAR α activity appeared to be blunted, was perhaps surprising. However, this apparent conundrum can be rationalized as follows. Free FAs are natural ligands for PPAR α , and a minimal FA threshold concentration may thus be required for the activation of PPAR α (15–17, 28). Moreover, acyl-CoA esters antagonize the activation of PPAR α by free FAs (37, 38). Because, due to the reduced expression of *Acots* in PAR bZip 3KO mice, these esters were probably less efficiently hydrolyzed, the ratio of free FAs to acyl-CoA esters is expected to be lower in these animals as compared to wild-type mice. The attenuation of PPAR α activity in the PAR bZip 3KO mice is expected to be associated with an impaired uptake of FAs from the blood (39–41).

PPAR α expression has first been found to follow a daily rhythm by Lemberger et al. (3). Subsequently, Oishi et al. (42) demonstrated that the core-clock transcription factor CLOCK is required for circadian *Ppara* transcription and that CLOCK binds to a series of E-box sequences within the first intron. This regulation by CLOCK might explain why *Ppara* expression is still circadian in PAR bZip 3KO mice, albeit with reduced amplitude and magnitude.

PPAR α Target Gene Expression is Rescued in PAR bZip 3KO Mice Fed with a Fat-Free Diet. In animals kept on a fat-free diet, hepatic FA synthesis is strongly induced (43). We thus suspected that the intracellular availability of FAs rescued PPAR α -mediated tran-

scription in PAR bZip 3KO mice. Indeed, the production of mRNAs encoding enzymes implicated in FAs synthesis, such as FASN, was strongly induced in wild-type and PAR bZip 3KO mice receiving a fat-free diet. Furthermore, in contrast to mice fed on a normal chow, PAR bZip 3KO and wild-type animals fed on a fat-free diet accumulated similar hepatic levels of mRNAs specified by *Ppara*, and the putative PPAR α target genes *Cyp4a10* and *Cyp4a14*. We did notice, however, that *Acot* expression, whose overall magnitude was only slightly changed in *Ppara* KO mice, was also rescued in PAR bZip 3KO mice kept on a fat-free diet. Hence, as previously suggested (21, 22), *Acot* transcription was also augmented by PPAR α , but probably required high concentrations of natural ligands (i.e., FAs). It is noteworthy that 1-palmitoyl-2-oleoyl-*sn*-glycerol-3-phosphocholine, whose FASN-dependent synthesis was activated under a fat-free diet, has recently been discovered as a highly potent PPAR α ligand (24).

PAR bZip 3KO Mice Are Unable to Adapt to Restricted Feeding. Wild-type mice exposed to caloric restriction lost about 13% of their body mass during the first 3 wk and then kept their mass within narrow boundaries over several months. In contrast, PAR bZip 3KO animals rapidly lost more than 20% of their weight and had to be killed after about a week, because they probably would have succumbed to wasting after this time period. At least in part, the failure of PAR bZip deficient mice may be due to a decreased PPAR α activity, as *Ppara* KO mice have been reported to adapt poorly to calorie restriction (29, 32–36). However, not all phenotypes of PAR bZip 3KO mice related to feeding could be assigned to an impaired PPAR α activity. Thus, in contrast to PAR bZip 3KO mice, *Ppara* KO mice did not exhibit an exacerbated FAA.

The capacity to adapt activity and metabolism to feeding–fasting cycles is primary to an animal's health and survival, and the disruption of the circadian timing system has indeed been linked to obesity and other metabolic disorders (44–46).

Experimental Procedures

Animal Housing Conditions. All animal studies were conducted in accordance with the regulations of the veterinary office of the State of Geneva and of the State of Vaud. PAR bZip 3KO mice with disrupted *Dbp*, *Tef*, and *Hlf* genes (8) and mice with *Ppara* null alleles (12) have been described previously. Mice were maintained under standard animal housing conditions, with free access to food and water, and a 12-h-light–12-h-dark cycle. Specific treatments and feeding regimens are described in *SI Text*.

Blood Chemistry. Blood samples were harvested after decapitation of the animals, and sera were obtained by centrifugation of coagulated samples for 10 min at 2,000 \times g at room temperature. The sera were stored at -20°C until analyzed. Triglycerides and total cholesterol were measured using commercially available enzymatic kits according to the manufacturer's instructions (Triglyceride; Cholesterol; Roche/Hitachi Mannheim GmbH). Glucose was measured using the glucose oxidase method adapted to rodent (GO assay kit Sigma-Aldrich, Handels GmbH).

Liver FA Measurement: Mouse livers were homogenized in 0.5 mL of phosphate buffered saline and 0.5 mL of methanol. This procedure inhibits triglycerides lipases and allows their elimination. Each sample was immediately spiked with 50 nmol of 15:0 FAs as an internal standard. Subsequently, lipids were extracted according to Bligh and Dyer (47) and FAs were then measured by GC-MS as described in *SI Text*.

RNA Isolation and Analysis. Livers were removed within 4 min after decapitation, frozen in liquid nitrogen, and stored at -70°C until use. The extraction of whole-cell RNA and its analysis by real-time RT-PCR were conducted as described previously (8). The

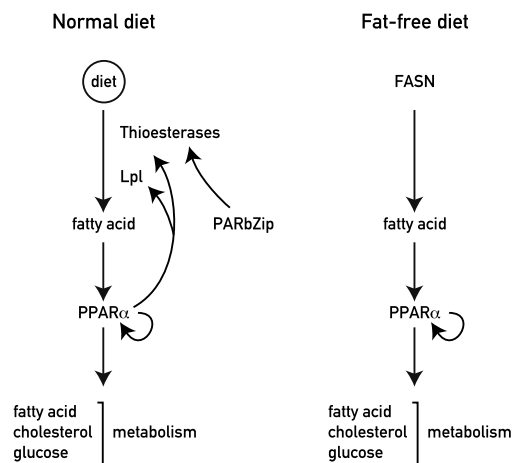


Fig. 5. Model showing the regulation of PPAR α by metabolism and PAR bZip transcription factors. (Left) Under normal diet conditions, the expression of ACOTs are under the control of circadian PAR bZip transcription factors. These transcription factors thus control the release of free FA from acyl-CoA thioesters, and the free FAs stimulate PPAR α activity. The activated PPAR α then stimulates transcription of *Acot* and *Lpl*, and in a feed-forward loop reinforces its own expression and activity. (Right) Under a fat-free diet, all free FAs are derived from the de novo synthesis pathway. Under these conditions, PPAR α activity is not dependent on PAR bZip transcription factors.

values were normalized to those obtained for *Gapdh* mRNA. Sequences of the oligonucleotides used are given in Table S2.

Preparation of Nuclear Protein Extracts and Western Blotting. Liver nuclear proteins were prepared by using the NaCl-Urea-NP40 procedure (48). Western blotting was carried out as described (9). The rabbit anti-PPAR α and murine anti-U2AF⁶⁵ antibodies were purchased from Cayman Chemical and Sigma, respectively.

1. Lamia KA, Storch K-F, Weitz CJ (2008) Physiological significance of a peripheral tissue circadian clock. *Proc Natl Acad Sci USA* 105:15172–15177.
2. Desvergne B, Michalik L, Wahli W (2006) Transcriptional regulation of metabolism. *Physiol Rev* 86:465–514.
3. Lemberger T, et al. (1996) Expression of the peroxisome proliferator-activated receptor α gene is stimulated by stress and follows a diurnal rhythm. *J Biol Chem* 271:1764–1769.
4. Yang X, et al. (2006) Nuclear receptor expression links the circadian clock to metabolism. *Cell* 126:801–810.
5. Damiola F, et al. (2000) Restricted feeding uncouples circadian oscillators in peripheral tissues from the central pacemaker in the suprachiasmatic nucleus. *Genes Dev* 14:2950–2961.
6. Stokkan K-A, Yamazaki S, Tei H, Sakaki Y, Menaker M (2001) Entrainment of the circadian clock in the liver by feeding. *Science* 291:490–493.
7. Gachon F (2007) Physiological function of PARbZip circadian clock-controlled transcription factors. *Ann Med* 39:562–571.
8. Gachon F, et al. (2004) The loss of circadian PAR bZip transcription factors results in epilepsy. *Genes Dev* 18:1397–1412.
9. Gachon F, Fleury Olela F, Schaad O, Descombes P, Schibler U (2006) The circadian PAR-domain basic leucine zipper transcription factors DBP, TEF, and HLF modulate basal and inducible xenobiotic detoxification. *Cell Metab* 4:25–36.
10. Leuenerberger N, Pradervand S, Wahli W (2009) Sumoylated PPAR α mediates sex-specific gene repression and protects the liver from estrogen-induced toxicity in mice. *J Clin Invest* 119:3138–3148.
11. Pineda Torra I, Jamshidi Y, Flavell DM, Fruchart J-C, Staels B (2002) Characterization of the human PPAR α promoter: Identification of a functional nuclear receptor response element. *Mol Endocrinol* 16:1013–1028.
12. Lee SS, et al. (1995) Targeted disruption of the α isoform of the peroxisome proliferator-activated receptor gene in mice results in abolishment of the pleiotropic effects of peroxisome proliferators. *Mol Cell Biol* 15:3012–3022.
13. Rochette-Egly C (2005) Dynamic combinatorial networks in nuclear receptor-mediated transcription. *J Biol Chem* 280:32565–32568.
14. Thomas D, Tyers M (2000) Transcriptional regulation: Kamikaze activators. *Curr Biol* 10:R341–R343.
15. Forman BM, Chen J, Evans RM (1997) Hypolipidemic drugs, polyunsaturated fatty acids, and eicosanoids are ligands for peroxisome proliferator-activated receptors α and δ . *Proc Natl Acad Sci USA* 94:4312–4317.
16. Kliewer SA, et al. (1997) Fatty acids and eicosanoids regulate gene expression through direct interactions with peroxisome proliferator-activated receptors α and γ . *Proc Natl Acad Sci USA* 94:4318–4323.
17. Krey G, et al. (1997) Fatty acids, eicosanoids, and hypolipidemic agents identified as ligands of peroxisome proliferator-activated receptors by coactivator-dependent receptor ligand assay. *Mol Endocrinol* 11:779–791.
18. Hunt MC, Alexson SEH (2002) The role Acyl-CoA thioesterases play in mediating intracellular lipid metabolism. *Prog Lipid Res* 41:99–130.
19. Ziouzenkova O, et al. (2003) Lipolysis of triglyceride-rich lipoproteins generates PPAR ligands: Evidence for an antiinflammatory role for lipoprotein lipase. *Proc Natl Acad Sci USA* 100:2730–2735.
20. Benavides A, Siches M, Llobera M (1998) Circadian rhythms of lipoprotein lipase and hepatic lipase activities in intermediate metabolism of adult rat. *Am J Physiol* 275:R811–817.
21. Hunt MC, et al. (2000) Involvement of the peroxisome proliferator-activated receptor α in regulating long-chain acyl-CoA thioesterases. *J Lipid Res* 41:814–823.
22. Hunt MC, Solaas K, Kase BF, Alexson SEH (2002) Characterization of an Acyl-CoA thioesterase that functions as a major regulator of peroxisomal lipid metabolism. *J Biol Chem* 277:1128–1138.
23. Schoonjans K, et al. (1996) PPAR α and PPAR γ activators direct a distinct tissue-specific transcriptional response via a PPRE in the lipoprotein lipase gene. *EMBO J* 15:5336–5348.
24. Chakravarthy MV, et al. (2009) Identification of a physiologically relevant endogenous ligand for PPAR α in liver. *Cell* 138:476–488.
25. Chakravarthy MV, et al. (2005) “New” hepatic fat activates PPAR α to maintain glucose, lipid, and cholesterol homeostasis. *Cell Metab* 1:309–322.
26. Patel DD, Knight BL, Wiggins D, Humphreys SM, Gibbons GF (2001) Disturbances in the normal regulation of SREBP-sensitive genes in PPAR α -deficient mice. *J Lipid Res* 42:328–337.
27. Knight BL, et al. (2005) A role for PPAR α in the control of SREBP activity and lipid synthesis in the liver. *Biochem J* 389:413–421.
28. Lin Q, Ruuska SE, Shaw NS, Dong D, Noy N (1999) Ligand selectivity of the peroxisome proliferator-activated receptor α . *Biochemistry* 38:185–190.
29. Hashimoto T, et al. (2000) Defect in peroxisome proliferator-activated receptor α -inducible fatty acid oxidation determines the severity of hepatic steatosis in response to fasting. *J Biol Chem* 275:28918–28928.
30. Bauer M, et al. (2004) Starvation response in mouse liver shows strong correlation with life-span-prolonging processes. *Physiol Genomics* 17:230–244.
31. Corton JC, et al. (2004) Mimetics of caloric restriction include agonists of lipid-activated nuclear receptors. *J Biol Chem* 279:46204–46212.
32. Badman MK, et al. (2007) Hepatic fibroblast growth factor 21 is regulated by PPAR α and is a key mediator of hepatic lipid metabolism in ketotic states. *Cell Metab* 5:426–437.
33. Inagaki T, et al. (2007) Endocrine regulation of the fasting response by PPAR α -mediated induction of fibroblast growth factor 21. *Cell Metab* 5:415–425.
34. Kersten S, et al. (1999) Peroxisome proliferator-activated receptor α mediates the adaptive response to fasting. *J Clin Invest* 103:1489–1498.
35. Lee SST, et al. (2004) Requirement of PPAR α in maintaining phospholipid and triacylglycerol homeostasis during energy deprivation. *J Lipid Res* 45:2025–2037.
36. Leone TC, Weinheimer CJ, Kelly DP (1999) A critical role for the peroxisome proliferator-activated receptor α (PPAR α) in the cellular fasting response: The PPAR α -null mouse as a model of fatty acid oxidation disorders. *Proc Natl Acad Sci USA* 96:7473–7478.
37. Elholm M, et al. (2001) Acyl-CoA esters antagonize the effects of ligands on peroxisome proliferator-activated receptor α conformation DNA binding, and interaction with co-factors. *J Biol Chem* 276:21410–21416.
38. Jørgensen C, et al. (2002) Opposing effects of fatty acids and Acyl-CoA esters on conformation and cofactor recruitment of peroxisome proliferator-activated receptors. *Ann N Y Acad Sci* 967:431–439.
39. Bremer J (2001) The biochemistry of hypo- and hyperlipidemic fatty acid derivatives: Metabolism and metabolic effects. *Prog Lipid Res* 40:231–268.
40. Fruchart J-C, Duriez P (2006) Mode of action of fibrates in the regulation of triglyceride and HDL-cholesterol metabolism. *Drugs Today* 42:39–64.
41. Martin G, Schoonjans K, Lefebvre A-M, Staels B, Auwerx J (1997) Coordinate regulation of the expression of the fatty acid transport protein and Acyl-CoA synthetase genes by PPAR α and PPAR γ activators. *J Biol Chem* 272:28210–28217.
42. Oishi K, Shirai H, Ishida N (2005) CLOCK is involved in the circadian transactivation of peroxisome-proliferator-activated receptor α (PPAR α) in mice. *Biochem J* 386:575–581.
43. Towle HC, Kaytor EN, Shih H-M (1997) Regulation of the expression of lipogenic enzyme genes by carbohydrate. *Annu Rev Nutr* 17:405–433.
44. Buijs RM, Kreier F (2006) The metabolic syndrome: A brain disease? *J Neuroendocrinol* 18:715–716.
45. Staels B (2006) When the clock stops ticking, metabolic syndrome explodes. *Nat Med* 12:54–55.
46. Turek FW, et al. (2005) Obesity and metabolic syndrome in circadian clock mutant mice. *Science* 308:1043–1045.
47. Bligh EG, Dyer WJ (1959) A rapid method of total lipid extraction and purification. *Can J Biochem Physiol* 37:911–917.
48. Lavery D, Schibler U (1993) Circadian transcription of the cholesterol 7 α hydroxylase gene may involve the liver-enriched bZIP protein DBP. *Genes Dev* 7:1871–1884.

Supporting Information

Gachon et al. 10.1073/pnas.1002862108

SI Experimental Procedures

Animal Experiments. WY14643 treatment by intraperitoneal injection.

Two groups of six proline- and acidic amino acid-rich domain basic leucine zipper (PAR bZip) 3KO male mice were injected intraperitoneally at ZT2 with 100 mg/Kg WY14643 (Biomol International) (10 mg/mL in 50% DMSO) or the equivalent volume of vehicle. Four hours after injection, mice were killed and livers were removed and snap-frozen in liquid nitrogen, or immediately processed for the purification of the nuclear proteins used in the immunoblot experiments.

In vivo siRNA treatment. Chemically modified Stealth RNAi™ siRNA duplexes (Invitrogen) complementary to the four *Acots* genes were complexed with InvivoFectamine® 2.0 (Invitrogen) according to manufacturer recommendation before the injection. For each of the four examined acyl-CoA thioesterases (*Acots* 1–4), six siRNAs with different sequences were tested in two different mice, and the one yielding maximal suppression was selected for the experiments shown in Fig. 2C and Fig. S5. The sequences of these siRNA are given in Table S1. The solution containing control siRNA (an siRNA with sequences that do not target any gene product that have been tested by microarray analysis and shown to have minimal effects on gene expression), individual *Acot* siRNAs, or an equimolar mix of the four *Acot* siRNAs were injected intravenously through the tail vein of 8-wk-old Balb/c mice at ZT12 at a dose of 7 mg/kg. Forty-eight hours after the injection, mice were killed and livers were removed and snap-frozen in liquid nitrogen, and stored at -70°C before RNA was extracted.

Calorie restriction. PAR bZip 3KO mice and wild-type siblings (nine KOs and seven wild-type 7–9-wk-old male mice) were fed regular chow (ref 3800 from Provimi Kliba. Diet composition: 24% protein, 47.5% carbohydrate, 4.9% fat) ad libitum for at least 3 mo. Mice were then separated (by placing them into individual cages) and fed with powdered food that was delivered by a computer-driven feeding machine (1). Average food consumption was determined to be 4.2 g per day, per mouse for animals fed ad libitum with regular chow, and this value was used as the normal diet control value in the caloric restriction studies. The animals were then subjected to a calorie diet reduced by 40% (i.e., 2.52 g per day, per animal, distributed into 20 daily portions delivered every 30 min between ZT12 and ZT22). The animals were weighed twice a week in the morning for 11 wk.

Temporally restricted feeding. Servings of 3.4 g powdered chow (80% of the normal diet control value) were offered in 12 portions between ZT03 and ZT09 by a computer-driven feeding machine (1). The wheel-running activities of the animals were recorded as described previously (2).

Fat-free feeding regimen. Eight-week-old PAR bZip 3KO mice and wild-type siblings (four males and four females of each genotype) were fed with regular chow ad libitum for at least 3 mo. The food was then replaced by a fat-free diet (TD.03314 from Harlan Teklad. Diet composition: 20.1% protein, 62.9% carbohydrate, 0% fat) for 5 wk.

Electromobility Shift Assay. The radiolabeled probe was prepared by annealing two oligonucleotides encompassing the PAR bZip binding site present in the *Acot* genes cluster and by filling in the 5' overhang with [α - ^{32}P]dCTP and Klenow DNA polymerase. The sequences of these oligonucleotides were 5'-CCATAAAAT-TACATAAG-3' and 5'-TTGATTACTTATGTAATTTTATGG-3'. Twenty micrograms of liver nuclear extract were incubated with 100 fmol of the double-stranded oligonucleotide in a 20- μL reaction containing 25 mM Hepes (pH 7.6), 60 mM KCl, 5 mM MgCl_2 , 0.1 mM EDTA, 7.5% glycerol, 1 mM DTT, 1 $\mu\text{g}/\mu\text{L}$ salmon sperm DNA. After an incubation of 10 min at room temperature, 2 μL of a 15% Ficoll solution were added, and the protein-DNA complexes were separated on a 5% polyacrylamide gel in 0.25 \times TBE (90 mM Tris/64.6 mM boric acid/2.5 mM EDTA, pH 8.3).

GC-MS Determination of Fatty Acids (FAs) Concentrations. Lipid extracts were taken to dryness in a speed-vac evaporator and resuspended in 240 μL of 50% wt/vol KOH and 800 μL ethanol for the alkaline hydrolysis of lipids. After a 60-min incubation at 75°C , FAs were extracted with 1 mL of water and 2 mL of hexane. The hexane phase was taken to dryness and redissolved in 50 μL of a pentafluoro-benzyl bromide solution (3.4% in acetonitrile) and 10 μL of *N,N*-diisopropyl ethanalamine. After 10 min of incubation at room temperature, samples were evaporated under a gentle stream of nitrogen and resuspended in 50 μL hexane.

A Trace-DSQ GC-MS (Thermo Scientific) equipped with a TR5MS 30-m column was used for the mass-spectrometric analysis of lipids by gas chromatography. Helium was used as carrier gas at 1 mL/min in splitless mode at 300°C injector temperature. The initial oven temperature of 150°C was held for 1 min and then the temperature first was ramped up to 200°C at a rate of $25^{\circ}\text{C}/\text{min}$, which was followed by a ramp of $12.5^{\circ}\text{C}/\text{min}$ up to 325°C , where the temperature was held for another 2 min. The mass spectrometer was run in negative ion chemical ionization mode where the FAs were detected in full scan as carboxylates after loss of the pentafluoro-benzyl moiety. Methane was used as CI gas, the source temperature was set to 250°C , and the transfer line temperature was 330°C . Peak areas for FAs were calculated by Xcalibur QuanBrowser and related to the internal standard peak area.

1. van der Veen DR, et al. (2006) Impact of behavior on central and peripheral circadian clocks in the common vole *Microtus arvalis*, a mammal with ultradian rhythms. *Proc Natl Acad Sci USA* 103:3393–3398.

2. Lopez-Molina L, Conquet F, Dubois-Dauphin M, Schibler U (1997) The DBP gene is expressed according to a circadian rhythm in the suprachiasmatic nucleus and influences circadian behavior. *EMBO J* 16:6762–6771.

A

Affy ID	Gene Symbol	Description	PPAR α KO	PARbZip 3KO
1424853_s_at	Cyp4a10	cytochrome P450, family 4, subfamily a, polypeptide 10	-61.23	-6.03
1423257_at	Cyp4a14	cytochrome P450, family 4, subfamily a, polypeptide 14	-32.25	-2.73
1424716_at	Retsat	retinol saturase (all trans retinol 13,14 reductase)	-4.49	-1.9
1419430_at	Cyp26a1	cytochrome P450, family 26, subfamily a, polypeptide 1	-4.12	-1.98
1424715_at	Retsat	retinol saturase (all trans retinol 13,14 reductase)	-3.88	-1.82
1440134_at	Cyp4a10	cytochrome P450, family 4, subfamily a, polypeptide 10	-3.65	-1.75
1448080_at	E2f8	E2F transcription factor 8	-3.44	-7.28
1448491_at	Ech1	enoyl coenzyme A hydratase 1, peroxisomal	-3.20	-1.35
1428223_at	Mfsd2	major facilitator superfamily domain containing 2	-3.11	-1.48
1451084_at	Etfhd	electron transferring flavoprotein, dehydrogenase	-2.57	-1.31
1421011_at	Dhrs8	dehydrogenase/reductase (SDR family) member 8	-2.49	-1.61
1431833_a_at	Hmgcs2	3-hydroxy-3-methylglutaryl-Coenzyme A synthase 2	-2.49	-1.23
1424451_at	Acaa1b	acetyl-Coenzyme A acyltransferase 1B	-2.45	-1.37
1423858_a_at	Hmgcs2	3-hydroxy-3-methylglutaryl-Coenzyme A synthase 2	-2.30	-1.21
1421430_at	Rad51l1	RAD51-like 1 (<i>S. cerevisiae</i>)	-2.18	-2.44
1416946_a_at	Acaa1b	acetyl-Coenzyme A acyltransferase 1B	-2.17	-1.27
1416947_s_at	Acaa1b	acetyl-Coenzyme A acyltransferase 1B	-2.14	-1.21
1454159_a_at	Igf1bp2	insulin-like growth factor binding protein 2	-2.13	-1.5
1449051_at	Ppara	peroxisome proliferator activated receptor alpha	-2.06	-1.55
1434642_at	Dhrs8	dehydrogenase/reductase (SDR family) member 8	-1.83	-1.28
1422526_at	Acs11	acyl-CoA synthetase long-chain family member 1	-1.70	-1.22
1415776_at	Aldh3a2	aldehyde dehydrogenase family 3, subfamily A2	-1.63	-1.29
1450643_s_at	Acs11	acyl-CoA synthetase long-chain family member 1	-1.61	-1.27
1415965_at	Scd1	stearoyl-Coenzyme A desaturase 1	-1.56	-1.49
1418989_at	Clse	cathepsin E	-1.54	-1.56
1438055_at	Rarres1	retinoic acid receptor responder (tazarotene induced) 1	-1.51	-1.44
1423883_at	Acs11	acyl-CoA synthetase long-chain family member 1	-1.49	-1.23
1415964_at	Scd1	stearoyl-Coenzyme A desaturase 1	-1.42	-1.45
1422032_a_at	Za20d3	zinc finger, A20 domain containing 3	-1.42	-1.37
1416409_at	Acox1	acyl-Coenzyme A oxidase 1, palmitoyl	-1.39	-1.25
1427229_at	Hmgcr	3-hydroxy-3-methylglutaryl-Coenzyme A reductase	-1.34	-1.47
1418654_at	Hao3	hydroxyacid oxidase (glycolate oxidase) 3	-1.27	-1.3
1424493_s_at	Ugt3a1	UDP glycosyltransferases 3 family, polypeptide A1	-1.25	-1.29
1416933_at	Por	P450 (cytochrome) oxidoreductase	-1.23	-1.41

B

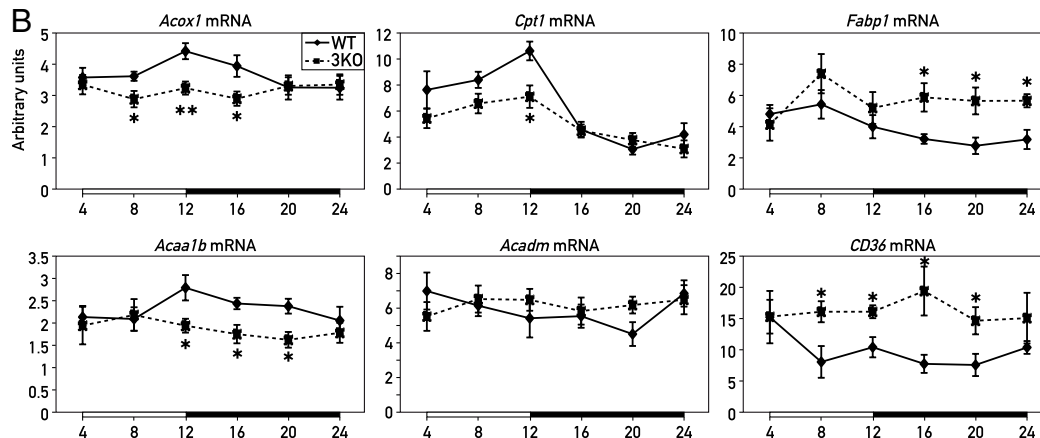


Fig. S1. Hepatic expression of peroxisome proliferator-activated receptors α (PPAR α) target genes in PAR bZip 3KO mice. (A) Microarray data obtained with PAR bZip 3KO mouse liver RNA (1) were compared to data obtained with *Ppara* KO mouse liver RNA (2). Genes down-regulated in both genotypes with regard to their wild-type counterparts are listed. The table corresponds to the list of genes down-regulated more than 1.25-fold in at least one of the KO genotypes (when compared to strain-matched wild-type mice). (B) Temporal hepatic expression of genes coding for enzymes involved in peroxisomal FA β -oxidation [acyl-CoA oxidase 1 (*Acox1*) and acyl-CoA acyltransferase 1B or thiolase B (*Acaa1b*)], mitochondrial FA β -oxidation [carnitine palmitoyltransferase 1 (*Cpt1*) and mitochondrial medium-chain acyl-CoA dehydrogenase (*Acadm*)], and FA binding and transport [FA-binding protein 1 (*Fabp1*) or liver FA-binding protein (L-FABP)] and CD36 (*Cd36*) in wild-type and PAR bZip 3KO mice, as determined by real-time RT-PCR. Mean values \pm SEM obtained from four animals are given ($*p \leq 0.05$, $**p \leq 0.01$, KO vs. WT, Student's *t* test). As for *Cyp4a* genes, the PPAR α target genes coding for enzymes involved in FA β -oxidation are also down-regulated [*Acox1*, *Acaa1b* (see also Fig. S1A for these genes) and *Cpt1*] or not changed (*Acadm*) in the liver of PAR bZip 3KO mice. Interestingly, the genes coding for proteins involved in the FA transport exhibit an increased expression in PAR bZip 3KO mice, confirming previously published microarray data (1). Similar to what has been observed for *Fasn* expression, the increased expression of these genes is probably an indirect consequence of the disrupted FA metabolism in PAR bZip 3KO mice, perhaps to compensate for the deficient import and/or metabolism of lipids absorbed with the food.

- Gachon F, Fleury Olela F, Schaad O, Descombes P, Schibler U (2006) The circadian PAR-domain basic leucine zipper transcription factors DBP, TEF, and HLF modulate basal and inducible xenobiotic detoxification. *Cell Metab* 4:25–36.
- Leuenerger N, Pradervand S, Wahli W (2009) Sumoylated PPAR α mediates sex-specific gene repression and protects the liver from estrogen-induced toxicity in mice. *J Clin Invest* 119:3138–3148.

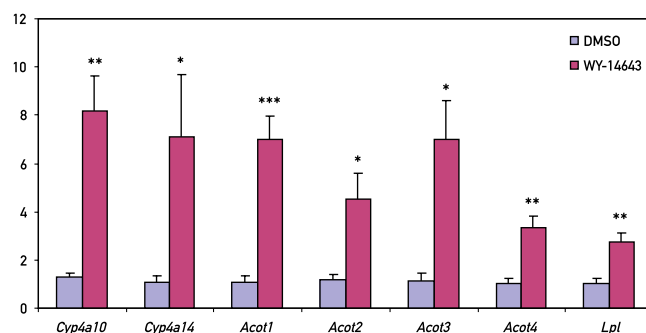


Fig. S4. Activation of hepatic *Cyp4a*, *Acots*, and *Lpl* expression after injection of the PPAR α activator WY14643. Six PAR bZip 3KO male mice were injected intraperitoneally with DMSO or PPAR α ligand WY14643 (100 mg/kg) at ZT2. Livers were harvested 4 h later, and whole-cell RNAs were extracted. The mRNAs of the indicated genes were quantified by real-time RT-PCR. Mean values \pm SEM are given (* $p \leq 0.05$, ** $p \leq 0.005$, *** $p \leq 0.0005$ DMSO vs. WY14643 injection, Student's *t* test).

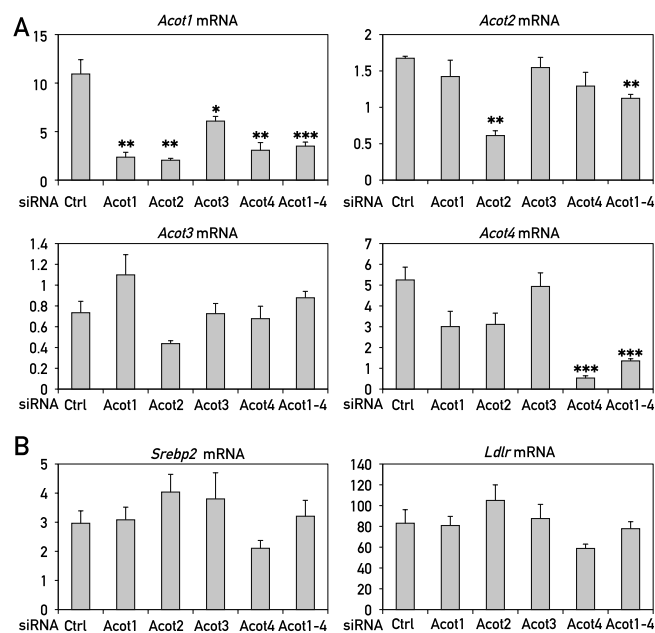


Fig. S5. Effect of ACOT siRNA on *Acot* genes and non-PPAR α regulated genes expression. (A) Accumulation of *Acot* mRNAs in mouse liver 48 h after the treatment with siRNA directed against *Acot* genes. The siRNAs act mainly by decreasing the levels of their target mRNA (1), and the cellular concentrations of *Acot1*, *Acot2*, and *Acot4* mRNA were indeed reduced to 10% to 50% after the injection of their respective siRNAs. None of the six examined *Acot3* siRNAs (see *SI Experimental Procedures*) reduced its target mRNA significantly, yet three of them did lower the expression of the PPAR α target genes *Cyp4a10* and *Cyp4a14*. A similar observation was made for the mix of the four *Acot* siRNAs. Indeed, it has recently been shown that siRNAs, similar to miRNAs, can also act by inhibiting translation of their target mRNA, without reducing the levels of their target mRNAs (2, 3). This phenomenon could explain the observation that *Acot3* siRNA and the mix of the four *Acot* siRNAs strongly reduced the expression of *Cyp4a10* and *Cyp4a14*. (B) Expression of genes involved in lipid metabolism (*Srebp2* and *Ldlr*), two transcripts whose levels were similar in wild-type and PPAR α or PAR bZip 3KO mice (4–6). Note that neither individual *Acot* siRNAs nor the mix of the four *Acot* siRNAs significantly affected the accumulation of *Srebp2* and *Ldlr* mRNAs. These results support the specificity of the effect of the *Acot* siRNAs for PPAR α target genes. Real-time RT-PCR experiments were conducted with whole-cell liver RNAs from four (control and individual *Acot* siRNAs) or six animals (pool of the four precedent *Acot* siRNAs). Mean values \pm SEM are given (* $p \leq 0.05$, ** $p \leq 0.01$, *** $p \leq 0.001$ control siRNA vs. *Acot* siRNAs, Student's *t* test).

- Guo H, Ingolia NT, Weissman JS, Bartel DP (2010) Mammalian microRNAs predominantly act to decrease target mRNA levels. *Nature* 466:835–840.
- Davidson TJ, et al. (2004) Highly efficient small interfering RNA delivery to primary mammalian neurons induces microRNA-like effects before mRNA degradation. *J Neurosci* 24:10040–10046.
- Tang G (2005) siRNA and miRNA: An insight into RISCs. *Trends Biochem Sci* 30:106–114.
- Gachon F, Fleury Olela F, Schaad O, Descombes P, Schibler U (2006) The circadian PAR-domain basic leucine zipper transcription factors DBP, TEF, and HLF modulate basal and inducible xenobiotic detoxification. *Cell Metab* 4:25–36.
- Knight BL, et al. (2005) A role for PPAR α in the control of SREBP activity and lipid synthesis in the liver. *Biochem J* 389:413–421.
- Patel DD, Knight BL, Wiggins D, Humphreys SM, Gibbons GF (2001) Disturbances in the normal regulation of SREBP-sensitive genes in PPAR α -deficient mice. *J Lipid Res* 42:328–337.

B. Sterol Carrier Protein 2 dependent diurnal lipid transport modulates rhythmic activation of signaling pathways in mouse liver

Lipid trafficking and especially cholesterol trafficking is involved in the activation of TORC1 pathway³⁰¹. Cholesterol, major constituent of the cellular membranes, is known to confer fluidity and impermeability on them. As an essential component of the lipid rafts/caveolae³⁰², it is involved in signal transduction³⁰³. These lipid rafts/caveolae are plasma membrane microdomains highly dynamics and enriched in sphingolipids, sterols such as cholesterol and certain lipid-anchored proteins³⁰⁴. These lipid rafts/caveolae are involved in the compartmentalized cellular processes³⁰⁵, as they are the preferential site of receptors whose activation leads to the activation of different signaling pathways like the PI3K/AKT and ERK/MAPK³⁰⁶⁻³⁰⁸.

Cells have two sources of cholesterol³⁰¹. One source is endogen as the cholesterol can be synthesized in the endoplasmic reticulum. The second cholesterol source is exogen, originates by food intake, and results in the internalization of cholesterol mediated by the LDL (Low-Density-Lipoproteins) endocytosis. Intracellular cholesterol trafficking of both sources requires transport proteins to reach their action localization in the plasma membrane and more precisely in microdomains termed lipid raft/caveolae. Here we will focus on SCP (Sterol Carrier Protein) 2, also known as non-specific lipid transfer protein.

As mentioned above, *de novo* cholesterol is synthesized in endoplasmic reticulum and must be transported to its action location at the inner leaflet of the plasma membrane³⁰⁹. SCP2 exhibits a diurnal expression pattern³¹⁰. Its role in cholesterol metabolism is not completely established but some evidence shows that SCP2 is localized in the cytoplasm and is involved

in *de novo* cholesterol transport from the endoplasmic reticulum to the plasma membrane³¹¹.

312.

In this study, we confirm SCP2 diurnal expression without exhibiting rhythmic mRNA transcription or translation. This suggests that degradation of this protein could be rhythmically in wild-type mouse liver. In *Bmal1* knockout mice, *Scp2* mRNA expression appeared higher as well as its protein expression with an anticipated manner. Even *Scp2* mRNA expression appeared similar in wild-type and *Cry1/2* knockout mice, the differences observed at the protein level showed the impact of the molecular clock for SCP2 expression in mouse liver.

Investigations on the effects of *Scp2* deletion on circadian physiology showed that *Scp2* KO mice present a longer period in locomotor activity accompanied by lower night and day activities. In addition, while no significant differences appeared at both mRNA and protein levels for most of the circadian machinery factors despite a delayed *Dbp* expression, we described decreased amplitude of BMAL1 expression as well as higher and slightly delayed PER2 expression in *Scp2* knockout mice compared to wild-type mice. All together, these results suggest that SCP2 could have an impact on the signaling pathways involved in the post-translational modifications regulating the stability of the circadian clock molecules.

In addition, we showed that serum glucose and insulin concentrations were similar in both wild-type and *Scp2* knockout mice. However, *Scp2* knockout mice exhibit less circulating cholesterol, and lower but still rhythmic serum triglyceride. In *Scp2* knockout mice liver, lipids content analyses showed disturbed rhythmic lipid accumulation. These results led us to the investigation of signaling pathways regulated by lipids like PPAR α , SREBP or LXR. Both PPAR α - and SREBP-regulated genes appeared up-regulated in *Scp2* knockout mice while no effect was observed in LXR target genes. We showed here that despite the fact that lipid

metabolism and UPR activation can be linked, it is not done *via* SCP2-dependent mechanisms as the UPR activation was not affected in *Scp2* knockout mice. We also investigate the possible involvement of SCP2 in TORC1 activated mechanism and the upstream TORC1 activating signaling pathways. We showed that even their mRNA expression did not differ, the different components of the translation initiation complex undergo significant difference in their activation by phosphorylation especially for EIF4B. In addition, AKT and ERK pathways exhibit a disturbed phosphorylation leading to disturbances in TORC1 activation in *Scp2* knockout mice.

All together, these results demonstrate new evidences of the orchestration of signaling pathways activation by circadian clock.

Sterol Carrier Protein 2 dependent diurnal lipid transport modulates rhythmic activation of signaling pathways in mouse liver

Céline Jouffe^{1,2}, Cédric Gobet², Eva Martin², Mojgan Masoodi³, and Frédéric Gachon^{1,2}

E-mails: celine.jouffe@rd.nestle.com

cedric.gobet@rd.nestle.com

eva.martin@rd.nestle.com

Mojgan.masoodi@rd.nestle.com

frederic.gachon@rd.nestle.com

Affiliation:

¹Department of Pharmacology and Toxicology, University of Lausanne, Lausanne, CH-1005, Switzerland

²Department of Diabetes and Circadian Rhythms, Nestlé Institute of Health Sciences, CH-1015 Lausanne, Switzerland

³Department of Molecular Biomarkers, Nestlé Institute of Health Sciences, CH-1015 Lausanne, Switzerland

Keywords:

Circadian clock, Target Of Rapamycin, mRNA translation, Peroxisome Proliferator Associated Receptor, Endoplasmic Reticulum stress, serum responsive element binding protein

Contacts:

Frédéric Gachon

Nestlé Institute of Health Sciences

EPFL Innovation Park

CH-1015 Lausanne

Switzerland

Tel: (00 41) 21 692 53 64

Fax: (00 41) 21 692 53 55

E-mail: Frederic.Gachon@rd.nestle.com

Abbreviations:

SCP2: Sterol Carrier Protein 2

TORC1: Target Of Rapamycin Complex 1

UPR: Unfolded Protein Response

PPAR α : Peroxisome Proliferator-Activated Receptor α

LXR: Liver X Receptor

SREBP: Sterol Regulatory Element-Binding Protein

SCN: SupraChiasmatic Nucleus

PI3K: Phosphatidylinositol-4,5-bisphosphate 3-Kinase

ERK: Extracellular-signal-Regulated Kinases

AMPK: 5' Adenosine Monophosphate-activated Protein Kinase

KO: KnockOut

Bmal1: Brain and Muscle Aryl hydrocarbon receptor nuclear translocator-Like 1

Cry: Cryptochrome

Per: Period

Dbp: D site of albumin promoter Binding Protein

TAG: TriAcylGlyceride

DAG: DiAcylGlyceride

SE: Sterol Esther

PC: PhosphatidylCholine

Cer: Ceramide

PG: PhosphatidylGlycerol

PE: PhosphatidylEthanolamin

PI: PhosphatidylInositol

Cyp4a14: Cytochrome P450, family 4, subfamily a, polypeptide 14

Acox1: peroxisomal Acyl-coenzyme A Oxidase 1

Lpl: LipoProtein Lipase

Cd36: Cluster of Differentiation 36

ER: Endoplasmic Reticulum

Hmgcr: 3-Hydroxy-3-MethylGlutaryl-CoA Reductase

Fasn: Fatty Acid Synthase

4E-BP1: eukaryotic translation initiation factor 4E-Binding Protein 1

EIF4G: Eukaryotic translation Initiation Factor 4G

EIF4B: Eukaryotic translation Initiation Factor 4B

RPS6: Ribosomal Protein S6

CK1: Casein Kinase 1

NPC1: Niemann-Pick disease, type C1

Financial Support:

This research was supported by the Swiss National Science Foundation (grant 31003A_129940/1), the European Research Council (grant ERC-2010-StG-260988), and the Canton of Vaud.

Abstract

Most of the living species on earth have evolutionary acquired a time keeper system to anticipate daily changes caused by the light-dark cycle caused the rotation of the earth. This pacemaker is based in all the system on a molecular transcriptional/translational negative feedback loop able to generate rhythmic gene expression with a 24 hours period. Recent evidences suggest that post-transcriptional regulations play also a fundamental role at different steps of the process, fine tuning in this way the time keeping system and linking it to animal physiology. Systemic cues can indeed activate specific signaling pathways controlling gene expression at the transcriptional and post-transcriptional level. Among this signals, we consider here the possible role of lipid transport in this system, and more particularly the SCP2-dependent lipid transport. Indeed mice with a deletion of the *Scp2* gene coding for a rhythmic lipid transporter present a modulated rhythmic activation of the lipid regulated transcription factors PPAR α and SREBP. Moreover, these mice present a perturbed rhythmic activation of TORC1 and its upstream pathways, whereas rhythmic UPR activation is not affected. Finally, this defect in signaling pathways activation feedbacks on the clock by lengthening the circadian period of animals through post-translational regulation of core clock regulators. *Conclusion:* We show here that the rhythmic lipid transporter SCP2 modulates rhythmic activation of several signaling pathways in mouse liver, becoming in this way a new player involved in the establishment of the rhythmic mRNA and protein expression landscape.

Introduction

As a result of living in an environment subject to light-dark cycles caused by Earth's rotation, organisms from bacteria to mammals acquired during evolution a timing system allowing their anticipation of these diurnal variations. In mammals, this timer is called the circadian clock, circadian meaning about a day, and influences most aspects of physiology and behavior (1). As a consequence, perturbations or misalignments of the circadian clock in human, like for example in the case of shift-workers, lead to diverse pathologies including metabolic disorders and obesity (2), vascular diseases (3), and psychiatric disorders (4). If the oscillatory timing system is cell-autonomous, timing at the organism scale is based on a hierarchal organization. Indeed, a "master clock" within the SCN of the hypothalamus, which is daily resynchronized through light input via ganglionar cells of the retina, communicates timing signals to "slave" oscillators in other peripheral tissues which are more sensitive to systemic signals like metabolic signals coming from food (5).

In mammals, the molecular oscillator consists in interconnected transcriptional and translational feedback loops with additional layers of control including temporal post-transcriptional and post-translational regulations (6). This additional layer of regulation is largely regulated by systemic signals coming from circadian clock and/or feeding coordinated rhythmic metabolism allowing in this way the adjustment of the molecular clockwork with the metabolic state of the cell (7). At least in part, this effect is mediated through the rhythmic activation of signaling pathways. In parallel, these signaling pathways also feedback on metabolism. We have for example recently shown that circadian-clock orchestrated liver metabolism regulate rhythmic activation of UPR (8) and mRNA translation through rhythmic activation of TORC1 pathway and the upstream pathways PI3K, ERK, and AMPK (9).

To gain more insight about the metabolic pathways involved in this process, we speculate about the potential role of rhythmic lipid transport. Indeed, recent evidences show that lipid metabolism and transport is involved in the activation of the UPR (10), TORC1 (11), or ERK (12) pathways. This activation often involved lipid-dependent organization of membrane proteins in lipid rafts (13) which produced changes in their structure and potential activation (14). In parallel, several signaling pathways are directly regulated by lipid metabolism. It is for example the case for PI3K/AKT (15, 16), LXR (17), PPAR α (18), or SREBP (19). Interestingly, the two last one present a rhythmic activation caused by interconnection between circadian clock and rhythmic lipid metabolism (20, 21).

In this context, we want to study the potential influence of rhythmic liver lipid transport on the activation of this pathway. Until now, SCP2 is the only intracellular lipid transporter that presents a diurnal expression in mouse liver. However, this rhythmic expression at the protein level is regulated at the post-transcriptional level as *Scp2* mRNA does not present rhythmic expression (22, 23). SCP2 is involved in the transfer of many lipid species from the endoplasmic reticulum where they are synthesized to the plasma membrane (24), affecting in this way the formation of lipid rafts and cell signaling (for a review see (25)). The *Scp2* locus

also encodes the *Scpx* mRNA through alternative transcription start site usage, the later encoded protein presenting peroxisomal 3-ketoacyl-CoA thiolase activity involved in the oxidation of branched-chain lipids (26). As a consequence, lipid metabolism (27) and expression of proteins at the plasma membrane in lipid raft domains is perturbed in *Scp2* deficient animals (28, 29). If the differential role of the two proteins encoded by the *Scp2* locus in the process is not clearly established yet, *in vitro* experiments suggest that the lipid transport activity of SCP2 is required (30).

We thus speculate that SCP2 could affect liver rhythmic lipid metabolism and transport and, as a consequence, rhythmic activation of signaling pathways through modification of the distribution of proteins in lipid rafts at the plasma membrane. We indeed show that rhythmic lipid content is affected in the liver of *Scp2* KO mice which present also a perturbed rhythmic activation of several signaling pathways including PPAR α , SREBP, and TORC1 which also appeared to feedback on the molecular clock itself. If increasing evidences show that lipid metabolism and accumulation in mouse liver follow a diurnal rhythm controlled by feeding and the circadian clock (31, 32), we show for the first time that this rhythmic lipid metabolism and transport in turn affect activation of signaling pathways and participates in the global rhythmic transcriptome of the mouse liver.

Experimental Procedures

Animal experiments

All animal studies were conducted in accordance with the regulations of the veterinary office of the Canton of Vaud. Eight-week-old male C57Bl/6J mice were purchased from Charles River Laboratory (L'Arbresle). *Scp2* KO mice have been previously described (27) and have been acquired from Jackson Laboratory. In all experiments, male mice between 10 and 12 weeks of age are used. Unless noted otherwise, mice were maintained under standard animal housing conditions, with free access to food and water and in 12 hours light/12 hours dark cycles. However, for all experiments, animals were fed only at night during 4 days before the sacrifice to reduce effects of feeding rhythm and mice were sacrificed every 2 hours.

The running-wheel activity has been monitored as previously described (33). Briefly, the mice were housed individually in cages equipped with running-wheel. The activity has been measured during 5 days in light-dark cycles followed by 18 days in constant darkness. Data were acquired and analysed with the Clocklab software (Actimetrics).

RNA extraction and analysis

Liver RNA were extracted and analysed by real-time quantitative RT-PCR, mostly as previously described (34). Briefly, 0.5 µg of liver RNA was reverse transcribed using random hexamers and SuperScript® II reverse transcriptase (Life Technologies). The cDNAs equivalent to 20 ng of RNA were PCR amplified in a LightCycler® 480 II System (Roche) using the TaqMan® or the SYBR® Green technologies. References and sequences of the probes are given in the tables. In each case, averages from at least three independent experiments are given, using *Gapdh* mRNA as controls. Probes references are given in Supplemental table X.

Nuclear protein extractions and analysis

Nuclear proteins were extracted mostly as described (34). Briefly, liver were homogenized in sucrose homogenization buffer containing 2.2 M sucrose, 15 mM KCl, 2 mM EDTA, 10 mM HEPES (pH7.6), 0.15 mM spermin, 0.5 mM spermidin, 1 mM DTT, and a protease inhibitor cocktail containing 0.5 mM PMSF, 10 µg/ml Aprotinin, 0.7 µg/ml Pepstatin A, and 0.7 µg/ml Leupeptin. Lysates were deposited on a sucrose cushion containing 2.05 M sucrose, 10 % glycerol, 15 mM KCl, 2 mM EDTA, 10 mM HEPES (pH7.6), 0.15 mM spermin, 0.5 mM spermidin, 1 mM DTT, and a protease inhibitor cocktail. Tubes were centrifuged during 45 min at 105 000 g at 4 °C. After ultra-centrifugation, the nucleus pellets were suspended in a nucleus lysis buffer composed of 10 mM HEPES (pH7.6), 100 mM KCl, 0.1 mM EDTA, 10 % Glycérol, 0.15 mM spermin, 0.5 mM spermidin, 0.1 mM NaF, 0.1 mM sodium orthovanadate, 0.1 mM ZnSO₄, 1 mM DTT, and the previously described protease inhibitor cocktail. Nuclear extracts were obtained by the addition of an equal volume of NUN buffer composed of 2 M urea, 2 % Nonidet P-40, 600

mM NaCl, 50 mM HEPES (pH7.6), 1 mM DTT and a cocktail of protease inhibitors, and incubation 20 min on ice. After centrifugation during 10 min at 21 000 g, the supernatants were harvested and constitute nuclear extracts.

12.5 µg nuclear extracts were used for western blotting. After migration, proteins were transferred to PVDF membranes and western blotting was realized according to standard procedures. References for the antibodies are given in the table.

Total protein extractions and analysis

Frozen organs were homogenized in lysis buffer containing 20 mM HEPES (pH 7.6), 100 mM KCl, 0.1 mM EDTA, 1 mM NaF, 1 mM sodium orthovanadate, 1 % Triton X-100, 0.5% Nonidet P-40, 0.15 mM spermin, 0.5 mM spermidin, 1 mM DTT, and the same protease inhibitor cocktail as for nuclear protein extractions. After incubation 30 min on ice, extracts were centrifuged 10 min at 21 000 g and the supernatants were harvested to obtain total extracts.

65 µg of extract was used for western blotting. After migration, proteins were transferred to PVDF membranes and western blotting was realized according to standard procedures. References for the antibodies are given in Table Y.

Serum chemistry analysis

Blood samples are collected every 2 hrs and sera are obtained after a centrifugation of 10 min at 10 000 rpm at room temperature. Sera are kept at -80°C until analysis. Insulin, glucose, cholesterol and triglycerides are respectively measured accordingly with the protocols of the Mouse Insulin ELISA kit (Merckodia), and the Glucose, Cholesterol, Triglycerides LabAssay kits (Wako).

Results

SCP2 diurnal expression is regulated at the post-translational level but orchestrated by the circadian clock

Diurnal expression of SCP2 has been originally described in rat liver in 1984 with an increased expression in the dark period (23). Post-transcriptional regulation has been suggested as neither *Scp2* mRNA nor its translation appeared rhythmic in these conditions (22). We confirmed the rhythmic expression of SCP2 in mouse liver but with a different phase as the maximum of expression takes place around ZT 9 (Fig. 1A). As previously described, this rhythmic accumulation is not due to the rhythmic expression of *Scp2* mRNA (Fig. 1B) or its translation evaluated by the presence of the mRNA in the polysomes (Fig. 1C). Non-characterized post-translational modifications of SCP2, and more particularly degradation, are thus probably involved in the rhythmic expression of SCP2, as suggested by the numerous SCP2 ubiquitylation sites characterized in mouse liver (35).

We are nevertheless interested by the fact that the molecular circadian clock can regulate rhythmic SCP2 expression. To study this possibility, we measured SCP2 expression at both mRNA and protein levels in *Bmal1* (36) and *Cry1/Cry2* (37) KO which present a non-functional molecular oscillator and an arrhythmic behavior in constant darkness. As shown in Fig. 1D, *Bmal1* KO mice present an increased expression of *Scp2* mRNA at all the time points, whereas no changes were observed in *Cry1/Cry2* KO. However, at the protein level, it appears that the clock affects the rhythmic accumulation of SCP2: SCP2 accumulates at high level and high amplitude in *Bmal1* KO mice, whereas its rhythmic expression is phase advanced and with lower amplitude in *Cry1/Cry2* KO mice. This result demonstrates that if the circadian clock does not regulate directly SCP2 expression, it influences its stability, potentially through the regulation of lipid metabolism by the clock. Indeed, SCP2 accumulation exactly follows triglycerides levels in mouse liver (31), suggesting a possible stabilization of SCP2 by triglycerides.

SCP2 influences circadian physiology and diurnal lipid metabolism

Scp2 KO mice (27) were used to study the potential role of SCP2 on rhythmic liver lipid physiology and cell signaling. To control that circadian behavior is not altered in these animals, we measured their running wheel activity in constant darkness. As shown in Fig. 2A, *Scp2* KO mice present a period longer by 16 min compared to wild-type mice and reduced locomotor activity that did not affect their day-night difference (around 1% activity during the day). Interestingly, the *Scp2* locus has been linked to dystonia and motor neuropathy in human, pathology that can explain this reduced activity (38).

To study the possible influence of *Scp2* deletion on circadian genes expression, we measured their rhythmic expression in mouse liver. As shown in Fig. 2B, diurnal expression of *Bmal1*, *Cry1*, and *Per2* are not significantly different between *Scp2* KO and wild-type animals, whereas *Dbp* expression is slightly delayed. However, at the protein level, BMAL1 expression presents decreased amplitude and an advanced phase in KO animals, whereas PER2 presents an increased expression and a delayed phase

(Fig. 2C). As accumulation of these proteins is strongly under the control of post-translational modifications (39), this differences may reflect changes in the rhythmic activation of signaling pathways that controls their stability and can explain delayed phase of the circadian activity and *Dbp* expression (see below).

As SCP2 played an important role in liver lipid metabolism and transport (27), we investigated general diurnal metabolic parameters in *Scp2* KO mice. As shown in Fig. 3A, diurnal serum glucose concentration is identical between WT and KO animals, whereas diurnal insulin concentration presents only a mild delay (Fig. 3B). However, diurnal serum triglyceride (Fig. 3C) and cholesterol (Fig. 3D) concentrations are significantly decreased and present a lower amplitude in KO compare to WT. It strongly suggests that diurnal lipid metabolism is perturbed in *Scp2* KO mice. To gain insight into this perturbed metabolism in the liver, we analyze the diurnal concentration of several lipid species in WT and KO mice. As show in Figure 3D, lipidomic analysis revealed that several lipid species identified and quantified in both species presents a rhythmic pattern in agreement with the previously published data (31): TAG, DAG and SE reach their maximum during the day, PC and Cer at the day-night transition, and PG, PE, and PI during the night (Fig. 3E). Among them, around 25 %, mostly TAG and SE, are not rhythmic in *Scp2* KO mice liver, showing perturbed rhythmic lipid transport and metabolism in these animals.

Diurnal activation of lipids regulated pathways is perturbed in *Scp2* KO mice

Several signaling pathways are directly regulated by lipids. For example the nuclear receptor PPAR α , directly binds lipid molecules and activates its target genes implied in different physiological pathways including lipid metabolism (18). PPAR α has been described as regulated in part by the circadian clock *via* its interaction with PER2 (40, 41). However, we have previously shown that *Ppara* transcription and activation is under the control of the circadian clock and its output pathways through direct transcriptional control and synthesis of its ligands (20). As availability of these ligands, through control of their transport and synthesis, is potentially under the control of SCP2, we investigated diurnal activation of PPAR α in *Scp2* KO mice. As shown in Fig. 4A, the PPAR α target genes *Cyp4a14*, *Acox1*, *Lpl*, and *Cd36* present all an increased expression throughout the diurnal cycle, indicating an overall increase activation of the PPAR α pathway. This is in accordance with the previously, but not explained, proliferation of peroxisomes in the liver of *Scp2* KO mice (27). Interestingly, *Ppara* itself presents an increased and delayed expression probably as a consequence of the regulation of the *Ppara* promoter by PPAR α itself (42).

SREPB is another lipid regulated transcription factor: SREBP is an ER membrane bound protein that, under low sterol conditions, translocates to the Golgi to be cleaved. The remaining peptide is released and migrates to the nucleus where it activates the transcription of genes coding for enzymes involved in cholesterol and fatty acid metabolism (19). As shown in Fig. 4B, the SREBP target genes *Hmgcr* and *Fasn* are upregulated in KO, especially *Hmgcr*. Interestingly, if *Fasn* is mostly regulated by

SREBP1, *Hmgcr* is regulated by both isoforms of SREBP (43), suggesting a prominent activation of SREBP2 in *Scp2* KO mice. Remarkably *Srebp2* diurnal expression is upregulated at the transcriptional level in *Scp2* KO mice, confirming this hypothesis.

Diurnal activation of several signaling pathways is perturbed in SCP2 KO mice

We have previously shown that several signaling pathways are rhythmically activated in mouse liver. Among them, UPR presents a 12 hours period rhythmic activation orchestrated by the circadian clock (8). As shown in Fig. 5, rhythmic maturation of *Xbp1* and nuclear expression of XBP1 are identical in WT and KO animals, as well expression of the UPR regulated genes *Bip* and *Chop*. Despite published link between lipid metabolism and UPR activation (10), this pathway is not affected by SCP2 deficiency. However, rhythmic activation of the TORC1 pathway is clearly altered, probably as a consequence of the disturbed activation of the pathways involved in its activation. Indeed, TORC1 activation depends on several upstream kinases activation: AMPK inhibits TORC1 through the phosphorylation of TSC2 whereas TSC2 phosphorylation AKT activates TORC1 (44). Once activated, TORC1 activation leads to translational activation through the phosphorylation of 4E-BP1, EIF4G, EIF4B, and RPS6 (45). In parallel, phosphorylation of EIF4E is mediated through activation of the ERK pathway (46). As shown in Fig. 6, rhythmic phosphorylation of the TORC1 targets RPS6, EIF4B, and EIF4G is perturbed in *Scp2* KO mice with, in addition to the normal maximum of phosphorylation that appeared in the beginning of the night in WT mice (9), a second peak of phosphorylation in the beginning of the day. In addition, phosphorylation of 4E-BP1 and EIF4B present an overall high phosphorylation level. Interestingly, differences are observed only at post-translational modifications as no differences are observed at the protein and mRNA expression levels, except for EIF4G which protein stability is linked to phosphorylation state (47) (Fig. 6 and S1). Concerning the upstream pathways, AKT rhythmic activation during the night (9) is preserved in *Scp2* KO mice but with a high level of activation throughout the time (Fig. 7). By contrast, rhythmic ERK activation during the day (9, 48) is lost in *Scp2* KO mice, which present a high activation throughout the time. These data converge in a perturbed activation of the TORC1 pathway in *Scp2* KO mice, at rhythmic parameters and activation level, which can lead to perturbed rhythmic ribosome biogenesis.

Discussion

Interplay between the circadian clock and SCP2-regulated lipid transport in mouse liver

If lipid synthesis and accumulation follow a diurnal rhythm in mouse liver controlled by feeding and the circadian clock-regulated lipid metabolism (31, 32), we show here that rhythmic lipid transport regulated by SCP2 contributes to this diurnal accumulation. Rhythmic SCP2 accumulation seems to be controlled by a clock-orchestrated mechanism occurring at the post-translational level. Interestingly, SCP2 and TAG accumulate in the liver with the same rhythmic pattern (Fig 1A and 3E), suggesting a possible stabilization of SCP2 through TAG binding. Protein stabilization through lipid binding is well known for membrane protein (49), but has been also described for lipid-bound cytosolic protein like Perilipin (50). Considering the modification of rhythmic lipid content in circadian clock mutant mice (31, 51), it is thus conceivable that circadian clock-controlled lipid metabolism adjust rhythmic SCP2 half-life through formation of stable SCP2-TAG complexes. This will constitute according to our knowledge the first example of a rhythmic protein induced by protein-metabolite interaction. Considering the crucial role of post-translational regulations in the establishment of the rhythmic liver proteome (52, 53), it will be not surprising that such kinds of regulation will be described in a near future.

The consequence of this disturbed lipid accumulation on rhythmic activation of signaling pathways seems also feedback on the clock itself. Indeed, *Scp2* KO mice present an increased and delayed PER2 expression regulated at the post-translational level, in addition to a lengthening of the free running period. Interestingly, stabilization of PER2, for example through the inhibition of CK1 activity which controls PER2 degradation (54), leads also to period lengthening. It is thus conceivable that SCP2 regulated signaling pathways perturbed in *Scp2* KO animals are involved in this period lengthening through the regulation of PER2 degradation. If no clear regulation of CK1 by lipids has been demonstrated despite a possible regulation by PI (55), it has been shown that PPAR α (56), AKT (57), and mTOR (57-59) pathways interfere with circadian clock genes expression and/or circadian behavior and physiology. In parallel, high fat diet has been linked also to modification of clock genes expression and circadian behavior (60). Taken together, these data suggest that lipid transport and metabolism, which are themselves regulated by the clock, are potentially important regulator of circadian clock function.

Rhythmic activation of cell signaling by lipid metabolism and transport in mouse liver

Increasing evidences link lipid metabolism and transport and cell signaling through different ways. Lipid metabolism can affect directly the activation of lipid-regulated proteins involved in several signaling pathways. It is for example the case for the nuclear receptors PPAR α and LXR for which the rhythmic activation is directly regulated by the rhythmic activation of their respective ligands (20, 21). Interestingly, these pathways are also regulated by lipid intracellular transport which facilitates direct interaction

between these lipids and their ligands through appropriate intracellular transport (61). However, in other cases, lipid metabolism acts through the regulation of the cellular localization of the signaling molecules which influence in this way their maturation (for example in the case of SREBP (19)) or their potential activation by second signaling pathways through their correct localization in a favorable environment or conformation at the plasma membranes, for example in lipid rafts (13, 14). As expected, perturbation of lipid metabolism and transport also affect this pathway in all cases (15, 62, 63). Some interconnections between these two pathways are possible since for example LXR-regulated cholesterol metabolism perturbed AKT activation through perturbation of its localization in lipid rafts (64). Nevertheless, no rhythmic activation of signaling pathway by this mechanism has been reported yet. In this condition, our result showing that SCP2-regulated rhythmic lipid transport is involved in the rhythmic activation of signaling pathways is the first description of such regulation.

However, involvement of other lipid transporter in this mechanism is not excluded. For example, the NPC1 protein, which is specifically involved in intracellular cholesterol transporter, is involved in the regulation of several signaling pathway (65). Indeed, NPC1 inhibition interfere with lipid rafts formation and, as a consequence, activation of the LXR and SREBP (66), PI3K/AKT (67), Insulin Receptor (68), and MAPK (69) pathways. Interestingly, we report here that NPC1 expression is rhythmic at both mRNA and protein levels and regulated by the circadian clock in mouse liver through transcriptional and post-transcriptional regulations (Fig. S2), suggesting a potential role of NPC1 in diurnal activation of signaling pathways. Further experiments are however required to characterize the importance of these two, or additional, lipid transporters in rhythmic activation of signaling pathways.

References

1. Bass J. Circadian topology of metabolism. *Nature* 2012;491:348-356.
2. Garaulet M, Gomez-Abellan P. Chronobiology and obesity. *Nutr Hosp* 2013;28 Suppl 5:114-120.
3. Vyas MV, Garg AX, Iansavichus AV, Costella J, Donner A, Laugsand LE, Janszky I, et al. Shift work and vascular events: systematic review and meta-analysis. *BMJ* 2012;345:e4800.
4. Baron KG, Reid KJ. Circadian misalignment and health. *Int Rev Psychiatry* 2014;26:139-154.
5. Mohawk JA, Green CB, Takahashi JS. Central and peripheral circadian clocks in mammals. *Annu Rev Neurosci* 2012;35:445-462.
6. Feng D, Lazar MA. Clocks, metabolism, and the epigenome. *Mol Cell* 2012;47:158-167.
7. Asher G, Schibler U. Crosstalk between components of circadian and metabolic cycles in mammals. *Cell Metab* 2011;13:125-137.
8. Cretenet G, Le Clech M, Gachon F. Circadian clock-coordinated 12 Hr period rhythmic activation of the IRE1alpha pathway controls lipid metabolism in mouse liver. *Cell Metab* 2010;11:47-57.
9. Jouffe C, Cretenet G, Symul L, Martin E, Atger F, Naef F, Gachon F. The circadian clock coordinates ribosome biogenesis. *PLoS Biol* 2013;11:e1001455.
10. Fu S, Yang L, Li P, Hofmann O, Dicker L, Hide W, Lin X, et al. Aberrant lipid metabolism disrupts calcium homeostasis causing liver endoplasmic reticulum stress in obesity. *Nature* 2011;473:528-531.
11. Xu J, Dang Y, Ren YR, Liu JO. Cholesterol trafficking is required for mTOR activation in endothelial cells. *Proc Natl Acad Sci U S A* 2010;107:4764-4769.
12. Nada S, Hondo A, Kasai A, Koike M, Saito K, Uchiyama Y, Okada M. The novel lipid raft adaptor p18 controls endosome dynamics by anchoring the MEK-ERK pathway to late endosomes. *EMBO J* 2009;28:477-489.
13. Lingwood D, Simons K. Lipid rafts as a membrane-organizing principle. *Science* 2010;327:46-50.
14. Laganowsky A, Reading E, Allison TM, Ulmschneider MB, Degiacomi MT, Baldwin AJ, Robinson CV. Membrane proteins bind lipids selectively to modulate their structure and function. *Nature* 2014;510:172-175.
15. Sanchez-Wandelmer J, Davalos A, Herrera E, Giera M, Cano S, de la Pena G, Lasuncion MA, et al. Inhibition of cholesterol biosynthesis disrupts lipid raft/caveolae and affects insulin receptor activation in 3T3-L1 preadipocytes. *Biochim Biophys Acta* 2009;1788:1731-1739.
16. Vanhaesebroeck B, Guillermet-Guibert J, Graupera M, Bilanges B. The emerging mechanisms of isoform-specific PI3K signalling. *Nat Rev Mol Cell Biol* 2010;11:329-341.
17. Hong C, Tontonoz P. Liver X receptors in lipid metabolism: opportunities for drug discovery. *Nat Rev Drug Discov* 2014;13:433-444.
18. Rakhshandehroo M, Knoch B, Muller M, Kersten S. Peroxisome proliferator-activated receptor alpha target genes. *PPAR Res* 2010;2010.
19. Jeon TI, Osborne TF. SREBPs: metabolic integrators in physiology and metabolism. *Trends Endocrinol Metab* 2012;23:65-72.
20. Gachon F, Leuenberger N, Claudel T, Gos P, Jouffe C, Fleury Olela F, de Mollerat du Jeu X, et al. Proline- and acidic amino acid-rich basic leucine zipper proteins modulate peroxisome proliferator-activated receptor alpha (PPARalpha) activity. *Proc Natl Acad Sci U S A* 2011;108:4794-4799.
21. Le Martelot G, Claudel T, Gatfield D, Schaad O, Kornmann B, Lo Sasso G, Moschetta A, et al. REV-ERBalpha participates in circadian SREBP signaling and bile acid homeostasis. *PLoS Biol* 2009;7:e1000181.

22. McGuire DM, Chan L, Smith LC, Towle HC, Dempsey ME. Translational control of the circadian rhythm of liver sterol carrier protein. Analysis of mRNA sequences with a specific cDNA probe. *J Biol Chem* 1985;260:5435-5439.
23. McGuire DM, Olson CD, Towle HC, Dempsey ME. Translational control of the circadian rhythm of liver sterol carrier protein. *J Biol Chem* 1984;259:5368-5371.
24. Puglielli L, Rigotti A, Greco AV, Santos MJ, Nervi F. Sterol carrier protein-2 is involved in cholesterol transfer from the endoplasmic reticulum to the plasma membrane in human fibroblasts. *J Biol Chem* 1995;270:18723-18726.
25. Schroeder F, Atshaves BP, McIntosh AL, Gallegos AM, Storey SM, Parr RD, Jefferson JR, et al. Sterol carrier protein-2: new roles in regulating lipid rafts and signaling. *Biochim Biophys Acta* 2007;1771:700-718.
26. Gallegos AM, Atshaves BP, Storey SM, Starodub O, Petrescu AD, Huang H, McIntosh AL, et al. Gene structure, intracellular localization, and functional roles of sterol carrier protein-2. *Prog Lipid Res* 2001;40:498-563.
27. Seedorf U, Raabe M, Ellinghaus P, Kannenberg F, Fobker M, Engel T, Denis S, et al. Defective peroxisomal catabolism of branched fatty acyl coenzyme A in mice lacking the sterol carrier protein-2/sterol carrier protein-x gene function. *Genes Dev* 1998;12:1189-1201.
28. Atshaves BP, McIntosh AL, Payne HR, Gallegos AM, Landrock K, Maeda N, Kier AB, et al. SCP-2/SCP-x gene ablation alters lipid raft domains in primary cultured mouse hepatocytes. *J Lipid Res* 2007;48:2193-2211.
29. Cerqueira DM, Tran U, Romaker D, Abreu JG, Wessely O. Sterol carrier protein 2 regulates proximal tubule size in the *Xenopus* pronephric kidney by modulating lipid rafts. *Dev Biol* 2014;394:54-64.
30. Gallegos AM, Storey SM, Kier AB, Schroeder F, Ball JM. Structure and cholesterol dynamics of caveolae/raft and nonraft plasma membrane domains. *Biochemistry* 2006;45:12100-12116.
31. Adamovich Y, Rousoo-Noori L, Zwighaft Z, Neufeld-Cohen A, Golik M, Kraut-Cohen J, Wang M, et al. Circadian clocks and feeding time regulate the oscillations and levels of hepatic triglycerides. *Cell Metab* 2014;19:319-330.
32. Gorne LD, Acosta-Rodriguez VA, Pasquare SJ, Salvador GA, Giusto NM, Guido ME. The mouse liver displays daily rhythms in the metabolism of phospholipids and in the activity of lipid synthesizing enzymes. *Chronobiol Int* 2015;32:11-26.
33. Lopez-Molina L, Conquet F, Dubois-Dauphin M, Schibler U. The DBP gene is expressed according to a circadian rhythm in the suprachiasmatic nucleus and influences circadian behavior. *EMBO J* 1997;16:6762-6771.
34. Gachon F, Olela FF, Schaad O, Descombes P, Schibler U. The circadian PAR-domain basic leucine zipper transcription factors DBP, TEF, and HLF modulate basal and inducible xenobiotic detoxification. *Cell Metab* 2006;4:25-36.
35. Wagner SA, Beli P, Weinert BT, Scholz C, Kelstrup CD, Young C, Nielsen ML, et al. Proteomic analyses reveal divergent ubiquitylation site patterns in murine tissues. *Mol Cell Proteomics* 2012;11:1578-1585.
36. Storch KF, Paz C, Signorovitch J, Raviola E, Pawlyk B, Li T, Weitz CJ. Intrinsic circadian clock of the mammalian retina: importance for retinal processing of visual information. *Cell* 2007;130:730-741.
37. van der Horst GT, Muijtjens M, Kobayashi K, Takano R, Kanno S, Takao M, de Wit J, et al. Mammalian Cry1 and Cry2 are essential for maintenance of circadian rhythms. *Nature* 1999;398:627-630.
38. Ferdinandusse S, Kostopoulos P, Denis S, Rusch H, Overmars H, Dillmann U, Reith W, et al. Mutations in the gene encoding peroxisomal sterol carrier protein X (SCPx) cause leukoencephalopathy with dystonia and motor neuropathy. *Am J Hum Genet* 2006;78:1046-1052.
39. Reischl S, Kramer A. Kinases and phosphatases in the mammalian circadian clock. *FEBS Lett* 2011;585:1393-1399.

40. Schmutz I, Ripperger JA, Baeriswyl-Aebischer S, Albrecht U. The mammalian clock component PERIOD2 coordinates circadian output by interaction with nuclear receptors. *Genes Dev* 2010;24:345-357.
41. Chappuis S, Ripperger JA, Schnell A, Rando G, Jud C, Wahli W, Albrecht U. Role of the circadian clock gene *Per2* in adaptation to cold temperature. *Mol Metab* 2013;2:184-193.
42. Pineda Torra I, Jamshidi Y, Flavell DM, Fruchart JC, Staels B. Characterization of the human PPARalpha promoter: identification of a functional nuclear receptor response element. *Mol Endocrinol* 2002;16:1013-1028.
43. Horton JD, Shah NA, Warrington JA, Anderson NN, Park SW, Brown MS, Goldstein JL. Combined analysis of oligonucleotide microarray data from transgenic and knockout mice identifies direct SREBP target genes. *Proc Natl Acad Sci U S A* 2003;100:12027-12032.
44. Laplante M, Sabatini DM. mTOR signaling in growth control and disease. *Cell* 2012;149:274-293.
45. Ma XM, Blenis J. Molecular mechanisms of mTOR-mediated translational control. *Nat Rev Mol Cell Biol* 2009;10:307-318.
46. Silva RL, Wendel HG. MNK, EIF4E and targeting translation for therapy. *Cell Cycle* 2008;7:553-555.
47. Berset C, Trachsel H, Altmann M. The TOR (target of rapamycin) signal transduction pathway regulates the stability of translation initiation factor eIF4G in the yeast *Saccharomyces cerevisiae*. *Proc Natl Acad Sci U S A* 1998;95:4264-4269.
48. Tsuchiya Y, Minami I, Kadotani H, Todo T, Nishida E. Circadian clock-controlled diurnal oscillation of Ras/ERK signaling in mouse liver. *Proc Jpn Acad Ser B Phys Biol Sci* 2013;89:59-65.
49. White SH, Wimley WC. Membrane protein folding and stability: physical principles. *Annu Rev Biophys Biomol Struct* 1999;28:319-365.
50. Hall AM, Brunt EM, Chen Z, Viswakarma N, Reddy JK, Wolins NE, Finck BN. Dynamic and differential regulation of proteins that coat lipid droplets in fatty liver dystrophic mice. *J Lipid Res* 2010;51:554-563.
51. Paschos GK, Ibrahim S, Song WL, Kunieda T, Grant G, Reyes TM, Bradfield CA, et al. Obesity in mice with adipocyte-specific deletion of clock component *Arntl*. *Nat Med* 2012;18:1768-1777.
52. Mauvoisin D, Wang J, Jouffe C, Martin E, Atger F, Waridel P, Quadroni M, et al. Circadian clock-dependent and -independent rhythmic proteomes implement distinct diurnal functions in mouse liver. *Proc Natl Acad Sci U S A* 2014;111:167-172.
53. Robles MS, Cox J, Mann M. In-vivo quantitative proteomics reveals a key contribution of post-transcriptional mechanisms to the circadian regulation of liver metabolism. *PLoS Genet* 2014;10:e1004047.
54. Hirota T, Lee JW, Lewis WG, Zhang EE, Breton G, Liu X, Garcia M, et al. High-throughput chemical screen identifies a novel potent modulator of cellular circadian rhythms and reveals CKIalpha as a clock regulatory kinase. *PLoS Biol* 2010;8:e1000559.
55. Brockman JL, Anderson RA. Casein kinase I is regulated by phosphatidylinositol 4,5-bisphosphate in native membranes. *J Biol Chem* 1991;266:2508-2512.
56. Canaple L, Rambaud J, Dkhissi-Benyahya O, Rayet B, Tan NS, Michalik L, Delaunay F, et al. Reciprocal regulation of brain and muscle *Arnt*-like protein 1 and peroxisome proliferator-activated receptor alpha defines a novel positive feedback loop in the rodent liver circadian clock. *Mol Endocrinol* 2006;20:1715-1727.
57. Zheng X, Sehgal A. AKT and TOR signaling set the pace of the circadian pacemaker. *Curr Biol* 2010;20:1203-1208.
58. Cao R, Robinson B, Xu H, Gkogkas C, Khoutorsky A, Alain T, Yanagiya A, et al. Translational control of entrainment and synchrony of the suprachiasmatic circadian clock by mTOR/4E-BP1 signaling. *Neuron* 2013;79:712-724.
59. Cornu M, Oppliger W, Albert V, Robitaille AM, Trapani F, Quagliata L, Fuhrer T, et al. Hepatic mTORC1 controls locomotor activity, body temperature, and lipid metabolism through FGF21. *Proc Natl Acad Sci U S A* 2014;111:11592-11599.

60. Kohsaka A, Laposky AD, Ramsey KM, Estrada C, Joshu C, Kobayashi Y, Turek FW, et al. High-fat diet disrupts behavioral and molecular circadian rhythms in mice. *Cell Metab* 2007;6:414-421.
61. Schroeder F, Petrescu AD, Huang H, Atshaves BP, McIntosh AL, Martin GG, Hostetler HA, et al. Role of fatty acid binding proteins and long chain fatty acids in modulating nuclear receptors and gene transcription. *Lipids* 2008;43:1-17.
62. Zhu X, Owen JS, Wilson MD, Li H, Griffiths GL, Thomas MJ, Hiltbold EM, et al. Macrophage ABCA1 reduces MyD88-dependent Toll-like receptor trafficking to lipid rafts by reduction of lipid raft cholesterol. *J Lipid Res* 2010;51:3196-3206.
63. Zhang J, Dudley-Rucker N, Crowley JR, Lopez-Perez E, Issandou M, Schaffer JE, Ory DS. The steroidal analog GW707 activates the SREBP pathway through disruption of intracellular cholesterol trafficking. *J Lipid Res* 2004;45:223-231.
64. Pommier AJ, Alves G, Viennois E, Bernard S, Communal Y, Sion B, Marceau G, et al. Liver X Receptor activation downregulates AKT survival signaling in lipid rafts and induces apoptosis of prostate cancer cells. *Oncogene* 2010;29:2712-2723.
65. Karten B, Peake KB, Vance JE. Mechanisms and consequences of impaired lipid trafficking in Niemann-Pick type C1-deficient mammalian cells. *Biochim Biophys Acta* 2009;1791:659-670.
66. Ishibashi M, Masson D, Westerterp M, Wang N, Sayers S, Li R, Welch CL, et al. Reduced VLDL clearance in Apoe(-/-)Npc1(-/-) mice is associated with increased Pcsk9 and Idol expression and decreased hepatic LDL-receptor levels. *J Lipid Res* 2010;51:2655-2663.
67. Bi X, Liu J, Yao Y, Baudry M, Lynch G. Deregulation of the phosphatidylinositol-3 kinase signaling cascade is associated with neurodegeneration in Npc1^{-/-} mouse brain. *Am J Pathol* 2005;167:1081-1092.
68. Vainio S, Bykov I, Hermansson M, Jokitalo E, Somerharju P, Ikonen E. Defective insulin receptor activation and altered lipid rafts in Niemann-Pick type C disease hepatocytes. *Biochem J* 2005;391:465-472.
69. Yang SR, Kim SJ, Byun KH, Hutchinson B, Lee BH, Michikawa M, Lee YS, et al. NPC1 gene deficiency leads to lack of neural stem cell self-renewal and abnormal differentiation through activation of p38 mitogen-activated protein kinase signaling. *Stem Cells* 2006;24:292-298.

Figures legends

Figure 1: Temporal mRNA and protein expressions of Sterol Carrier Protein 2

A. F. G. Temporal protein expression of SCP2 in wild-type (A), *Bmal1* knockout and control (F) and *Cry 1/2* double knockout and control (G) mouse liver. Western blots were realized on total liver extracts. Naphtol blue black staining of the membranes was used as a loading control. Each graph corresponds to the mean densitometric values of the western blot data associated.

B. F. E. Temporal mRNA expression profile of *Scp2* in wild-type (B), *Bmal1* knockout and control (D) and *Cry 1/2* double knockout and control (E) mouse liver.

C. Temporal localization of *Scp2* mRNA in the polysomal fraction.

The zeitgeber times (ZT), with ZT0: lights on, ZT12: lights off, at which the animals were sacrificed, are indicated on each panel. For each time point, data are Mean \pm SEM obtained from three independent animals.

Figure 2: Influence of SCP2 in the circadian physiology

A. Circadian locomotor (running-wheel) activity of *Scp2* knockout (right panel) and wild-type (left panel) mice.

B. Temporal mRNA expression profile of *Bmal1*, *Cry1*, *Dbp* and *Per2* in *Scp2* knockout (dotted line) and wild-type (solid line) mouse liver.

C. Temporal protein expression of BMAL1 and PER2 in *Scp2* knockout (right panel) and wild-type (left panel) mouse liver. Western blots were realized on nuclear liver extracts. Naphtol blue black staining of the membranes was used as a loading control. Each graph corresponds to the mean densitometric values of the western blot data associated.

The zeitgeber times (ZT), with ZT0: lights on, ZT12: lights off, at which the animals were sacrificed, are indicated on each panel. For each time point, data are Mean \pm SEM obtained from three independent animals.

Figure 3: Perturbation of the diurnal lipid metabolism in *Scp2* knockout mice

A-D. Temporal serum concentration of glucose (A), insulin (B), triglycerides (C) and cholesterol (D) in *Scp2* knockout (dotted line) and wild-type (solid line) mouse.

E. F. Heatmap of the abundance of cycling (E) or non-cycling (F) lipid species in *Scp2* knockout mice.

The zeitgeber times (ZT), with ZT0: lights on, ZT12: lights off, at which the animals were sacrificed, are indicated on each panel. For each time point, data are Mean \pm SEM obtained from three independent animals.

Figure 4: Alteration of the activation of lipids regulated pathways in *Scp2* knockout mice

A. Temporal mRNA expression profile of PPAR α target genes *Cyp4a14*, *Acox1*, *Lpl*, *Cd36* and *Ppara* in *Scp2* knockout (dotted line) and wild-type (solid line) mouse liver.

B. Temporal mRNA expression profile of SREBP target genes *Hmgcr*, *Fasn*, *Srebp1c* and *Srebp2* in *Scp2* knockout (dotted line) and wild-type (solid line) mouse liver.

C. Temporal protein expression of SREBP1 and SREBP2 in *Scp2* knockout (right panels) and wild-type (left panels) mouse liver. Western blots were realized on nuclear liver extracts. Naphtol blue black staining of the membranes was used as a loading control. Each graph corresponds to the mean densitometric values of the western blot data associated.

The zeitgeber times (ZT), with ZT0: lights on, ZT12: lights off, at which the animals were sacrificed, are indicated on each panel. For each time point, data are Mean \pm SEM obtained from three independent animals.

Figure 5: The regulation of the UPR stress pathway is not affected in *Scp2* knockout mice

A. Temporal mRNA expression profile of genes involved in the regulation of the UPR stress *Bip*, *Chop*, and *sXbp1* in *Scp2* knockout (dotted line) and wild-type (solid line) mouse liver.

B. Temporal protein expression of sXBP1 in *Scp2* knockout (right panel) and wild-type (left panel) mouse liver. Western blots were realized on nuclear liver extracts. Naphtol blue black staining of the membranes was used as a loading control. Each graph corresponds to the mean densitometric values of the western blot data associated.

The zeitgeber times (ZT), with ZT0: lights on, ZT12: lights off, at which the animals were sacrificed, are indicated on each panel. For each time point, data are Mean \pm SEM obtained from three independent animals.

Figure 6: The rhythmic phosphorylation of translation initiation factors is altered in *Scp2* knockout mice

Temporal protein expression and phosphorylation profile of translation initiation factors in *Scp2* knockout (right panel) and wild-type (left panel) mouse liver. Western blots were realized on total liver extracts. Naphtol blue black staining of the membranes was used as a loading control. Each graph corresponds to the mean densitometric values of the western blot data associated.

The zeitgeber times (ZT), with ZT0: lights on, ZT12: lights off, at which the animals were sacrificed, are indicated on each panel. For each time point, data are Mean \pm SEM obtained from three independent animals.

Figure 7: The rhythmic activation of signaling pathways controlling translation initiation is altered in *Scp2* knockout mice

Temporal protein expression and phosphorylation profile of representative proteins of key signaling pathways involved in the regulation of translation initiation in *Scp2* knockout (right panel) and wild-type (left panel) mouse liver. Western blots were realized on total liver extracts. Naphtol blue black staining of the membranes was used as a loading control. Each graph corresponds to the mean densitometric values of the western blot data associated.

The zeitgeber times (ZT), with ZT0: lights on, ZT12: lights off, at which the animals were sacrificed, are indicated on each panel. For each time point, data are Mean \pm SEM obtained from three independent animals.

Figure S1: Temporal expression of translation initiation complex factors

Temporal expression of factors involved in translation initiation in *Scp2* KO mice and their control littermates. Temporal real-time RT-PCR expression profile translation initiation factors in mouse liver. For each time point, data are Mean \pm SEM obtained from three independent animals. The Zeitgeber times (ZT), with ZT0: lights on, ZT12: lights off, at which the animals were sacrificed, are indicated on each panel.

Figure S2: Rhythmic expression of NPC1 is circadian clock dependent.

A. *Npc1* expression was measured by real-time RT-PCR on liver RNAs obtained from arrhythmic *Bmal1* (left panel) and *Cry1/Cry2* (right panel) KO mice and their control littermates. Data are Mean \pm SEM obtained from three independent animals. B. Protein levels were assessed by western-blot on total extracts in *Bmal1* (upper panel) and *Cry1/Cry2* (lower panel) KO mice and their control littermates. Naphtol blue black staining of the membranes was used as a loading control. The *Zeitgeber* times (ZT), with ZT0: lights on, ZT12: lights off, at which the animals were sacrificed, are indicated on each panel.

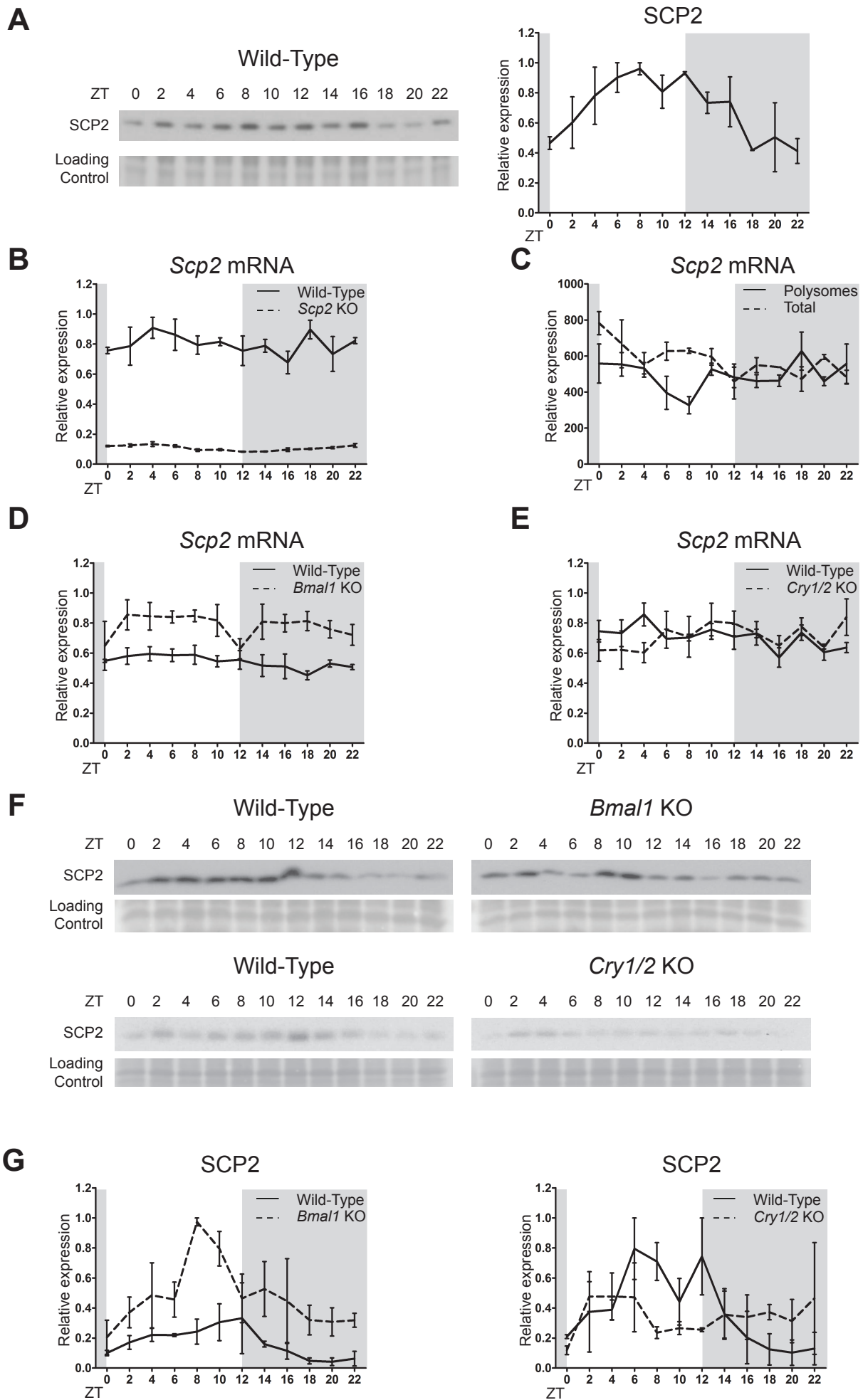


Figure 1

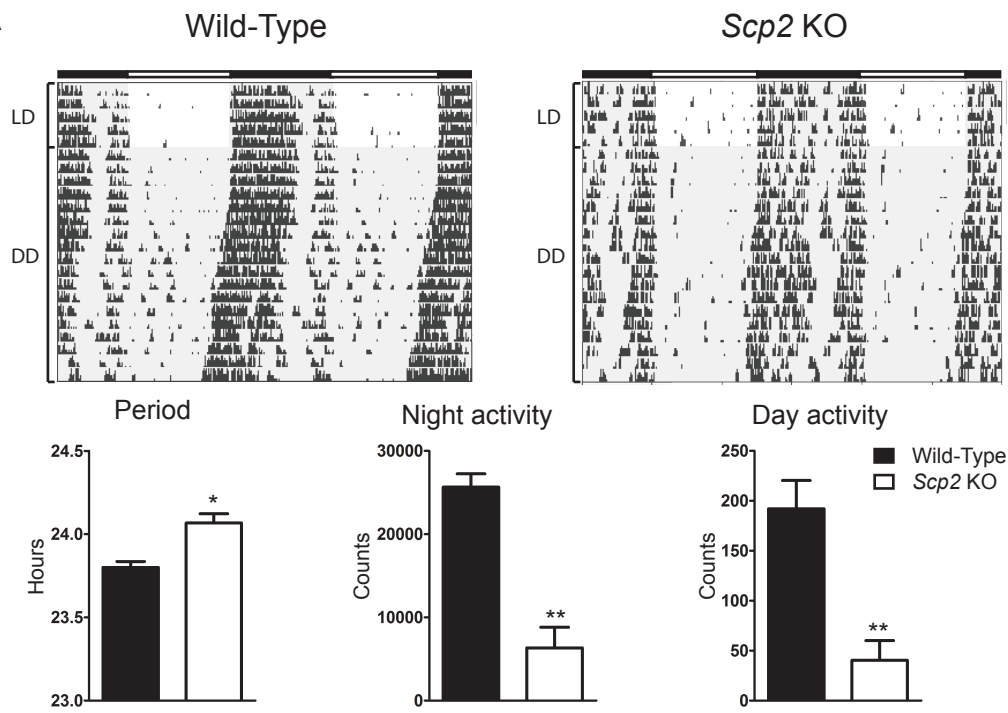
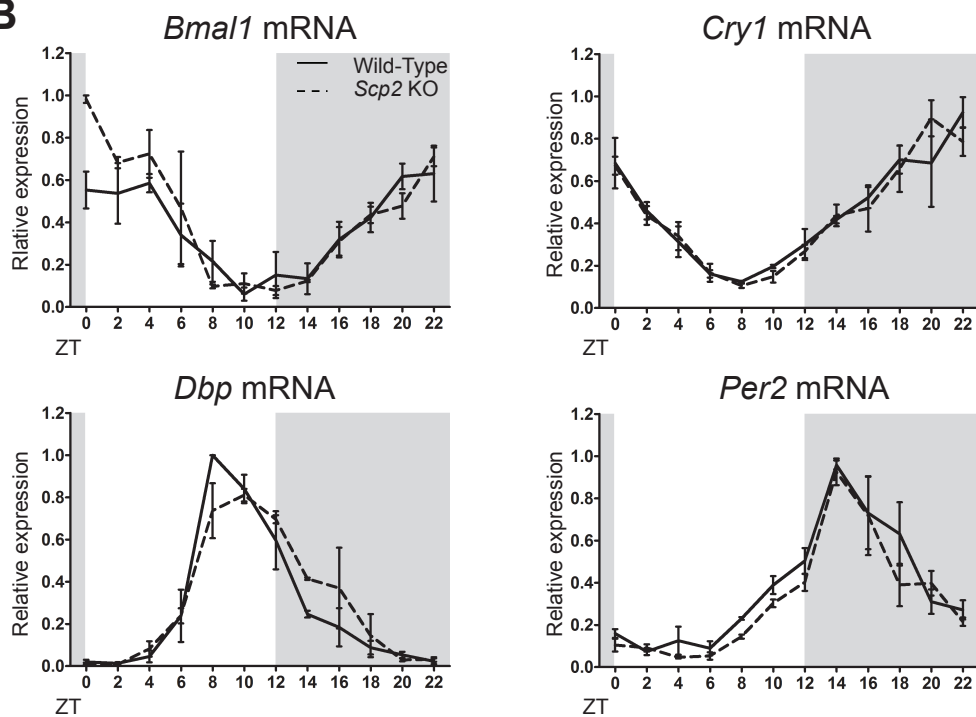
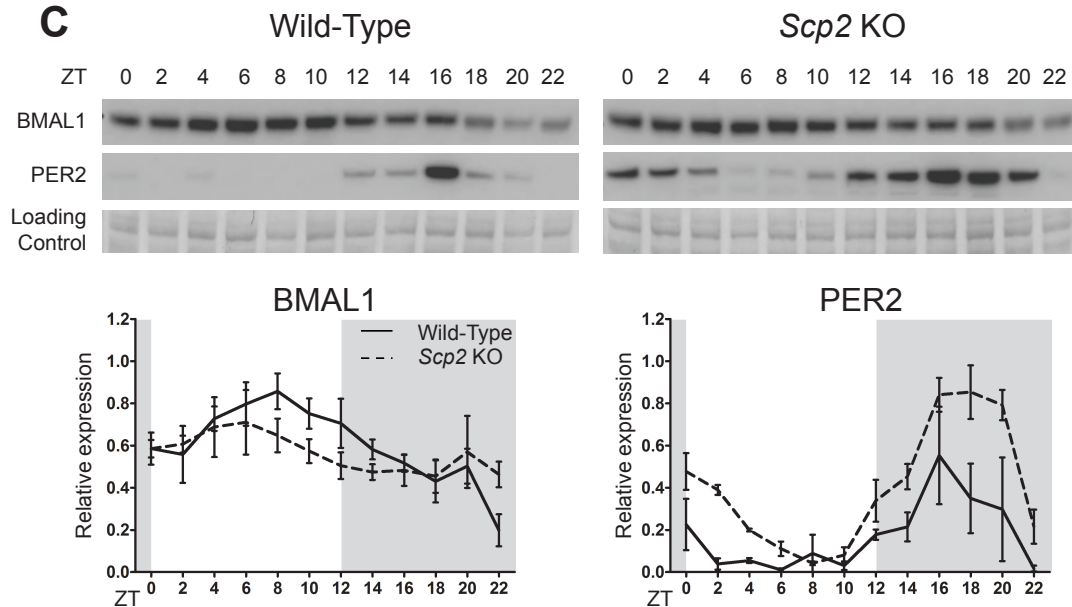
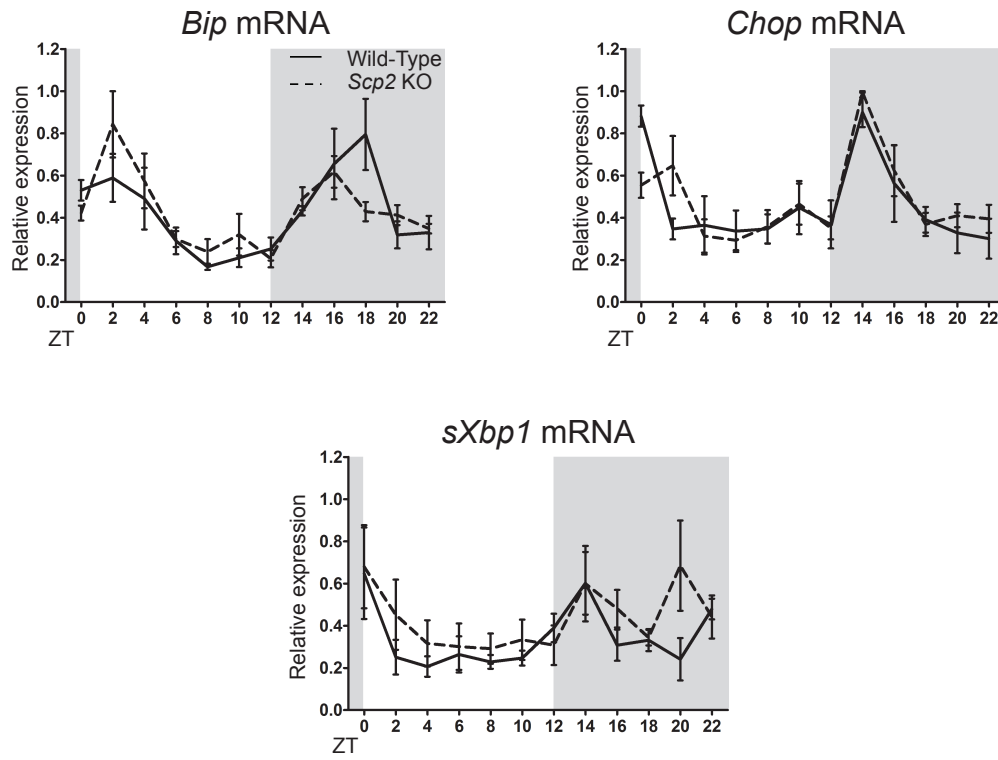
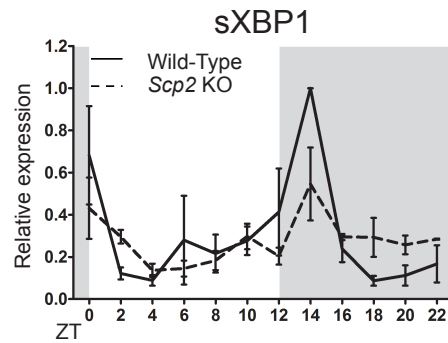
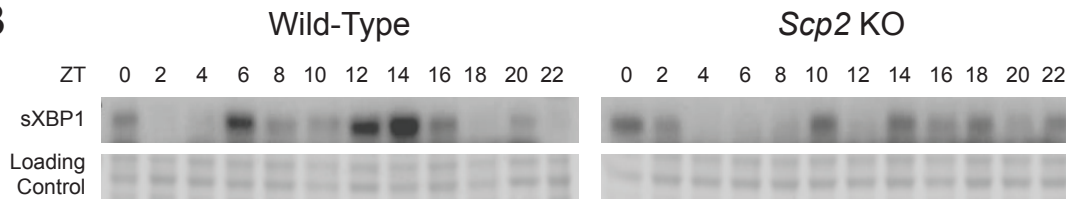
A**B****C**

Figure 2

A**B**

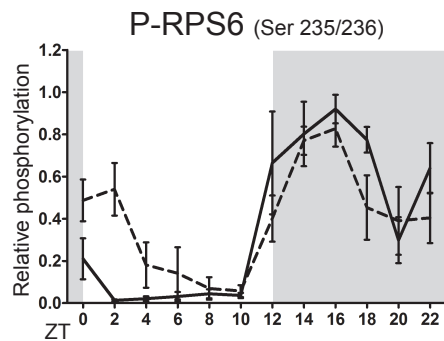
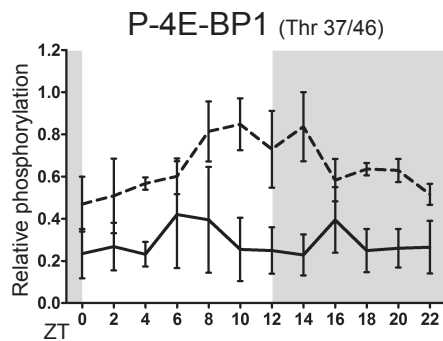
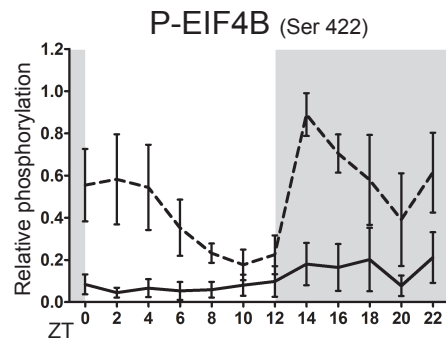
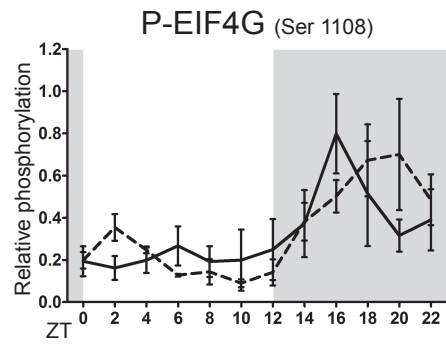
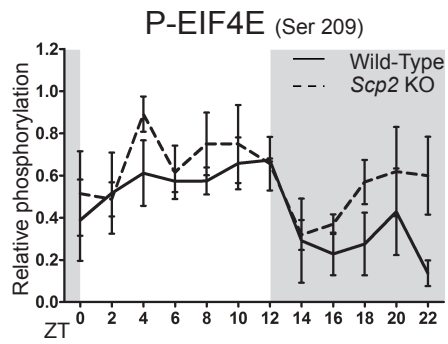
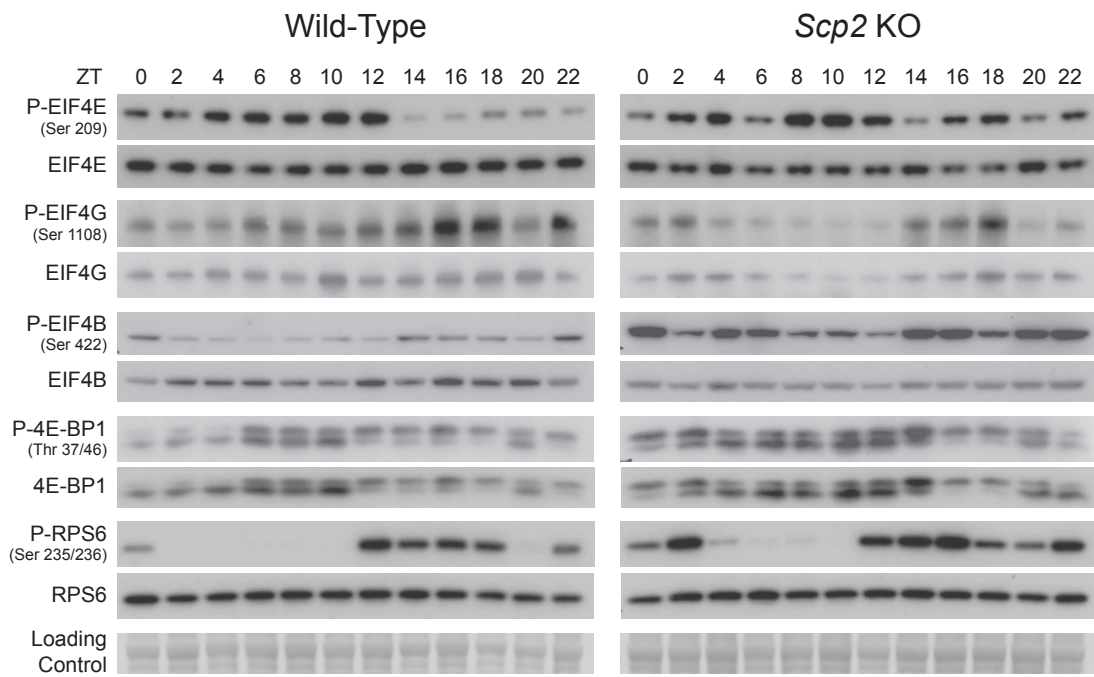


Figure 6

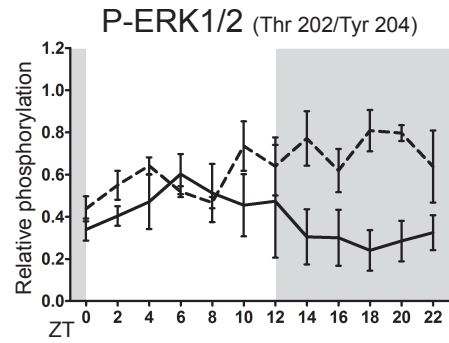
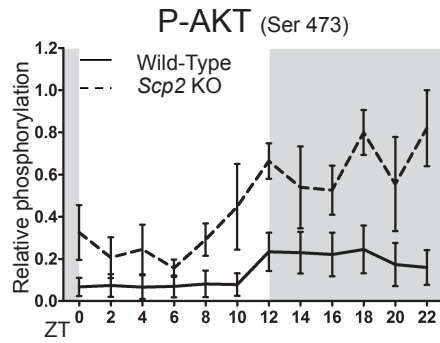
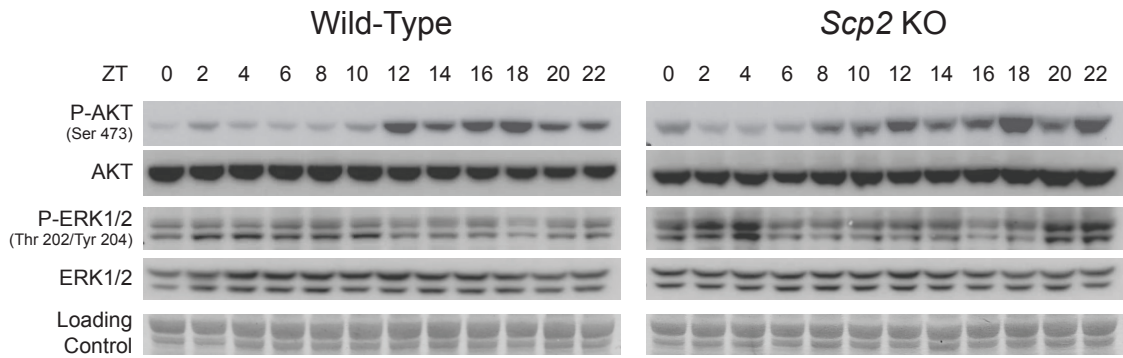


Figure 7

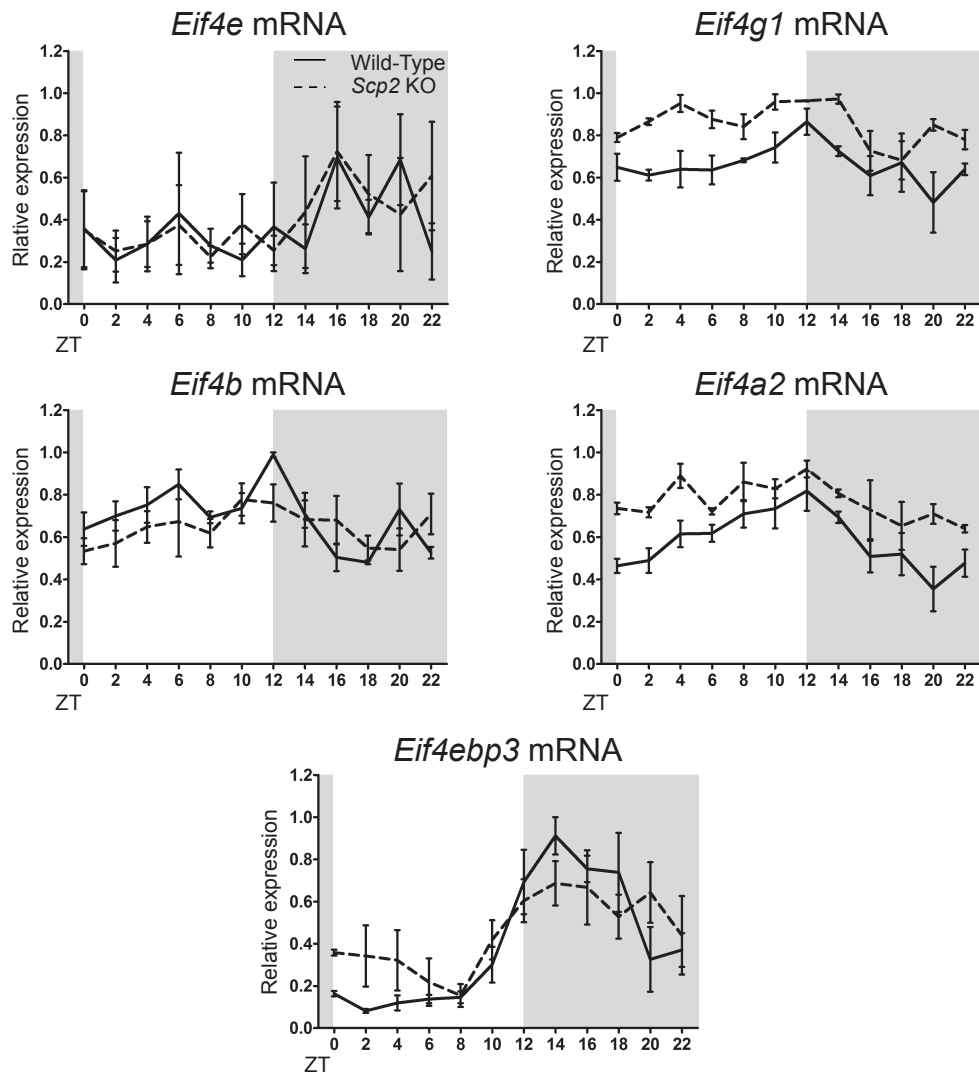


Figure S1

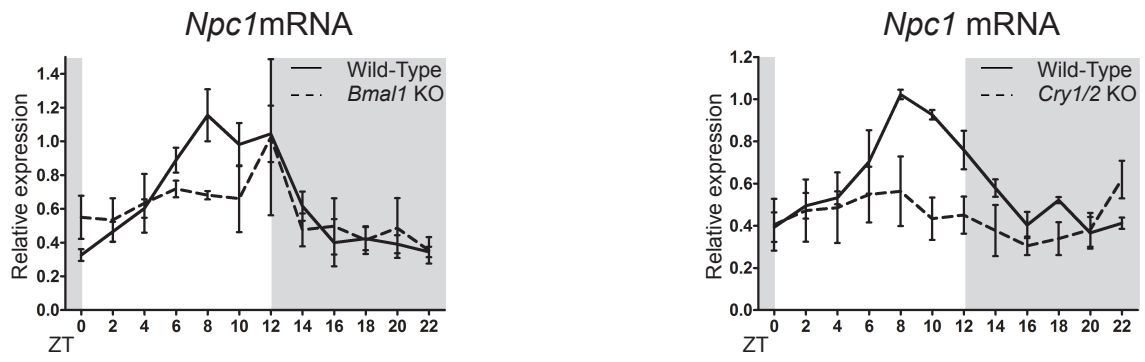
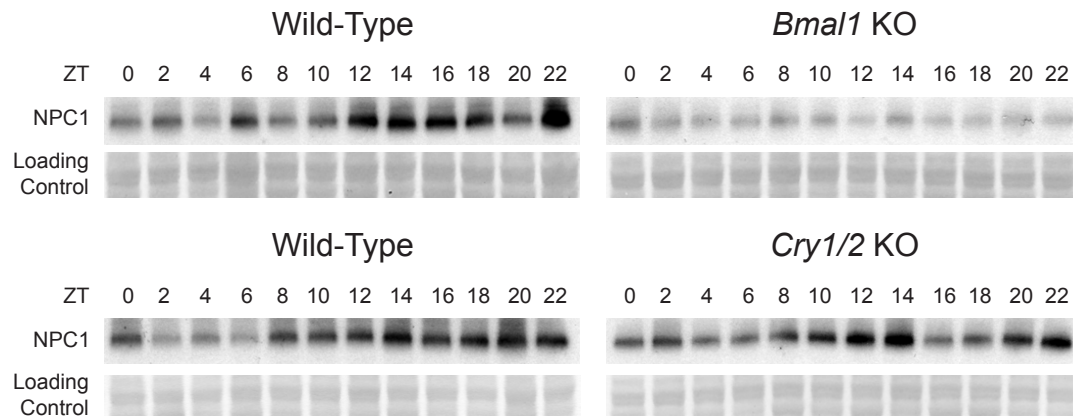
A**B**

Table S1 : Cosinor statistical values related to rhythmic mRNA expression involved in the circadian clock and signaling pathways in *Scp2* KO and wild-type mice

	Genotype	p value	F(2,9)	robustness (%)	Mesor	Amplitude	Acrophase (h)	fold change
<i>Scp2</i>	KO	0.000177	35.129	84.9	0.1074	0.022	1.26	1.613074418
	WT	0.589938	0.992	0				1.340930239
<i>Bmal1</i>	KO	0.000121	41.208	86.9	0.4332	0.384	0.07	12.61631342
	WT	0.000068	53.309	89.6	0.3804	0.2672	23.32	10.40495458
<i>Cry1</i>	KO	0.000022	94.51	93.9	0.4488	0.3437	20.58	8.547864226
	WT	0.000051	61.04	90.8	0.4574	0.3293	20.56	7.427079148
<i>Dbp</i>	KO	0.000272	29.608	82.4	0.2977	0.3832	10.92	103.9179487
	WT	0.0048	10.456	59.9	0.2789	0.3881	10.04	77.63975155
<i>Per2</i>	KO	0.001026	18.074	73.4	0.3157	0.3327	15.28	19.99675886
	WT	0.000309	28.166	81.6	0.3726	0.3529	15.06	13.07585266
<i>Cyp4a14</i>	KO	0.010681	7.881	51.5	0.4512	0.1803	3.66	4.723795676
	WT	0.903592	0.102	0				16.26319397
<i>Acox1</i>	KO	0.868388	0.143	0				1.437809548
	WT	0.000325	27.636	81.3	0.3653	0.0805	10.74	1.777709226
<i>Lpl</i>	KO	0.003978	11.219	61.8	0.6235	20.95	5.92	2.74628662
	WT	0.000165	36.21	85.3	0.3261	0.1627	4.1	3.560435931
<i>Cd36</i>	KO	0.124428	2.641	16				1.689982604
	WT	0.045111	4.434	32.8	0.2017	0.0499	9.14	2.412037037
<i>Ppara</i>	KO	0.001166	17.265	72.4	0.5497	0.28	11.44	2.751498133
	WT	0.001987	14.308	68.1	0.3715	0.1705	10.24	2.989282697
<i>Hmgcr</i>	KO	0.049291	4.26	31.5	0.5061	0.1816	17.5	3.50465868
	WT	0.101446	2.97	19.7				3.936582196
<i>Fasn</i>	KO	0.028951	5.361	39.2	0.4667	0.1847	20.24	4.327027666
	WT	0.023321	5.852	42	0.3698	0.153	20.45	5.043459365
<i>Srebp1c</i>	KO	0.025914	5.609	40.6	0.3913	0.0876	17.49	2.082407166
	WT	0.011033	7.788	51.2	0.4562	0.1824	17.35	4.7716141
<i>Srebp2</i>	KO	0.125254	2.63	15.9				1.722547904
	WT	0.157798	2.276	11.4				1.986686232
<i>Bip</i>	KO	0.392926	1.044	0				4.097817103
	WT	0.155558	2.297	11.7				4.749656285
<i>Chop</i>	KO	0.515685	0.721	0				3.404024186
	WT	0.717126	0.35	0				2.99215582
<i>sXbp1</i>	KO	0.072583	3.542	25.4				2.349473251
	WT	0.513584	0.789	0				3.139220905

Table S2 : Cosinor statistical values related to rhythmic phosphorylation and expression protein involved in the circadian clock and signaling pathways in *Scp2* KO and wild-type mice

	Genotype	p value	F(2,9)	robustness (%)	Mesor	Amplitude	Acrophase (h)	fold change
SCP2	WT	0.000183	34.679	84.7	0.6877	0.2565	9.15	2.328796
BMAL1	KO	0.001085	17.718	73	0.5631	0.1071	5.02	1.562068
	WT	0.001149	17.357	72.5	0.6008	0.2196	8.11	4.327242
PER2	KO	0.002614	12.996	65.7	0.3992	0.3437	18.48	20.46211
	WT	0.013169	7.293	49.1	0.1716	0.1775	17.06	50.78053
sXBP1	KO	0.280083	1.47	0				3.996046
	WT	0.589666	0.568	0				11.51941
P-EIF4E	KO	0.144284	2.411	13.2				2.798669
	WT	0.007071	9.152	56	0.4462	0.2009	7.37	4.925861
P-EIF4G	KO	0.001123	17.499	72.7	0.3367	0.2584	19.33	7.857111
	WT	0.023242	5.859	42.1	0.3209	0.1865	16.93	4.94066
P-EIF4B	KO	0.18052	2.077	8.8				5.035737
	WT	0.015436	6.869	47.2	0.11	0.0645	17.43	4.713967
P-4EBP1	KO	0.00182	14.754	68.8	0.6445	0.1565	11.54	1.806493
	WT	0.564615	0.617	0				1.837553
P-RPS6	KO	0.044081	4.48	33.2	0.3932	0.2396	18.07	14.56473
	WT	0.001068	17.818	73.1	0.371	0.4352	16.6	71.2969
P-AKT	KO	0.006582	9.384	56.8	0.4645	0.25	17.2	5.245264
	WT	0.000314	27.99	81.5	0.1417	0.0952	16.17	3.710415
P-ERK	KO	0.064351	3.759	27.4				1.846368
	WT	0.000174	35.391	85	0.3925	0.1403	6.87	2.503327

Table S3 : Cosinor statistical values related to serum measurements in *Scp2* KO and wild-type mice

	Genotype	p value	F(2,9)	robustness (%)	Mesor	Amplitude	Acrophase (h)	fold change
Glucose	KO	0.129815	2.574	15.2				1.475746295
	WT	0.023216	5.862	42.1	1.8317	0.1582	13.34	1.376423221
Insulin	KO	0.002756	23.758	15.2	2.1325	1.2766	19.42	4.162980759
	WT	0.002608	13.006	42.1	2.1876	1.7963	17.1	7.270994261
Triglycerides	KO	0.013342	7.257	49	0.9336	0.2063	23.36	1.936409188
	WT	0.00089	19.014	74.5	1.1907	0.3991	0.13	2.477136213
Cholesterol	KO	0.166743	2.194	10.4				1.623615585
	WT	0.249314	1.625	2				1.65562497

References of the antibodies used for Western blotting

Protein	Reference	Company
P-EIF4E (Ser 209)	9741	Cell Signaling Technology
EIF4E	2067	Cell Signaling Technology
P-EIF4G (Ser 1108)	2441	Cell Signaling Technology
EIF4G	2469	Cell Signaling Technology
P-EIF4B (Ser 422)	3591	Cell Signaling Technology
EIF4B	3592	Cell Signaling Technology
P-4EBP1 (Thr 37/46)	2855	Cell Signaling Technology
4EBP1	9644	Cell Signaling Technology
P-RPS6 (Ser 235/236)	2211	Cell Signaling Technology
RPS6	2217	Cell Signaling Technology
P-TSC2 (Ser 1387)	5584	Cell Signaling Technology
TSC2	4308	Cell Signaling Technology
P-AKT (Ser 473)	4060	Cell Signaling Technology
AKT	4691	Cell Signaling Technology
P-p44/42 MAPK (Erk1/2)	4376	Cell Signaling Technology
(The 202 / Tyr 204)		
P44/42 MAPK (Erk1/2)	9102	Cell Signaling Technology
SCP2	HPA027101	Sigma
sXBP1	Sc-7160	Santa Cruz Biotechnology
BMAL1	Preitner et al., 2002	
PER2	Brown et al., 2005	
NPC1	Ab36983	Abcam

Taqman probes used for real-time PCR (Life technologies)

Gene	Probe reference
<i>Gapdh</i>	Mm 99999915_g1
<i>Eif4e</i>	Mm 00725633_s1
<i>Eif4g1</i>	Mm 00524099_m1
<i>Eif4a2</i>	Mm 00778003_s1
<i>Eif4ebp3</i>	Mm 01406408_m1
<i>Fasn</i>	Mm00662319_m1
<i>Lpl</i>	Mm00434770_m1
<i>Ppara</i>	Mm00440939_m1
<i>Scd1</i>	Mm00772290_m1

Sequences of the primers used for real-time PCR

Gene	Forward primer	Reverse primer
<i>Gapdh</i>	CATGGCCTTCCGTGTTCCCTA	CCTGCTCTTCCGTGTTCCCTA
<i>Scp2</i>	GGCCTTCTTTCAAGGGAAAC	CTAAGCCCTGACGACGAGAC
<i>Bip</i>	GAAAGGATGGTTAATGATGCTGAG	GTCTTCAATGTCCGCATCCTG
<i>Chop</i>	CATACACCACCACACCTGAAAG	CCGTTTCCTAGTTCTTCCTTGC
<i>sXbp1</i>	CTGAGTCCGAATCAGGTGCAG	TGGCCGGGTCTGCTGAGTCCG
<i>Cyp4a14</i>	TCTCTGGCTTTTCTGTACTTTGCTT	CAGAAAGATGAGATGACAGGACACA
<i>Acox1</i>	GGATGGTAGTCCGGAGAACA	AGTCTGGATCGTTCAGAATCAAG
<i>Cd36</i>	GATGACGTGGCAAAGAACAG	TCCTCGGGGTCCTGAGTTAT
<i>Hmgcr</i>	AGCTTGCCCGAATTGTATGTG	TCTGTTGTGAACCATGTGACTTC
<i>Srebp1c</i>	GGAGCCATGGATTGCACATT	GGCCCGGGAAGTCACTGT
<i>Srebp2</i>	GCGTTCTGGAGACCATGGA	ACAAAGTTGCTCTGAAAACAAATCA
<i>Npc1</i>	TGAATGCGGTCTCCTTGGTC	CTCACTGGCTTCCTTTGGTA
<i>Bmal1</i>	GCATTCTTGATCCTTCTTTGGT	CCAAGAAGGTATGGACACAGACAAA
<i>Cry1</i>	CTGGCGTGGAAGTCATCGT	CTGTCCGCCATTGAGTTCTATG
<i>Dbp</i>	CGTGGAGGTGCTTAATGACCTTT	CATGGCCTGGAATGCTTGA
<i>Per2</i>	ATGCTCGCCATCCACAAGA	GCGGAATCGAATGGGAGAAT

III. Metabolic defects in *Bmal1* knockout mice

Deficiency in the molecular circadian clock has been shown to be involved in metabolic syndromes and obesity. Indeed, several studies present evidence of impaired glucose and insulin metabolism in various clock deficient mice models^{66, 313-315}. Some characteristics observed in circadian clock genes deficient mice, such as glucose intolerance defect and hyperglycemia were also observed in obesity mice models as *Ob/Ob* and *Db/Db* mice³¹⁶. Feeding is also an important parameter involved in metabolic defects. Indeed, feeding/fasting cycle constitutes an external cue involved in the synchronization of peripheral organs like the liver. Mice challenged with a high-fat diet exhibit obesity characteristics, but it has been shown that their molecular circadian clock was also disrupted because of changes in feeding behaviour³¹⁷. However, mice fed a high-fat diet in restricted conditions exhibit a normal circadian clock function without presented metabolic disorders³¹⁸.

To investigate involvement of the circadian clock in metabolic disorders, we used two approaches. First, obesity has been induced by the *Ob* mutation in the gene encoding for leptin. Second, it was induced by a high-fat challenge in *Bmal1* knockout mice.

A. Metabolic defects in genetically obese *Bmal1* KO mice

(1) *Bmal1* KO mice harboring the *Ob* mutation exhibit premature death.

We generated a new mice line that is deficient in a functional circadian clock and obese. To this end we used *Bmal1* KO and *Ob* mice that carry a mutation in the gene encoding for leptin (*Ob* mutation). Because both *Bmal1* KO and *Ob/Ob* mice are infertile^{319, 320}, we crossed mice

expressing both knockout and mutation at the heterozygote state: $Bmal1^{KO/WT} Ob^{Ob/WT}$ and the littermates were used as control in this study. As shown in figure 16A, the proportions of each of the 9 genotypes obtained of the born pups are in accordance with the theoretical Mendelian proportions. This first result means that this crossing did not generate embryonic lethality. However, we did observe some dead mice after birth. It appeared that these deaths were genotype-related, as we estimated 45% of $Bmal1^{KO/KO} Ob^{Ob/WT}$ and 60% of $Bmal1^{KO/KO} Ob^{Ob/Ob}$ mice died (figure 16B) between 4 and 5 weeks after birth (figure 16C).

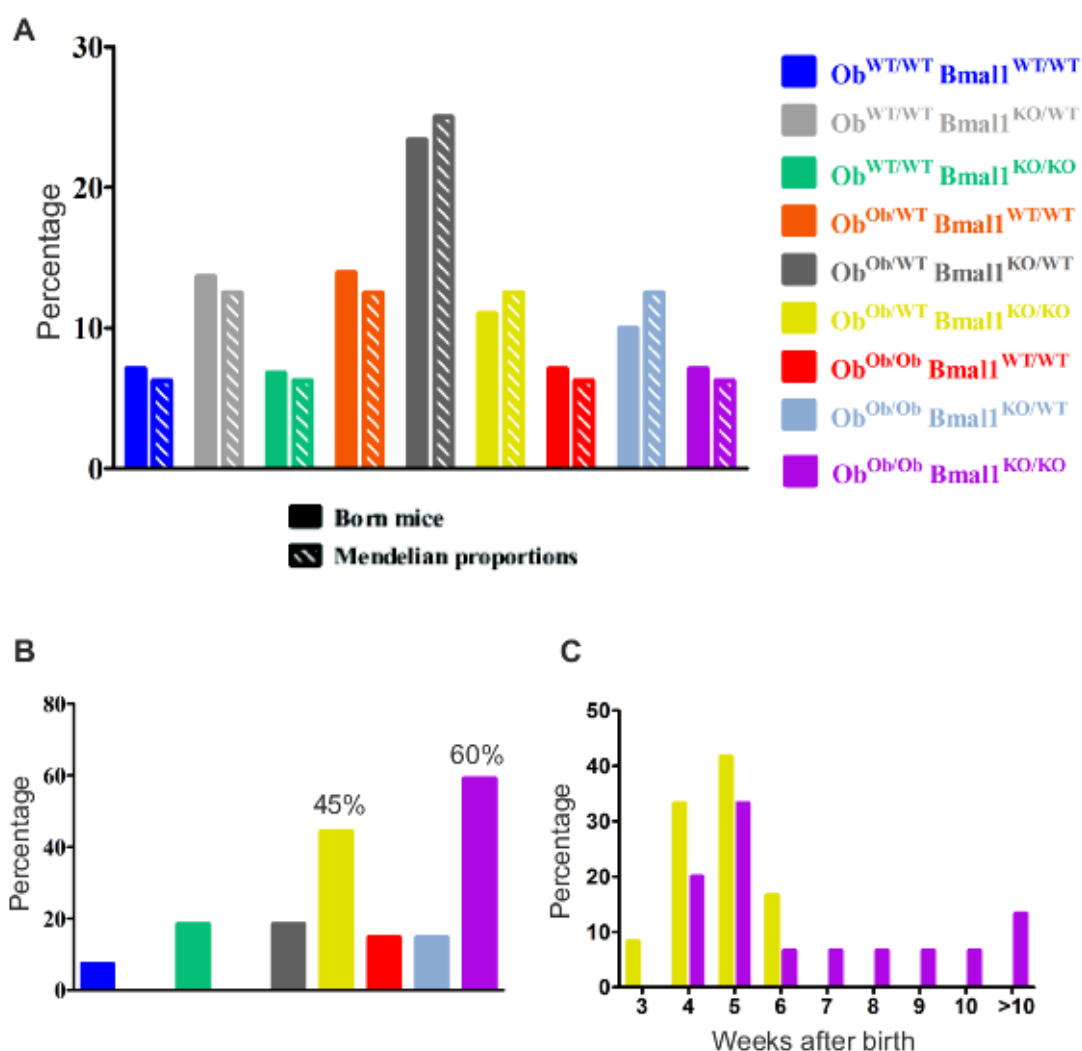


Figure 16: Obese *Bmal1* knockout mice died prematurely.

A. Proportions of each genotype of born mice (filled bars) compared to the theoretical Mendelian proportions (streaked bars). B. Proportions of death for each genotype. C. Repartition of dead $Bmal1^{KO/KO} Ob^{Ob/WT}$ and $Bmal1^{KO/KO} Ob^{Ob/Ob}$ mice depending on their age.

During this study we performed experiments on male mice belonging to the following four genotypes: *Bmal1*^{WT/WT} *Ob*^{WT/WT}, *Bmal1*^{KO/KO} *Ob*^{WT/WT}, *Bmal1*^{WT/WT} *Ob*^{Ob/Ob} and *Bmal1*^{KO/KO} *Ob*^{Ob/Ob} respectively called WT (wild-type), KO (*Bmal1* KO), Ob (obese) and ObKO (Obese *Bmal1* KO) mice.

(2) ObKO mice exhibit an obese phenotype

The first step of this study consisted in the characterization of this new mice line. The mice have been weighted every week at ZT3 from the weaning to 16 weeks. As shown in the figure 17A, while the Ob mice exhibit a rapid weight gain, the ObKO mice body weight curve appeared similar to WT and KO mice. The pictures of the different mice (figure 17B) showed that WT and KO mice were not recognizable without molecular genotyping. However, Ob and ObKO mice exhibit clear phenotyping marks. To understand why the ObKO mice appear “kind of obese” without exhibiting a high weight gain, we measured some parameters. At 6 weeks and at ZT3, the mice underwent body weight, size measurements and an analysis of the body composition *via* EchoMRI technology. The first parameter, the body mass index (figure 17C) resulted in part of these measurements showed that WT and KO mice have a similar body mass index of about 2.7 Kg/m² while the ObKO mice exhibit an intermediate body mass index (3.5 Kg/m²) between the WT/KO mice and the Ob mice (4.2 Kg/m²). The differences in body mass index are also due to mice size variations between genotypes. Indeed, KO and ObKO mice exhibit a smaller size than WT and Ob mice (data not shown) reflecting thus growth defects. Concerning the fat content analysis (figure 17D), we showed a clear distinction between the obese and non-obese mice as WT and KO mice present 8.7 and 9.6% of fat while the fat content in Ob and ObKO mice is respectively 38.7 and 34.8%. The last argument allowing us to assimilate the ObKO mice to an obese phenotype is the weight of

different organs as liver or white adipose tissue. Indeed, in WT and KO mice, liver weight represented from 3 to 4% of the total mice weight while it represented a significant higher percentage in Ob and ObKO mice (figure 17F). The same observation was done concerning the proportion of white adipose tissue as it represented less than 2% of the body weight in WT and KO mice while the proportion of this tissue reached 8.8 and 6.7% of the whole mouse weight in Ob and ObKO mice respectively.

(3) Glucose homeostasis is impaired in ObKO mice

Ob/Ob mice are described as hyperglycemic and insulin resistant, that is why they are frequently used as model for studies on diabetes. Recent evidences shown that pancreatic molecular circadian clock coordinates insulin release. Deficient molecular clock is sufficient to generate diabetes mellitus³¹³. We hypothesized here that mice harboring both *Ob* mutation and molecular clock deficiency could undergo severe diabetes which may explain the premature death of ObKO mice previously described (figure 16).

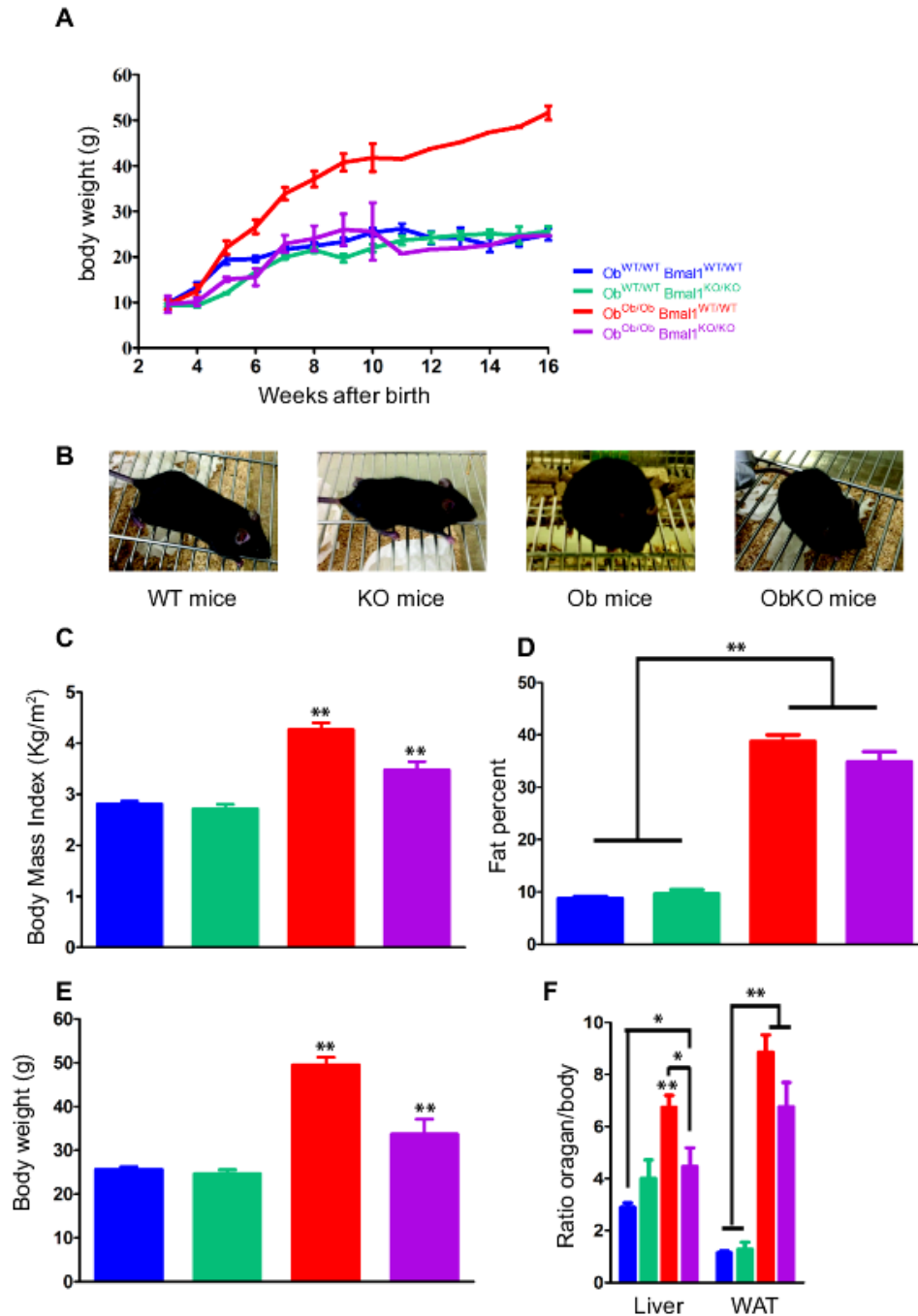


Figure 17: ObKO mice exhibit obese phenotype.

A. Body weight curves corresponding to WT (blue), KO (green), Ob (red) and ObKO (purple) mice. Each mouse is weighted from 3 to 16 weeks after birth at ZT6. B. Representative pictures of mice of interest. The mice are all 12 week-old. C. Body Mass Index of each 6 week-old mice of interest. D. Proportion of fat content for each mice of interest. The fat content is given by the EchoMRI analyser on 6 week-old fed mice at ZT3. E. Body weight of fed mice before the sacrifice at ZT12. F. Proportion of organs. Liver and white adipose tissues (WAT) were weighted after dissection. Data are Mean \pm SEM obtained from 7 to 10 independent animals for each genotype. The *Zeitgeber* Times (ZT) are defined as followed: ZT0 lights on; ZT12: lights off. Statistical analysis were done with the *t*-test (** $P < 0.01$ and * $P < 0.05$ compared to other genotypes).

We first measured the glycemia on the 10 week-old mice after 15 hour-starvation (ZT3) and then after 6 hour-refeeding (ZT9). In WT mice, the glycemia after starvation is 6 mmol/l and after refeeding the glycemia increased to reach 10.3 mmol/l (figure 18A). The KO mice exhibit a higher glycemia after starvation (8.3 mmol/l) than WT mice, but the glycemia did not increase as much as we could expect after the refeeding period (9.9 mmol/l). KO mice are thus insulin-sensitive. It may thus suggest a defect in enzymes, such as amylases, catalyzing glucose release from the food. The food intake, leading to activation of insulin-related signaling pathways, allows the glucose entry into cells through different glucose transporters. Indeed, glucose entry in hepatocytes and pancreatic β -islets is mediated by GLUT2³²¹ while GLUT4 is responsible for glucose internalization in adipose tissue and skeletal muscles³²². Ob and ObKO mice exhibit starved glycemia a little higher (respectively 7.2 and 7.7 mmol/l) compared to WT mice, but glycemia after refeeding reaches a very high level (respectively 15.7 and 12 mmol/l). In these mice, the post-prandial glycemia may reflect impairment in insulin-activated pathways leading defects in glucose clearance.

Glucose and insulin concentrations measurements in the serum at ZT12 on 13 week-old mice (figure 18 B and C) showed that WT and KO mice exhibit the same behavior: their serum glucose concentration at this time point was 12 mmol/l and their serum insulin concentration was about 2 μ g/l. In Ob mice the glucose concentration in the serum was the double (22 mmol/l) and the serum insulin concentration was more than 6 times higher than the WT and KO mice (12.9 μ g/l). These results are in accordance with hyperglycemic and hyperinsulinemic phenotype of *Ob/Ob* mice. Leptin deficient mice eat much more which can explain the hyperglycemia and insulin resistance. The hyperinsulinemia is the result of insulin resistance. ObKO mice exhibit also a high serum glucose (18 mmol/l), certainly due to high food intake. However, their serum insulin concentration was quite low (4.4 μ g/l) oppositely to Ob mice. This result can be explained by low pancreatic insulin secretion.

The glycogen accumulation in the liver reflects the glucose storage. GSK (Glycogen Synthase Kinase) 3 is a key enzyme involved in glucose conversion to glycogen. The glycogen accumulates rhythmically in the liver in WT mice, the lower accumulation corresponding time point occurring at ZT12. Moreover, this rhythm seems to be dependent on the molecular clock as it is impaired in *Bmal1* KO mice liver (figure 18D, left panel). In addition, *Bmal1* KO mice exhibit a lower glycogen accumulation (almost the half) throughout the entire day compared to WT mice (figure 18E, right panel). We extracted the glycogen from liver samples of the 13 week-old mice sacrificed at ZT12 (figure 18F). In WT mice liver, the glycogen concentration was 19 $\mu\text{g}/\text{mg}$ of tissue. The glycogen proportion in KO mice liver (39.6 $\mu\text{g}/\text{mg}$ of tissue) doubled compared to the one in WT mice liver. The glycogen accumulation in Ob mice liver appeared to be intermediate (28.9 $\mu\text{g}/\text{mg}$ of tissue) compared to the WT and KO mice liver. ObKO mice exhibit a liver glycogen accumulation 1.5 fold higher than in obese mice liver (45.2 $\mu\text{g}/\text{mg}$ of tissue). High glycogen accumulation through over-activation of GSK3 has been linked to insulin resistance. It was thus surprising to observe high glycogen accumulation in ObKO mice while they are apparently insulin-sensitive. Considering the fact that ZT12 corresponds to the highest glycogen accumulation in *Bmal1* KO mice compared to WT, we may suppose that at ZT20 or ZT0, glycogen accumulation would be still the same than at ZT12 in ObKO mice while it would be much higher in Ob mice.

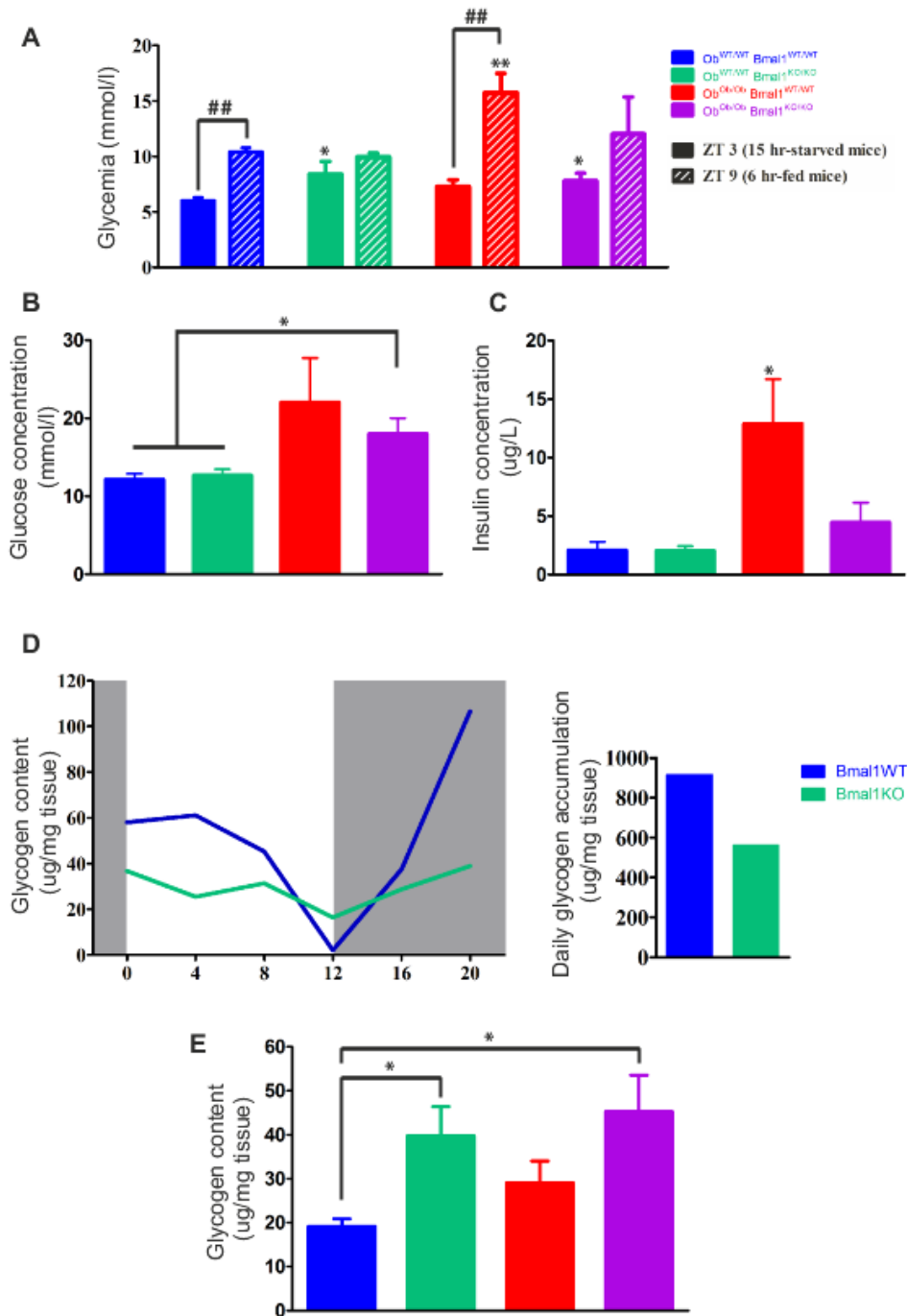


Figure 18: The glucose homeostasis is impaired in obese knockout mice.

A. Glycemia measurements after 15 hour starvation (filled bars) and after 6 hour-refeeding (streaked bars) on 10 week-old mice. B and C. Serum glucose (B) and insulin (C) measurements performed on 13 week-old mice at ZT12. D. Temporal glycogen accumulation in *Bmal1* wild-type (blue) and knockout (green) mice liver (left panel) and whole day glycogen accumulation corresponding(right panel). E. Glycogen accumulation in the liver of 13 week-old mice at ZT12. Data are Mean \pm SEM obtained from 6 to 8 independent animals for each genotype of interest. The *Zeitgeber* Times (ZT) are defined as followed: ZT0 lights on; ZT12: lights off. Statistical analysis were done with the *t*-test (** $P < 0.01$ and * $P < 0.05$ compared to other genotypes; ## $P < 0.01$ comparison between starved and refeed conditions).

(4) ObKO mice exhibit an impaired glucose clearance but are insulin sensitive.

We performed both glucose and insulin tolerance tests on 11 and 12 week-old mice respectively. We choose to perform these experiments at ZT3 because it appeared to be the most responding time-point³²³.

After glucose injection, all the mice exhibit an increased glycemia (figure 19A, right panel). However, in WT mice, after 15 min the glycemia stabilizes and starts to decrease after 30 min to reach the basal glycemic level at 90 minutes after the glucose injection. In KO, Ob and ObKO mice, the glycemia continues to increase until 30 minutes after the injection. The curve slopes (figure 19A, left panel) reflect the capacity of glucose elimination from the blood called glucose clearance. We can observe that KO and ObKO mice exhibit faster clearance than wild-type mice. Ob mice can be qualified as glucose resistant because of their lower glucose clearance capacity.

Concerning insulin tolerance tests, we show here (figure 19B) that all the mice exhibit a decreased glycemia after insulin injection except the Ob mice which revealed insulin intolerance or resistance. We can also observe that KO mice are highly insulin sensitive as the glycemia did not reach the basal level even after 180 min. In ObKO mice, we can observe a similar effect even the basal glycemia was higher.

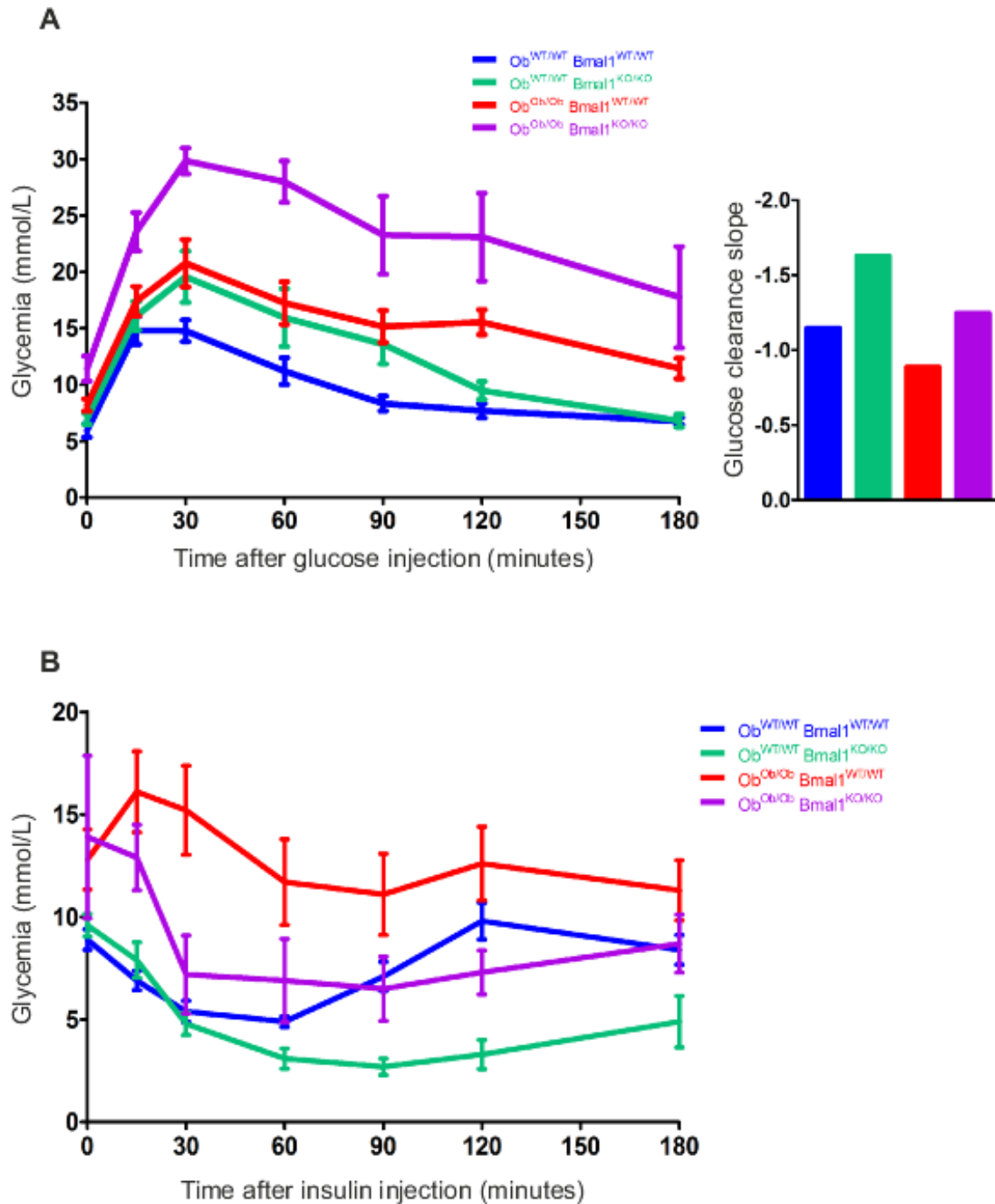


Figure 19: Glucose and insulin tolerance tests.

A. Glucose tolerance test realized on 11 week-old mice at ZT3 after 15 hour-starvation (left panel) and the clearance slopes (right panel) associated. The mice underwent intra-peritoneal injection of glucose (1g/Kg of mice). B. Insulin tolerance test realized on 12 week-old mice at ZT3. The mice underwent intra-peritoneal injection of insulin (1UI/Kg of mice). Data are Mean \pm SEM obtained from 6 to 10 independent animals for each genotype of interest.

(5) ObKO mice exhibit low hepatosteatosis but high circulating triglycerides concentration.

Liver steatosis consisted in an excess of fatty acids mostly as triglycerides accumulation³²⁴. Steatosis has been shown to be related to obesity and insulin resistance. *Ob/Ob* mice have been described as exhibiting extended adipose tissue and liver steatosis³²⁵. We performed liver slices of each of our mice of interest (figure 20A-D). The slices treated with HE coloration have been analysed by a histopathologist who did not know the genotype of the mice. In WT (figure 20A) and KO (figure 20B) mice liver, no steatosis has been noticed while *Ob* mice liver (figure 20C) showed steatosis estimated in 90-100% of hepatocytes. In *ObKO* mice (figure 20D), liver steatosis has also been found but with a lower degree as only 20 to 30% of hepatocytes exhibited triglycerides droplets. This result is consistent with the lower insulin resistance observed in obese knockout mice previously described. We also looked at the circulating triglycerides in the serum (figure 20E). In 13 week-old mice, at ZT12, circulating triglycerides levels are significantly higher in KO and *ObKO* mice as they are respectively 1.8 and 2 fold higher than in WT mice.

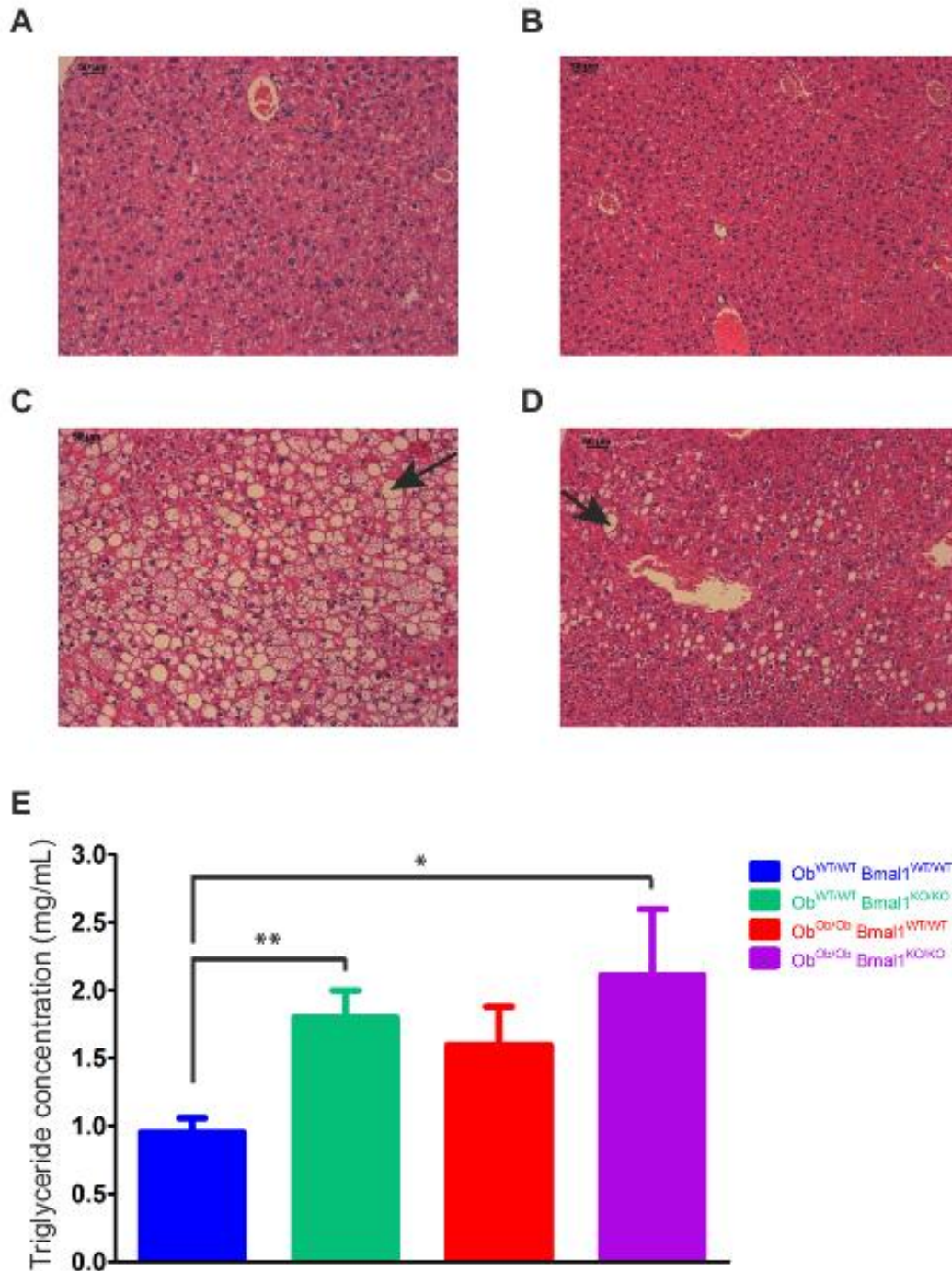


Figure 20: Triglyceride homeostasis in obese *Bmal1* knockout mice.

A-D. Representative histology of WT (A), KO (B), Ob (C) and ObKO (D) mice liver. Liver slices have been realized from 15 week-old mice. The slices were treated with Hematoxylin/Eosin coloration. The scale bars are indicated on the pictures (50 μ m) and the objective used is 10X. The arrows showed lipid droplets. E. Serum triglyceride concentration on 13 week-old mice at ZT12. Data are Mean \pm SEM obtained from 6 independent animals for each genotype of interest. The *Zeitgeber* Times (ZT) are defined as followed: ZT0 lights on; ZT12: lights off. Statistical analysis were done with the *t*-test (** $P < 0.01$; * $P < 0.05$).

B. Metabolic defects in diet-induced obese *Bmal1* KO mice

In order to study the evolution of obesity induced by the food in molecular circadian clock deficient mice, we fed 8 week-old *Bmal1* KO and WT mice with high-fat and control diet during 12 weeks. The mice are weight before starting the experimentation and then every week until the sacrifice time. From the 4th week of the experiment, mice underwent different *in vivo* measurements as analysis of the body composition *via* EchoMRI technology, starved and refeed glycemia measurements, glucose and insulin tolerance tests.

(1) *Bmal1* KO mice fed with high-fat diet become obese prematurely

It appeared that the mice fed with control diet, whatever their genotype, exhibit similar gain of weight (figure 21A), body mass index (figure 21B), but the fat content of *Bmal1* knockout mice is a little higher than wild-type mice during the first weeks of the experiment to become similar at the end (figure 21C). While no difference in the organs weight ratio was observe at the sacrifice time (figure 21E), it appeared however that the *Bmal1* KO mice fed with control diet exhibit a lighter body weight compared to the wild-type (figure 21D). Concerning the mice fed with high-fat diet, more differences were observed. Indeed, the weight gain (figure 21A), the increased of the body mass index (figure 21B) and the proportion of fat (figure 21C) appeared faster in *Bmal1* knockout mice than in wild-type mice. However, at the end of the experiment, they reach the same level for each of these characteristics. We can notice that liver/body ratio appeared lower for WT mice fed with high-fat diet compared to control diet fed WT mice (figure 21E, right panel), but liver mass is actually higher. This can be explained by the difference of their body weight measured at the sacrifice time (figure 21D).

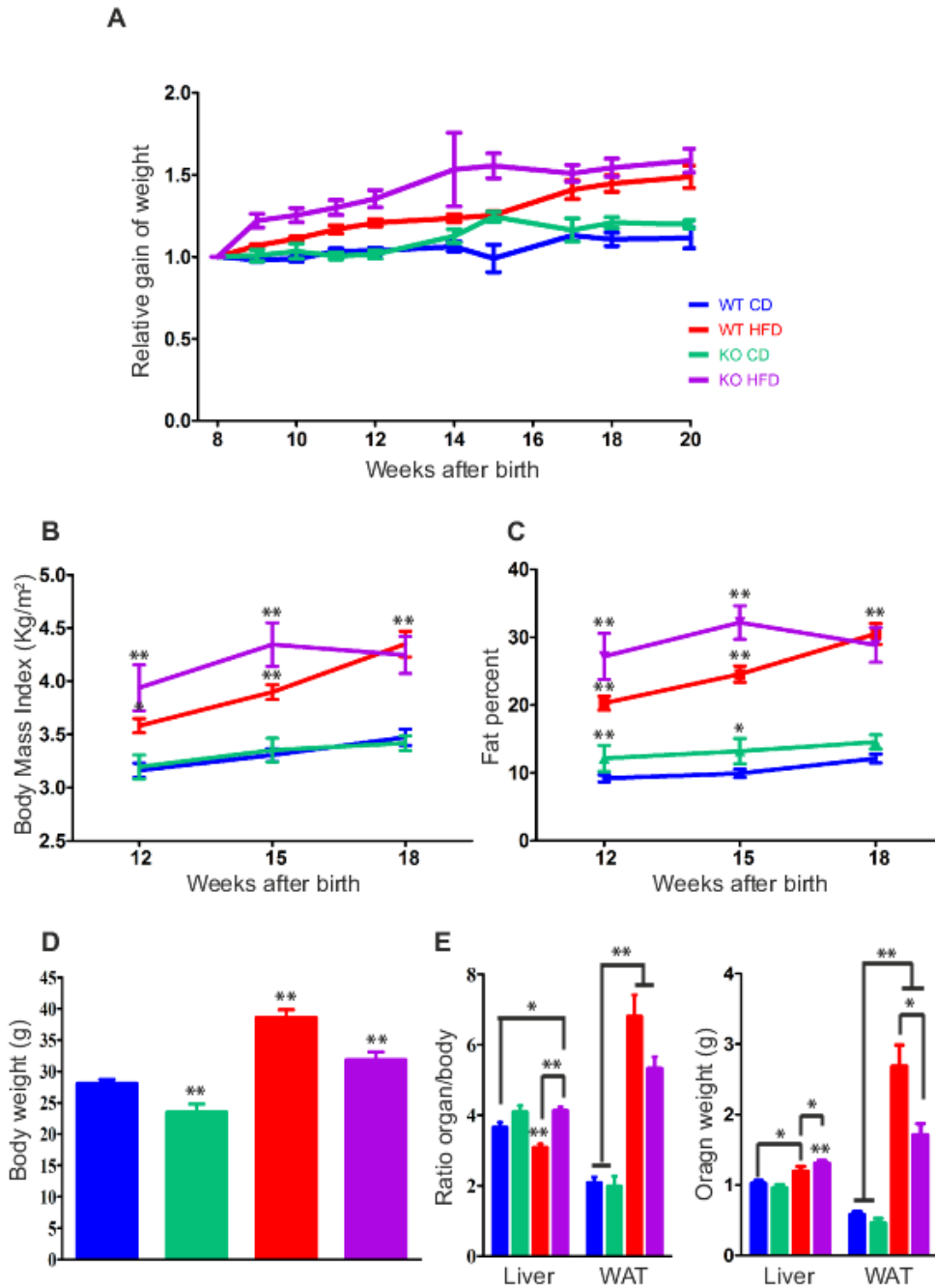


Figure 21: *Bmal1* knockout mice present obese phenotype.

A. Relative gain of weight of each group of mice. Each mouse is weighted from 8 (beginning of the experiment) to 20 weeks after birth at ZT6. B. Evolution of the Body Mass Index of the mice. D. Proportion of fat content for each group of mice. The fat content is given by the EchoMRI analyser on fed mice at ZT3. D. Body weight of fed mice before the sacrifice at ZT12. E. Proportion of organs (right panel) and organs weight (left panel). Liver and white adipose tissues (WAT) were weighted after dissection. Data are Mean \pm SEM obtained from 6 to 10 independent animals for each condition. The *Zeitgeber* Times (ZT) are defined as followed: ZT0 lights on; ZT12: lights off. Statistical analysis were done with the *t*-test (** $P < 0.01$; * $P < 0.05$).

WT mice fed with high-fat regimen become obese but the mice were not fed long enough to observe a significant increase in liver weight ratio.

(2) Glucose homeostasis is impaired in diet-induced obese mice

Before starting the feeding experiment, we measured the glycemia on the 8 week-old mice after 15 hour-starvation (ZT3) and then after 6 hour-refeeding (ZT9). The results obtained are in accordance with the ones observed on wild-type and knockout mice coming from the *Ob.Bmal1* mice line. Indeed, in wild-type mice, the glycemia after starvation is 5 mmol/l and after refeeding the glycemia increased to reach 10.5 mmol/l (figure 22A). The knockout mice exhibit a higher glycemia after starvation (6.8 mmol/l) than wild-type mice. But the glycemia did not increase as much as we could expect after the refeeding period (9.3 mmol/l). During the experiment (figure 22B) the glycemia after starvation in control diet fed mice did not change. However, after refeeding, their glycemia tended to decrease at the end of the experiment especially in wild-type mice. Concerning the high-fat fed mice, *Bmal1* knockout mice exhibit higher glycemia after starvation than the wild-type, but at the end of the experiment, *Bmal1* knockout mice exhibit a decreased glycemia to present the same glycemia than the wild-type mice. The same observation was done on glycemia measured after refeeding.

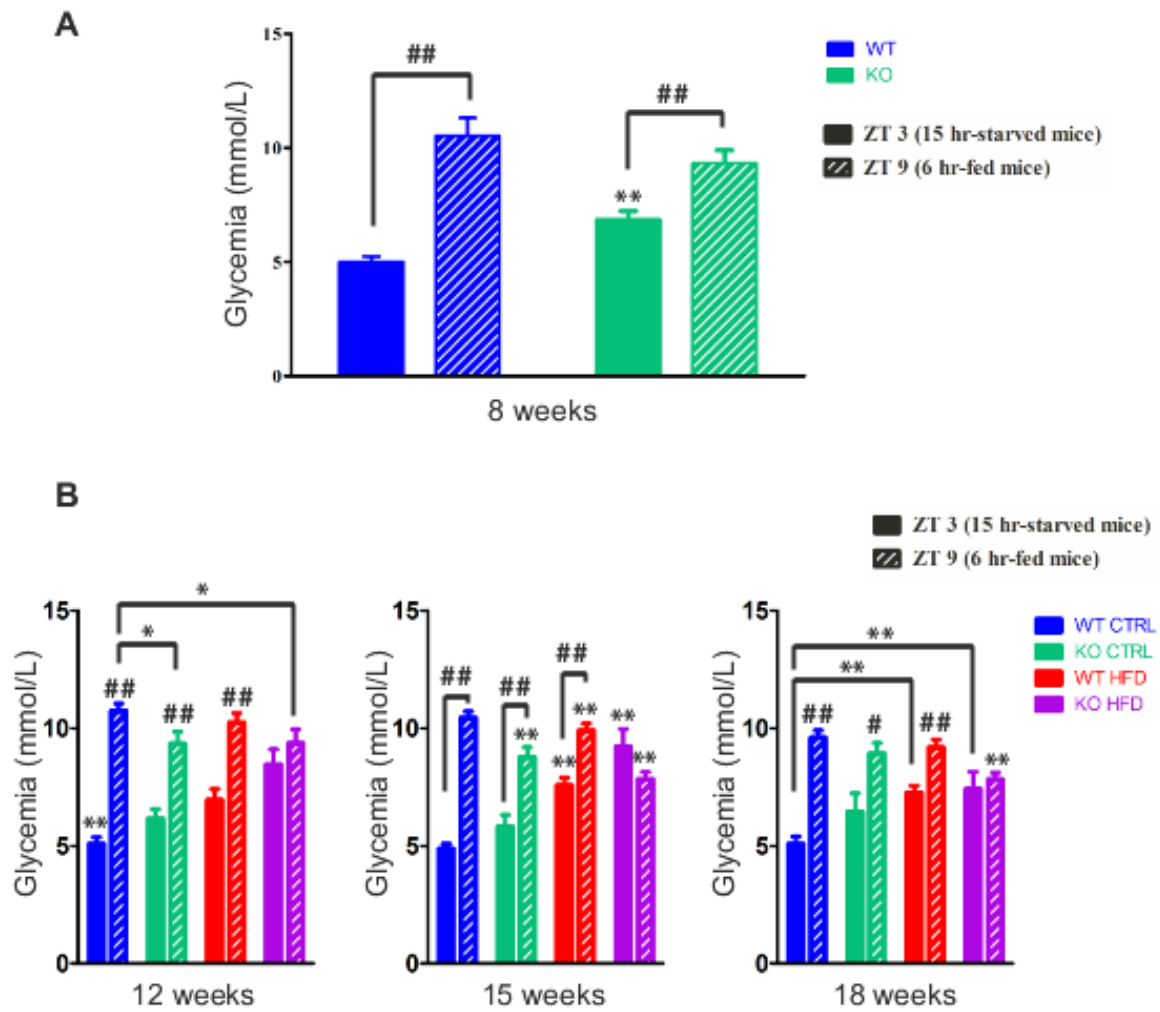


Figure 22: Impairment of glucose homeostasis in mice fed with high-fat diet.

A. B. Glycemia measurements after 15 hour starvation (filled bars or lines) and after 6 hour-refeeding (streaked bars or dashed lines) on 8 week-old wild-type and *Bmal1* knockout mice before the beginning of the feeding experiment(A) and every 3 weeks during the experiment (B). Data are Mean \pm SEM obtained from 6 to 8 independent animals for each genotype of interest. The *Zeitgeber* Times (ZT) are defined as followed: ZT0 lights on; ZT12: lights off. Statistical analysis were done with the *t*-test (** $P < 0.01$; * $P < 0.05$ compared to other genotypes; ### $P < 0.01$; # $P < 0.05$ comparison between starved and refed conditions).

(3) *Bmal1* KO liver exhibit less steatosis

We performed liver slices of mice in each condition (figure 23). Both control diet fed wild-type (figure 23A) and *Bmal1* knockout mice (figure 23B) present normal liver without

steatosis. When wild-type mice are fed with high-fat diet during 12 weeks, we can notice the presence of lipid droplets in hepatocytes. This steatosis is however very low compared to obese mice previously described (figure 20C). In contrast, high-fat diet fed *Bmal1* knockout mice liver exhibit much less lipid droplets than the high-fat diet mice liver. In this condition, *Bmal1* deletion prevents triglycerides accumulation in liver leading to hepatosteatosis.

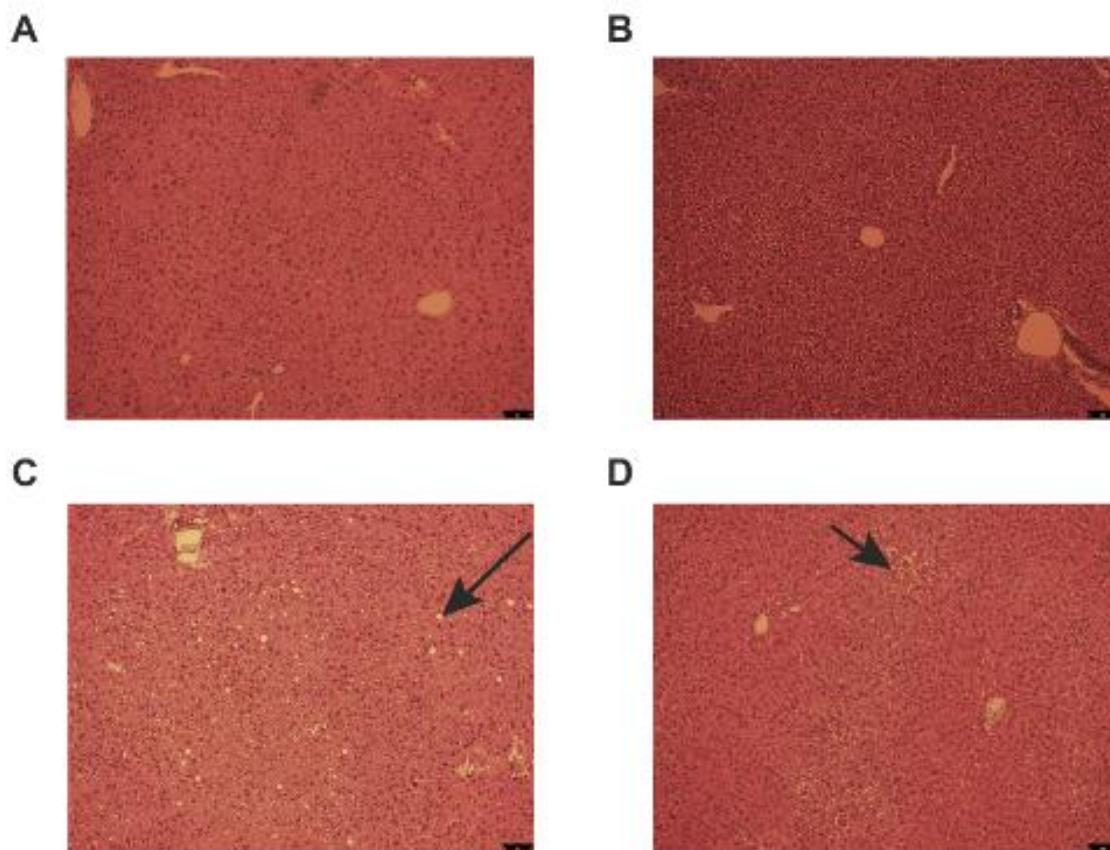


Figure 23: Triglyceride homeostasis in obese *Bmal1* knockout mice.

A-D. Representative histology of WT CD (A), KO CD (B), WT HFD (C) and KO HFD (D) mice liver. Liver slices have been realized from 21 week-old mice. The slices were treated with Hematoxylin/Eosin coloration. The scale bars are indicated on the pictures (50 μ m) and the objective used is 10X. The arrows showed lipid droplets.

(4) Delayed glucose clearance in high-fat diet fed mice

During the feeding experiment, we followed the evolution of the response of the mice to glucose injection. It appeared that the way organisms manage the excess of circulating glucose did not change so much weeks after weeks (figure 24, left panels). In addition, it is clear that we have two different groups depending on the feeding. Indeed, high-fat diet mice exhibit a delayed glucose clearance as it started 30 to 60 minutes after the injection. However, the slopes reflecting glucose clearance showed increased glucose intolerance in wild-type mice fed with high fat diet (figure 24, right panels) in function of the time. Indeed, while the glucose clearance do not change in control diet fed mice and in high fat diet *Bmal1* knockout fed mice, the speed of glucose elimination from the blood is low at 13 weeks and became even lower.

Concerning the insulin tolerance test, we show here (figure 25) that all the mice exhibit a decreased glycemia after insulin injection. However the wild-type mice fed with high-fat diet exhibit less important insulin sensitivity. While they were fed with high-fat diet, *Bmal1* knockout mice remained still very sensitive to insulin even it was clear that this sensitivity appeared less important than in mice fed with control diet especially during the first weeks of the experiment.

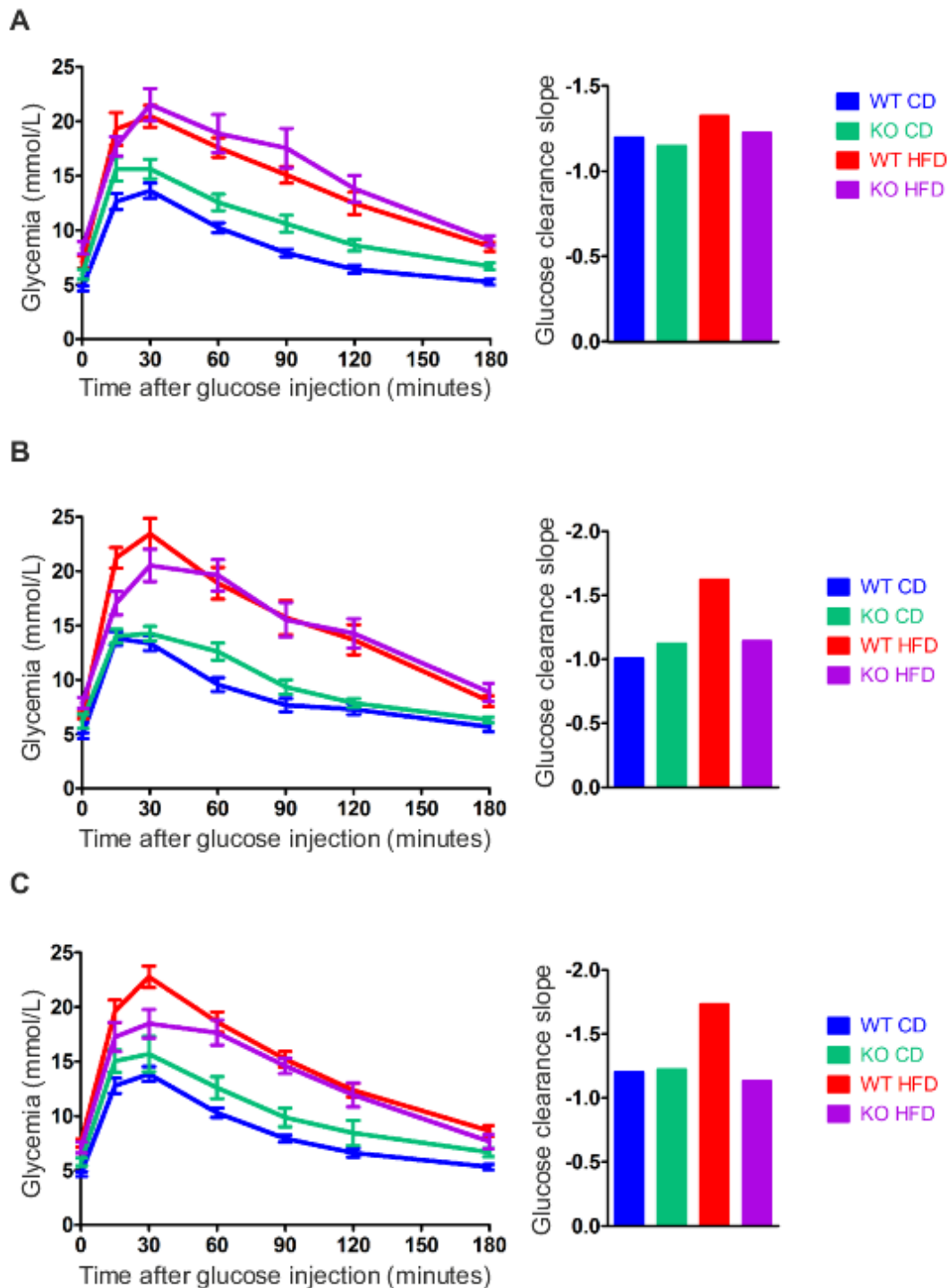


Figure 24: Evolution of the glucose clearance.

A-C Glucose tolerance tests performed on 13 (A), 16 (B) and 19 (C) week-old mice at ZT3 after 15 hour-starvation. The mice underwent intra-peritoneal injection of glucose (1g/Kg of mice). Right panels correspond to the clearance slopes for each experiment. Data are Mean \pm SEM obtained from 6 to 10 independent animals for each genotype of interest. The *Zeitgeber* Times (ZT) are defined as followed: ZT0 lights on; ZT12: lights off.

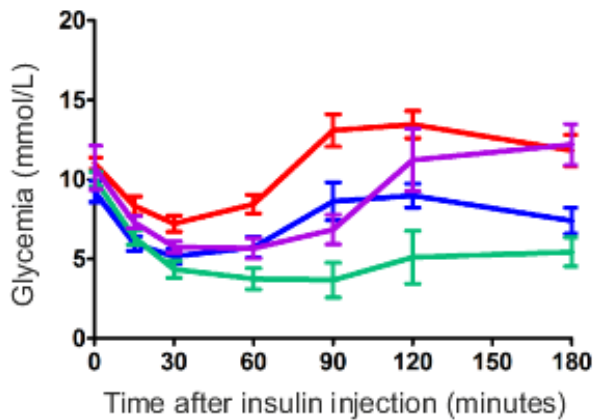
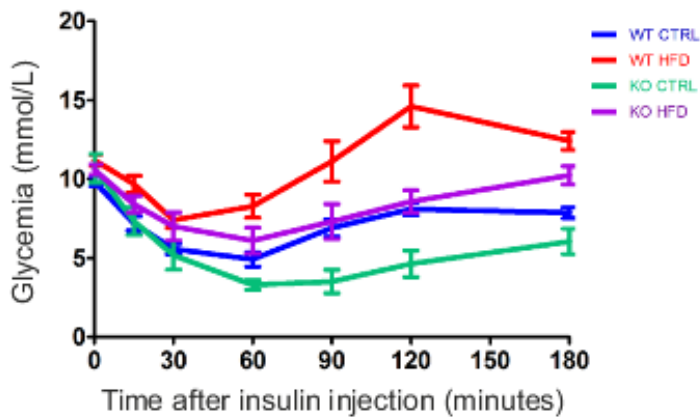
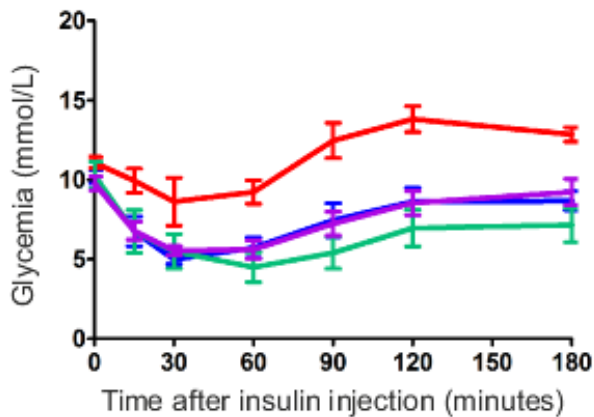
A**B****C**

Figure 25: Evolution of the insulin sensitivity.

A-C Insulin tolerance tests performed on 14 (A), 17 (B) and 20 (C) week-old mice at ZT3. The mice underwent intra-peritoneal injection of insulin (0.5UI/Kg of mice). Data are Mean \pm SEM obtained from 6 to 10 independent animals for each genotype of interest. The *Zeitgeber* Times (ZT) are defined as followed: ZT0 lights on; ZT12: lights off.

DISCUSSION

Circadian rhythms involvement in metabolism consists in activation of the right signaling pathway at the right time to ensure an adapted physiology. To study metabolic defects due to misalignments of circadian clock, we used both genetic and diet-induced obesity models as previously described.

I. Premature death for *Bmal1* KO mice harboring *Ob* mutation

As both *Ob/Ob* and *Bmal1* KO mice are infertile^{319, 320}, it is thus necessary to cross heterozygotes to generate these mice. For both mice lines, no embryonic or premature death has been reported. It was thus surprising to observe 45% and 60% of dead *Ob*^{Ob/+} *Bmal1*^{KO/KO} and *Ob*^{Ob/Ob} *Bmal1*^{KO/KO} mice respectively. *Ob* mutation in one allele is thus sufficient to cause death *Bmal1* deficient mice. Experiments on *Ob*^{Ob/+} *Bmal1*^{KO/KO} mice did not show any differences with *Bmal1* KO mice concerning the glucose homeostasis, and glucose and insulin tolerance. However, Leptin deficiency in one allele in *Bmal1* KO mice leads to increasing fat percentage (data not shown). This is in accordance with intermediate obese phenotype already described in *Ob*^{Ob/+} mice³²⁶. It seems thus that BMAL1 and Leptin may directly or indirectly interact in a critical physiological process. In addition, most of these deaths occurs during a particular 2-3 weeks period after weaning but after this critical period, obese knockout mice do not exhibit significant mortality until 13 weeks after birth, age of the sacrifices. We thus have no information concerning their ageing.

II. Involvement in bone metabolism

In our experiments, to calculate the body mass index of each mice, we measured their size. Wild-type and obese mice measured 8.5 and 8.3 cm respectively while knockout and obese knockout mice exhibit significant smaller size (8.1 and 7.6 cm respectively).

Recently, circadian clock³²⁷ and leptin³²⁸ have been shown to be involved in bone metabolism at different levels. Indeed, synchronized by glucocorticoids releasing, the clock resided in osteoclasts contributes to circadian expression of osteoclast-related genes³²⁷. In addition, osteoblasts number and activity are increased by leptin through peripheral pathways³²⁸. The disruption of circadian clock through *Bmal1* deletion associated with leptin defect created smaller size of the mice revealing their importance in bone metabolism.

III. Food intake consequences

During our experiments, we did not measure food intake. However, leptin defect leads to increasing food intake especially during the light phase compared to wild-type mice. High-fat diet can also influence time and amount of food intake. Indeed, wild-type mice under high-fat regimen exhibit higher food intake during the light (about 20% of total food intake) phase compared to control animals³¹⁷. This abnormal feeding behaviour impacts on regulation of circadian clock as fasting/feeding cycles which are considered as a strong Zeitgeber. This leads to consequences at the metabolic level. Indeed, activation of SREBP1c in liver has been linked to feeding behaviour³²⁹. When fasting/feeding cycles are altered by disrupted light/dark cycles, clock genes deletion, leptin deficiency, or induced by high-fat regimen, this leads to abnormal activation of the lipogenesis through SREBP1c signaling pathway, leading as a

consequence to obesity. In addition, mice fed with high-fat diet only during the night exhibit restored circadian gene oscillations. They also exhibit alteration in fatty acid and glucose metabolisms preventing thus obesity and liver steatosis and glucose tolerance³¹⁸.

IV. Protective effect of *Bmal1* deletion in obesity

Insulin resistance, a consequence of T2D (Type 2 Diabetes), is characterized by high serum glucose and insulin levels due to high pancreatic insulin secretion. In addition, animal liver exhibits steatosis and high glycogen accumulation. We show here that genetic obese mice exhibit hyperglycemia, hyperinsulinemia, liver steatosis, glucose and insulin resistances. In contrast, while they exhibit an obese phenotype, genetic and diet-induced obese *Bmal1* KO mice present characteristics of insulin sensitivity such as low steatosis in liver and low insulin levels in the serum. It has been recently reported in *Bmal1* KO and *Clock*^{A19} mutant mice that pancreatic insulin secretion was impaired^{313, 323}. In these studies, the authors demonstrated that circadian clock is involved in both size and proliferation of pancreatic β islets. In addition, as islet insulin content does not vary between wild-type and *Clock*^{A19} mutant mice, the low pancreatic insulin secretion may thus be explained mainly by defects in size, proliferation and function (insulin exocytosis) of the endocrine part of pancreas. They also reported the same defect in pancreas-specific *Bmal1* KO mice which activity and feeding behaviour and body composition are not affected. *Clock*^{A19} mutant mice have been described as developing metabolic syndrome under high-fat diet³³⁰. As both mice models present the same defect in insulin secretion, it thus suggests that disruption of core clock in pancreas is sufficient to generate defect in insulin secretion independently to adipogenesis.

Interestingly, *Ob/Ob* mice which both *Lxr α* and *Lxr β* genes are deleted (LOKO mice)³³¹ present a similar phenotype than ObKO mice without exhibiting mortality. Indeed, these LOKO mice are clearly obese, but protected from hepatosteatosis. In addition, LOKO mice are insulin-sensitive, β cell expansion is impaired and *de novo* lipogenesis occurs especially in adipose tissue. Rhythmic LXR activation has been proposed²⁸². Indeed, rhythmic REV-ERB α accumulation in hepatocytes leads to rhythmic activation of SREBP pathway which thus rhythmically activates LXR pathway. As REV-ERB α expression is activated by CLOCK:BMAL1 heterodimer, the similar phenotypes observed in LOKO and obese *Bmal1* knockout mice may thus suggest circadian clock control of LXR pathway *via* REV-ERB α .

V. Involvement of mitochondrial metabolism in insulin sensitivity

Ob/Ob mice exhibit higher levels of plasma NEFA (Non Esterified Fatty Acids)³³². UCP (UnCoupling Protein) 2 is a mitochondrial protein involved in oxidative phosphorylation. Its activity has been shown to be increased by fatty acid³³³ and ROS (Reactive Oxygen Species) which are generated during oxidative phosphorylation³³⁴. UCP2 plays a role in insulin secretion in β -islets^{332, 335-337}. Several *in vivo* studies of the role of UCP2 in insulin secretion lead to controversial results^{335, 336}. However, the hypothesis of insulin secretion inhibition by UCP2 has been shown by UCP2 overexpression or inhibition in isolated pancreatic β -cells³³⁷. In addition to insulin secretion, UCP2 has also been reported to be involved in glucagon secretion from pancreatic α -islets³³⁸. Indeed, deletion of UCP2 in α -islets leads to impaired glucagon secretion during fasting.

Recently, β -islets specific *Bmal1* knockout mice exhibit high accumulation of ROS and as a consequence high UCP2 activity. *Nrf2* (*Nuclear factor erythroid 2-related factor 2*), a regulator of antioxidant, has been shown to be a direct target of *Bmal1*. In this model, its own expression and antioxidant *Nrf2*-induced expression are disrupted contributing in ROS accumulation³¹⁴. In addition, oxidative phosphorylation has been reported to be dependent on circadian clock³³⁹. Mitochondrial fatty acid oxidation exhibits a circadian oscillation in wild-type mice. This phenomenon has been shown to be dependent on clock gene in MEF (Mouse Embryonic Fibroblast) deleted of *Clock*, or *Bmal1* or *Cry1/2*. It appears thus that mitochondria and circadian clock play interconnected role in insulin resistance and as a consequence in type 2 diabetes.

CONCLUSION AND FURTHER WORK

During this doctoral work, we were interested in the influence of circadian clock on metabolism. We thus present evidences of circadian clock orchestrated activation of signaling pathways. Indeed, AMPK, PI3K/AKT, ERK pathways are rhythmically activated leading to rhythmic modulation of TORC1. We showed that TORC1 downstream targets, 4EBP1 and RPS6, exhibit also rhythmic phosphorylation leading to rhythmic translation initiation. The study of these mechanisms in circadian clock deficient mice (*Bmal1* and *Cry1/2* KO mice) led us to clearly link them to circadian core clock. As a consequence, we demonstrated major role of circadian clock in ribosome biogenesis which occurs mostly at the beginning of the dark phase when energy and nutrients are available in sufficient amount, which is during the night in rodents³⁴⁰.

We reported also that signaling pathways activation depends on circadian clock indirectly. Indeed, SCP2, a lipid transporter from the endoplasmic reticulum to the lipid rafts localized in plasma membrane, is rhythmically expressed in liver. SCP2 deficiency leads to defects in the activation of PI3K/AKT and ERK signaling pathways in mice liver. It may suggest thus that ribosome biogenesis could be also influenced by circadian clock controlled-lipid trafficking but this remains to be investigated. In addition, *Scp2* KO mice exhibit impairments in insulin, triglycerides and cholesterol concentration in serum. As these mice present a longer free running period, it is possible to envisage a shift in feeding behavior. As a consequence of *Scp2* deletion, PPAR α and SREBP target genes expressions are impaired in liver, reflecting thus its impacts in lipid homeostasis. Rhythmic PPAR α activation has been shown to be

dependent on the circadian clock *via* PAR bZip-dependent fatty acids release³⁰⁰. Interestingly, while PPAR α itself and its target genes are down regulated in PAR bZip KO mice liver, SCP2 deficiency leads to their up regulation. As both PAR bZip and SCP2 expressions are circadian clock controlled, it suggests that PPAR α pathway activation is restricted at a precise time controlled by circadian clock. SREBP signaling pathway is stimulated by insulin dependent PI3K/AKT – TORC1 pathways²¹⁵. We thus suppose that delayed circulating insulin in *Scp2* KO mice may lead to upregulation of PI3K/AKT – TORC1 pathways and *in fine* SREBP activation. Further genomic analysis may help in the understanding of SCP2 controlled PPAR α and SREBP pathways hyper activation.

Plasma membrane lipid rafts, as preferential site of receptors, have been linked to promotion of signaling pathways activation for example PI3K/AKT and ERK/MAPK³⁰⁶⁻³⁰⁸. While SCP2 is involved in lipid rafts formation, we surprisingly found signaling pathways hyperactivation in *Scp2* deleted mice liver. SCP2 is one intracellular lipid transporter among others in the cell. SCP2 deficiency may thus provoke compensatory effects leading to upregulation of other lipid transporters which lipid specificity would be different. As a consequence, this phenomenon may lead to changes in the nature of components constituting lipid rafts. To answer this question, investigation of lipid raft composition would be helpful.

All these signaling pathways play crucial role in metabolic processes. For example, PI3K/AKT signaling pathway activation *via* insulin is involved in lipogenesis through SREBP activation²¹⁵. Abnormal high insulin levels in serum could thus induce abnormal lipogenesis and as a consequence deregulated glucose/lipid homeostasis. This is what happens in case of insulin resistance caused by metabolic defects. In order to better understand involvements of circadian clock in metabolic defects, we generated and characterized genetic obese *Bmal1* KO

mice. Besides premature death of *Ob*^{Ob/+} *Bmal1*^{KO/KO} and *Ob*^{Ob/Ob} *Bmal1*^{KO/KO} (ObKO) mice which remains unexplained, ObKO mice exhibit obese phenotype accompanied with hyperglycemia, glucose resistance, but insulin sensitivity and reduced liver steatosis. In parallel, diet-induced obese *Bmal1* KO mice present the same characteristics, showing thus a protected effect of *Bmal1* deletion against insulin resistance. To further investigate how BMAL1 is involved in this phenomenon, it would be interesting first to characterized feeding and drinking behavior of both obese *Bmal1* KO mice models. It has been shown, both *Bmal1* KO and *Clock*^{A19} mutant mice present defects in pancreatic insulin secretion^{313, 323}. Glucose stimulated-insulin secretion assay in β -islets of our models would give us more precise information on endocrine pancreatic function. As oxidation level through ROS detection³¹⁴ and the activity of UCP2^{330, 333-335} have been linked to defect of pancreatic insulin secretion, further investigation of mitochondrial function may give answers in understanding of insulin resistance mechanisms. Energy balance regulation is appealing different tissues such as liver, adipose tissues, muscles, and pancreas. Genomic and proteomic studies on these different tissues are necessary to have information on regulation of signaling pathways involved in energy balance.

EXPERIMENTAL PROCEDURES

I. Animal experiments

All animal studies were conducted in accordance with our regional committee for ethics in the regulations of the veterinary office of the Canton of Vaud.

The generation of obese *Bmal1* knockout mice resulted in crossing $Ob^{Ob/+} Bmal1^{KO/+}$ mice. The male mice harboring the following genotyping were used for the experiments: $Ob^{+/+} Bmal1^{+/+}$, $Ob^{+/+} Bmal1^{KO/KO}$, $Ob^{Ob/+} Bmal1^{KO/KO}$, $Ob^{Ob/Ob} Bmal1^{+/+}$, and $Ob^{Ob/Ob} Bmal1^{KO/KO}$.

Bmal1 floxed mice, previously described (Storch et al, 2007) were crossed with the mice expressing the CRE recombinase under the control of the CMV promoter (Schweng et al, 1995) to obtain *Bmal1* knockout mice. Eight-week-old *Bmal1* wild-type and knockout male mice were fed with high-fat or control diets for 12 weeks to study the diet-induced obesity.

In all experiments, unless noted otherwise, mice are maintained under standard animal housing conditions, with free access to the food and water and in a 12 hours light / 12 hours dark cycles. Mice were weighted every week and were sacrificed at ZT0 and ZT12.

A. Body composition analysis

For *Ob.Bmal1* KO mice, echoMRI experiments are done at 6 weeks and *Bmal1* WT and KO mice in high fat and control diets undergo EchoMRI at 12, 15 and 18 weeks. These measurements to determine the body composition are performed at ZT3. Mice are weighted

and their size between the snout and the tail base was measured in order to determine the body mass index (BMI).

B. Glycemia measurements

For *Ob.Bmal1* KO mice, the experiment is done at 10 weeks and *Bmal1* WT and KO mice in high fat and control diets undergo these glycemia measurements at 12, 15 and 18 weeks. Mice undergo glycemia measurements (Breeze2 system, Bayer) after 15 hours of starvation (ZT3) and after 6 hours of refeeding (ZT9). At both time-points, blood samples from the vain tail are collected and sera are obtained after a 10 minute-centrifugation at 10 000 rpm at room temperature. Sera are kept at -80°C until analysis.

C. Glucose tolerance test

At 11 weeks, *Ob.Bmal1* KO mice undergo a glucose tolerance test at ZT3. Concerning the *Bmal1* WT and KO mice put under high-fat or control diet, glucose tolerance tests are performed at 13, 16 and 19 weeks. The glucose tolerance test is performed after 15 hours of starvation (ZT3). Glycemia measurements (Breeze2 system, Bayer) occurred 0, 15, 30, 60, 90, 120 and 180 minutes after the intra-peritoneal injection of glucose (1g/Kg).

D. Insulin tolerance test

At 12 weeks, Ob.*Bmal1* KO mice undergo an insulin tolerance test at ZT3. Concerning the *Bmal1* WT and KO mice put under high-fat or control diet, glucose tolerance tests are performed at 14, 17 and 20 weeks. At ZT3, glycemia measurements (Breeze2 system, Bayer) occurred 0, 15, 30, 60, 90, 120 and 180 minutes after the intra-peritoneal injection of insulin (1UI/Kg for the Ob.*Bmal1* KO mice line and 0.5UI/Kg for *Bmal1* WT and KO mice put under high-fat or control diet).

II. Serum chemistry analysis

Blood samples are collected every 2 hrs and sera are obtained after a centrifugation of 10 min at 10 000 rpm at room temperature. Sera are kept at -80°C until analysis. Insulin, glucose, cholesterol and triglycerides are respectively measured accordingly with the protocols of the Mouse Insulin ELISA kit (Mercodia), and the Glucose, Cholesterol, Triglycerides LabAssay kits (Wako).

III. Glycogen extraction

The tissue glycogen extractions have been previously described³⁴¹. Briefly, frozen tissues were incubated 20 minutes at 100°C in KOH solution. Ethanol 95% solution is added and a 20 minutes centrifugation at 840g at 4°C allows the precipitation of glycogen in a pellet. The

glycogen is then diluted in water. Glycogen measurements are performed in phenol 5% and sulphuric acid solutions. The optic density used is 490 nm.

IV. Liver slices

Liver pieces were fixed overnight in 10% formalin solution. Pieces were then washed three times in PBS solution. Liver slices underwent standard Hematoxylin/Eosin coloration.

REFERENCES

1. Kressler D, Hurt E, Bassler J. Driving ribosome assembly. *Biochimica et biophysica acta*. 2010;1803:673-683
2. Mayer C, Grummt I. Ribosome biogenesis and cell growth: Mtor coordinates transcription by all three classes of nuclear rna polymerases. *Oncogene*. 2006;25:6384-6391
3. Gachon F, Olela FF, Schaad O, Descombes P, Schibler U. The circadian par-domain basic leucine zipper transcription factors dbp, tef, and hlf modulate basal and inducible xenobiotic detoxification. *Cell metabolism*. 2006;4:25-36
4. Cretenet G, Le Clech M, Gachon F. Circadian clock-coordinated 12 hr period rhythmic activation of the ire1alpha pathway controls lipid metabolism in mouse liver. *Cell metabolism*. 2010;11:47-57
5. Simpson S, Galbraith JJ. An investigation into the diurnal variation of the body temperature of nocturnal and other birds, and a few mammals. *The Journal of physiology*. 1905;33:225-238
6. Pittendrigh CS. On temperature independence in the clock system controlling emergence time in drosophila. *Proceedings of the National Academy of Sciences of the United States of America*. 1954;40:1018-1029
7. Aschoff J. Circadian rhythms in man. *Science*. 1965;148:1427-1432
8. Pittendrigh CS. Circadian rhythms and the circadian organization of living systems. *Cold Spring Harbor symposia on quantitative biology*. 1960;25:159-184
9. Konopka RJ, Benzer S. Clock mutants of drosophila melanogaster. *Proceedings of the National Academy of Sciences of the United States of America*. 1971;68:2112-2116
10. Bargiello TA, Young MW. Molecular genetics of a biological clock in drosophila. *Proceedings of the National Academy of Sciences of the United States of America*. 1984;81:2142-2146
11. Garaulet M, Gomez-Abellan P. Chronobiology and obesity. *Nutricion hospitalaria*. 2013;28 Suppl 5:114-120
12. Vyas MV, Garg AX, Iansavichus AV, Costella J, Donner A, Laugsand LE, Janszky I, Mrkobrada M, Parraga G, Hackam DG. Shift work and vascular events: Systematic review and meta-analysis. *Bmj*. 2012;345:e4800
13. Baron KG, Reid KJ. Circadian misalignment and health. *Int Rev Psychiatry*. 2014;26:139-154
14. Bass J, Takahashi JS. Circadian integration of metabolism and energetics. *Science*. 2010;330:1349-1354
15. Yagita K, Tamanini F, van Der Horst GT, Okamura H. Molecular mechanisms of the biological clock in cultured fibroblasts. *Science*. 2001;292:278-281
16. Balsalobre A, Damiola F, Schibler U. A serum shock induces circadian gene expression in mammalian tissue culture cells. *Cell*. 1998;93:929-937
17. Klein DC, Moore, R.Y., and Reppert, S.M. . Suprachiasmatic nucleus: Themind's clock. 1991
18. Stephan FK, Zucker I. Circadian rhythms in drinking behavior and locomotor activity of rats are eliminated by hypothalamic lesions. *Proceedings of the National Academy of Sciences of the United States of America*. 1972;69:1583-1586
19. Ralph MR, Foster RG, Davis FC, Menaker M. Transplanted suprachiasmatic nucleus determines circadian period. *Science*. 1990;247:975-978
20. Berson DM. Strange vision: Ganglion cells as circadian photoreceptors. *Trends in neurosciences*. 2003;26:314-320
21. Hannibal J, Hindersson P, Knudsen SM, Georg B, Fahrenkrug J. The photopigment melanopsin is exclusively present in pituitary adenylate cyclase-activating polypeptide-containing retinal ganglion cells of the retinohypothalamic tract. *The Journal of neuroscience : the official journal of the Society for Neuroscience*. 2002;22:RC191
22. Hattar S, Liao HW, Takao M, Berson DM, Yau KW. Melanopsin-containing retinal ganglion cells: Architecture, projections, and intrinsic photosensitivity. *Science*. 2002;295:1065-1070
23. Tischkau SA, Mitchell JW, Tyan SH, Buchanan GF, Gillette MU. Ca²⁺/camp response element-binding protein (creb)-dependent activation of per1 is required for light-induced

- signaling in the suprachiasmatic nucleus circadian clock. *The Journal of biological chemistry*. 2003;278:718-723
24. Shigeyoshi Y, Taguchi K, Yamamoto S, Takekida S, Yan L, Tei H, Moriya T, Shibata S, Loros JJ, Dunlap JC, Okamura H. Light-induced resetting of a mammalian circadian clock is associated with rapid induction of the mper1 transcript. *Cell*. 1997;91:1043-1053
 25. Dibner C, Schibler U, Albrecht U. The mammalian circadian timing system: Organization and coordination of central and peripheral clocks. *Annual review of physiology*. 2010;72:517-549
 26. Liu AC, Welsh DK, Ko CH, Tran HG, Zhang EE, Priest AA, Buhr ED, Singer O, Meeker K, Verma IM, Doyle FJ, 3rd, Takahashi JS, Kay SA. Intercellular coupling confers robustness against mutations in the scn circadian clock network. *Cell*. 2007;129:605-616
 27. Guo H, Brewer JM, Lehman MN, Bittman EL. Suprachiasmatic regulation of circadian rhythms of gene expression in hamster peripheral organs: Effects of transplanting the pacemaker. *The Journal of neuroscience : the official journal of the Society for Neuroscience*. 2006;26:6406-6412
 28. Yoo SH, Yamazaki S, Lowrey PL, Shimomura K, Ko CH, Buhr ED, Sieppka SM, Hong HK, Oh WJ, Yoo OJ, Menaker M, Takahashi JS. Period2::Luciferase real-time reporting of circadian dynamics reveals persistent circadian oscillations in mouse peripheral tissues. *Proceedings of the National Academy of Sciences of the United States of America*. 2004;101:5339-5346
 29. Guo H, Brewer JM, Champhekar A, Harris RB, Bittman EL. Differential control of peripheral circadian rhythms by suprachiasmatic-dependent neural signals. *Proceedings of the National Academy of Sciences of the United States of America*. 2005;102:3111-3116
 30. Damiola F, Le Minh N, Preitner N, Kornmann B, Fleury-Olela F, Schibler U. Restricted feeding uncouples circadian oscillators in peripheral tissues from the central pacemaker in the suprachiasmatic nucleus. *Genes & development*. 2000;14:2950-2961
 31. Stokkan KA, Yamazaki S, Tei H, Sakaki Y, Menaker M. Entrainment of the circadian clock in the liver by feeding. *Science*. 2001;291:490-493
 32. Oster H, Damerow S, Kiessling S, Jakubcakova V, Abraham D, Tian J, Hoffmann MW, Eichele G. The circadian rhythm of glucocorticoids is regulated by a gating mechanism residing in the adrenal cortical clock. *Cell metabolism*. 2006;4:163-173
 33. Cailotto C, Lei J, van der Vliet J, van Heijningen C, van Eden CG, Kalsbeek A, Pevet P, Buijs RM. Effects of nocturnal light on (clock) gene expression in peripheral organs: A role for the autonomic innervation of the liver. *PloS one*. 2009;4:e5650
 34. Lowrey PL, Takahashi JS. Genetics of the mammalian circadian system: Photic entrainment, circadian pacemaker mechanisms, and posttranslational regulation. *Annual review of genetics*. 2000;34:533-562
 35. Albrecht U. The mammalian circadian clock: A network of gene expression. *Frontiers in bioscience : a journal and virtual library*. 2004;9:48-55
 36. Zhang EE, Kay SA. Clocks not winding down: Unravelling circadian networks. *Nature reviews. Molecular cell biology*. 2010;11:764-776
 37. Vitaterna MH, King DP, Chang AM, Kornhauser JM, Lowrey PL, McDonald JD, Dove WF, Pinto LH, Turek FW, Takahashi JS. Mutagenesis and mapping of a mouse gene, clock, essential for circadian behavior. *Science*. 1994;264:719-725
 38. King DP, Zhao Y, Sangoram AM, Wilsbacher LD, Tanaka M, Antoch MP, Steeves TD, Vitaterna MH, Kornhauser JM, Lowrey PL, Turek FW, Takahashi JS. Positional cloning of the mouse circadian clock gene. *Cell*. 1997;89:641-653
 39. Debruyne JP, Noton E, Lambert CM, Maywood ES, Weaver DR, Reppert SM. A clock shock: Mouse clock is not required for circadian oscillator function. *Neuron*. 2006;50:465-477
 40. Hogenesch JB, Gu YZ, Jain S, Bradfield CA. The basic-helix-loop-helix-pas orphan mop3 forms transcriptionally active complexes with circadian and hypoxia factors. *Proceedings of the National Academy of Sciences of the United States of America*. 1998;95:5474-5479
 41. Gekakis N, Staknis D, Nguyen HB, Davis FC, Wilsbacher LD, King DP, Takahashi JS, Weitz CJ. Role of the clock protein in the mammalian circadian mechanism. *Science*. 1998;280:1564-1569

42. Bunker MK, Wilsbacher LD, Moran SM, Clendenin C, Radcliffe LA, Hogenesch JB, Simon MC, Takahashi JS, Bradfield CA. Mop3 is an essential component of the master circadian pacemaker in mammals. *Cell*. 2000;103:1009-1017
43. Ueda HR, Hayashi S, Chen W, Sano M, Machida M, Shigeyoshi Y, Iino M, Hashimoto S. System-level identification of transcriptional circuits underlying mammalian circadian clocks. *Nature genetics*. 2005;37:187-192
44. Garcia JA, Zhang D, Estill SJ, Michnoff C, Rutter J, Reick M, Scott K, Diaz-Arrastia R, McKnight SL. Impaired cued and contextual memory in npas2-deficient mice. *Science*. 2000;288:2226-2230
45. Dudley CA, Erbel-Sieler C, Estill SJ, Reick M, Franken P, Pitts S, McKnight SL. Altered patterns of sleep and behavioral adaptability in npas2-deficient mice. *Science*. 2003;301:379-383
46. DeBruyne JP, Weaver DR, Reppert SM. Clock and npas2 have overlapping roles in the suprachiasmatic circadian clock. *Nature neuroscience*. 2007;10:543-545
47. Okano T, Sasaki M, Fukada Y. Cloning of mouse bmal2 and its daily expression profile in the suprachiasmatic nucleus: A remarkable acceleration of bmal2 sequence divergence after bmal gene duplication. *Neuroscience letters*. 2001;300:111-114
48. Shi S, Hida A, McGuinness OP, Wasserman DH, Yamazaki S, Johnson CH. Circadian clock gene bmal1 is not essential; functional replacement with its paralog, bmal2. *Current biology : CB*. 2010;20:316-321
49. Masri S, Sassone-Corsi P. Plasticity and specificity of the circadian epigenome. *Nature neuroscience*. 2010;13:1324-1329
50. Zheng B, Albrecht U, Kaasik K, Sage M, Lu W, Vaishnav S, Li Q, Sun ZS, Eichele G, Bradley A, Lee CC. Nonredundant roles of the mper1 and mper2 genes in the mammalian circadian clock. *Cell*. 2001;105:683-694
51. van der Horst GT, Muijtjens M, Kobayashi K, Takano R, Kanno S, Takao M, de Wit J, Verkerk A, Eker AP, van Leenen D, Buijs R, Bootsma D, Hoeijmakers JH, Yasui A. Mammalian cry1 and cry2 are essential for maintenance of circadian rhythms. *Nature*. 1999;398:627-630
52. Albrecht U, Sun ZS, Eichele G, Lee CC. A differential response of two putative mammalian circadian regulators, mper1 and mper2, to light. *Cell*. 1997;91:1055-1064
53. Shearman LP, Zylka MJ, Weaver DR, Kolakowski LF, Jr., Reppert SM. Two period homologs: Circadian expression and photic regulation in the suprachiasmatic nuclei. *Neuron*. 1997;19:1261-1269
54. Sun ZS, Albrecht U, Zhuchenko O, Bailey J, Eichele G, Lee CC. Rigi, a putative mammalian ortholog of the drosophila period gene. *Cell*. 1997;90:1003-1011
55. Tei H, Okamura H, Shigeyoshi Y, Fukuhara C, Ozawa R, Hirose M, Sakaki Y. Circadian oscillation of a mammalian homologue of the drosophila period gene. *Nature*. 1997;389:512-516
56. Zylka MJ, Shearman LP, Levine JD, Jin X, Weaver DR, Reppert SM. Molecular analysis of mammalian timeless. *Neuron*. 1998;21:1115-1122
57. Zhong HH, Resnick AS, Straume M, Robertson McClung C. Effects of synergistic signaling by phytochrome a and cryptochrome1 on circadian clock-regulated catalase expression. *The Plant cell*. 1997;9:947-955
58. Thresher RJ, Vitaterna MH, Miyamoto Y, Kazantsev A, Hsu DS, Petit C, Selby CP, Dawut L, Smithies O, Takahashi JS, Sancar A. Role of mouse cryptochrome blue-light photoreceptor in circadian photoresponses. *Science*. 1998;282:1490-1494
59. Kiyohara YB, Tagao S, Tamanini F, Morita A, Sugisawa Y, Yasuda M, Yamanaka I, Ueda HR, van der Horst GT, Kondo T, Yagita K. The bmal1 c terminus regulates the circadian transcription feedback loop. *Proceedings of the National Academy of Sciences of the United States of America*. 2006;103:10074-10079
60. Kume K, Zylka MJ, Sriram S, Shearman LP, Weaver DR, Jin X, Maywood ES, Hastings MH, Reppert SM. Mcry1 and mcry2 are essential components of the negative limb of the circadian clock feedback loop. *Cell*. 1999;98:193-205

61. Sato TK, Yamada RG, Ukai H, Baggs JE, Miraglia LJ, Kobayashi TJ, Welsh DK, Kay SA, Ueda HR, Hogenesch JB. Feedback repression is required for mammalian circadian clock function. *Nature genetics*. 2006;38:312-319
62. Oishi K, Sakamoto K, Okada T, Nagase T, Ishida N. Antiphase circadian expression between *bmal1* and period homologue mRNA in the suprachiasmatic nucleus and peripheral tissues of rats. *Biochemical and biophysical research communications*. 1998;253:199-203
63. Field MD, Maywood ES, O'Brien JA, Weaver DR, Reppert SM, Hastings MH. Analysis of clock proteins in mouse *scn* demonstrates phylogenetic divergence of the circadian clockwork and resetting mechanisms. *Neuron*. 2000;25:437-447
64. Shearman LP, Sriram S, Weaver DR, Maywood ES, Chaves I, Zheng B, Kume K, Lee CC, van der Horst GT, Hastings MH, Reppert SM. Interacting molecular loops in the mammalian circadian clock. *Science*. 2000;288:1013-1019
65. Ye R, Selby CP, Chiou YY, Ozkan-Dagliyan I, Gaddameedhi S, Sancar A. Dual modes of clock: *Bmal1* inhibition mediated by cryptochrome and period proteins in the mammalian circadian clock. *Genes & development*. 2014;28:1989-1998
66. Cho H, Zhao X, Hatori M, Yu RT, Barish GD, Lam MT, Chong LW, DiTacchio L, Atkins AR, Glass CK, Liddle C, Auwerx J, Downes M, Panda S, Evans RM. Regulation of circadian behaviour and metabolism by *rev-erb-alpha* and *rev-erb-beta*. *Nature*. 2012;485:123-127
67. Akashi M, Takumi T. The orphan nuclear receptor *roralpha* regulates circadian transcription of the mammalian core-clock *bmal1*. *Nature structural & molecular biology*. 2005;12:441-448
68. Ueda HR, Chen W, Adachi A, Wakamatsu H, Hayashi S, Takasugi T, Nagano M, Nakahama K, Suzuki Y, Sugano S, Iino M, Shigeyoshi Y, Hashimoto S. A transcription factor response element for gene expression during circadian night. *Nature*. 2002;418:534-539
69. Sato TK, Panda S, Miraglia LJ, Reyes TM, Rudic RD, McNamara P, Naik KA, FitzGerald GA, Kay SA, Hogenesch JB. A functional genomics strategy reveals *rora* as a component of the mammalian circadian clock. *Neuron*. 2004;43:527-537
70. Preitner N, Damiola F, Lopez-Molina L, Zakarija J, Duboule D, Albrecht U, Schibler U. The orphan nuclear receptor *rev-erbalpha* controls circadian transcription within the positive limb of the mammalian circadian oscillator. *Cell*. 2002;110:251-260
71. Crumbley C, Wang Y, Kojetin DJ, Burris TP. Characterization of the core mammalian clock component, *npas2*, as a *rev-erbalpha*/*roralpha* target gene. *The Journal of biological chemistry*. 2010;285:35386-35392
72. Crumbley C, Burris TP. Direct regulation of clock expression by *rev-erb*. *PloS one*. 2011;6:e17290
73. Takeda Y, Jothi R, Birault V, Jetten AM. *Rorgamma* directly regulates the circadian expression of clock genes and downstream targets in vivo. *Nucleic acids research*. 2012;40:8519-8535
74. So WV, Rosbash M. Post-transcriptional regulation contributes to drosophila clock gene mRNA cycling. *The EMBO journal*. 1997;16:7146-7155
75. Woo KC, Kim TD, Lee KH, Kim DY, Kim W, Lee KY, Kim KT. Mouse period 2 mRNA circadian oscillation is modulated by *ptb*-mediated rhythmic mRNA degradation. *Nucleic acids research*. 2009;37:26-37
76. Woo KC, Ha DC, Lee KH, Kim DY, Kim TD, Kim KT. Circadian amplitude of cryptochrome 1 is modulated by mRNA stability regulation via cytoplasmic *hnrnp d* oscillation. *Molecular and cellular biology*. 2010;30:197-205
77. Kojima S, Hirose M, Tokunaga K, Sakaki Y, Tei H. Structural and functional analysis of 3' untranslated region of mouse *period1* mRNA. *Biochemical and biophysical research communications*. 2003;301:1-7
78. Kojima S, Ina K, Futamura Y, Ito Y, Hibi S, Nagaoka M, Yuasa S, Kawai M, Nagao S, Kataoka T. [a phase I study of modified folfox 6 therapy for advanced colorectal cancer]. *Gan to kagaku ryoho. Cancer & chemotherapy*. 2007;34:203-206
79. Dupressoir A, Morel AP, Barbot W, Loireau MP, Corbo L, Heidmann T. Identification of four families of *yccr4*- and *mg2+*-dependent endonuclease-related proteins in higher eukaryotes, and characterization of orthologs of *yccr4* with a conserved leucine-rich repeat essential for *hcaf1/hpop2* binding. *BMC genomics*. 2001;2:9

80. Green CB, Besharse JC. Identification of a novel vertebrate circadian clock-regulated gene encoding the protein nocturnin. *Proceedings of the National Academy of Sciences of the United States of America*. 1996;93:14884-14888
81. Stubblefield JJ, Terrien J, Green CB. Nocturnin: At the crossroads of clocks and metabolism. *Trends in endocrinology and metabolism: TEM*. 2012;23:326-333
82. Kojima S, Sher-Chen EL, Green CB. Circadian control of mrna polyadenylation dynamics regulates rhythmic protein expression. *Genes & development*. 2012;26:2724-2736
83. Majercak J, Sidote D, Hardin PE, Edery I. How a circadian clock adapts to seasonal decreases in temperature and day length. *Neuron*. 1999;24:219-230
84. Diernfellner AC, Schafmeier T, Merrow MW, Brunner M. Molecular mechanism of temperature sensing by the circadian clock of *neurospora crassa*. *Genes & development*. 2005;19:1968-1973
85. McGlincy NJ, Valomon A, Chesham JE, Maywood ES, Hastings MH, Ule J. Regulation of alternative splicing by the circadian clock and food related cues. *Genome biology*. 2012;13:R54
86. Preussner M, Wilhelmi I, Schultz AS, Finkernagel F, Michel M, Moroy T, Heyd F. Rhythmic u2af26 alternative splicing controls period1 stability and the circadian clock in mice. *Molecular cell*. 2014;54:651-662
87. Cheng HY, Papp JW, Varlamova O, Dziema H, Russell B, Curfman JP, Nakazawa T, Shimizu K, Okamura H, Impey S, Obrietan K. MicroRNA modulation of circadian-clock period and entrainment. *Neuron*. 2007;54:813-829
88. Gatfield D, Le Martelot G, Vejnar CE, Gerlach D, Schaad O, Fleury-Olela F, Ruskeepaa AL, Oresic M, Esau CC, Zdobnov EM, Schibler U. Integration of microRNA mir-122 in hepatic circadian gene expression. *Genes & development*. 2009;23:1313-1326
89. Chen R, D'Alessandro M, Lee C. Mirnas are required for generating a time delay critical for the circadian oscillator. *Current biology : CB*. 2013;23:1959-1968
90. Du NH, Arpat AB, De Matos M, Gatfield D. MicroRNAs shape circadian hepatic gene expression on a transcriptome-wide scale. *eLife*. 2014;3:e02510
91. Vanselow K, Vanselow JT, Westermarck PO, Reischl S, Maier B, Korte T, Herrmann A, Herzog H, Schlosser A, Kramer A. Differential effects of per2 phosphorylation: Molecular basis for the human familial advanced sleep phase syndrome (fasps). *Genes & development*. 2006;20:2660-2672
92. Shirogane T, Jin J, Ang XL, Harper JW. Scfbeta-trcp controls clock-dependent transcription via casein kinase 1-dependent degradation of the mammalian period-1 (per1) protein. *The Journal of biological chemistry*. 2005;280:26863-26872
93. Eide EJ, Woolf MF, Kang H, Woolf P, Hurst W, Camacho F, Vielhaber EL, Giovanni A, Virshup DM. Control of mammalian circadian rhythm by ckiepsilon-regulated proteasome-mediated per2 degradation. *Molecular and cellular biology*. 2005;25:2795-2807
94. Eide EJ, Vielhaber EL, Hinz WA, Virshup DM. The circadian regulatory proteins bmal1 and cryptochromes are substrates of casein kinase iepsilon. *The Journal of biological chemistry*. 2002;277:17248-17254
95. Harada Y, Sakai M, Kurabayashi N, Hirota T, Fukada Y. Ser-557-phosphorylated mcry2 is degraded upon synergistic phosphorylation by glycogen synthase kinase-3 beta. *The Journal of biological chemistry*. 2005;280:31714-31721
96. Iitaka C, Miyazaki K, Akaike T, Ishida N. A role for glycogen synthase kinase-3beta in the mammalian circadian clock. *The Journal of biological chemistry*. 2005;280:29397-29402
97. Yin L, Wang J, Klein PS, Lazar MA. Nuclear receptor rev-erbalpha is a critical lithium-sensitive component of the circadian clock. *Science*. 2006;311:1002-1005
98. Lamia KA, Sachdeva UM, DiTacchio L, Williams EC, Alvarez JG, Egan DF, Vasquez DS, Juguilon H, Panda S, Shaw RJ, Thompson CB, Evans RM. Ampk regulates the circadian clock by cryptochrome phosphorylation and degradation. *Science*. 2009;326:437-440
99. Gallego M, Kang H, Virshup DM. Protein phosphatase 1 regulates the stability of the circadian protein per2. *The Biochemical journal*. 2006;399:169-175

100. Partch CL, Shields KF, Thompson CL, Selby CP, Sancar A. Posttranslational regulation of the mammalian circadian clock by cryptochrome and protein phosphatase 5. *Proceedings of the National Academy of Sciences of the United States of America*. 2006;103:10467-10472
101. Kornitzer D, Ciechanover A. Modes of regulation of ubiquitin-mediated protein degradation. *Journal of cellular physiology*. 2000;182:1-11
102. Busino L, Bassermann F, Maiolica A, Lee C, Nolan PM, Godinho SI, Draetta GF, Pagano M. Scffbx13 controls the oscillation of the circadian clock by directing the degradation of cryptochrome proteins. *Science*. 2007;316:900-904
103. Siepka SM, Yoo SH, Park J, Song W, Kumar V, Hu Y, Lee C, Takahashi JS. Circadian mutant overtime reveals f-box protein fbx13 regulation of cryptochrome and period gene expression. *Cell*. 2007;129:1011-1023
104. Godinho SI, Maywood ES, Shaw L, Tucci V, Barnard AR, Busino L, Pagano M, Kendall R, Quwailid MM, Romero MR, O'Neill J, Chesham JE, Brooker D, Lallanne Z, Hastings MH, Nolan PM. The after-hours mutant reveals a role for fbx13 in determining mammalian circadian period. *Science*. 2007;316:897-900
105. Hirano A, Yumimoto K, Tsunematsu R, Matsumoto M, Oyama M, Kozuka-Hata H, Nakagawa T, Lanjakornsiripan D, Nakayama KI, Fukada Y. Fbx121 regulates oscillation of the circadian clock through ubiquitination and stabilization of cryptochromes. *Cell*. 2013;152:1106-1118
106. Cardone L, Hirayama J, Giordano F, Tamaru T, Palvimo JJ, Sassone-Corsi P. Circadian clock control by sumoylation of bmal1. *Science*. 2005;309:1390-1394
107. Lee J, Lee Y, Lee MJ, Park E, Kang SH, Chung CH, Lee KH, Kim K. Dual modification of bmal1 by sumo2/3 and ubiquitin promotes circadian activation of the clock/bmal1 complex. *Molecular and cellular biology*. 2008;28:6056-6065
108. Etchegaray JP, Lee C, Wade PA, Reppert SM. Rhythmic histone acetylation underlies transcription in the mammalian circadian clock. *Nature*. 2003;421:177-182
109. Doi M, Hirayama J, Sassone-Corsi P. Circadian regulator clock is a histone acetyltransferase. *Cell*. 2006;125:497-508
110. Hirayama J, Sahar S, Grimaldi B, Tamaru T, Takamatsu K, Nakahata Y, Sassone-Corsi P. Clock-mediated acetylation of bmal1 controls circadian function. *Nature*. 2007;450:1086-1090
111. Naruse Y, Oh-hashi K, Iijima N, Naruse M, Yoshioka H, Tanaka M. Circadian and light-induced transcription of clock gene per1 depends on histone acetylation and deacetylation. *Molecular and cellular biology*. 2004;24:6278-6287
112. Yin L, Lazar MA. The orphan nuclear receptor rev-erbalpha recruits the n-cor/histone deacetylase 3 corepressor to regulate the circadian bmal1 gene. *Molecular endocrinology*. 2005;19:1452-1459
113. Ripperger JA, Schibler U. Rhythmic clock-bmal1 binding to multiple e-box motifs drives circadian dbp transcription and chromatin transitions. *Nature genetics*. 2006;38:369-374
114. Brown SA, Ripperger J, Kadener S, Fleury-Olela F, Vilbois F, Rosbash M, Schibler U. Period1-associated proteins modulate the negative limb of the mammalian circadian oscillator. *Science*. 2005;308:693-696
115. DiTacchio L, Le HD, Vollmers C, Hatori M, Witcher M, Secombe J, Panda S. Histone lysine demethylase jarid1a activates clock-bmal1 and influences the circadian clock. *Science*. 2011;333:1881-1885
116. Asher G, Gatfield D, Stratmann M, Reinke H, Dibner C, Kreppel F, Mostoslavsky R, Alt FW, Schibler U. Sirt1 regulates circadian clock gene expression through per2 deacetylation. *Cell*. 2008;134:317-328
117. Nakahata Y, Kaluzova M, Grimaldi B, Sahar S, Hirayama J, Chen D, Guarente LP, Sassone-Corsi P. The nad⁺-dependent deacetylase sirt1 modulates clock-mediated chromatin remodeling and circadian control. *Cell*. 2008;134:329-340
118. Masri S, Rigor P, Cervantes M, Ceglia N, Sebastian C, Xiao C, Roqueta-Rivera M, Deng C, Osborne TF, Mostoslavsky R, Baldi P, Sassone-Corsi P. Partitioning circadian transcription by sirt6 leads to segregated control of cellular metabolism. *Cell*. 2014;158:659-672

119. Ramsey KM, Yoshino J, Brace CS, Abrassart D, Kobayashi Y, Marcheva B, Hong HK, Chong JL, Buhr ED, Lee C, Takahashi JS, Imai S, Bass J. Circadian clock feedback cycle through nampt-mediated nad⁺ biosynthesis. *Science*. 2009;324:651-654
120. Komar AA, Mazumder B, Merrick WC. A new framework for understanding ires-mediated translation. *Gene*. 2012;502:75-86
121. Pestova TV, Kolupaeva VG, Lomakin IB, Pilipenko EV, Shatsky IN, Agol VI, Hellen CU. Molecular mechanisms of translation initiation in eukaryotes. *Proceedings of the National Academy of Sciences of the United States of America*. 2001;98:7029-7036
122. Gingras AC, Raught B, Sonenberg N. Eif4 initiation factors: Effectors of mrna recruitment to ribosomes and regulators of translation. *Annual review of biochemistry*. 1999;68:913-963
123. Heitman J, Movva NR, Hall MN. Targets for cell cycle arrest by the immunosuppressant rapamycin in yeast. *Science*. 1991;253:905-909
124. Wullschleger S, Loewith R, Hall MN. Tor signaling in growth and metabolism. *Cell*. 2006;124:471-484
125. Fingar DC, Salama S, Tsou C, Harlow E, Blenis J. Mammalian cell size is controlled by mtor and its downstream targets s6k1 and 4ebp1/eif4e. *Genes & development*. 2002;16:1472-1487
126. Hay N, Sonenberg N. Upstream and downstream of mtor. *Genes & development*. 2004;18:1926-1945
127. Hara K, Yonezawa K, Weng QP, Kozlowski MT, Belham C, Avruch J. Amino acid sufficiency and mtor regulate p70 s6 kinase and eif-4e bp1 through a common effector mechanism. *The Journal of biological chemistry*. 1998;273:14484-14494
128. Kimball SR, Shantz LM, Horetsky RL, Jefferson LS. Leucine regulates translation of specific mRNAs in 16 myoblasts through mtor-mediated changes in availability of eif4e and phosphorylation of ribosomal protein s6. *The Journal of biological chemistry*. 1999;274:11647-11652
129. Xu G, Kwon G, Cruz WS, Marshall CA, McDaniel ML. Metabolic regulation by leucine of translation initiation through the mtor-signaling pathway by pancreatic beta-cells. *Diabetes*. 2001;50:353-360
130. Manning BD. Balancing akt with s6k: Implications for both metabolic diseases and tumorigenesis. *The Journal of cell biology*. 2004;167:399-403
131. Li Y, Corradetti MN, Inoki K, Guan KL. Tsc2: Filling the gap in the mtor signaling pathway. *Trends in biochemical sciences*. 2004;29:32-38
132. Long X, Lin Y, Ortiz-Vega S, Yonezawa K, Avruch J. Rheb binds and regulates the mtor kinase. *Current biology : CB*. 2005;15:702-713
133. Inoki K, Zhu T, Guan KL. Tsc2 mediates cellular energy response to control cell growth and survival. *Cell*. 2003;115:577-590
134. Gwinn DM, Shackelford DB, Egan DF, Mihaylova MM, Mery A, Vasquez DS, Turk BE, Shaw RJ. Ampk phosphorylation of raptor mediates a metabolic checkpoint. *Molecular cell*. 2008;30:214-226
135. Ma L, Chen Z, Erdjument-Bromage H, Tempst P, Pandolfi PP. Phosphorylation and functional inactivation of tsc2 by erk implications for tuberous sclerosis and cancer pathogenesis. *Cell*. 2005;121:179-193
136. Roux PP, Ballif BA, Anjum R, Gygi SP, Blenis J. Tumor-promoting phorbol esters and activated ras inactivate the tuberous sclerosis tumor suppressor complex via p90 ribosomal s6 kinase. *Proceedings of the National Academy of Sciences of the United States of America*. 2004;101:13489-13494
137. Meyuhas O. Synthesis of the translational apparatus is regulated at the translational level. *European journal of biochemistry / FEBS*. 2000;267:6321-6330
138. Jackson RJ, Hellen CU, Pestova TV. The mechanism of eukaryotic translation initiation and principles of its regulation. *Nature reviews. Molecular cell biology*. 2010;11:113-127
139. Magnuson B, Ekim B, Fingar DC. Regulation and function of ribosomal protein s6 kinase (s6k) within mtor signalling networks. *The Biochemical journal*. 2012;441:1-21
140. Pestova D, Macek M, Elena Martinez Perez M. Ciliates and their picophytoplankton-feeding activity in a high-altitude warm-monomictic saline lake. *European journal of protistology*. 2008;44:13-25

141. Lomakin IB, Kolupaeva VG, Marintchev A, Wagner G, Pestova TV. Position of eukaryotic initiation factor eif1 on the 40s ribosomal subunit determined by directed hydroxyl radical probing. *Genes & development*. 2003;17:2786-2797
142. Simonetti A, Marzi S, Myasnikov AG, Fabbretti A, Yusupov M, Gualerzi CO, Klaholz BP. Structure of the 30s translation initiation complex. *Nature*. 2008;455:416-420
143. Allen GS, Zavialov A, Gursky R, Ehrenberg M, Frank J. The cryo-em structure of a translation initiation complex from escherichia coli. *Cell*. 2005;121:703-712
144. Pestova TV, Kolupaeva VG. The roles of individual eukaryotic translation initiation factors in ribosomal scanning and initiation codon selection. *Genes & development*. 2002;16:2906-2922
145. LeFebvre AK, Korneeva NL, Trutschl M, Cvek U, Duzan RD, Bradley CA, Hershey JW, Rhoads RE. Translation initiation factor eif4g-1 binds to eif3 through the eif3e subunit. *The Journal of biological chemistry*. 2006;281:22917-22932
146. Passmore LA, Schmeing TM, Maag D, Applefield DJ, Acker MG, Algire MA, Lorsch JR, Ramakrishnan V. The eukaryotic translation initiation factors eif1 and eif1a induce an open conformation of the 40s ribosome. *Molecular cell*. 2007;26:41-50
147. Matsuda D, Dreher TW. Close spacing of aug initiation codons confers dicistronic character on a eukaryotic mrna. *RNA*. 2006;12:1338-1349
148. Kozak M. Structural features in eukaryotic mRNAs that modulate the initiation of translation. *The Journal of biological chemistry*. 1991;266:19867-19870
149. Pisarev AV, Kolupaeva VG, Pisareva VP, Merrick WC, Hellen CU, Pestova TV. Specific functional interactions of nucleotides at key -3 and +4 positions flanking the initiation codon with components of the mammalian 48s translation initiation complex. *Genes & development*. 2006;20:624-636
150. Pestova TV, Shatsky IN, Fletcher SP, Jackson RJ, Hellen CU. A prokaryotic-like mode of cytoplasmic eukaryotic ribosome binding to the initiation codon during internal translation initiation of hepatitis c and classical swine fever virus mRNAs. *Genes & development*. 1998;12:67-83
151. Paulin FE, Campbell LE, O'Brien K, Loughlin J, Proud CG. Eukaryotic translation initiation factor 5 (eif5) acts as a classical gtpase-activator protein. *Current biology : CB*. 2001;11:55-59
152. Marintchev A, Wagner G. Translation initiation: Structures, mechanisms and evolution. *Quarterly reviews of biophysics*. 2004;37:197-284
153. Pestova TV, Lomakin IB, Lee JH, Choi SK, Dever TE, Hellen CU. The joining of ribosomal subunits in eukaryotes requires eif5b. *Nature*. 2000;403:332-335
154. Unbehauen A, Borukhov SI, Hellen CU, Pestova TV. Release of initiation factors from 48s complexes during ribosomal subunit joining and the link between establishment of codon-anticodon base-pairing and hydrolysis of eif2-bound gtp. *Genes & development*. 2004;18:3078-3093
155. Olsen DS, Savner EM, Mathew A, Zhang F, Krishnamoorthy T, Phan L, Hinnebusch AG. Domains of eif1a that mediate binding to eif2, eif3 and eif5b and promote ternary complex recruitment in vivo. *The EMBO journal*. 2003;22:193-204
156. Marintchev A, Kolupaeva VG, Pestova TV, Wagner G. Mapping the binding interface between human eukaryotic initiation factors 1a and 5b: A new interaction between old partners. *Proceedings of the National Academy of Sciences of the United States of America*. 2003;100:1535-1540
157. Poyry TA, Kaminski A, Jackson RJ. What determines whether mammalian ribosomes resume scanning after translation of a short upstream open reading frame? *Genes & development*. 2004;18:62-75
158. Reed VS, Wastney ME, Yang DC. Mechanisms of the transfer of aminoacyl-trna from aminoacyl-trna synthetase to the elongation factor 1 alpha. *The Journal of biological chemistry*. 1994;269:32932-32936
159. Carvalho MD, Carvalho JF, Merrick WC. Biological characterization of various forms of elongation factor 1 from rabbit reticulocytes. *Archives of biochemistry and biophysics*. 1984;234:603-611
160. Browne GJ, Proud CG. Regulation of peptide-chain elongation in mammalian cells. *European journal of biochemistry / FEBS*. 2002;269:5360-5368

161. Yonath A. Ribosomal crystallography: Peptide bond formation, chaperone assistance and antibiotics activity. *Molecules and cells*. 2005;20:1-16
162. Taylor DJ, Nilsson J, Merrill AR, Andersen GR, Nissen P, Frank J. Structures of modified eef2 80s ribosome complexes reveal the role of gtp hydrolysis in translocation. *The EMBO journal*. 2007;26:2421-2431
163. Wang X, Li W, Williams M, Terada N, Alessi DR, Proud CG. Regulation of elongation factor 2 kinase by p90(rsk1) and p70 s6 kinase. *The EMBO journal*. 2001;20:4370-4379
164. Zhouravleva G, Frolova L, Le Goff X, Le Guellec R, Inge-Vechtomov S, Kisselev L, Philippe M. Termination of translation in eukaryotes is governed by two interacting polypeptide chain release factors, erf1 and erf3. *The EMBO journal*. 1995;14:4065-4072
165. Alkalaeva EZ, Pisarev AV, Frolova LY, Kisselev LL, Pestova TV. In vitro reconstitution of eukaryotic translation reveals cooperativity between release factors erf1 and erf3. *Cell*. 2006;125:1125-1136
166. Nierhaus KH. The allosteric three-site model for the ribosomal elongation cycle: Features and future. *Biochemistry*. 1990;29:4997-5008
167. Powers T, Walter P. Regulation of ribosome biogenesis by the rapamycin-sensitive tor-signaling pathway in *saccharomyces cerevisiae*. *Molecular biology of the cell*. 1999;10:987-1000
168. Grandi P, Rybin V, Bassler J, Petfalski E, Strauss D, Marzioch M, Schafer T, Kuster B, Tschochner H, Tollervey D, Gavin AC, Hurt E. 90s pre-ribosomes include the 35s pre-rrna, the u3 snorncp, and 40s subunit processing factors but predominantly lack 60s synthesis factors. *Molecular cell*. 2002;10:105-115
169. Hannan KM, Brandenburger Y, Jenkins A, Sharkey K, Cavanaugh A, Rothblum L, Moss T, Poortinga G, McArthur GA, Pearson RB, Hannan RD. Mtor-dependent regulation of ribosomal gene transcription requires s6k1 and is mediated by phosphorylation of the carboxy-terminal activation domain of the nucleolar transcription factor ubf. *Molecular and cellular biology*. 2003;23:8862-8877
170. Schneider DA, Michel A, Sikes ML, Vu L, Dodd JA, Salgia S, Osheim YN, Beyer AL, Nomura M. Transcription elongation by rna polymerase i is linked to efficient rrna processing and ribosome assembly. *Molecular cell*. 2007;26:217-229
171. Fromont-Racine M, Senger B, Saveanu C, Fasiolo F. Ribosome assembly in eukaryotes. *Gene*. 2003;313:17-42
172. Henras AK, Soudet J, Gerus M, Lebaron S, Caizergues-Ferrer M, Mouglin A, Henry Y. The post-transcriptional steps of eukaryotic ribosome biogenesis. *Cellular and molecular life sciences : CMLS*. 2008;65:2334-2359
173. Perez-Fernandez J, Roman A, De Las Rivas J, Bustelo XR, Dosil M. The 90s preribosome is a multimodular structure that is assembled through a hierarchical mechanism. *Molecular and cellular biology*. 2007;27:5414-5429
174. Schafer T, Maco B, Petfalski E, Tollervey D, Bottcher B, Aebi U, Hurt E. Hrr25-dependent phosphorylation state regulates organization of the pre-40s subunit. *Nature*. 2006;441:651-655
175. Fatica A, Oeffinger M, Dlakic M, Tollervey D. Nob1p is required for cleavage of the 3' end of 18s rrna. *Molecular and cellular biology*. 2003;23:1798-1807
176. Granneman S, Nandineni MR, Baserga SJ. The putative ntpase fap7 mediates cytoplasmic 20s pre-rrna processing through a direct interaction with rps14. *Molecular and cellular biology*. 2005;25:10352-10364
177. Fatica A, Cronshaw AD, Dlakic M, Tollervey D. Ssf1p prevents premature processing of an early pre-60s ribosomal particle. *Molecular cell*. 2002;9:341-351
178. Kressler D, Roser D, Pertschy B, Hurt E. The aaa atpase rix7 powers progression of ribosome biogenesis by stripping nsal from pre-60s particles. *The Journal of cell biology*. 2008;181:935-944
179. Nissan TA, Bassler J, Petfalski E, Tollervey D, Hurt E. 60s pre-ribosome formation viewed from assembly in the nucleolus until export to the cytoplasm. *The EMBO journal*. 2002;21:5539-5547

180. Ulbrich C, Diepholz M, Bassler J, Kressler D, Pertschy B, Galani K, Bottcher B, Hurt E. Mechanochemical removal of ribosome biogenesis factors from nascent 60s ribosomal subunits. *Cell*. 2009;138:911-922
181. Ansel KM, Pastor WA, Rath N, Lapan AD, Glasmacher E, Wolf C, Smith LC, Papadopoulou N, Lamperti ED, Tahiliani M, Ellwart JW, Shi Y, Kremmer E, Rao A, Heissmeyer V. Mouse eri1 interacts with the ribosome and catalyzes 5.8s rna processing. *Nature structural & molecular biology*. 2008;15:523-530
182. Senger B, Lafontaine DL, Graindorge JS, Gadal O, Camasses A, Sanni A, Garnier JM, Breitenbach M, Hurt E, Fasiolo F. The nucle(ol)ar tif6p and efl1p are required for a late cytoplasmic step of ribosome synthesis. *Molecular cell*. 2001;8:1363-1373
183. Hurt E, Hannus S, Schmelzl B, Lau D, Tollervey D, Simos G. A novel in vivo assay reveals inhibition of ribosomal nuclear export in ran-cycle and nucleoporin mutants. *The Journal of cell biology*. 1999;144:389-401
184. Moy TI, Silver PA. Nuclear export of the small ribosomal subunit requires the ran-gtpase cycle and certain nucleoporins. *Genes & development*. 1999;13:2118-2133
185. Ho JH, Kallstrom G, Johnson AW. Nascent 60s ribosomal subunits enter the free pool bound by nmd3p. *RNA*. 2000;6:1625-1634
186. Yao W, Roser D, Kohler A, Bradatsch B, Bassler J, Hurt E. Nuclear export of ribosomal 60s subunits by the general mrna export receptor mex67-mtr2. *Molecular cell*. 2007;26:51-62
187. Bradatsch B, Katahira J, Kowalinski E, Bange G, Yao W, Sekimoto T, Baumgartel V, Boese G, Bassler J, Wild K, Peters R, Yoneda Y, Sinning I, Hurt E. Arx1 functions as an unorthodox nuclear export receptor for the 60s preribosomal subunit. *Molecular cell*. 2007;27:767-779
188. Ferreira-Cerca S, Poll G, Gleizes PE, Tschochner H, Milkereit P. Roles of eukaryotic ribosomal proteins in maturation and transport of pre-18s rna and ribosome function. *Molecular cell*. 2005;20:263-275
189. Towle HC. Glucose as a regulator of eukaryotic gene transcription. *Trends in endocrinology and metabolism: TEM*. 2005;16:489-494
190. Shimomura I, Bashmakov Y, Ikemoto S, Horton JD, Brown MS, Goldstein JL. Insulin selectively increases srebp-1c mrna in the livers of rats with streptozotocin-induced diabetes. *Proceedings of the National Academy of Sciences of the United States of America*. 1999;96:13656-13661
191. Azzout-Marniche D, Becard D, Guichard C, Foretz M, Ferre P, Foufelle F. Insulin effects on sterol regulatory-element-binding protein-1c (srebp-1c) transcriptional activity in rat hepatocytes. *The Biochemical journal*. 2000;350 Pt 2:389-393
192. Yabe D, Komuro R, Liang G, Goldstein JL, Brown MS. Liver-specific mrna for insig-2 down-regulated by insulin: Implications for fatty acid synthesis. *Proceedings of the National Academy of Sciences of the United States of America*. 2003;100:3155-3160
193. Horton JD, Bashmakov Y, Shimomura I, Shimano H. Regulation of sterol regulatory element binding proteins in livers of fasted and refed mice. *Proceedings of the National Academy of Sciences of the United States of America*. 1998;95:5987-5992
194. Kim JB, Sarraf P, Wright M, Yao KM, Mueller E, Solanes G, Lowell BB, Spiegelman BM. Nutritional and insulin regulation of fatty acid synthetase and leptin gene expression through add1/srebp1. *The Journal of clinical investigation*. 1998;101:1-9
195. Liang G, Yang J, Horton JD, Hammer RE, Goldstein JL, Brown MS. Diminished hepatic response to fasting/refeeding and liver x receptor agonists in mice with selective deficiency of sterol regulatory element-binding protein-1c. *The Journal of biological chemistry*. 2002;277:9520-9528
196. Horton JD, Shah NA, Warrington JA, Anderson NN, Park SW, Brown MS, Goldstein JL. Combined analysis of oligonucleotide microarray data from transgenic and knockout mice identifies direct srebp target genes. *Proceedings of the National Academy of Sciences of the United States of America*. 2003;100:12027-12032
197. Foretz M, Pacot C, Dugail I, Lemarchand P, Guichard C, Le Liepvre X, Berthelie-Lubrano C, Spiegelman B, Kim JB, Ferre P, Foufelle F. Add1/srebp-1c is required in the activation of hepatic lipogenic gene expression by glucose. *Molecular and cellular biology*. 1999;19:3760-3768

198. Tang X, Ma H, Shen Z, Zou S, Xu X, Lin C. Dehydroepiandrosterone activates cyclic adenosine 3',5'-monophosphate/protein kinase a signalling and suppresses sterol regulatory element-binding protein-1 expression in cultured primary chicken hepatocytes. *The British journal of nutrition*. 2009;102:680-686
199. Vallett SM, Sanchez HB, Rosenfeld JM, Osborne TF. A direct role for sterol regulatory element binding protein in activation of 3-hydroxy-3-methylglutaryl coenzyme a reductase gene. *The Journal of biological chemistry*. 1996;271:12247-12253
200. Nohturfft A, Yabe D, Goldstein JL, Brown MS, Espenshade PJ. Regulated step in cholesterol feedback localized to budding of scap from er membranes. *Cell*. 2000;102:315-323
201. Yang T, Espenshade PJ, Wright ME, Yabe D, Gong Y, Aebersold R, Goldstein JL, Brown MS. Crucial step in cholesterol homeostasis: Sterols promote binding of scap to insig-1, a membrane protein that facilitates retention of srebps in er. *Cell*. 2002;110:489-500
202. Rawson RB, Zelenski NG, Nijhawan D, Ye J, Sakai J, Hasan MT, Chang TY, Brown MS, Goldstein JL. Complementation cloning of s2p, a gene encoding a putative metalloprotease required for intramembrane cleavage of srebps. *Molecular cell*. 1997;1:47-57
203. Sakai J, Rawson RB, Espenshade PJ, Cheng D, Seegmiller AC, Goldstein JL, Brown MS. Molecular identification of the sterol-regulated luminal protease that cleaves srebps and controls lipid composition of animal cells. *Molecular cell*. 1998;2:505-514
204. Goldstein JL, DeBose-Boyd RA, Brown MS. Protein sensors for membrane sterols. *Cell*. 2006;124:35-46
205. Magana MM, Osborne TF. Two tandem binding sites for sterol regulatory element binding proteins are required for sterol regulation of fatty-acid synthase promoter. *The Journal of biological chemistry*. 1996;271:32689-32694
206. Ikonen E. Cellular cholesterol trafficking and compartmentalization. *Nature reviews. Molecular cell biology*. 2008;9:125-138
207. Manning BD, Cantley LC. Akt/pkb signaling: Navigating downstream. *Cell*. 2007;129:1261-1274
208. Lizcano JM, Alessi DR. The insulin signalling pathway. *Current biology : CB*. 2002;12:R236-238
209. Porstmann T, Santos CR, Griffiths B, Cully M, Wu M, Leever S, Griffiths JR, Chung YL, Schulze A. Srebp activity is regulated by mtorc1 and contributes to akt-dependent cell growth. *Cell metabolism*. 2008;8:224-236
210. Owen JL, Zhang Y, Bae SH, Farooqi MS, Liang G, Hammer RE, Goldstein JL, Brown MS. Insulin stimulation of srebp-1c processing in transgenic rat hepatocytes requires p70 s6-kinase. *Proceedings of the National Academy of Sciences of the United States of America*. 2012;109:16184-16189
211. Li S, Brown MS, Goldstein JL. Bifurcation of insulin signaling pathway in rat liver: Mtorc1 required for stimulation of lipogenesis, but not inhibition of gluconeogenesis. *Proceedings of the National Academy of Sciences of the United States of America*. 2010;107:3441-3446
212. Hegarty BD, Bobard A, Hainault I, Ferre P, Bossard P, Foufelle F. Distinct roles of insulin and liver x receptor in the induction and cleavage of sterol regulatory element-binding protein-1c. *Proceedings of the National Academy of Sciences of the United States of America*. 2005;102:791-796
213. Yellaturu CR, Deng X, Cagen LM, Wilcox HG, Mansbach CM, 2nd, Siddiqi SA, Park EA, Raghov R, Elam MB. Insulin enhances post-translational processing of nascent srebp-1c by promoting its phosphorylation and association with copii vesicles. *The Journal of biological chemistry*. 2009;284:7518-7532
214. Yecies JL, Zhang HH, Menon S, Liu S, Yecies D, Lipovsky AI, Gorgun C, Kwiatkowski DJ, Hotamisligil GS, Lee CH, Manning BD. Akt stimulates hepatic srebp1c and lipogenesis through parallel mtorc1-dependent and independent pathways. *Cell metabolism*. 2011;14:21-32
215. Xu X, So JS, Park JG, Lee AH. Transcriptional control of hepatic lipid metabolism by srebp and chrebp. *Seminars in liver disease*. 2013;33:301-311
216. Peet DJ, Janowski BA, Mangelsdorf DJ. The lxrs: A new class of oxysterol receptors. *Current opinion in genetics & development*. 1998;8:571-575

217. Peet DJ, Turley SD, Ma W, Janowski BA, Lobaccaro JM, Hammer RE, Mangelsdorf DJ. Cholesterol and bile acid metabolism are impaired in mice lacking the nuclear oxysterol receptor lxr alpha. *Cell*. 1998;93:693-704
218. Hong C, Tontonoz P. Liver x receptors in lipid metabolism: Opportunities for drug discovery. *Nature reviews. Drug discovery*. 2014;13:433-444
219. Repa JJ, Turley SD, Lobaccaro JA, Medina J, Li L, Lustig K, Shan B, Heyman RA, Dietschy JM, Mangelsdorf DJ. Regulation of absorption and abc1-mediated efflux of cholesterol by rxr heterodimers. *Science*. 2000;289:1524-1529
220. Yu L, Hammer RE, Li-Hawkins J, Von Bergmann K, Lutjohann D, Cohen JC, Hobbs HH. Disruption of abcg5 and abcg8 in mice reveals their crucial role in biliary cholesterol secretion. *Proceedings of the National Academy of Sciences of the United States of America*. 2002;99:16237-16242
221. Repa JJ, Berge KE, Pomajzl C, Richardson JA, Hobbs H, Mangelsdorf DJ. Regulation of atp-binding cassette sterol transporters abcg5 and abcg8 by the liver x receptors alpha and beta. *The Journal of biological chemistry*. 2002;277:18793-18800
222. Tarling EJ, Edwards PA. Atp binding cassette transporter g1 (abcg1) is an intracellular sterol transporter. *Proceedings of the National Academy of Sciences of the United States of America*. 2011;108:19719-19724
223. Chen G, Liang G, Ou J, Goldstein JL, Brown MS. Central role for liver x receptor in insulin-mediated activation of srebp-1c transcription and stimulation of fatty acid synthesis in liver. *Proceedings of the National Academy of Sciences of the United States of America*. 2004;101:11245-11250
224. Repa JJ, Liang G, Ou J, Bashmakov Y, Lobaccaro JM, Shimomura I, Shan B, Brown MS, Goldstein JL, Mangelsdorf DJ. Regulation of mouse sterol regulatory element-binding protein-1c gene (srebp-1c) by oxysterol receptors, lxralpha and lxrbeta. *Genes & development*. 2000;14:2819-2830
225. Yoshikawa T, Shimano H, Amemiya-Kudo M, Yahagi N, Hasty AH, Matsuzaka T, Okazaki H, Tamura Y, Iizuka Y, Ohashi K, Osuga J, Harada K, Gotoda T, Kimura S, Ishibashi S, Yamada N. Identification of liver x receptor-retinoid x receptor as an activator of the sterol regulatory element-binding protein 1c gene promoter. *Molecular and cellular biology*. 2001;21:2991-3000
226. Zhang Y, Breevoort SR, Angdisen J, Fu M, Schmidt DR, Holmstrom SR, Kliewer SA, Mangelsdorf DJ, Schulman IG. Liver lxralpha expression is crucial for whole body cholesterol homeostasis and reverse cholesterol transport in mice. *The Journal of clinical investigation*. 2012;122:1688-1699
227. Kalaany NY, Gauthier KC, Zavacki AM, Mammen PP, Kitazume T, Peterson JA, Horton JD, Garry DJ, Bianco AC, Mangelsdorf DJ. Lxrs regulate the balance between fat storage and oxidation. *Cell metabolism*. 2005;1:231-244
228. Kok T, Wolters H, Bloks VW, Havinga R, Jansen PL, Staels B, Kuipers F. Induction of hepatic abc transporter expression is part of the pparalpha-mediated fasting response in the mouse. *Gastroenterology*. 2003;124:160-171
229. Bloks VW, Bakker-Van Waarde WM, Verkade HJ, Kema IP, Wolters H, Vink E, Groen AK, Kuipers F. Down-regulation of hepatic and intestinal abcg5 and abcg8 expression associated with altered sterol fluxes in rats with streptozotocin-induced diabetes. *Diabetologia*. 2004;47:104-112
230. Iizuka K, Bruick RK, Liang G, Horton JD, Uyeda K. Deficiency of carbohydrate response element-binding protein (chrebp) reduces lipogenesis as well as glycolysis. *Proceedings of the National Academy of Sciences of the United States of America*. 2004;101:7281-7286
231. Yamashita H, Takenoshita M, Sakurai M, Bruick RK, Henzel WJ, Shillinglaw W, Arnot D, Uyeda K. A glucose-responsive transcription factor that regulates carbohydrate metabolism in the liver. *Proceedings of the National Academy of Sciences of the United States of America*. 2001;98:9116-9121
232. Cairo S, Merla G, Urbinati F, Ballabio A, Reymond A. Wbscr14, a gene mapping to the williams-beuren syndrome deleted region, is a new member of the mlx transcription factor network. *Human molecular genetics*. 2001;10:617-627

233. Stoeckman AK, Ma L, Towle HC. Mlx is the functional heteromeric partner of the carbohydrate response element-binding protein in glucose regulation of lipogenic enzyme genes. *The Journal of biological chemistry*. 2004;279:15662-15669
234. Ishii S, Iizuka K, Miller BC, Uyeda K. Carbohydrate response element binding protein directly promotes lipogenic enzyme gene transcription. *Proceedings of the National Academy of Sciences of the United States of America*. 2004;101:15597-15602
235. Herman MA, Peroni OD, Villoria J, Schon MR, Abumrad NA, Bluher M, Klein S, Kahn BB. A novel chrebp isoform in adipose tissue regulates systemic glucose metabolism. *Nature*. 2012;484:333-338
236. Kabashima T, Kawaguchi T, Wadzinski BE, Uyeda K. Xylulose 5-phosphate mediates glucose-induced lipogenesis by xylulose 5-phosphate-activated protein phosphatase in rat liver. *Proceedings of the National Academy of Sciences of the United States of America*. 2003;100:5107-5112
237. Kawaguchi T, Takenoshita M, Kabashima T, Uyeda K. Glucose and camp regulate the l-type pyruvate kinase gene by phosphorylation/dephosphorylation of the carbohydrate response element binding protein. *Proceedings of the National Academy of Sciences of the United States of America*. 2001;98:13710-13715
238. Bricambert J, Miranda J, Benhamed F, Girard J, Postic C, Dentin R. Salt-inducible kinase 2 links transcriptional coactivator p300 phosphorylation to the prevention of chrebp-dependent hepatic steatosis in mice. *The Journal of clinical investigation*. 2010;120:4316-4331
239. Guinez C, Filhoulaud G, Rayah-Benhamed F, Marmier S, Dubuquoy C, Dentin R, Moldes M, Burnol AF, Yang X, Lefebvre T, Girard J, Postic C. O-glcnaacylation increases chrebp protein content and transcriptional activity in the liver. *Diabetes*. 2011;60:1399-1413
240. Sakiyama H, Fujiwara N, Noguchi T, Eguchi H, Yoshihara D, Uyeda K, Suzuki K. The role of o-linked glcnac modification on the glucose response of chrebp. *Biochemical and biophysical research communications*. 2010;402:784-789
241. Ido-Kitamura Y, Sasaki T, Kobayashi M, Kim HJ, Lee YS, Kikuchi O, Yokota-Hashimoto H, Iizuka K, Accili D, Kitamura T. Hepatic foxo1 integrates glucose utilization and lipid synthesis through regulation of chrebp o-glycosylation. *PloS one*. 2012;7:e47231
242. Sakiyama H, Wynn RM, Lee WR, Fukasawa M, Mizuguchi H, Gardner KH, Repa JJ, Uyeda K. Regulation of nuclear import/export of carbohydrate response element-binding protein (chrebp): Interaction of an alpha-helix of chrebp with the 14-3-3 proteins and regulation by phosphorylation. *The Journal of biological chemistry*. 2008;283:24899-24908
243. Davies MN, O'Callaghan BL, Towle HC. Activation and repression of glucose-stimulated chrebp requires the concerted action of multiple domains within the mondo conserved region. *American journal of physiology. Endocrinology and metabolism*. 2010;299:E665-674
244. Li MV, Chang B, Imamura M, Pongvarin N, Chan L. Glucose-dependent transcriptional regulation by an evolutionarily conserved glucose-sensing module. *Diabetes*. 2006;55:1179-1189
245. Li MV, Chen W, Pongvarin N, Imamura M, Chan L. Glucose-mediated transactivation of carbohydrate response element-binding protein requires cooperative actions from mondo conserved regions and essential trans-acting factor 14-3-3. *Molecular endocrinology*. 2008;22:1658-1672
246. McFerrin LG, Atchley WR. A novel n-terminal domain may dictate the glucose response of mondo proteins. *PloS one*. 2012;7:e34803
247. Dentin R, Tomas-Cobos L, Fougelle F, Leopold J, Girard J, Postic C, Ferre P. Glucose 6-phosphate, rather than xylulose 5-phosphate, is required for the activation of chrebp in response to glucose in the liver. *Journal of hepatology*. 2012;56:199-209
248. Iizuka K, Takeda J, Horikawa Y. Hepatic overexpression of dominant negative mlx improves metabolic profile in diabetes-prone c57bl/6j mice. *Biochemical and biophysical research communications*. 2009;379:499-504
249. Iizuka K, Wu W, Horikawa Y, Takeda J. Role of glucose-6-phosphate and xylulose-5-phosphate in the regulation of glucose-stimulated gene expression in the pancreatic beta cell line, ins-1e. *Endocrine journal*. 2013;60:473-482

250. Iizuka K, Wu W, Horikawa Y, Saito M, Takeda J. Feedback looping between chrebp and pparalpha in the regulation of lipid metabolism in brown adipose tissues. *Endocrine journal*. 2013;60:1145-1153
251. Iizuka K. Recent progress on the role of chrebp in glucose and lipid metabolism. *Endocrine journal*. 2013;60:543-555
252. Berger J, Moller DE. The mechanisms of action of ppars. *Annual review of medicine*. 2002;53:409-435
253. Rogue A, Lambert C, Josse R, Antherieu S, Spire C, Claude N, Guillouzo A. Comparative gene expression profiles induced by ppargamma and pparalpha/gamma agonists in human hepatocytes. *PloS one*. 2011;6:e18816
254. Rogue A, Spire C, Brun M, Claude N, Guillouzo A. Gene expression changes induced by ppar gamma agonists in animal and human liver. *PPAR research*. 2010;2010:325183
255. Issemann I, Green S. Activation of a member of the steroid hormone receptor superfamily by peroxisome proliferators. *Nature*. 1990;347:645-650
256. Gottlicher M, Widmark E, Li Q, Gustafsson JA. Fatty acids activate a chimera of the clofibrac acid-activated receptor and the glucocorticoid receptor. *Proceedings of the National Academy of Sciences of the United States of America*. 1992;89:4653-4657
257. Zhu Y, Alvares K, Huang Q, Rao MS, Reddy JK. Cloning of a new member of the peroxisome proliferator-activated receptor gene family from mouse liver. *The Journal of biological chemistry*. 1993;268:26817-26820
258. Tontonoz P, Hu E, Graves RA, Budavari AI, Spiegelman BM. Mppar gamma 2: Tissue-specific regulator of an adipocyte enhancer. *Genes & development*. 1994;8:1224-1234
259. Kliewer SA, Forman BM, Blumberg B, Ong ES, Borgmeyer U, Mangelsdorf DJ, Umesono K, Evans RM. Differential expression and activation of a family of murine peroxisome proliferator-activated receptors. *Proceedings of the National Academy of Sciences of the United States of America*. 1994;91:7355-7359
260. Sertznig P, Seifert M, Tilgen W, Reichrath J. Present concepts and future outlook: Function of peroxisome proliferator-activated receptors (ppars) for pathogenesis, progression, and therapy of cancer. *Journal of cellular physiology*. 2007;212:1-12
261. Fruchart JC, Staels B, Duriez P. The role of fibric acids in atherosclerosis. *Current atherosclerosis reports*. 2001;3:83-92
262. Rao MS, Papreddy K, Musunuri S, Okonkwo A. Prevention/reversal of choline deficiency-induced steatohepatitis by a peroxisome proliferator-activated receptor alpha ligand in rats. *In vivo*. 2002;16:145-152
263. Rao MS, Reddy JK. Pparalpha in the pathogenesis of fatty liver disease. *Hepatology*. 2004;40:783-786
264. Ip E, Farrell GC, Robertson G, Hall P, Kirsch R, Leclercq I. Central role of pparalpha-dependent hepatic lipid turnover in dietary steatohepatitis in mice. *Hepatology*. 2003;38:123-132
265. Wang YX, Lee CH, Tiep S, Yu RT, Ham J, Kang H, Evans RM. Peroxisome-proliferator-activated receptor delta activates fat metabolism to prevent obesity. *Cell*. 2003;113:159-170
266. Berger J, Leibowitz MD, Doebber TW, Elbrecht A, Zhang B, Zhou G, Biswas C, Cullinan CA, Hayes NS, Li Y, Tanen M, Ventre J, Wu MS, Berger GD, Mosley R, Marquis R, Santini C, Sahoo SP, Tolman RL, Smith RG, Moller DE. Novel peroxisome proliferator-activated receptor (ppar) gamma and ppardelta ligands produce distinct biological effects. *The Journal of biological chemistry*. 1999;274:6718-6725
267. Yu BC, Chang CK, Ou HY, Cheng KC, Cheng JT. Decrease of peroxisome proliferator-activated receptor delta expression in cardiomyopathy of streptozotocin-induced diabetic rats. *Cardiovascular research*. 2008;80:78-87
268. Ren D, Collingwood TN, Rebar EJ, Wolffe AP, Camp HS. Ppargamma knockdown by engineered transcription factors: Exogenous ppargamma2 but not ppargamma1 reactivates adipogenesis. *Genes & development*. 2002;16:27-32
269. Werman A, Hollenberg A, Solanes G, Bjorbaek C, Vidal-Puig AJ, Flier JS. Ligand-independent activation domain in the n terminus of peroxisome proliferator-activated receptor

- gamma (ppargamma). Differential activity of ppargamma1 and -2 isoforms and influence of insulin. *The Journal of biological chemistry*. 1997;272:20230-20235
270. Medina-Gomez G, Gray SL, Yetukuri L, Shimomura K, Virtue S, Campbell M, Curtis RK, Jimenez-Linan M, Blount M, Yeo GS, Lopez M, Seppanen-Laakso T, Ashcroft FM, Oresic M, Vidal-Puig A. Ppar gamma 2 prevents lipotoxicity by controlling adipose tissue expandability and peripheral lipid metabolism. *PLoS genetics*. 2007;3:e64
271. Kintscher U, Law RE. Ppargamma-mediated insulin sensitization: The importance of fat versus muscle. *American journal of physiology. Endocrinology and metabolism*. 2005;288:E287-291
272. Lehrke M, Lazar MA. The many faces of ppargamma. *Cell*. 2005;123:993-999
273. Ahmadian M, Suh JM, Hah N, Liddle C, Atkins AR, Downes M, Evans RM. Ppargamma signaling and metabolism: The good, the bad and the future. *Nature medicine*. 2013;19:557-566
274. Lemberger T, Saladin R, Vazquez M, Assimacopoulos F, Staels B, Desvergne B, Wahli W, Auwerx J. Expression of the peroxisome proliferator-activated receptor alpha gene is stimulated by stress and follows a diurnal rhythm. *The Journal of biological chemistry*. 1996;271:1764-1769
275. Yang X, Downes M, Yu RT, Bookout AL, He W, Straume M, Mangelsdorf DJ, Evans RM. Nuclear receptor expression links the circadian clock to metabolism. *Cell*. 2006;126:801-810
276. Wang N, Yang G, Jia Z, Zhang H, Aoyagi T, Soodvilai S, Symons JD, Schnermann JB, Gonzalez FJ, Litwin SE, Yang T. Vascular ppargamma controls circadian variation in blood pressure and heart rate through bmal1. *Cell metabolism*. 2008;8:482-491
277. Oishi K, Shirai H, Ishida N. Clock is involved in the circadian transactivation of peroxisome-proliferator-activated receptor alpha (pparalpha) in mice. *The Biochemical journal*. 2005;386:575-581
278. Canaple L, Rambaud J, Dkhissi-Benyahya O, Rayet B, Tan NS, Michalik L, Delaunay F, Wahli W, Laudet V. Reciprocal regulation of brain and muscle arnt-like protein 1 and peroxisome proliferator-activated receptor alpha defines a novel positive feedback loop in the rodent liver circadian clock. *Molecular endocrinology*. 2006;20:1715-1727
279. Gervois P, Chopin-Delannoy S, Fadel A, Dubois G, Kosykh V, Fruchart JC, Najib J, Laudet V, Staels B. Fibrates increase human rev-erbalpha expression in liver via a novel peroxisome proliferator-activated receptor response element. *Molecular endocrinology*. 1999;13:400-409
280. Schmutz I, Ripperger JA, Baeriswyl-Aebischer S, Albrecht U. The mammalian clock component period2 coordinates circadian output by interaction with nuclear receptors. *Genes & development*. 2010;24:345-357
281. Fontaine C, Dubois G, Duguay Y, Helledie T, Vu-Dac N, Gervois P, Soncin F, Mandrup S, Fruchart JC, Fruchart-Najib J, Staels B. The orphan nuclear receptor rev-erbalpha is a peroxisome proliferator-activated receptor (ppar) gamma target gene and promotes ppargamma-induced adipocyte differentiation. *The Journal of biological chemistry*. 2003;278:37672-37680
282. Le Martelot G, Claudel T, Gatfield D, Schaad O, Kornmann B, Lo Sasso G, Moschetta A, Schibler U. Rev-erbalpha participates in circadian srebp signaling and bile acid homeostasis. *PLoS biology*. 2009;7:e1000181
283. Doherty CJ, Kay SA. Circadian control of global gene expression patterns. *Annual review of genetics*. 2010;44:419-444
284. Akhtar RA, Reddy AB, Maywood ES, Clayton JD, King VM, Smith AG, Gant TW, Hastings MH, Kyriacou CP. Circadian cycling of the mouse liver transcriptome, as revealed by cDNA microarray, is driven by the suprachiasmatic nucleus. *Current biology : CB*. 2002;12:540-550
285. Panda S, Antoch MP, Miller BH, Su AI, Schook AB, Straume M, Schultz PG, Kay SA, Takahashi JS, Hogenesch JB. Coordinated transcription of key pathways in the mouse by the circadian clock. *Cell*. 2002;109:307-320
286. Storch KF, Lipan O, Leykin I, Viswanathan N, Davis FC, Wong WH, Weitz CJ. Extensive and divergent circadian gene expression in liver and heart. *Nature*. 2002;417:78-83

287. Reddy AB, Karp NA, Maywood ES, Sage EA, Deery M, O'Neill JS, Wong GK, Chesham J, Odell M, Lilley KS, Kyriacou CP, Hastings MH. Circadian orchestration of the hepatic proteome. *Current biology : CB*. 2006;16:1107-1115
288. Mauvoisin D, Wang J, Jouffe C, Martin E, Atger F, Waridel P, Quadroni M, Gachon F, Naef F. Circadian clock-dependent and -independent rhythmic proteomes implement distinct diurnal functions in mouse liver. *Proceedings of the National Academy of Sciences of the United States of America*. 2014;111:167-172
289. Robles MS, Cox J, Mann M. In-vivo quantitative proteomics reveals a key contribution of post-transcriptional mechanisms to the circadian regulation of liver metabolism. *PLoS genetics*. 2014;10:e1004047
290. Hughes ME, DiTacchio L, Hayes KR, Vollmers C, Pulivarthy S, Baggs JE, Panda S, Hogenesch JB. Harmonics of circadian gene transcription in mammals. *PLoS genetics*. 2009;5:e1000442
291. Dong W, Tang X, Yu Y, Nilsen R, Kim R, Griffith J, Arnold J, Schuttler HB. Systems biology of the clock in *Neurospora crassa*. *PloS one*. 2008;3:e3105
292. Xu W, Yang R, Li M, Xing Z, Yang W, Chen G, Guo H, Gong X, Du Z, Zhang Z, Hu X, Wang D, Qian Q, Wang T, Su Z, Xue Y. Transcriptome phase distribution analysis reveals diurnal regulated biological processes and key pathways in rice flag leaves and seedling leaves. *PloS one*. 2011;6:e17613
293. Piques M, Schulze WX, Hohne M, Usadel B, Gibon Y, Rohwer J, Stitt M. Ribosome and transcript copy numbers, polysome occupancy and enzyme dynamics in *Arabidopsis*. *Molecular systems biology*. 2009;5:314
294. Warner JR. The economics of ribosome biosynthesis in yeast. *Trends in biochemical sciences*. 1999;24:437-440
295. Bianchini A, Loiirro M, Bielli P, Busa R, Paronetto MP, Loreni F, Geremia R, Sette C. Phosphorylation of eif4e by mnks supports protein synthesis, cell cycle progression and proliferation in prostate cancer cells. *Carcinogenesis*. 2008;29:2279-2288
296. Ripperger JA, Shearman LP, Reppert SM, Schibler U. Clock, an essential pacemaker component, controls expression of the circadian transcription factor dbp. *Genes & development*. 2000;14:679-689
297. Falvey E, Marcacci L, Schibler U. DNA-binding specificity of par and c/ebp leucine zipper proteins: A single amino acid substitution in the c/ebp DNA-binding domain confers par-like specificity to c/ebp. *Biological chemistry*. 1996;377:797-809
298. Gachon F, Fonjallaz P, Damiola F, Gos P, Kodama T, Zakany J, Duboule D, Petit B, Tafti M, Schibler U. The loss of circadian par bzip transcription factors results in epilepsy. *Genes & development*. 2004;18:1397-1412
299. Wang Q, Maillard M, Schibler U, Burnier M, Gachon F. Cardiac hypertrophy, low blood pressure, and low aldosterone levels in mice devoid of the three circadian par bzip transcription factors dbp, hlf, and tef. *American journal of physiology. Regulatory, integrative and comparative physiology*. 2010;299:R1013-1019
300. Gachon F, Leuenberger N, Claudel T, Gos P, Jouffe C, Fleury Olela F, de Mollerat du Jeu X, Wahli W, Schibler U. Proline- and acidic amino acid-rich basic leucine zipper proteins modulate peroxisome proliferator-activated receptor alpha (pparalpha) activity. *Proceedings of the National Academy of Sciences of the United States of America*. 2011;108:4794-4799
301. Xu J, Dang Y, Ren YR, Liu JO. Cholesterol trafficking is required for mtor activation in endothelial cells. *Proceedings of the National Academy of Sciences of the United States of America*. 2010;107:4764-4769
302. Parton RG. Caveolae and caveolins. *Current opinion in cell biology*. 1996;8:542-548
303. Simons K, Ikonen E. Functional rafts in cell membranes. *Nature*. 1997;387:569-572
304. Silvius JR. Role of cholesterol in lipid raft formation: Lessons from lipid model systems. *Biochimica et biophysica acta*. 2003;1610:174-183
305. Michel V, Bakovic M. Lipid rafts in health and disease. *Biology of the cell / under the auspices of the European Cell Biology Organization*. 2007;99:129-140
306. Patra SK. Dissecting lipid raft facilitated cell signaling pathways in cancer. *Biochimica et biophysica acta*. 2008;1785:182-206

307. George KS, Wu S. Lipid raft: A floating island of death or survival. *Toxicology and applied pharmacology*. 2012;259:311-319
308. Gao X, Lowry PR, Zhou X, Depry C, Wei Z, Wong GW, Zhang J. Pi3k/akt signaling requires spatial compartmentalization in plasma membrane microdomains. *Proceedings of the National Academy of Sciences of the United States of America*. 2011;108:14509-14514
309. Seedorf U, Ellinghaus P, Roch Nofer J. Sterol carrier protein-2. *Biochimica et biophysica acta*. 2000;1486:45-54
310. McGuire DM, Olson CD, Towle HC, Dempsey ME. Translational control of the circadian rhythm of liver sterol carrier protein. *The Journal of biological chemistry*. 1984;259:5368-5371
311. Puglielli L, Rigotti A, Greco AV, Santos MJ, Nervi F. Sterol carrier protein-2 is involved in cholesterol transfer from the endoplasmic reticulum to the plasma membrane in human fibroblasts. *The Journal of biological chemistry*. 1995;270:18723-18726
312. Schroeder F, Atshaves BP, McIntosh AL, Gallegos AM, Storey SM, Parr RD, Jefferson JR, Ball JM, Kier AB. Sterol carrier protein-2: New roles in regulating lipid rafts and signaling. *Biochimica et biophysica acta*. 2007;1771:700-718
313. Marcheva B, Ramsey KM, Buhr ED, Kobayashi Y, Su H, Ko CH, Ivanova G, Omura C, Mo S, Vitaterna MH, Lopez JP, Philipson LH, Bradfield CA, Crosby SD, JeBailey L, Wang X, Takahashi JS, Bass J. Disruption of the clock components clock and bmal1 leads to hypoinsulinaemia and diabetes. *Nature*. 2010;466:627-631
314. Lee J, Moulik M, Fang Z, Saha P, Zou F, Xu Y, Nelson DL, Ma K, Moore DD, Yechoor VK. Bmal1 and beta-cell clock are required for adaptation to circadian disruption, and their loss of function leads to oxidative stress-induced beta-cell failure in mice. *Molecular and cellular biology*. 2013;33:2327-2338
315. Zhang EE, Liu Y, Dentin R, Pongsawakul PY, Liu AC, Hirota T, Nusinow DA, Sun X, Landais S, Kodama Y, Brenner DA, Montminy M, Kay SA. Cryptochrome mediates circadian regulation of camp signaling and hepatic gluconeogenesis. *Nature medicine*. 2010;16:1152-1156
316. Amitani M, Asakawa A, Amitani H, Inui A. The role of leptin in the control of insulin-glucose axis. *Frontiers in neuroscience*. 2013;7:51
317. Kohsaka A, Laposky AD, Ramsey KM, Estrada C, Joshu C, Kobayashi Y, Turek FW, Bass J. High-fat diet disrupts behavioral and molecular circadian rhythms in mice. *Cell metabolism*. 2007;6:414-421
318. Hatori M, Vollmers C, Zarrinpar A, DiTacchio L, Bushong EA, Gill S, Leblanc M, Chaix A, Joens M, Fitzpatrick JA, Ellisman MH, Panda S. Time-restricted feeding without reducing caloric intake prevents metabolic diseases in mice fed a high-fat diet. *Cell metabolism*. 2012;15:848-860
319. Alvarez JD, Hansen A, Ord T, Bebas P, Chappell PE, Giebultowicz JM, Williams C, Moss S, Sehgal A. The circadian clock protein bmal1 is necessary for fertility and proper testosterone production in mice. *Journal of biological rhythms*. 2008;23:26-36
320. Ingalls AM, Dickie MM, Snell GD. Obese, a new mutation in the house mouse. *The Journal of heredity*. 1950;41:317-318
321. Thorens B, Sarkar HK, Kaback HR, Lodish HF. Cloning and functional expression in bacteria of a novel glucose transporter present in liver, intestine, kidney, and beta-pancreatic islet cells. *Cell*. 1988;55:281-290
322. James DE, Strube M, Mueckler M. Molecular cloning and characterization of an insulin-regulatable glucose transporter. *Nature*. 1989;338:83-87
323. Sadacca LA, Lamia KA, deLemos AS, Blum B, Weitz CJ. An intrinsic circadian clock of the pancreas is required for normal insulin release and glucose homeostasis in mice. *Diabetologia*. 2011;54:120-124
324. Bradbury MW, Berk PD. Lipid metabolism in hepatic steatosis. *Clinics in liver disease*. 2004;8:639-671, xi
325. Anstee QM, Goldin RD. Mouse models in non-alcoholic fatty liver disease and steatohepatitis research. *International journal of experimental pathology*. 2006;87:1-16

326. Chung WK, Belfi K, Chua M, Wiley J, Mackintosh R, Nicolson M, Boozer CN, Leibel RL. Heterozygosity for *lep(ob)* or *lep(rdb)* affects body composition and leptin homeostasis in adult mice. *The American journal of physiology*. 1998;274:R985-990
327. Fujihara Y, Kondo H, Noguchi T, Togari A. Glucocorticoids mediate circadian timing in peripheral osteoclasts resulting in the circadian expression rhythm of osteoclast-related genes. *Bone*. 2014;61:1-9
328. Turner RT, Kalra SP, Wong CP, Philbrick KA, Lindenmaier LB, Boghossian S, Iwaniec UT. Peripheral leptin regulates bone formation. *Journal of bone and mineral research : the official journal of the American Society for Bone and Mineral Research*. 2013;28:22-34
329. Matsumoto E, Ishihara A, Tamai S, Nemoto A, Iwase K, Hiwasa T, Shibata S, Takiguchi M. Time of day and nutrients in feeding govern daily expression rhythms of the gene for sterol regulatory element-binding protein (*sreb*p)-1 in the mouse liver. *The Journal of biological chemistry*. 2010;285:33028-33036
330. Turek FW, Joshu C, Kohsaka A, Lin E, Ivanova G, McDearmon E, Laposky A, Losee-Olson S, Easton A, Jensen DR, Eckel RH, Takahashi JS, Bass J. Obesity and metabolic syndrome in circadian clock mutant mice. *Science*. 2005;308:1043-1045
331. Beaven SW, Matveyenko A, Wroblewski K, Chao L, Wilpitz D, Hsu TW, Lentz J, Drew B, Hevener AL, Tontonoz P. Reciprocal regulation of hepatic and adipose lipogenesis by liver x receptors in obesity and insulin resistance. *Cell metabolism*. 2013;18:106-117
332. Saleh MC, Wheeler MB, Chan CB. Endogenous islet uncoupling protein-2 expression and loss of glucose homeostasis in *ob/ob* mice. *The Journal of endocrinology*. 2006;190:659-667
333. Beck V, Jaburek M, Demina T, Rupprecht A, Porter RK, Jezek P, Pohl EE. Polyunsaturated fatty acids activate human uncoupling proteins 1 and 2 in planar lipid bilayers. *FASEB journal : official publication of the Federation of American Societies for Experimental Biology*. 2007;21:1137-1144
334. Echtay KS, Esteves TC, Pakay JL, Jekabsons MB, Lambert AJ, Portero-Otin M, Pamplona R, Vidal-Puig AJ, Wang S, Roebuck SJ, Brand MD. A signalling role for 4-hydroxy-2-nonenal in regulation of mitochondrial uncoupling. *The EMBO journal*. 2003;22:4103-4110
335. Zhang CY, Baffy G, Perret P, Krauss S, Peroni O, Grujic D, Hagen T, Vidal-Puig AJ, Boss O, Kim YB, Zheng XX, Wheeler MB, Shulman GI, Chan CB, Lowell BB. Uncoupling protein-2 negatively regulates insulin secretion and is a major link between obesity, beta cell dysfunction, and type 2 diabetes. *Cell*. 2001;105:745-755
336. Pi J, Bai Y, Daniel KW, Liu D, Lyght O, Edelstein D, Brownlee M, Corkey BE, Collins S. Persistent oxidative stress due to absence of uncoupling protein 2 associated with impaired pancreatic beta-cell function. *Endocrinology*. 2009;150:3040-3048
337. Pi J, Collins S. Reactive oxygen species and uncoupling protein 2 in pancreatic beta-cell function. *Diabetes, obesity & metabolism*. 2010;12 Suppl 2:141-148
338. Allister EM, Robson-Doucette CA, Prentice KJ, Hardy AB, Sultan S, Gaisano HY, Kong D, Gilon P, Herrera PL, Lowell BB, Wheeler MB. *Ucp2* regulates the glucagon response to fasting and starvation. *Diabetes*. 2013;62:1623-1633
339. Peek CB, Affinati AH, Ramsey KM, Kuo HY, Yu W, Sena LA, Ilkayeva O, Marcheva B, Kobayashi Y, Omura C, Levine DC, Bacsik DJ, Gius D, Newgard CB, Goetzman E, Chandel NS, Denu JM, Mrksich M, Bass J. Circadian clock *nad*⁺ cycle drives mitochondrial oxidative metabolism in mice. *Science*. 2013;342:1243417
340. Jouffe C, Cretenet G, Symul L, Martin E, Atger F, Naef F, Gachon F. The circadian clock coordinates ribosome biogenesis. *PLoS biology*. 2013;11:e1001455
341. Lo S, Russell JC, Taylor AW. Determination of glycogen in small tissue samples. *Journal of applied physiology*. 1970;28:234-236